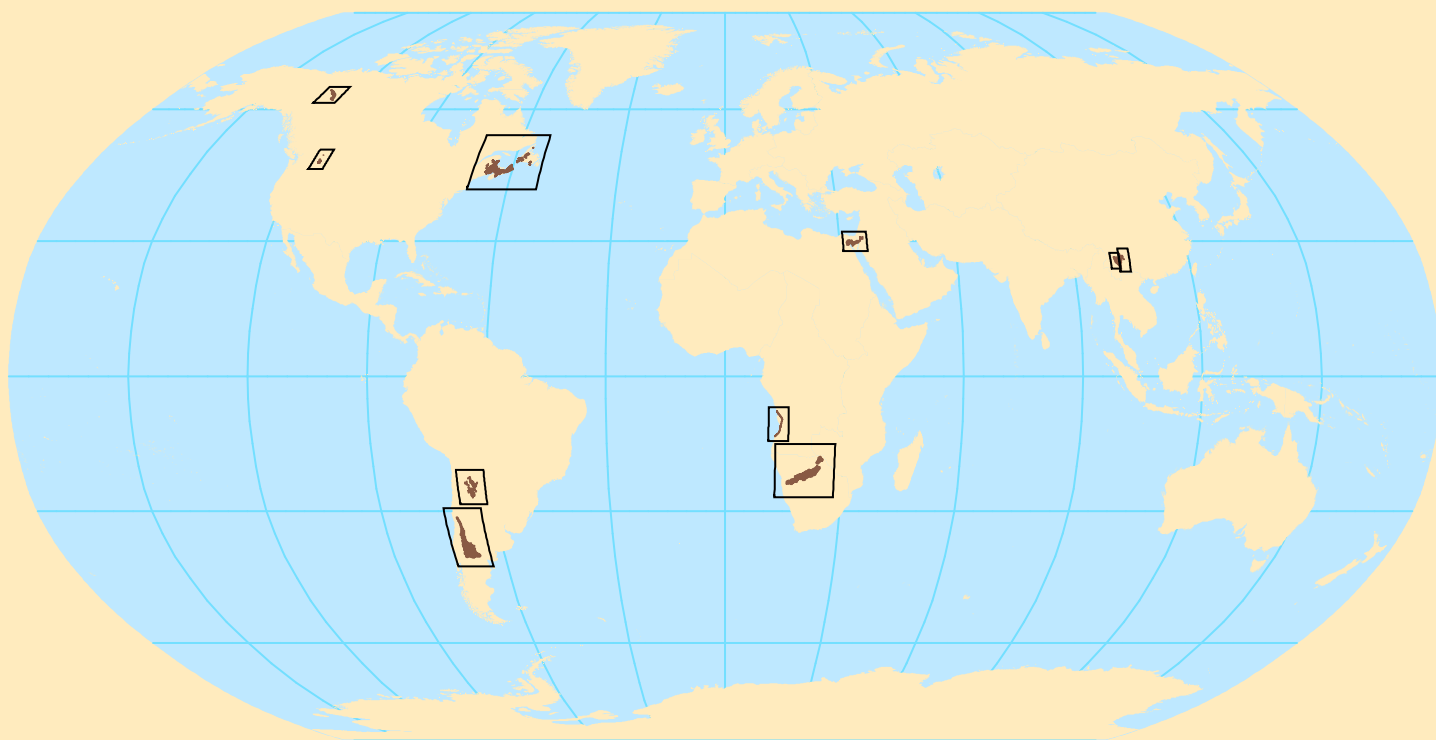


**Global Mineral Resource Assessment**

**Qualitative Assessment of Selected Areas of the World  
for Undiscovered Sediment-Hosted Stratabound Copper  
Deposits**



Scientific Investigations Report 2010–5090–Y

This page left intentionally blank.

## **Global Mineral Resource Assessment**

Michael L. Zientek, Jane M. Hammarstrom, and Kathleen M. Johnson, editors

# **Qualitative Assessment of Selected Areas of the World for Undiscovered Sediment- Hosted Stratabound Copper Deposits**

By Michael L. Zientek, Niki E. Wintzer, Timothy S. Hayes, Heather L. Parks,  
Deborah A. Briggs, J. Douglas Causey, Shyla A. Hatch, M. Christopher Jenkins,  
and David J. Williams

Scientific Investigations Report 2010–5090–Y

**U.S. Department of the Interior**  
**U.S. Geological Survey**

**U.S. Department of the Interior**  
SALLY JEWELL, Secretary

**U.S. Geological Survey**  
Suzette M. Kimball, Acting Director

U.S. Geological Survey, Reston, Virginia: 2015

For more information on the USGS—the Federal source for science about the Earth, its natural and living resources, natural hazards, and the environment—visit <http://www.usgs.gov/> or call 1-888-ASK-USGS (1-888-275-8747).

For an overview of USGS information products, including maps, imagery, and publications, visit <http://www.usgs.gov/pubprod/>.

To order USGS information products, visit <http://store.usgs.gov/>.

Any use of trade, firm, or product names is for descriptive purposes only and does not imply endorsement by the U.S. Government.

Although this information product, for the most part, is in the public domain, it also may contain copyrighted materials as noted in the text. Permission to reproduce copyrighted items must be secured from the copyright owner.

Suggested citation:

Zientek, M.L., Wintzer, N.E., Hayes, T.S., Parks, H.L., Briggs, D.A., Causey, J.D., Hatch, S.A., Jenkins, M.C., and Williams, D.J., 2015, Qualitative assessment of selected areas of the world for undiscovered sediment-hosted stratabound copper deposits: U.S. Geological Survey Scientific Investigations Report 2010-5090-Y, 143 p., and spatial data, <http://dx.doi.org/10.3133/sir20105090Y>.



# Contents

Abstract.....	1
Chapter 1. Qualitative Assessment of Sediment-Hosted Stratabound Copper Permissive Tracts.....	3
Introduction.....	3
Deposit Type Assessed.....	5
Mineral System for the Deposit Type .....	5
Data Collected .....	7
Permissive Tract Delineation .....	7
Qualitative Assessment of the Areas .....	7
Results .....	22
Chapter 2. Tectonics, Stratigraphy, and Economic Geology of Qualitatively Assessed Tracts.....	25
Introduction.....	25
Northwest Botswana Rift, Botswana and Namibia—Assessment Tract 002rfCu2002 .....	25
Tectonic Setting .....	25
Stratigraphy .....	26
Deposits and Occurrences .....	26
Reduced-Facies-Type Deposits.....	26
Sandstone-Copper Deposits .....	35
Mineral System Components.....	36
Principal Sources of Information .....	36
Benguela and Cuanza Basins, Angola—Assessment Tract 002rfCu2000 .....	36
Tectonic Setting .....	36
Stratigraphy .....	37
Deposits and Occurrences .....	37
Reduced-Facies-Subtype Deposits .....	37
Red-Bed-Subtype Deposits.....	37
Mineral System Components.....	41
Principal Sources of Information .....	41
Egypt–Israel–Jordan Rift, Egypt, Israel, and Jordan—Assessment Tract 002rfCu2001 .....	41
Tectonic Setting .....	42
Stratigraphy .....	42
Deposits and Occurrences .....	47
Mineral System Components .....	52
Principal Sources of Information .....	52
Redstone Copperbelt, Canada—Assessment Tract 003rfCu3000.....	52
Tectonic Setting .....	52
Stratigraphy .....	54
Deposits and Occurrences .....	54
Mineral System Components.....	57
Principal Sources of Information .....	62
Dongchuan Group Rocks, South Central China—Assessment Tract 142rfCu4000.....	62
Tectonic Setting .....	62
Stratigraphy .....	64

Deposits and Occurrences .....	64
Mineral System Components.....	70
Principal Sources of Information .....	70
Belt-Purcell Basin, United States and Canada—Assessment Tract 003ssCu3100.....	70
Tectonic Setting .....	70
Stratigraphy .....	72
Deposits and Occurrences .....	72
Mineral System Components.....	79
Principal Sources of Information .....	79
Neuquén Basin, Argentina—Assessment Tract 005ssCu5100.....	79
Tectonic Setting .....	80
Stratigraphy .....	80
Deposits and Occurrences .....	84
Mineral System Components.....	89
Principal Sources of Information .....	89
Maritimes Basin, Canada—Assessment Tract 003shCu1000.....	89
Tectonic Setting .....	89
Stratigraphy .....	91
Deposits and Occurrences .....	94
Mineral System Components.....	94
Principal Sources of Information .....	100
Chuxiong Basin, China—Assessment Tract 142ssCu6000.....	100
Tectonic Setting .....	100
Stratigraphy .....	102
Deposits and Occurrences .....	102
Mineral System Components.....	102
Principal Sources of Information .....	109
Salta Rift System, Argentina—Assessment Tract 005ssCu5101 .....	109
Tectonic Setting .....	109
Stratigraphy .....	109
Deposits and Occurrences .....	109
Mineral System Components.....	114
Principal Sources of Information .....	114
Conclusions.....	114
Acknowledgments.....	117
References Cited .....	118
Appendix A. Description of GIS Files .....	140
Appendix B. Analytic Hierarchy Process Input.....	142
Appendix C. Assessment Team .....	143

## Figures

1-1.	Map showing the 10 assessment areas that were qualitatively assessed for undiscovered sediment-hosted stratabound copper deposits .....	4
1-2.	Schematic section of a sedimentary basin showing the mineral system components.....	6
1-3.	Map showing the sediment-hosted copper permissive tract, deposits, and occurrences of the Northwest Botswana Rift, Botswana and Namibia.....	12
1-4.	Map showing the sediment-hosted copper permissive tract, deposits, and occurrences of the Benguela and Cuanza Basins, Angola.....	13
1-5.	Map showing the sediment-hosted copper permissive tract, deposits, and occurrences of the Egypt–Israel–Jordan Rift, Egypt, Israel, and Jordan.....	14
1-6.	Map showing the sediment-hosted copper permissive tract, deposits, and occurrences of the Redstone Copperbelt, Canada.....	15
1-7.	Map showing the sediment-hosted copper permissive tract, deposits, and occurrences of the Dongchuan Group Rocks, south central China .....	16
1-8.	Map showing the sediment-hosted copper permissive tract, deposits, and occurrences of the Belt-Purcell Basin, United States and Canada.....	17
1-9.	Map showing the sediment-hosted copper permissive tract, deposits, and occurrences of the Neuquén Basin, Argentina.....	18
1-10.	Map showing the sediment-hosted copper permissive tract, deposits, and occurrences of the Maritimes Basin, Canada .....	19
1-11.	Map showing the sediment-hosted copper permissive tract, deposits, and occurrences of the Chuxiong Basin, China .....	20
1-12.	Map showing the sediment-hosted copper permissive tract, deposits, and occurrences of the Salta Rift System, Argentina.....	21
1-13.	Chart showing criteria hierarchy used for the analytic hierarchy process.....	23
1-14.	Stacked bar graph showing group analytic hierarchy process .....	23
2-1.	Map of the Proterozoic rocks associated with the Northwest Botswana Rift, Botswana and Namibia.....	27
2-2.	Map showing the reconstruction of southwestern Gondwana .....	28
2-3.	Cross section through the Northwest Botswana Rift showing folding and faulting of Proterozoic Ghanzi Group rocks .....	29
2-4.	Stratigraphic columns of the Neoproterozoic rocks that host reduced-facies-type stratabound copper mineralization of the Kalahari Copperbelt, Botswana and Namibia.....	30
2-5.	Geologic map of the western part of the Kalahari Copperbelt, Northwest Botswana Rift, Botswana and Namibia .....	32
2-6.	Geologic map of the eastern part of the Kalahari Copperbelt, Northwest Botswana Rift, Botswana and Namibia .....	33
2-7.	Schematic block diagram showing the location of several reduced-facies-type sediment-hosted copper deposits and occurrences .....	34
2-8.	Map showing the onshore parts of the Benguela and Cuanza Basins, Angola.....	38
2-9.	Geologic cross section of the Cuanza Basin, Angola.....	39
2-10.	Chronostratigraphic column of the Cuanza Basin, Angola.....	40
2-11.	Map showing the Egypt–Israel–Jordan Rift permissive tract.....	43
2-12.	Geologic cross section based on a seismic profile through southern Jordan .....	44
2-13.	Stratigraphic columns of lower Paleozoic sedimentary rocks, Egypt, Israel, and Jordan.....	45
2-14.	Stratigraphic columns of Early to Middle Cambrian rocks in Jordan.....	46

## Figures—Continued

2-15.	Map showing sediment-hosted copper permissive tract, deposits, and occurrences in Early to Middle Cambrian rocks in the Egypt–Israel–Jordan Rift.....	48
2-16.	Two geologic cross sections showing subsurface extent of Paleozoic rocks in Egypt, Israel, and Jordan.....	49
2-17.	Map showing the relation between Cambrian sedimentary host rocks and associated sediment-hosted stratabound copper deposits and occurrences to protected areas in Israel and Jordan.....	50
2-18.	Map showing the distribution of Neoproterozoic rocks in northwestern Canada .....	53
2-19.	Stratigraphic column showing the position of reduced-facies-type copper mineralization in Neoproterozoic rocks of the Redstone Copper Belt, Canada .....	55
2-20.	Schematic cross section illustrating stratigraphic relations of Neoproterozoic units in the central Mackenzie Mountains, Northwest Territories, Canada .....	56
2-21.	Map showing sediment-hosted copper permissive geologic units, deposits, and occurrences of the northern part of the Redstone Copperbelt, Canada .....	58
2-22.	Map showing sediment-hosted copper permissive geologic units, deposits, and occurrences of the southern part of the Redstone Copperbelt, Canada.....	59
2-23.	Map and cross sections through the Coates Lake deposit showing reduced-facies copper mineralization, Canada .....	60
2-24.	Stratigraphic column of the mineralized transition zone of the Coates Lake Group, Canada.....	61
2-25.	Simplified tectonic map showing part of the Yangtze Craton and rocks associated with the Kunyang Aulacogen, China .....	63
2-26.	Stratigraphic columns illustrating the position of copper mineralization in the Yinmin, Luoxue, and Luzhijiang Formations, China .....	65
2-27.	Map showing the northern part of permissive Paleoproterozoic to early Mesoproterozoic geologic units and associated sediment-hosted copper deposits and occurrences.....	66
2-28.	Map showing the southern part of permissive Paleoproterozoic to early Mesoproterozoic geologic units and associated sediment-hosted copper deposits and occurrences.....	67
2-29.	Cross section of the Tangdan deposit, a reduced-facies deposit in Dongchuan Group strata, China.....	69
2-30.	Map showing the Revett/Creston Formations, Belt-Purcell Basin, and sediment-hosted copper permissive tract the United States and Canada .....	71
2-31.	Diagram showing approximate thicknesses of stratigraphic divisions of the Belt-Purcell Supergroup, United States and Canada .....	73
2-32.	Stratigraphic column of the Middle Proterozoic Belt-Purcell Supergroup emphasizing sedimentary structures in the area of Revett-hosted deposits and occurrences.....	74
2-33.	Map showing the sediment-hosted copper permissive tract, deposits, and occurrences associated with the Revett/Creston Formations, United States and Canada.....	76
2-34.	Stratigraphic columns of the Belt Supergroup of western Montana and northern Idaho.....	77
2-35.	Map and cross sections through the Rock Creek deposit, Montana .....	78
2-36.	Map showing the distribution of Lower Jurassic to Upper Cretaceous sedimentary rocks and deposits and occurrences, Argentina.....	81
2-37.	Stratigraphic column of the Neuquén Basin with regional tectonic history and depositional settings of sedimentary rocks, Argentina.....	82
2-38.	Cross sections through the Neuquén Basin illustrating stratigraphic relations across the Huincul High, Argentina.....	83
2-39.	Stratigraphic column of the Neuquén Group in the Huincul High area, Argentina.....	86

## Figures—Continued

2-40.	Map showing late Paleozoic subbasins and faults related to the Maritimes Basin, Canada.....	90
2-41.	Stratigraphic column of the Maritimes Basin, Canada, showing the position of sediment-hosted copper mineralization .....	92
2-42.	Schematic geologic cross section of the Maritimes Basin, Canada .....	93
2-43.	Geologic map of western Nova Scotia and eastern New Brunswick showing deposits and occurrences associated with the Maritimes Basin, Canada .....	97
2-44.	Geologic map of eastern Nova Scotia showing sediment-hosted copper occurrences associated with the Maritimes Basin, Canada.....	98
2-45.	Geologic map of eastern New Brunswick and western Newfoundland showing deposits and occurrences associated with the Maritimes Basin, Canada .....	99
2-46.	Simplified tectonic map of southern China showing major structural units in the region.....	101
2-47.	Correlated stratigraphic columns for the Chuxiong Basin, China .....	106
2-48.	Map showing the Chuxiong Basin, Cretaceous rocks permissive for sediment-hosted copper mineralization, and deposits and occurrences, China .....	107
2-49.	Cross sections illustrating aspects of sediment-hosted copper mineralization in the Chuxiong Basin, China .....	108
2-50.	Map showing areas of Early Cretaceous rifting, South Atlantic Ocean.....	110
2-51.	Map showing the subbasins of the Salta Rift System, outcrop of the Salta Group, deposits, occurrences, and sites, Argentina .....	111
2-52.	Stratigraphic correlation chart showing lateral variation of the Salta Group in northeastern Chile and northern Argentina .....	112
2-53.	Stratigraphic column of the Salta Group, Argentina .....	113
2-54.	Stratigraphic column showing sediment-hosted copper mineralization in the Balbuena Subgroup of the Salta Group at the Leon deposit, Argentina .....	115
2-55.	Geologic map and cross section through the Leon deposit, Argentina .....	116

## Tables

1-1.	Mineral-system components present in each assessment area .....	8
1-2.	Geologic units and methods used for permissive tract delineation.....	11
1-3.	Ranked lists of the assessment areas showing results based on expert opinion and group analytic hierarchy process analysis.....	22
2-1.	Sediment-hosted stratabound copper deposits within the Northwest Botswana Rift, Botswana and Namibia .....	31
2-2.	Sediment-hosted stratabound copper deposits within the Cuvo and Binga Formations of the Benguela and Cuanza Basins, Angola .....	41
2-3.	Sediment-hosted stratabound copper deposits in Early to Middle Cambrian rocks of the Egypt–Israel–Jordan Rift.....	51
2-4.	Geologic maps used by the assessment team for the Egypt–Israel–Jordan Rift.....	52
2-5.	Sediment-hosted stratabound copper deposits in the Redstone Copperbelt, Canada .....	57
2-6.	Geologic maps used by the assessment team for the Redstone Copperbelt, Canada .....	62
2-7.	Sediment-hosted stratabound copper deposits within the Proterozoic Dongchuan Group rocks, China .....	68

## Tables—Continued

2-8.	Sediment-hosted stratabound copper deposits within the Revett Formation of the Belt-Purcell Basin, United States .....	75
2-9.	Sediment-hosted stratabound copper deposits within the Neuquén Basin, Argentina.....	85
2-10.	Summary table for selected deposits and occurrences within the Neuquén Basin, Argentina.....	87
2-11.	Sediment-hosted stratabound copper deposits and occurrences within the Maritimes Basin, Canada .....	95
2-12.	Names of deposits and occurrences that correlate to numbers in figure 2-43 .....	95
2-13.	Names of occurrences that correlate to numbers in figure 2-44 .....	96
2-14.	Stratigraphic units of the Chuxiong Basin, Sichuan and Yunnan, China.....	103
2-15.	Sediment-hosted stratabound copper deposits within the Matoushan Formation, and lateral equivalents, of the Chuxiong Basin.....	105
2-16.	Sediment-hosted stratabound copper deposits within the Salta Rift System, Argentina.....	114
A1.	Definitions of GMRA_SSCqual_pts.shp attribute table fields .....	140
A2.	Definitions of GMRA_SSCqual_tracts.shp attribute table fields .....	141

## Conversion Factors, Abbreviations and Acronyms, and Chemical Symbols

Inch/Pound to SI

<b>Multiply</b>	<b>By</b>	<b>To obtain</b>
Length		
foot (ft)	0.3048	meter (m)
mile (mi)	1.609	kilometer (km)
yard (yd)	0.9144	meter (m)
Area		
acre	0.4047	hectare (ha)
acre	0.004047	square kilometer (km <sup>2</sup> )
square mile (mi <sup>2</sup> )	259.0	hectare (ha)
square mile (mi <sup>2</sup> )	2.590	square kilometer (km <sup>2</sup> )
Mass		
ounce, troy (troy oz)	31.015	gram (g)
ounce, troy (troy oz)	0.0000311	megagram (Mg)
ton, short (2,000 lb)	0.9072	megagram (Mg)

Inch/Pound to SI

<b>Multiply</b>	<b>By</b>	<b>To obtain</b>
Length		
meter (m)	3.281	foot (ft)
kilometer (km)	0.6214	mile (mi)
meter (m)	1.094	yard (yd)
Area		
hectare (ha)	2.471	acre
square kilometer (km <sup>2</sup> )	247.1	acre
hectare (ha)	0.003861	square mile (mi <sup>2</sup> )
square kilometer (km <sup>2</sup> )	0.3861	square mile (mi <sup>2</sup> )
Mass		
gram (g)	0.03215	ounce, troy (troy oz)
megagram (Mg)	1.102	ton, short (2,000 lb)
megagram (Mg)	0.9842	ton, long (2,240 lb)

Other conversions used in this report

<b>Multiply</b>	<b>By</b>	<b>To obtain</b>
metric ton (t)	1	megagram (Mg)
troy ounce per short ton	34.2857	gram per metric ton (g/t)
percent	10,000	parts per million (ppm) or grams per metric ton (g/t)
percent metal	0.01 × metal grade, percent x ore tonnage, metric tons	metric tons of metal

## Datum

Vertical coordinate information is referenced to the World Geodetic System 1984 (WGS 84), reported in decimal degrees.

Horizontal coordinate information is referenced to the World Geodetic System 1984 (WGS 84), reported in decimal degrees.

## Acronyms and Abbreviations Used

A.D.	Anno Domini—A designation used to label or number years used with the Gregorian calendar
AHP	analytic hierarchy process
Ant	antlerite
Atc	atacamite
Az	azurite
B.C.	Before Christ—A designation used to label or number years used with the Gregorian calendar
Bh	brochantite
Bn	bornite
Cc	chalcocite
Ccl	chrysocolla
Ccp	chalcopyrite
Cp	cuprite
Ct	chalcanthite
Cv	covellite
Dg	digenite
Dj	djurleite
DRC	Democratic Republic of the Congo
Enr	enargite
Ga	billion years before the present
GIS	geographic information system
Gn	galena
g/t	grams per metric ton
Hem	hematite
Holcor	hollandite–coronadite solid solution
Ida	idaite
Ma	million years before the present
Mal	malachite
Mo	molybdenite
Mt	million metric tons
m.y.	million years
NA	not available
NWBR	Northwest Botswana Rift
oz/t	troy ounces per ton



## Acronyms and Abbreviations Used—Continued

Patc	paratacamite
ppm	parts per million
Py	pyrite
Pyl	pyrolusite
SEGEMAR	Servicio Geológico Minero Argentino (Geological and Mining Services of Argentina)
Sp	sphalerite
t	metric tons
Tet	tetrahedrite
Trn	tenorite
Turq	turquoise
USGS	U.S. Geological Survey

## Chemical Symbols Used

Ag	silver
Au	gold
Co	cobalt
Cu	copper
Mo	molybdenum
Pb	lead
REE	rare earth elements
Sb	antimony
Se	selenium
U	uranium
V	vanadium
Zn	zinc

This page left intentionally blank.

# Qualitative Assessment of Selected Areas of the World for Undiscovered Sediment-Hosted Stratabound Copper Deposits

By Michael L. Zientek<sup>1</sup>, Niki E. Wintzer<sup>1</sup>, Timothy S. Hayes<sup>2</sup>, Heather L. Parks<sup>1</sup>, Deborah A. Briggs<sup>1</sup>, J. Douglas Causey<sup>1</sup>, Shyla A. Hatch<sup>3</sup>, M. Christopher Jenkins<sup>3</sup>, and David J. Williams<sup>3</sup>

## Abstract

A qualitative mineral resource assessment of sediment-hosted stratabound copper mineralized areas for undiscovered copper deposits was performed for 10 selected areas of the world. The areas, in alphabetical order, are (1) Belt-Purcell Basin, United States and Canada; (2) Benguela and Cuanza Basins, Angola; (3) Chuxiong Basin, China; (4) Dongchuan Group rocks, China; (5) Egypt–Israel–Jordan Rift, Egypt, Israel, and Jordan; (6) Maritimes Basin, Canada; (7) Neuquén Basin, Argentina; (8) Northwest Botswana Rift, Botswana and Namibia; (9) Redstone Copperbelt, Canada; and (10) Salta Rift System, Argentina. This assessment (1) outlines the main characteristics of the areas, (2) classifies known deposits by deposit model subtypes, and (3) ranks the areas according to their potential to contain undiscovered copper deposits.

An analytic hierarchy process (AHP) was used to rank assessment areas according to their potential for undiscovered

copper deposits. Once the main characteristics of each area were compiled (age of host rock, geologic setting, stratigraphy, host lithology, deposit subtype(s), known deposits and occurrences, and mineral system components), three criteria (mineralization, extent of study area, and lithostratigraphic framework, each with multiple subcriteria) were scored for all assessment areas. Relative weights and scores were assigned to all criteria by three geologists. In addition, the assessment areas were ranked for comparison exclusively on the basis of professional opinion. The AHP and professional opinion lists are similar but not the same. Both the professional opinion and the cumulative AHP lists rate the Northwest Botswana Rift in Botswana and Namibia as the area most likely to contain the most undiscovered copper deposits. The Salta Rift System in Argentina is rated lowest among the 10 qualitatively assessed areas.

---

<sup>1</sup>U.S. Geological Survey, Spokane, Washington, United States.

<sup>2</sup>U.S. Geological Survey, Tucson, Arizona, United States.

<sup>3</sup>Eastern Washington University, Cheney, Washington, United States.

This page left intentionally blank.

# Chapter 1. Qualitative Assessment of Sediment-Hosted Stratabound Copper Permissive Tracts

By Michael L. Zientek<sup>1</sup>, Timothy S. Hayes<sup>2</sup>, Niki E. Wintzer<sup>1</sup>, and Heather L. Parks<sup>1</sup>

## Introduction

A qualitative mineral resource assessment of undiscovered deposits that could be associated with sediment-hosted stratabound copper mineralization was undertaken as part of a U.S. Geological Survey (USGS) global mineral resource assessment. The study resulted in (1) permissive tracts for undiscovered sediment-hosted stratabound copper deposits for 10 areas, (2) a database of known sediment-hosted stratabound copper deposits and occurrences, and (3) a ranked list of the 10 permissive tracts according to their potential to contain undiscovered copper deposits.

During the USGS global mineral assessment study, the areas for quantitative study were prioritized. In addition, a method was developed to provide a qualitative expression of value for areas that have insufficient information for a complete quantitative assessment. The method needed to be science based, unbiased, robust, and transparent (Harris, 1984; Sinclair and Blackwell, 2002; Charpentier and Klett, 2005; Singer and Menzie, 2010). Methods are science based if evaluation criteria are based on the concept that mineral-deposit types are the product of processes that take place in larger mineral systems. Bias can be minimized if the methodology incorporates an operating policy and documented procedures that allow consistent application of the technique. A robust method tends to produce correct predictions or estimates regardless of flaws in the data (Charpentier and Klett, 2005). Finally, transparency implies that the principles and process of the assessment method are defensible and documented.

In this study, a decision support tool, the analytic hierarchy process (AHP), was applied to consistently rank areas for their potential to contain undiscovered sediment-hosted stratabound copper deposits. The AHP is a structured technique to analyze complex decisions (Saaty, 1980; Meyer and Booker, 2001; Saaty and Vargas, 2010, 2012). The decision process is organized into a hierarchy of pairwise choices that can be evaluated qualitatively (for example, better, worse, or equal) as well as quantitatively by numerical scores or values. The pairwise comparisons made by professionals are converted into relative numerical weights using matrix algebra for all the

alternatives being considered. The technique also advises the assessors if pairwise comparisons are inconsistent.

About 30 sedimentary basins worldwide are known to contain sediment-hosted stratabound copper deposits (localities with reported tonnage and grade) (Zientek, Hayes, and Taylor, 2013). Almost 90 percent of the known contained resources were found in four areas that were quantitatively assessed for the USGS global assessment study: the Katanga Basin, Democratic Republic of the Congo and Zambia (Zientek, Bliss, and others, 2014); the Southern Permian Basin, northern Europe (Zientek and others, 2015); the Chu-Sarysu Basin, Kazakhstan (Box and others, 2012); and the Kodar-Udokan area, Russia (Zientek, Chechetkin, and others, 2014). Quantitative assessments for this deposit type have recently been published for Afghanistan and Greenland (Ludington and others, 2007; Peters and others, 2007; Stensgaard and others, 2011) and for the Teniz Basin, Kazakhstan (Cossette and others, 2014). Of the remaining basins, 10 were selected for qualitative assessment: the Belt-Purcell Basin, United States and Canada; a basin with Cambrian rocks in Egypt, Israel, and Jordan; the Chuxiong Basin, China; the Benguela and Cuanza Basins, Angola; the basin that contains the Dongchuan Group rocks, China; the Northwest Botswana Rift (which includes the Kalahari Copperbelt), Botswana and Namibia; the Maritimes Basin, Canada; the Neuquén Basin, Argentina; Neoproterozoic rocks that host the Redstone Copperbelt, Canada; and the Salta Rift System, Argentina (fig. 1-1). Study areas were selected so there would be a range of data quality and availability, exposure, level of exploration, and known deposits and occurrences.

This chapter describes the deposit type, data sources, methods, and results of the assessment. Chapter 2 is a summary of the available information that was used to qualitatively rank the tracts. For each study area, the tectonic setting and stratigraphy are described, and a map, stratigraphic column, cross section, and compilation of known deposits and occurrences are provided. Spatial data for permissive tract polygons and deposit and prospect point locations are included in geographic information system (GIS) files that accompany this report (appendix A).

<sup>1</sup>U.S. Geological Survey, Spokane, Washington, United States.

<sup>2</sup>U.S. Geological Survey, Tucson, Arizona, United States.

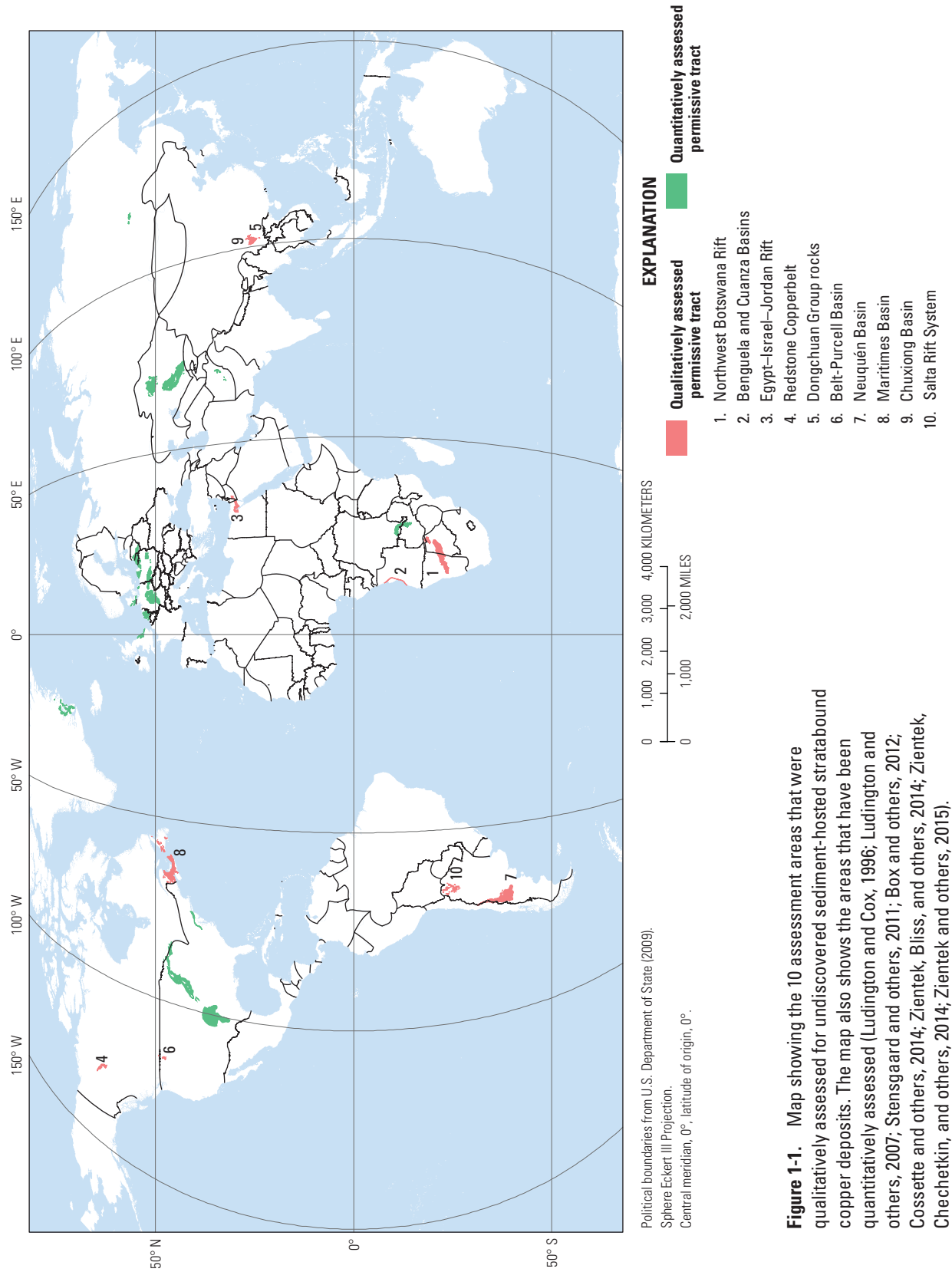


**Figure 1-1.** Map showing the 10 assessment areas that were qualitatively assessed for undiscovered sediment-hosted stratabound copper deposits. The map also shows the areas that have been quantitatively assessed (Ludington and Cox, 1996; Ludington and others, 2007; Stensgaard and others, 2011; Box and others, 2012; Cosssette and others, 2014; Zientek, Bliss, and others, 2014; Zientek, Chechetkin, and others, 2014; Zientek and others, 2015).

## Deposit Type Assessed

Sediment-hosted stratabound copper deposits consist of fine-grained, copper-sulfide and copper-iron-sulfide minerals that form stratabound to stratiform disseminations in sedimentary rocks (Cox and others, 2003; Hitzman and others, 2005; Zientek, Hayes, and Hammarstrom, 2013). Ore minerals, such as chalcocite and bornite, occur as cements and replacements in the matrix of sedimentary rocks and, less commonly, as veinlets. The concentration of sulfide minerals is broadly conformable with stratification in the host rocks. In more detail, deposits are characterized by systematic changes (zonation) in ore mineralogy along and across bedding from pyrite to chalcopyrite to bornite to chalcocite to hematite.

Subtypes of sediment-hosted stratabound copper deposits are distinguished by host lithology and the nature of organic material in the sedimentary rocks (Zientek, Hayes, and Hammarstrom, 2013; Zientek, Hayes, and Taylor, 2013). In some literature two types of sediment-hosted stratabound copper deposits are distinguished on the basis of the rocks hosting the deposits: (1) sandstones (Dzhezkazgan deposits of Bogdanov and others, 1973; continental red-bed deposits of Kirkham, 1989, and Kirkham and others, 1994; and red-bed deposits of Hitzman and others, 2005); and (2) shales and marls (copper shale deposits of Bogdanov and others, 1973; paralic marine deposits of Kirkham, 1989 and Kirkham and others, 1994; reduced-facies deposits of Cox and others, 2003; Kupferschiefer deposits of Hitzman and others, 2005; and reduced-facies [nonbrecciated] deposits, this study). The sandstone-hosted deposits have been divided still further into two additional types based on the nature of the organic material that localizes ore minerals in the rock: (1) patchy concentrations of plant remains (the Uralian deposits of Bogdanov and others, 1973; red-bed deposits of Lindsey and Cox, 2003); and (2) a diffusely distributed reductant, probably a mobile hydrocarbon (Revett deposits of Cox and others, 2003; sandstone copper, this study).

Two deposit subtypes were considered for this assessment: reduced facies [nonbrecciated] (shortened to reduced facies for this report) and sandstone (Zientek, Hayes, and Hammarstrom, 2013). Host rocks for the reduced-facies subtype include black shale, dark gray to black siltstone, dark gray dolosiltstone, gray shale, and locally green shale or siltstone, all of which contain varying amounts of solid organic material. Well-sorted sandstones from a variety of deltaic topset depositional environments are the host rocks for sandstone-type copper deposits. Petroleum-bearing fluid inclusions and solid amorphous hydrocarbons, which stain authigenic minerals and locally form meniscus cements, indicate that the mineralized strata once contained liquid or gaseous hydrocarbon accumulations. For other sandstone-copper deposits, the hydrocarbons could have been sour gas (natural gas containing substantial amounts of hydrogen sulfide) (Hayes and others, 2012). Lateral dimensions of deposits are large relative to deposit thickness, and deposit morphology varies by deposit type (Zientek, Hayes, and Hammarstrom,

2013). Reduced-facies deposits have sheet-like geometry with lateral dimensions hundreds to thousands of times greater than thicknesses. For example, strike lengths may be 3,000 to 5,000 meters (m) and widths from 500 to 2,000 m, whereas ore body thicknesses range from less than a meter to 50 m. Sandstone-copper deposits are tabular to lens-like; lateral dimensions are from 20 to 100 times their thicknesses. Vertically stacked or clustered sandstone ore bodies are a characteristic feature of large sandstone-type deposits like Udokan, Russia (Volodin and others, 1994), Dzhezkazgan, Kazakhstan (Box and others, 2013), and Rock Creek-Montanore, Montana (Balla, 2003).

Grade and tonnage models for subtypes of sediment-hosted stratabound copper were compiled by Zientek, Hayes, and Taylor (2013). Their data indicate that for reduced-facies-type deposits, median and mean values (1) for ore tonnage are 10 and 42 million metric tons and (2) for copper grades are 2.9 and 3.3 percent, respectively. The median and mean contained-copper values for reduced-facies-type deposits are 0.46 and 3.5 million metric tons, respectively. For sandstone-type deposits, median and mean values for (1) ore tonnage are 10 and 77 million metric tons and (2) copper grades are 1.2 and 1.4 percent, respectively. The median and mean contained-copper values for sandstone-type deposits are 0.12 and 1.0 million metric tons, respectively.

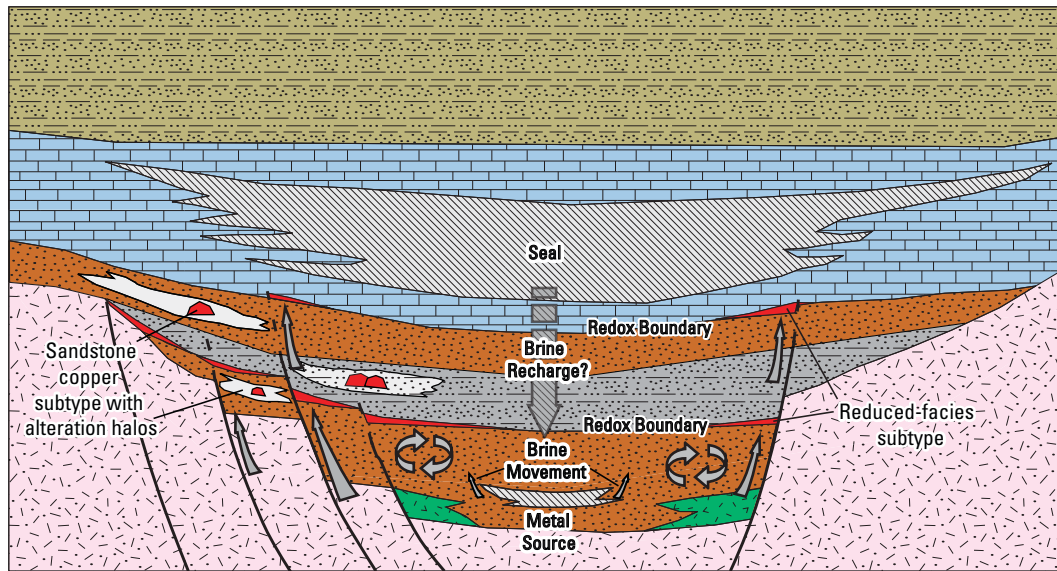
Deposits of the red-bed-copper type of Lindsey and Cox (2003) are interesting because the deposits indicate the presence of copper-bearing fluids in sedimentary basins, yet their contribution to global mineral endowment is negligible. These deposits are commonly found as mineral occurrences, but tonnage and grade have been formally reported for only a few sites. Only 3 of the 20 deposits in the model developed by Lindsey and Cox (2003) contain more than 50,000 metric tons contained copper (a “significant” copper deposit as defined by Singer, 1995). Therefore, red-bed-copper-type mineralization was not included in undiscovered copper that may be present.

## Mineral System for the Deposit Type











Sediment-hosted stratabound copper deposits are associated with evaporite minerals and continental red beds that formed in an arid climate. The host rock sedimentary depositional environments include aeolian dunes, sabkhas, playas, and sand sheets, together with minor alluvial fans, ephemeral rivers, and inland lakes (Davidson, 1965; Rose, 1976; Kirkham, 1989). Red beds and evaporite minerals typically form within 20 to 30 degrees of the equator in continental areas, (Kirkham, 1989) and red beds associated with stratabound sediment-hosted copper deposits are found in rift, transtensional, and intermontane basins. In this study, red beds were also found as molasse deposits in back-arc basins and foredeeps.

Sediment-hosted stratabound copper deposits formed from late diagenetic fluids generated during the compaction and lithification of sedimentary basins containing successions





## EXPLANATION

	Sediment-hosted stratabound copper deposits		Continental red beds
	Shallow-marine to continental sandstone, siltstone, and shale		Bimodal volcanic rocks
	Evaporite minerals		Basement rocks
	Marine carbonate rocks		Metal-bearing brine
	Marine sandstone, siltstone, and shale		Fault

**Figure 1-2.** Schematic section of a sedimentary basin showing the mineral system components required to form sediment-hosted copper deposits. Modified from Hitzman and others (2010).

of red beds and evaporite minerals (fig. 1-2). The metal-bearing fluids are thought to have been low temperature, hematite-stable (oxidized), sulfate- and chloride-rich, and subsurface sedimentary brines. The primary causes of base-metal sulfide precipitation are reduction of sulfate in the metal-bearing brine by organic material or mixing of the metal-bearing brine with hydrogen sulfide-bearing natural gas (Hitzman and others, 2005; Hayes and others, 2012).

Theories of regional ore genesis can be translated into criteria that are used in mineral resource assessment and exploration targeting studies using the concept of a mineral system (Wyborn and others, 1994; Knox-Robinson and Wyborn, 1997; Cox and others, 2003; Hronsky, 2004; Hitzman and others, 2005; Barnicoat, 2006; Hronsky and Groves, 2008; Blewett and others, 2010). For example, hydrothermal ore deposits can be understood by considering the source and physical and chemical character of the ore-forming fluid, the mechanisms for dissolving and transporting ore-forming components, and the causes of precipitation (Skinner and Barton, 1973). Locations with appropriate combinations of structural, chemical, and physical conditions that prompt ore-mineral-precipitation reactions are called ore traps (Reed, 1997). Variations of the source-transport-trap paradigm are used to define both petroleum and hydrothermal mineral systems models (Magoon and Dow, 1994; Wyborn and others, 1994; Magoon and Schmoker, 2000).

The formation of sediment-hosted stratabound copper deposits requires a source of metals, a fluid that extracts and moves metals away from the source rocks, a pathway that allows the movement of these ore-bearing fluids, and a physical and redox chemical trap that fixes metals in an ore body (Taylor, 2000; Hitzman and others, 2005; Hayes and others, 2015). The timing of the processes that control fluid generation, migration, and reaction to precipitate ore is critical; if a single element or process is missing or occurs out of order, the copper deposits cannot form (Magoon and Dow, 1994; Kreuzer and others, 2008; McCuaig and others, 2010).

Essential mineral system components for assessing sediment-hosted stratabound copper deposits include (1) permeable red-bed rocks juxtaposed against strata that contain reductants (typically organic material and early diagenetic pyrite, or for sandstone-hosted deposits, natural gas or petroleum); (2) basin history that indicates that the rocks underwent burial diagenesis (at depths of 1 to 5 kilometers (km) and temperatures ranging from 70 to 220 degrees Celsius (°C)); and (3) subsurface aqueous fluids that are enriched in copper. The lithostratigraphic relations in the first component are used to delineate areas where reduced-facies-type or sandstone-type copper deposits could occur. The second component is necessary because sediment-hosted copper ore fluids will not develop unless the sediments undergo burial diagenesis. The third component is vital in that only oxidized brines can



carry substantial quantities of copper in solution. Rocks with the appropriate lithostratigraphic relations can undergo burial diagenesis without developing subsurface fluids enriched in copper. Thus, the presence of copper deposits and occurrences can be used as evidence for the presence of copper-bearing ore fluids.

## Data Collected

The areas were assessed by using information readily available in the public domain. Stratigraphic columns and cross sections were used to identify lithostratigraphic relations that are characteristic of permissive rock units. Geologic maps used to construct the permissive tracts ranged in scale from 1:50,000 to 1:2,500,000, but most did not have structural data such as strike and dip of the beds. Data on sediment-hosted stratabound copper deposits and occurrences and copper sites came from mineral occurrence databases, metallogenic maps, journal articles, and company reports. Mineral system components for each assessment area are described in chapter 2 and summarized in table 1-1.

The deposit and mineral system models indicate that oil and gas well data, seismic data, facies maps, isopach maps, structure contour maps, basin burial curves, and petrogenetic studies of diagenetic and (or) alteration minerals would be useful for the assessment. This information, however, was not available for this study.

## Permissive Tract Delineation

For this assessment, geographic areas were defined where undiscovered mineral resources could be present. These areas, or “permissive tracts,” represent either the surface projection down to a specified depth or the areal extent of rocks where undiscovered mineral resources could be present. The criteria used to select the permissive volume of rock (herein referred to as assessment unit) are defined by the deposit type and its associated mineral system.

For sediment-hosted stratabound copper mineralization, lithostratigraphic relations and the presence of mineral deposits and occurrences are used to identify permissive geologic units. The permissive units project into the subsurface, forming a volume of rock that may contain sediment-hosted stratabound copper deposits if the necessary geologic, chemical, and tectonic processes took place. For areas where sufficient geologic data are available, permissive rock units are projected to a depth of about 2 km below the surface. For areas without sufficient geologic data, the permissive tract is defined using a buffered extent of the mapped geologic units.

The Belt-Purcell Basin and the Cambrian rocks of the Egypt–Israel–Jordan Rift permissive tracts were delineated to a projected subsurface depth of 2.4 and 2 km, respectively. The other eight tracts were delineated using the surface extent

of mapped permissive rock units (table 1-2). This method of delineation was performed using a multistep tool (prototract tool) created by the USGS using ArcGIS ModelBuilder. The tool incorporates standard tools available in the ArcGIS 10.1 Arc Toolbox. All parameter settings in the processes were empirically determined by delineation trials where computer-generated tracts were compared to manually generated tracts. The tool comprises four primary steps:

1. Combining all permissive units digitized from paper copies of geologic maps or ones sourced from digital geologic maps, as well as combining other polygon features that are necessary to the framework of the tract.
2. Aggregating the polygons that were located within 20 km of each other and filling in holes less than 2,000 square kilometers (km<sup>2</sup>).
3. Simplifying the aggregated polygons using a bend-simplify algorithm with a tolerance of 5 km.
4. Line smoothing the simplified polygons using a Bezier interpolation algorithm with a tolerance of 20 km.

After the tool was run, each tract was visually inspected, an additional smoothing or aggregation tool was run if needed, and in some cases minor manual edits were done to cover areas of permissive units that were missed by the tool. Permissive tracts for each study area as well as the locations of deposits and occurrences are shown in figures 1-3–1-12. Each permissive tract is assigned a unique identifier coded by United Nations region<sup>3</sup>, deposit type<sup>4</sup>, and a 4-digit identification number.

## Qualitative Assessment of the Areas

After data were compiled, two authors of this report, both economic geologists, qualitatively ranked the study areas according to the relative amount of undiscovered resource that may be present, where 1 represents the largest and 10 represents the smallest expected undiscovered copper resources (table 1-3). Their ranked lists are similar in that the same three areas are ranked high and the same three are ranked low. The process is useful because it is time efficient, as it relied on experience, intuition, and insight. To anyone else, however, the valuation process is opaque. Therefore, an expert-judgment-based method was sought to provide a similar outcome that would be more objective, transparent, reproducible, and defensible than the experience-driven-decision-making process used by the economic geologists.

The AHP was selected because it provides a consistent, quantifiable approach to problems involving a number of

<sup>3</sup>United Nation region codes: 002, Africa; 003, North America; 005, South America; 142, Asia (<http://unstats.un.org/unsd/methods/m49/m49regin.htm>).

<sup>4</sup>rfCu, reduced-facies copper; shCu, sediment-hosted copper, multiple subtypes; ssCu, sandstone copper.

**Table 1-1.** Mineral-system components present in each assessment area.

[km, kilometer; NA, not applicable]

Analytic hierarchy process rank	Assessment area	Deposit subtypes present	Extent of permissive tract (km <sup>2</sup> )	Basin type	Subaerial mafic volcanic rocks
1	Northwest Botswana Rift	Reduced-facies type; sandstone type	135,005	Tectonically inverted rift basin	Doornpoort, Eskadron, and Ngwako Pan Formation
2	Benguela and Cuanza Basins, Angola	Reduced-facies type; red-bed type	6,813	Rift basin related to opening of South Atlantic overlain by passive-margin sediments	Pre-Aptian tholeiitic basalt and basaltic andesite associated with the Central Atlantic Magmatic Province
3	Egypt-Israel-Jordan Rift	Reduced-facies type; sandstone type	31,649	Transensional basins related to the Najd Fault system, covered by passive-margin sedimentary rocks	Basaltic to andesitic rocks of the Ghuweir Mafics; basaltic trachyandesite, trachyandesite, trachyte/trachydacite and rhyolite of the Aheimir Volcanic Suite
4	Redstone Copper-belt, Canada	Reduced-facies type	8,923	Intracratonic basin (Mackenzie Mountains Supergroup), then rift and passive margin sedimentary associations (Windermere Supergroup)	Little Dal Basalt of Coates Lake Group; related to Gunbarrel magmatic event
5	Dongchuan Group, south central China	Reduced-facies type	8,747	An intracratonic rift, known as the Kunyang Aulacogen	The late Permian Emeishan large igneous province covers the western margin of the Yangtze structural unit and the Tibetan Plateau and underlies the Chuxiong Basin. Volcanic rocks with tuff and basalt in the Yinmin and Etouchang Formations in Central Yunnan; Yinmin Formation in Northern Yunnan, and the Limahe Formation in Southern Sichuan
6	Belt-Purcell Basin, USA	Sandstone type	1,633	Passive-type intracontinental rift or extensional domain along a collisional/convergent plate margin	Purcell Lava (basalt), near the base of the Missoula Group in Glacier National Park
7	Neuquén Basin, Argentina	Sandstone type	71,549	Isolated rift basins which formed in a strike-slip fault system, then extensional back-arc basin, then foreland basin	Volcanic rocks of the Lapa Formation; in Lower Jurassic rift basins, prior to development of back-arc basin
8	Maritimes Basin, Canada	Reduced-facies type; sandstone type; red-bed type	71,941	Extensional basins related to intracontinental transform zone lying between the east-west trending Hercynian belt of Europe and the northeast-southwest trending orogenic belt of the U.S. Appalachians	Continental flood basalt of the Diamond Brook Formation in the Fountain Lake Group
9	Chuxiong Basin, China	Sandstone type; red-bed type	19,847	Foredeep developed along the eastern margin of the Longmen Shan thrust belt and its southern extension	Emeishan flood basalts
10	Salta Rift System, Argentina	Reduced-facies type; sandstone type; red-bed type	27,384	Continental rift zones related to the opening of the Atlantic; followed by marine transgression and deposition of sedimentary rocks in back-arc basin	Isonza Basalt in the Alemania Subbasin; Las Conchas Basalt in the Alemania and Metan Subbasins; time-correlative with Paraná Volcanic Province magmatism but from different source regions and different processes

Table 1-1. Mineral-system components present in each assessment area.—Continued

Analytic hierarchy process rank	Red beds	Petroleum source	Evaporite-bearing rock units
1	Doornpoort and Eskadron Formations (Namibia); and Upper Kgwebe/Ngwako Pan Formations (Botswana)	NA	Sulfide minerals replace former evaporite minerals; however, substantial evaporites do not occur in either the footwall or hanging wall to the mineralized horizon
2	Lower Cuvo Formation	NA	The Upper Cuvo Formation includes thin beds of anhydrite, gypsum and other salts and finely bedded siltstones with plant and coal remains. Towards the center of the basin, the Upper Cuvo Formation passes laterally into and is overlain by a sequence of saline evaporitic cycles and calcareous units including the Loeme, Quianga, Binga, and Tuenza Formations
3	Salib (Jordan), Amudei Shelomo (Israel), and Serabit el-Khadim (Egypt) Formations	None known in the rift basins near copper-bearing rocks	None known in the rift basins near copper-bearing rocks
4	Shezal Formation of the Raptan Group; Redstone River Formation of Coates Lake Group; and Rusty Shale Formation of the Little Dal Group	NA	Thunder Cloud Formation of Coates Lake Group; Gypsum Formation of the Little Dal Group
5	Yinmin Formation in Yunnan	NA	Yinmin Formation breccias
6	Burke, Revett, and St. Regis Formations of the Ravalli Group; Snowslip, Shepard, Mount Shields, Bonnder, and McNamara (Libby) Formations of the Missoula Group	Gas observed in the Mesoproterozoic Prichard Formation	Missoula Group (contains casts and molds of halite, gypsum, and other evaporite minerals)
7	Tordillo Formation, Quebrada del Sapo Formation, Rayoso Group, and Neuquén Group	Los Molles, Vaca Muerta, and Agrio Formations (oil shale)	Tabanos, Auquilco, and Huitrin Formations
8	Horton, Mabou, Cumberland, and Pictou Groups	Horton Group (lacustrine oil shale) and Cumberland Group (coal beds) Lacustrine shales in the middle Horton Group (Type I-II organic matter) and coal deposits in the Cumberland and Pictou Groups (Type II-III organic matter). Coal seams are the most widespread source rocks (Dietrich and others, 2009)	Windsor Group (gypsum and anhydrite)
9	All Jurassic to Upper Cretaceous units in Yunnan and Sichuan	Coal beds in Upper Triassic Baoding, Daqiaodi, and Bingnan Formations in Yunnan; and Baiguowan Formation in Sichuan	Jiangdihe Formation in Yunnan and Xiaoba Formation in Sichuan (evaporite beds are interbedded with the red beds)
10	Pirgua Subgroup, including the La Yesera, Las Curtiembres, and Los Blanquitos Formations (Argentina); lower part of the Purilactis Group (Chile)	In Argentina, Olmedo/Tunal Formation (black shale) and Yacoraite Formation (marl and limestone)	Yacoraite Formation (gypsum and anhydrite)

Table 1-1. Mineral-system components present in each assessment area.—Continued

Analytic hierarchy process rank	Reservoir units with sandstone copper mineralization	Stratigraphic redox boundary with copper mineralization	Fluid movement driver
1	NA	Marine carbonaceous units of the Klein Aub and D'Kar Formations overlie continental clastic rocks of the Doornpoort and Upper Kgwabe/Ngwako Pan Formations	Damara Orogen
2	NA	Marine carbonaceous strata of the Upper Cuvo Formation overlies the continental clastic Lower Cuvo Formation	In-situ fluids were likely mobilized due to compaction by rapidly deposited overburden, and migrated to the basin margins through the Lower Cuvo Formation
3	NA	Marine carbonaceous strata of the Burj, Timna, and Middle Araba Formations overlie continental clastic Salib, Amudei Shelomo, and basal Middle Araba and Serabit el-Khadim Formations	Oxidizing metalliferous brines likely dewatered from near the Cambrian depocenters to the north and then flowed upsection
4	NA	Marine carbonaceous strata of the Coppercap Formation overlies continental clastic of Redstone River Formation	NA
5	NA	Marine carbonaceous strata of the Luoxue Formation overlies the continental clastic Yinmin Formation	Sediment overburden likely caused ascent of mineralizing fluids through preexisting faults
6	Revet/Creston Formations	NA	Copper and silver were deposited where oxidized metal-bearing basinal brines upwelled (possibly along faults) and subsequently mixed and reacted with trapped sour (hydrogen sulfide-bearing) natural gas
7	Challaco Formation, Tordillo Formation, Rayoso Group, and Neuquén Group	NA	Andean Orogeny
8	Pictou and Cumberland Groups	Marine carbonaceous Macumber Formation (basal Windsor Group) overlies continental clastic Horton Group	NA
9	Gaofengsi, Puchenghe, Matoushan, and Jiangdihe Formations in Yunnan and Lower Xiaoba Formation in Sichuan	NA	Himalayan Orogeny
10	NA	Marine strata of the Yacoraite Formation overlies continental clastic rocks of the Pirgua Subgroup	Andean Orogeny

**Table 1-2.** Geologic units and methods used for permissive tract delineation.

[M, million; km, kilometer; NA, not applicable]

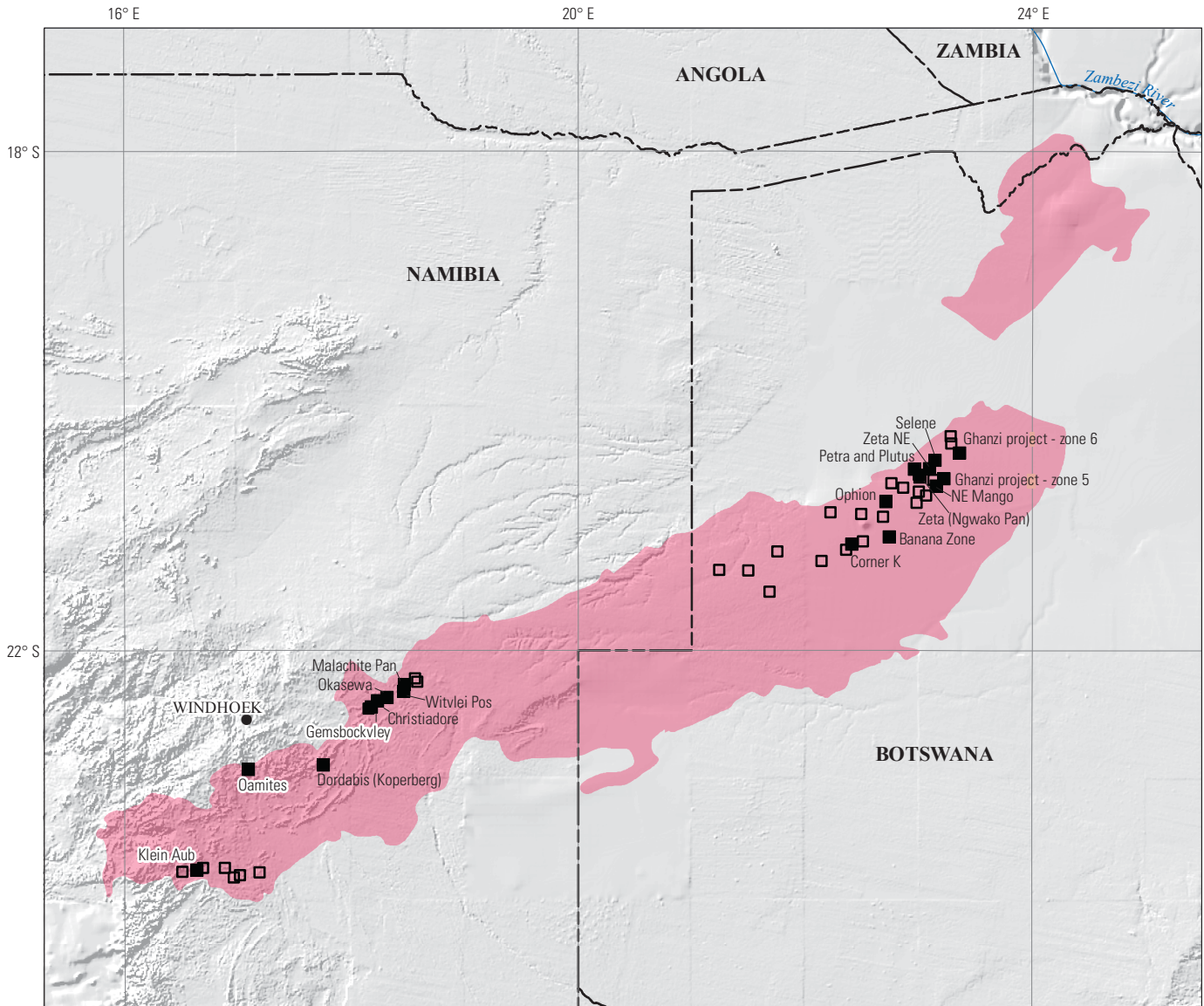
Tract	Permissive geologic units	Delineation method	Approximate depth
Northwest Botswana Rift	Ghanzi and Nosib Groups as shown on 1:1M geologic map of Namibia and the 1:2.5M sub-Kalahari map	Prototract tool	NA
Benguela and Cuanza Basins	Pre-Aptian, Aptian, and Albian-Aptian rocks (units K1 through K4) as shown on 1:1M map of Angola	Prototract tool	NA
Egypt–Israel–Jordan Rift	Facies transition between marine and near-shore facies of the Cambrian Nasib, Timna, and Burj Formations	Geologic analysis projected to depth of 2 km	Up to 2 km
Dongchuan Group rocks	Dongchuan Group Rocks as shown on 1:1M provincial geologic maps of China	Prototract tool	NA
Redstone Copperbelt	Rocks of the Twitya Formation, Rapitan, Coates Lake, and Little Dal Groups as shown on maps ranging from 1:50,000 to 1:250,000	Prototract tool	NA
Belt-Purcell Basin	Presence of indicative alteration minerals, and proximity to known stratabound copper-silver deposits or occurrences in the Revett Formation (on 1:250,000- or larger-scale maps)	Geologic analysis projected to depth of 2.4 km	Up to 2.4 km
Chuxiong Basin	Cretaceous Gaofengsi, Puchenghe, Matoushan, and Xiaoba Formations in south central China as shown on 1:1M provincial geologic maps of China	Prototract tool	NA
Neuquén Basin	Jurassic and Cretaceous sedimentary rocks of the Neuquén Basin as shown on 1:2.5M geologic maps	Prototract tool	NA
Maritimes Basin	Sedimentary rocks of the Carboniferous Windsor, Mabou, Cumberland, and Pictou Groups as shown on provincial Canadian maps ranging from 1:500,000 to 1:1M	Prototract tool	NA
Salta Rift System	Salta Group as shown on 1:2.5M geologic map	Prototract tool	NA

criteria or attributes (Coulter and others, 2006). In the geosciences, AHP has been used to weight spatial data in GIS models for assessing mineral resource potential (Hosseinali and Aleshiekh, 2008; Noori and others, 2011; Pazand and others, 2011) and landslide hazards (Komac, 2006; Yalcin, 2008; Moradi and others, 2012; Bhatt and others, 2013; Daneshvar, 2014).

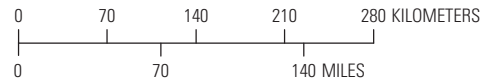
The AHP is a theory of measurement used to derive relative priorities on absolute scales from paired comparisons in multilevel hierarchic structures (Saaty, 1980; Malczewski, 1999; Coulter and others, 2006; Saaty and Vargas, 2010, 2012). The AHP involves (1) deconstructing the decision into a hierarchy of components that can be evaluated with pairwise comparisons, (2) creating sets of comparison matrices by evaluating the pairwise comparisons in the hierarchy, (3) calculating priorities from the comparison matrices for each element in the hierarchy, and (4) constructing a composite set of priorities for the alternatives being considered. In this study, the goal is to determine which of the 10 areas (the alternatives) have the greatest potential for undiscovered copper. Thus, this mineral resource assessment was deconstructed into a hierarchy (fig. 1-13) of pairwise comparisons that capture the necessary elements of the geologic environment (Saaty, 1980; Malczewski, 1999).

The top level of the hierarchy is ranking of tracts according to their potential for undiscovered sediment-hosted copper deposits, which is the goal of the decision making process (fig. 1-13). The hierarchy then descends through specific criteria, until a set of alternatives is reached. In this study, the alternatives are the 10 permissive areas. The criteria within the hierarchical structure are evaluated using pairwise comparisons, which reduce the conceptual complexity of decision making because only two components are considered at any given time. Paired comparisons can be made by (1) rating items relative to each other in a qualitative evaluation or (2) using numerical scales (Meyer and Brooker, 2001). The result is a set of pairwise comparison matrices. For each pairwise comparison matrix, the eigenvalue is used to obtain a priority weight vector (Saaty, 1980). In addition to the eigenvalue and the eigenvector, consistency tests are also computed (Saaty, 1990). A sequence of multiplications of the matrices of relative weights at each level of the hierarchy of criteria is used to calculate overall scores for each alternative (called alternative utility in this report). Alternatives can be ranked by their importance in contributing to the goal of the analysis by simply sorting alternatives on the basis of their overall score. The alternatives with higher scores receive a higher overall





Political boundaries from U.S. Department of State (2009).  
 Shaded relief from Earth Resources Observation and Science (EROS) Center (2001).  
 Africa Albers Equal-Area Conic Projection.  
 Central meridian, 20° E., latitude of origin, 0°.



**EXPLANATION**

- Assessed sediment-hosted copper tract 002rfCu2002
- Sediment-hosted copper deposit
- Sediment-hosted copper occurrence

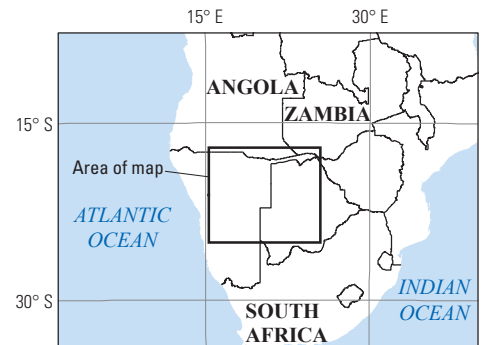


**Figure 1-3.** Map showing the sediment-hosted copper permissive tract, deposits, and occurrences of the Northwest Botswana Rift, Botswana and Namibia (002rfCu2002).

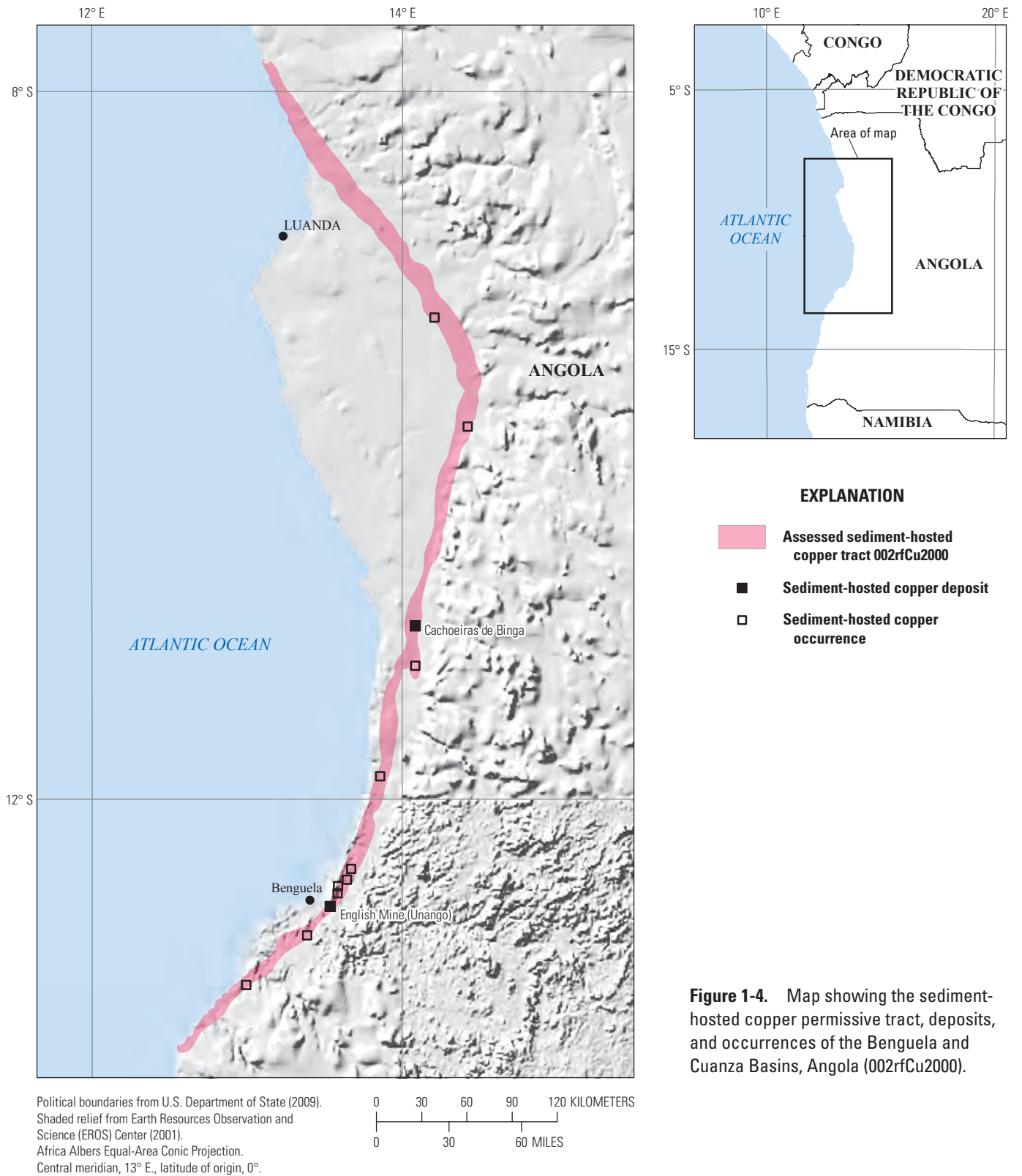
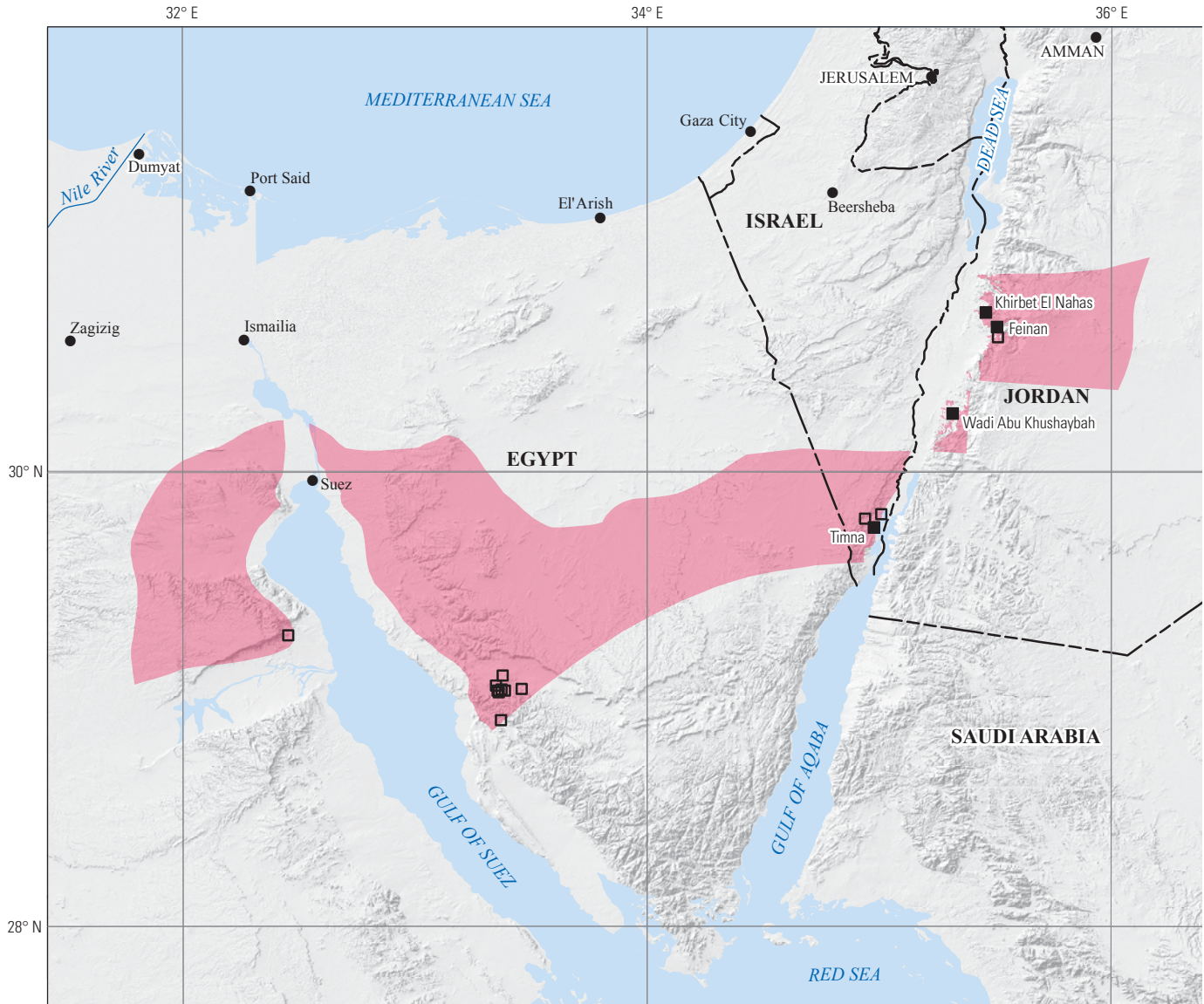
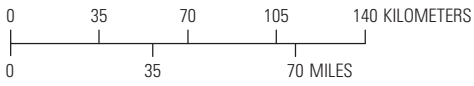


**Figure 1-4.** Map showing the sediment-hosted copper permissive tract, deposits, and occurrences of the Benguela and Cuanza Basins, Angola (002rfCu2000).





Political boundaries from U.S. Department of State (2009).  
 Shaded relief from Esri (2008).  
 Lambert Azimuthal Equal-Area Conic Projection.  
 Central meridian, 34° E., latitude of origin, 0°.



- EXPLANATION**
- Assessed sediment-hosted copper tract 002rfCu2001
  - Sediment-hosted copper deposit
  - Sediment-hosted copper occurrence

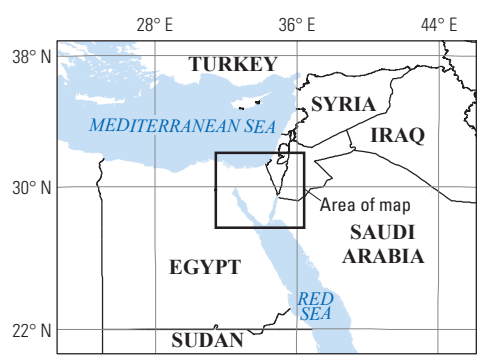


**Figure 1-5.** Map showing the sediment-hosted copper permissive tract, deposits, and occurrences of the Egypt–Israel–Jordan Rift, Egypt, Israel, and Jordan (002rfCu2001).



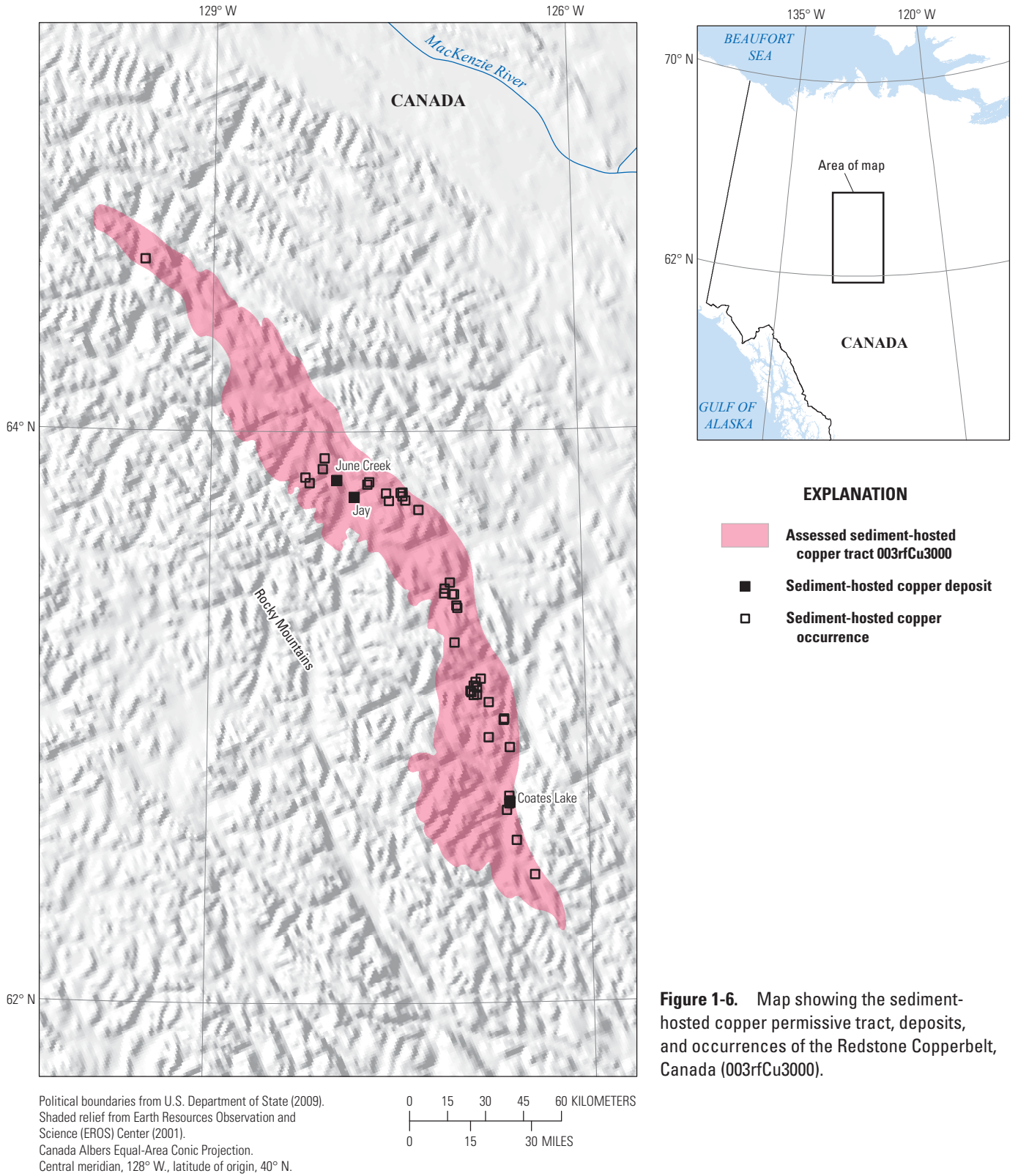


**Figure 1-6.** Map showing the sediment-hosted copper permissive tract, deposits, and occurrences of the Redstone Copperbelt, Canada (003rfCu3000).

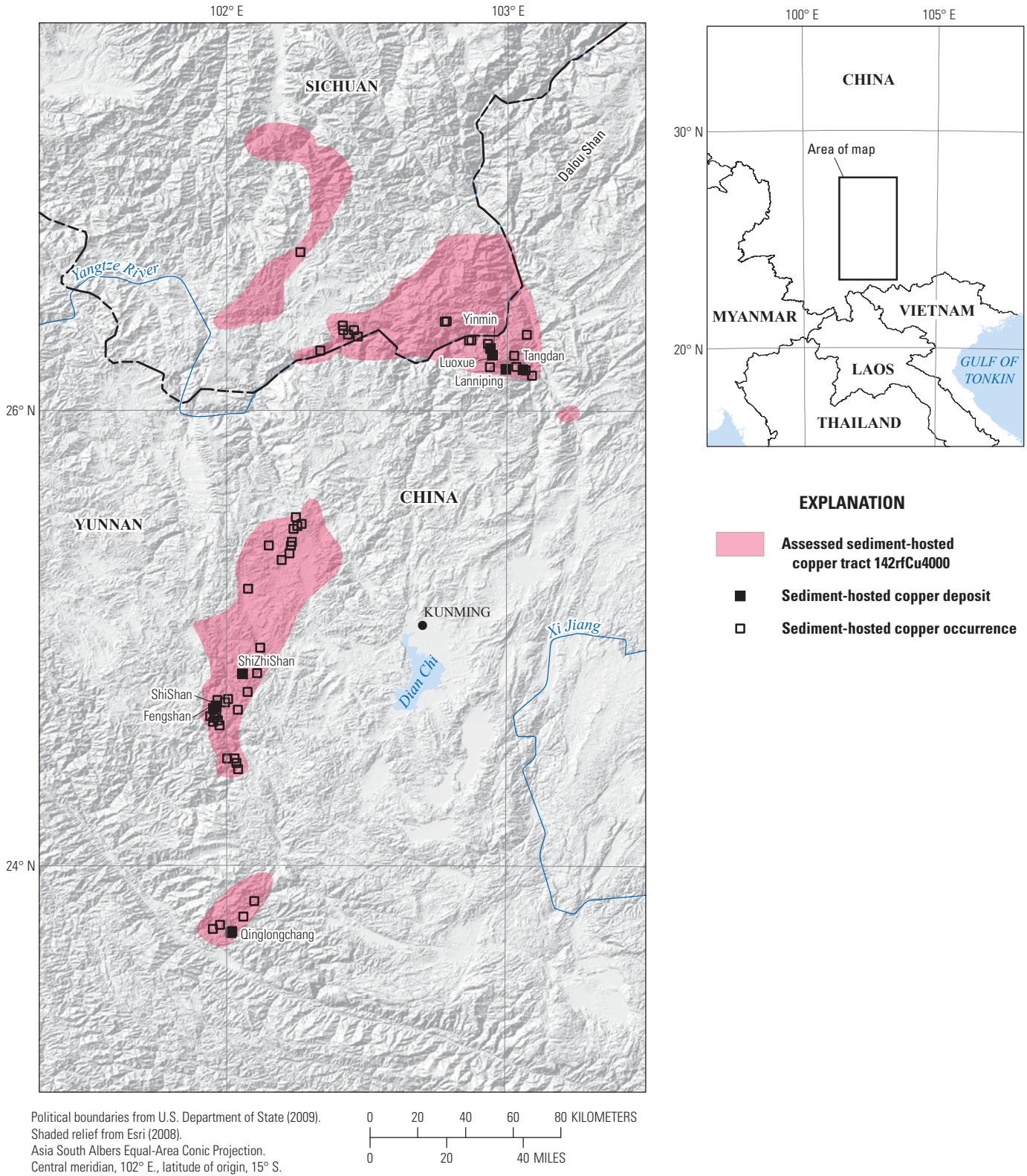


**Figure 1-7.** Map showing the sediment-hosted copper permissive tract, deposits, and occurrences of the Dongchuan Group Rocks, south central China (142rfCu4000).



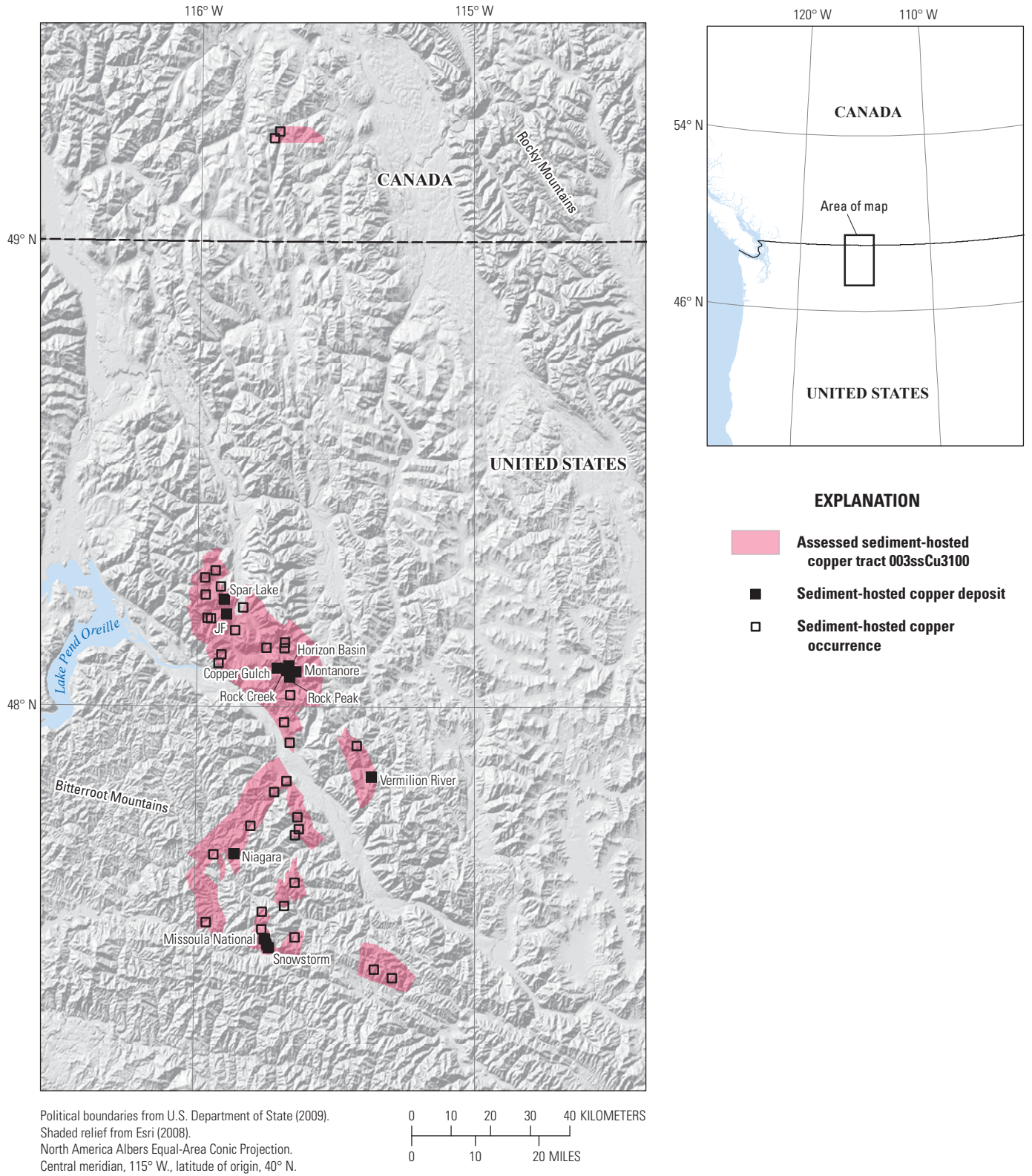


**Figure 1-8.** Map showing the sediment-hosted copper permissive tract, deposits, and occurrences of the Belt-Purcell Basin, United States and Canada (003ssCu3100).



18 Qualitative Assessment of Selected Areas of the World for Undiscovered Sediment-Hosted Stratabound Copper Deposits

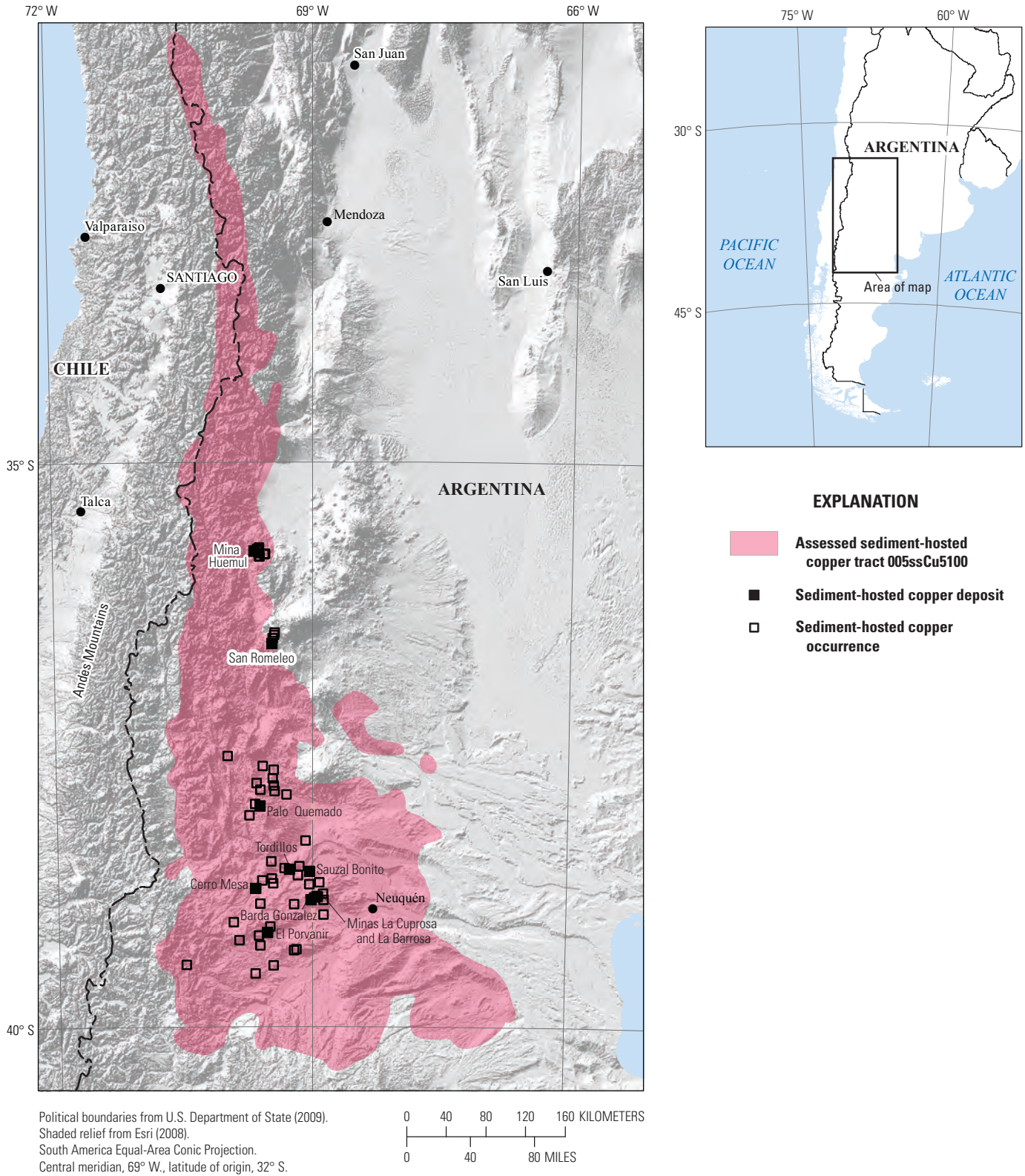
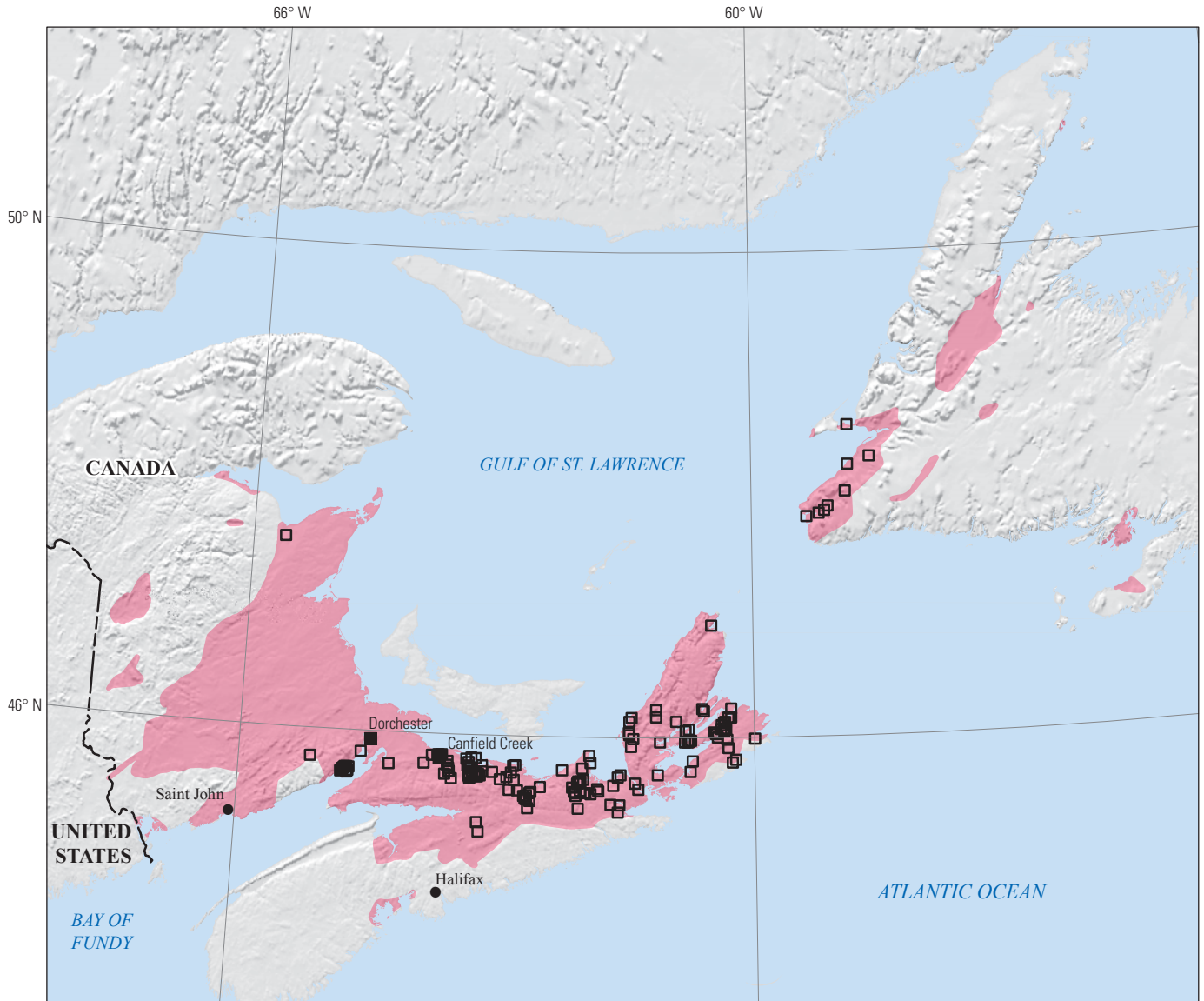
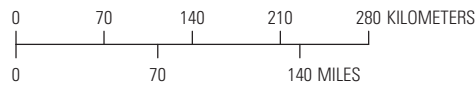


**Figure 1-9.** Map showing the sediment-hosted copper permissive tract, deposits, and occurrences of the Neuquén Basin, Argentina (005ssCu5100).



Political boundaries from U.S. Department of State (2009).  
 Shaded relief from Earth Resources Observation and Science (EROS) Center (2001).  
 Canada Albers Equal-Area Conic Projection,  
 Central meridian, 61° W., latitude of origin, 40° N.

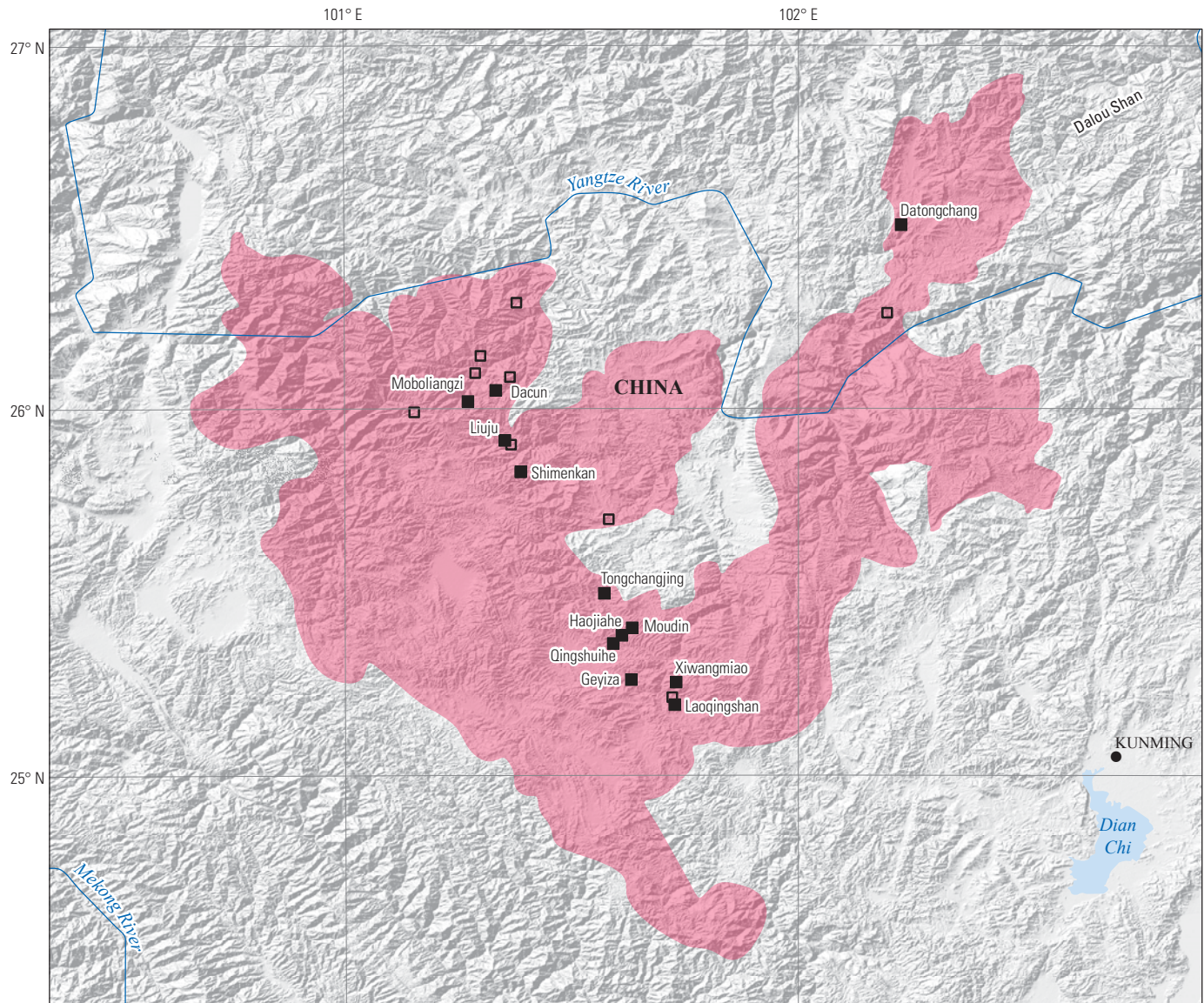


- EXPLANATION**
- Assessed sediment-hosted copper tract 003shCu1000
  - Sediment-hosted copper deposit
  - Sediment-hosted copper occurrence

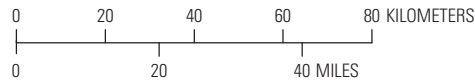


**Figure 1-10.** Map showing the sediment-hosted copper permissive tract, deposits, and occurrences of the Maritimes Basin, Canada (003shCu1000).





Political boundaries from U.S. Department of State (2009).  
 Shaded relief from Esri (2008).  
 Asia South Albers Equal-Area Conic Projection.  
 Central meridian, 102° E., latitude of origin, 15° S.



- EXPLANATION**
- Assessed sediment-hosted copper tract 142ssCu6000
  - Sediment-hosted copper deposit
  - Sediment-hosted copper occurrence

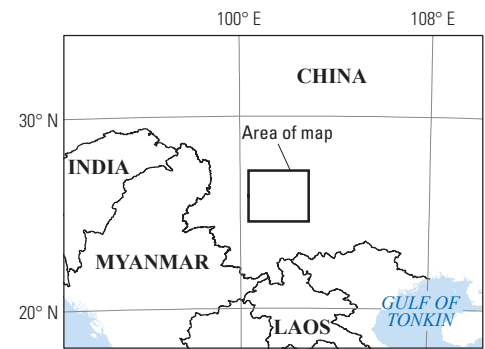


**Figure 1-11.** Map showing the sediment-hosted copper permissive tract, deposits, and occurrences of the Chuxiong Basin, China (142ssCu6000).



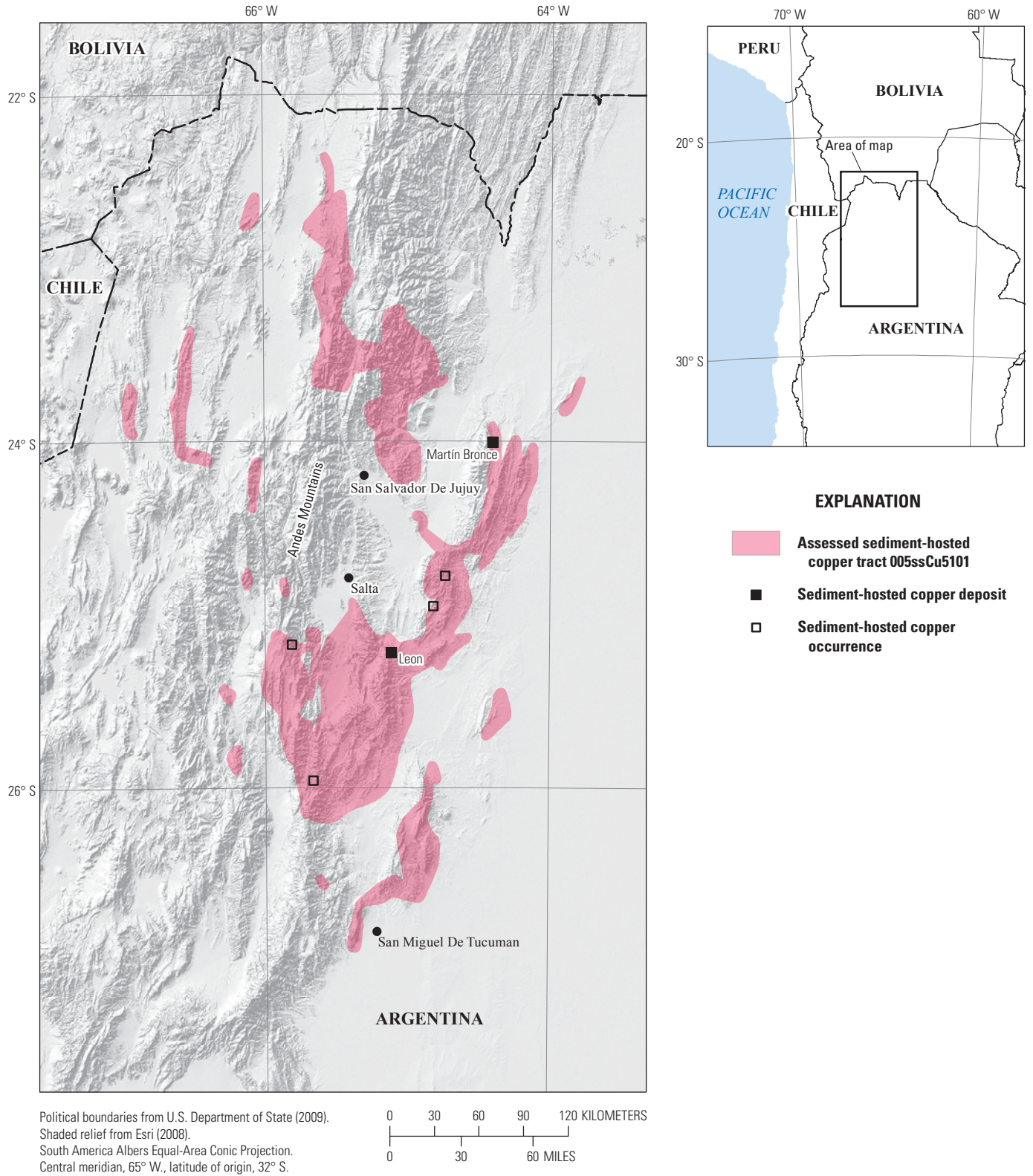


**Figure 1-12.** Map showing the sediment-hosted copper permissive tract, deposits, and occurrences of the Salta Rift System, Argentina (005ssCu5101).

**Table 1-3.** Ranked lists of the assessment areas showing results based on expert opinion and group analytic hierarchy process analysis. The highest ranked assessment areas are considered to have the highest potential for the largest amount of resources in undiscovered sediment-hosted stratabound copper deposits.

[AHP, analytic hierarchy process]

Rank	Economic geologist 1	Economic geologist 2	Group AHP
1	Northwest Botswana Rift	Northwest Botswana Rift	Northwest Botswana Rift
2	Benguela and Cuanza Basins	Egypt-Israel-Jordan Rift	Benguela and Cuanza Basins
3	Egypt-Israel-Jordan Rift	Benguela and Cuanza Basins	Egypt-Israel-Jordan Rift
4	Chuxiong Basin	Redstone Copperbelt	Redstone Copperbelt
5	Dongchuan Group rocks of China	Dongchuan Group rocks of China	Dongchuan Group rocks of China
6	Belt-Purcell Basin	Chuxiong Basin	Belt-Purcell Basin
7	Redstone Copperbelt	Belt-Purcell Basin	Neuquén Basin
8	Maritimes Basin	Maritimes Basin	Maritimes Basin
9	Neuquén Basin	Neuquén Basin	Chuxiong Basin
10	Salta Rift System	Salta Rift System	Salta Rift System

ranking. For a detailed guide on AHP, see the tutorial by Hass and Meixner (2006).

For this study, the goal (the top level of the hierarchy) is a qualitative assessment of the amount of undiscovered copper that may be present in each of the 10 prospective basins (fig. 1-13). The alternatives (the bottom of the hierarchy) are the 10 study areas. Three criteria are used at the second level of the hierarchy: (1) the extent of the study areas, (2) the lithostratigraphic framework, and (3) the evidence for fluids capable of forming sediment-hosted stratabound copper deposits (mineralization). In general, larger permissive tracts may have more undiscovered copper, all other variables being equal. However, the map resolution and the depth that could be assessed varied between the tracts, so extra elements are included to the hierarchy under the “size criterion” to account for these differences. The lithostratigraphic criterion considers features that can be observed on geologic maps and stratigraphic columns that indicate that geologic units permissive for sediment-hosted stratabound copper mineralization are present. Lithostratigraphic criteria are used to evaluate the mineral system components that can be observed on the stratigraphic columns. Examples include the presence of basaltic rocks that could be a source of copper for the ore fluids or the presence of salt layers that could form impermeable seals in the section. The “mineralization” criterion evaluates evidence suggestive of a copper-bearing ore fluid in the basin. The criteria used to evaluate the mineralization element include the deposit subtypes that are present, the degree (completeness) of exploration, and the size and number of known deposits, occurrences, and mineralized sites. For this report, deposits are defined as sediment-hosted stratabound copper localities with identified resources that have a defined tonnage and copper grade, occurrences are sediment-hosted stratabound copper localities with no known tonnage or grade, and sites are copper localities with an unknown deposit type and development status. The pairwise-comparisons used to evaluate the individual elements of the hierarchy are summarized in appendix B (AHP Input.

xlsx). The most important outcome is a chart that compares alternative utility scores for the study areas.

## Results

The AHP analysis ranks the Northwest Botswana Rift, the Benguela and Cuanza Basins, and the Egypt–Israel–Jordan Rift at the top of the list with the Maritimes Basin, Chuxiong Basin, and the Salta Rift System at the bottom (fig. 1-14). This outcome is consistent with the expert rankings done by the economic geologists (table 1-3) with the same three assessment areas ranked the highest. Thus, the Northwest Botswana Rift, the Benguela and Cuanza Basins, and the Egypt–Israel–Jordan Rift assessment areas have the highest potential for undiscovered copper in sediment-hosted stratabound copper deposits and are candidates for more in-depth research, analysis, and evaluation.

This study also shows that qualitative rankings of study areas using expert opinion and the AHP yield similar results, particularly for study areas that are likely to contain high amounts of undiscovered copper. The evaluation process using expert opinion is quick but lacks transparency. The benefit of the AHP approach is that the evaluation process is explicit and quantified. The process also appears to be robust, and the type of information required to make the decisions is straightforward. As part of this study, a simple hierarchy was developed in which the criteria were independent and what the criteria were measuring or comparing was clear.

Several areas not included in this study may have sufficient information to conduct a similar qualitative evaluation of the potential for undiscovered sediment-hosted stratabound copper deposits. Examples include areas in Australia (the Adelaide Geosyncline; Rowlands, 1974; Tonkin and Creelman, 1990), Canada (the Seal Lake Group; Gandhi and Brown, 1975), the United States (the Paradox Basin; Thorson, 2005), and Zimbabwe (the Deweras Group; Master, 1996).



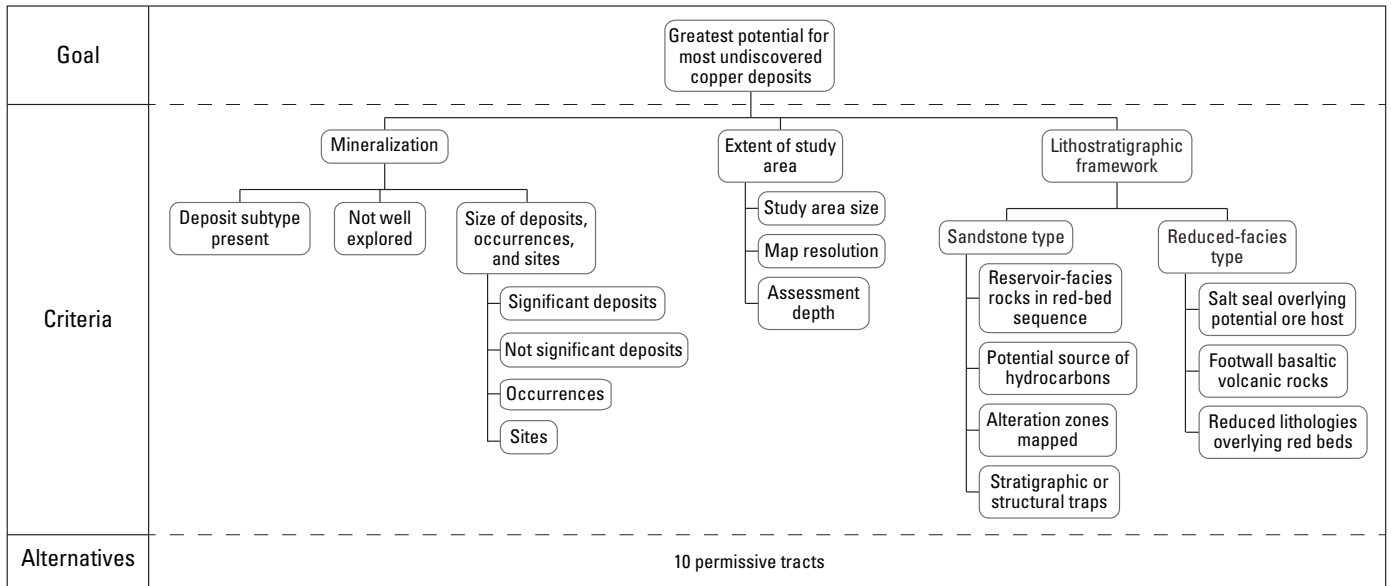


Figure 1-13. Chart showing criteria hierarchy used for the analytic hierarchy process analysis for 10 assessment areas that could contain undiscovered sediment-hosted stratabound copper deposits.

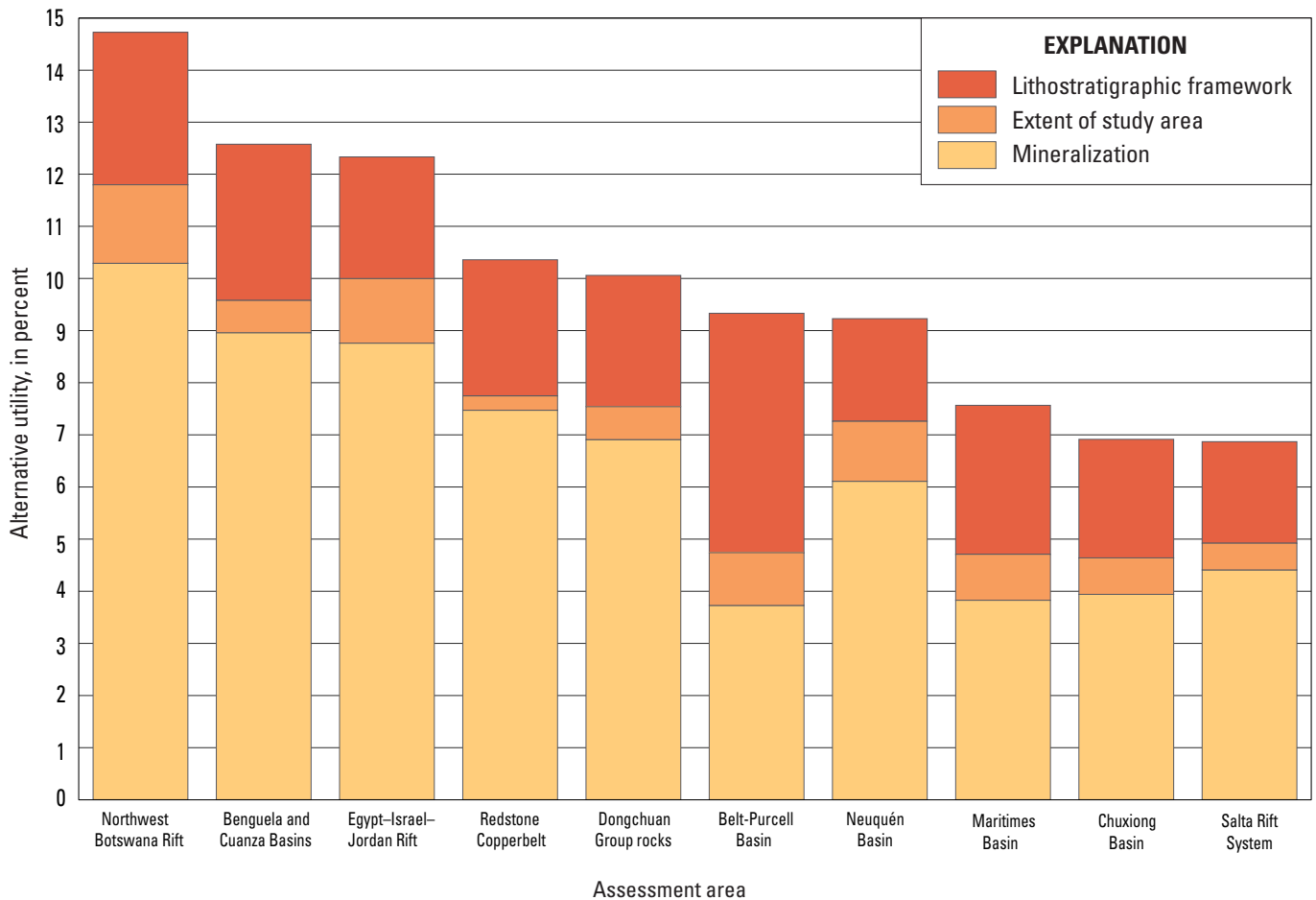


Figure 1-14. Stacked bar graph showing group analytic hierarchy process scores in order of decreasing potential of undiscovered copper for the 10 assessment areas. Each bar is segmented into the three main criteria used in the AHP analysis.

This page left intentionally blank.

## Chapter 2. Tectonics, Stratigraphy, and Economic Geology of Qualitatively Assessed Tracts

By Niki E. Wintzer<sup>1</sup>, Timothy S. Hayes<sup>2</sup>, Heather L. Parks<sup>1</sup>, Michael L. Zientek<sup>1</sup>, Deborah A. Briggs<sup>1</sup>, J. Douglas Causey<sup>1</sup>, Shyla A. Hatch<sup>3</sup>, M. Christopher Jenkins<sup>3</sup>, and David J. Williams<sup>3</sup>

### Introduction

This chapter summarizes information used to rank copper-permissive areas in 10 sedimentary basins that were selected for qualitative assessment as part of the U.S. Geological Survey (USGS) global mineral resource assessment. The areas assessed include the Northwest Botswana Rift (NWBR) (which includes the Kalahari Copperbelt), Namibia and Botswana; the Benguela and Cuanza Basins, Angola; a basin with Cambrian rocks in Egypt, Israel, and Jordan; Neoproterozoic rocks that host the Redstone Copperbelt, Canada; the basin that includes the Dongchuan Group rocks, China; the Belt-Purcell Basin, United States and Canada; the Neuquén Basin, Argentina; the Maritimes Basin, Canada; the Chuxiong Basin, China; and the Salta Rift System, Argentina (fig. 1-1). Areas are listed in order of descending likelihood to contain undiscovered copper deposits.

For decades, two competing concepts about the origin of sediment-hosted stratabound copper deposits have been discussed in scientific literature: (1) syngensis, in which the mineralization developed simultaneously with the deposition of the sediments, and (2) diagenesis, in which the mineralization formed later than the deposition of the sediments, from processes occurring at low temperatures and pressures during compaction and lithification. The diagenetic model of ore formation is now widely accepted. Essential mineral system components for diagenetic sediment-hosted stratabound copper deposits are (1) permeable red-bed rocks juxtaposed against strata that contain reductants (typically organic material and diagenetic pyrite, or, for sandstone-hosted deposits, natural gas or petroleum), (2) basin history that indicates that the rocks underwent burial diagenesis (depths of 1 to 5 km at temperatures ranging from 70 to 220 °C), and (3) subsurface aqueous fluids that are enriched in copper. All three components were used to create a template for the information that was compiled for the qualitative assessment.

Tectonic setting and stratigraphy are compiled for each area to explain basin history and stratigraphic relations. Each section includes one or more maps, stratigraphic columns, and cross sections to illustrate these relations. Known deposits

and occurrences are used to indicate fluid pathways and traps. Mineral system components are discussed for each basin as well as a brief statement on the quality of information that was available. Herein, deposits are defined as sediment-hosted stratabound copper localities with identified resources that have a defined tonnage and copper grade, occurrences are sediment-hosted stratabound copper localities with no known tonnage or grade, and sites are copper localities with an unknown deposit type and development status.

### Northwest Botswana Rift, Botswana and Namibia—Assessment Tract 002rfCu2002

Sedimentary rocks of the Neoproterozoic Ghanzi and Nosib Groups in Botswana and Namibia host reduced-facies and sandstone-copper subtypes of sediment-hosted stratabound copper deposits. These rock units extend about 1,070 km along strike and are part of the NWBR. The NWBR hosts 18 deposits, 27 occurrences, and 38 sites (fig. 1-3). Informally, the area containing these deposits, occurrences, and sites is known as the “Kalahari Copperbelt.”

### Tectonic Setting

A northeast-trending, tectonically inverted Mesoproterozoic and Neoproterozoic rift basin extends from central Namibia to northern Botswana (fig. 2-1). The rift is known by several names, including the Koras-Sinclair-Ghanzi Rift (Borg, 1988), the Ghanzi-Chobe Belt (Modie, 1996), and the NWBR (Key and Mapeo, 1999). The NWBR initially developed on the northern margin of the Kalahari Craton during the Mesoproterozoic Era (fig. 2-2); the age of the basal felsic volcanic rocks associated with initial rifting is  $1,106 \pm 2$  Ma (million years before the present; Schwartz and others, 1995). As much as 7.5 km of volcanic and sedimentary material was deposited in the rift from the late Mesoproterozoic to the early Neoproterozoic (Martin and Porada, 1977; Modie, 1996; Thomas and Jacobs, 1998; Key and Ayres, 2000; Singletary and others, 2003; Frimmel and others, 2011). To the northwest, the NWBR is faulted against deformed rocks associated

<sup>1</sup>U.S. Geological Survey, Spokane, Washington, United States.

<sup>2</sup>U.S. Geological Survey, Tucson, Arizona, United States.

<sup>3</sup>Eastern Washington University, Cheney, Washington, United States.

with the Damara Belt (fig. 2-3; Modie, 1996; Key and Mapeo, 1999; Key and Ayres, 2000). High-angle normal faults, part of the Kalahari Suture Zone, bound the rift to the southeast (fig. 2-3; Key and Mapeo, 1999). Deformation during the late Neoproterozoic, possibly associated with the Damara Orogeny (Modie, 1996), produced isoclinal to tight folds in the volcanic and sedimentary rift-fill rocks (fig. 2-3; Singletary and others, 2003). Kalahari sands, about 30 m thick, cover most of the NWBR (Haddon, 1999).

## Stratigraphy

Mesoproterozoic bimodal volcanic rocks form the base of the stratigraphic sequence of the NWBR. The volcanic rocks are unconformably overlain by continental red beds, which in turn are overlain by Neoproterozoic marine sedimentary rocks (fig. 2-4). The Mesoproterozoic bimodal volcanic rocks are known as the Kgwebe Formation in Botswana and the Nückopf and Grauwater Formations in the Klein Aub area in Namibia (fig. 2-4; Borg and Maiden, 1987). In Botswana, the volcanic rocks consist of porphyritic rhyolites and subalkaline basalts, with minor pyroclastic flow deposits, peperites, and subaerial basaltic lavas intercalated with localized epiclastic and tuffaceous sediments (Kampunzu and others, 1998). In Namibia, conglomerate and arkose are a minor component of the Nückopf Formation but make up almost 50 percent of the Grauwater Formation. On the basis of U-Pb dates from zircons, the age of the porphyritic rhyolites is 1,106 Ma (Schwartz and others, 1995).

The overlying Neoproterozoic red beds are named the Ngwako Pan Formation in Botswana and the Doornpoort Formation in the Klein Aub area of Namibia (fig. 2-4; Borg and Maiden, 1987; Modie, 2000; Pretorius and Park, 2011). In Botswana, these formations are composed of muddy sandstone characterized by parallel lamination with sporadic crossbedding and minor pebbly and granule-rich layers. The sandstone and mudstone rocks of this unit contain finely disseminated hematite that imparts a pink to maroon color to the rocks. Mafic volcanic rocks are intercalated with the red beds (Kampunzu and others, 2009).

The overlying Neoproterozoic marine rocks are referred to as the D'Kar Formation of the Ghanzi Group in Botswana, and the Klein Aub Formation of the Nosib Group in Namibia (fig. 2-4). The D'Kar Formation is parallel-laminated gray-green siltstone and mudstone with some interbedded fine-grained sandstone, some impure limestone beds with dark-and-white-banded rhythmites, and organic-rich shale (Modie, 2000; Pretorius and Park, 2011). This formation contains fine-to-coarse-grained pyrite. The D'Kar Formation is dated at  $810 \pm 10$  Ma on the basis of the correlation with the Bitter Springs  $\delta^{13}\text{C}$  event, which is interpreted to represent the end of the Snowball Earth event (Halverson and others, 2005). The Klein Aub Formation is made up of pyritic metasandstone, dark gray and black pyritic slate, detrital metacarbonate, and laminated shale (Borg and Maiden, 1987).

## Deposits and Occurrences

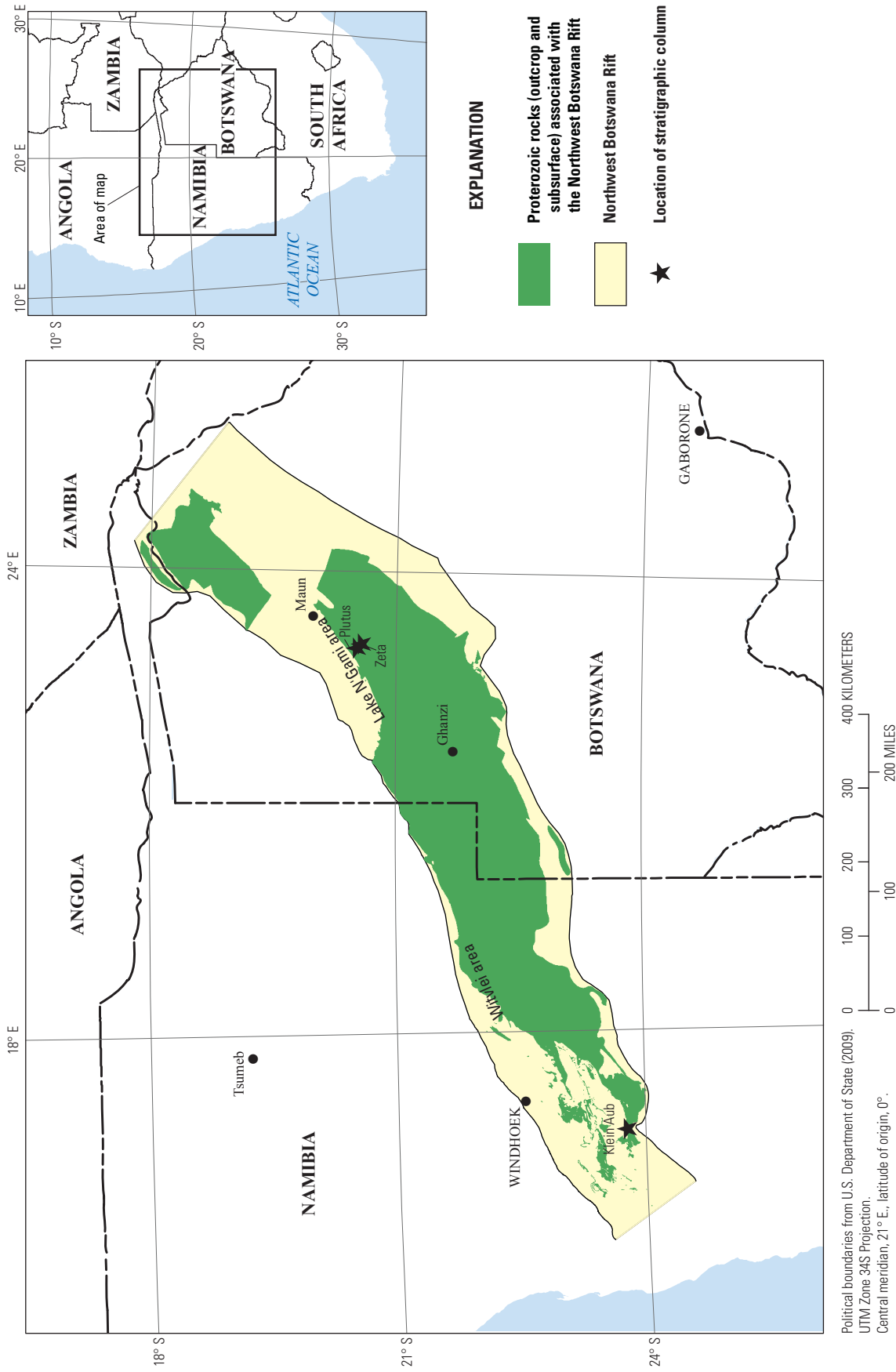
Eighteen deposits, 27 occurrences, and 38 sites have been identified within the NWBR (table 2-1; figs. 2-5 and 2-6). Both reduced-facies and sandstone-copper subtypes are present in this assessment area. Additional copper sites in sedimentary rock are shown in figures 2-5 and 2-6. Reduced-facies sediment-hosted stratabound deposits and occurrences are confined to the basal part of the gray-green, argillitic facies of the D'Kar Formation (Modie, 2000; Hall, 2013) and the Kagas member of the Klein Aub Formation (Borg and Maiden, 1987). Sandstone-copper subtypes are hosted in Doornpoort Formation red beds in Namibia.

Although the presence of copper ore within the NWBR was documented as early as 1855 (Mietzner, 2011), extensive Kalahari sands covering most of the rift limited exploration in the area. Beginning in the 1960s, airborne geophysical surveys, soil geochemical surveys, and drilling allowed exploration geologists to assess the geology and mineral potential of rocks under the Kalahari sands.

## Reduced-Facies-Type Deposits

The largest reduced-facies-type deposits are in the Lake N'Gami area in Botswana (fig. 2-1) in a belt of thick, laterally continuous, and folded rock units (figs. 2-6 and 2-7). The host rocks are dark, carbonate-bearing mudstone, siltstone, and very fine-grained sandstone (1 to 25 m thick) of the D'Kar Formation, which overlies the red beds of the Ngwako Pan Formation (more than 3,500 m thick; Modie, 2000). Low-grade copper (0.2 percent) concentrations at the base of the D'Kar Formation can be traced for hundreds of kilometers. Exploration along this trend delineated 10 deposits, including the Petra and Plutus, Zeta, and Zeta NE deposits, as well as the Nexus and Erebus copper occurrences (fig. 2-7). The rocks are isoclinally folded into southwest- and northeast-plunging, upright anticlines and synclines with wavelengths of 3 to 10 km. The mineralized area is more than 600 km long with a width of 30 km or greater (Modie, 2000). As of 2014, three companies hold license areas over permissive rocks in Botswana: Cupric Canyon Capital (a private equity company backed by Barclays Bank plc), Discovery Minerals Ltd. (a publicly traded company listed on the Botswana Stock Exchange and the Australian Securities Exchange), and MOD Resources Ltd. (a publicly traded company listed on the Australian Securities Exchange).






Johannesburg Consolidated Investments initiated exploration in the Lake N'Gami area (fig. 2-1), in 1962, but failed to find economic deposits. Between 1967 and 1970, a joint venture of Anglovaal, DeBeers, and Tsumeb Corporation conducted soil sampling and the first exploration drilling (Van Der Heever and Arengi, 2010) and discovered the Ngwako Pan deposit, subsequently renamed Zeta (fig. 2-6). Anglovaal and DeBeers left the joint venture, and U.S. Steel Corporation took over and was joined by Newmont Mining. The latter

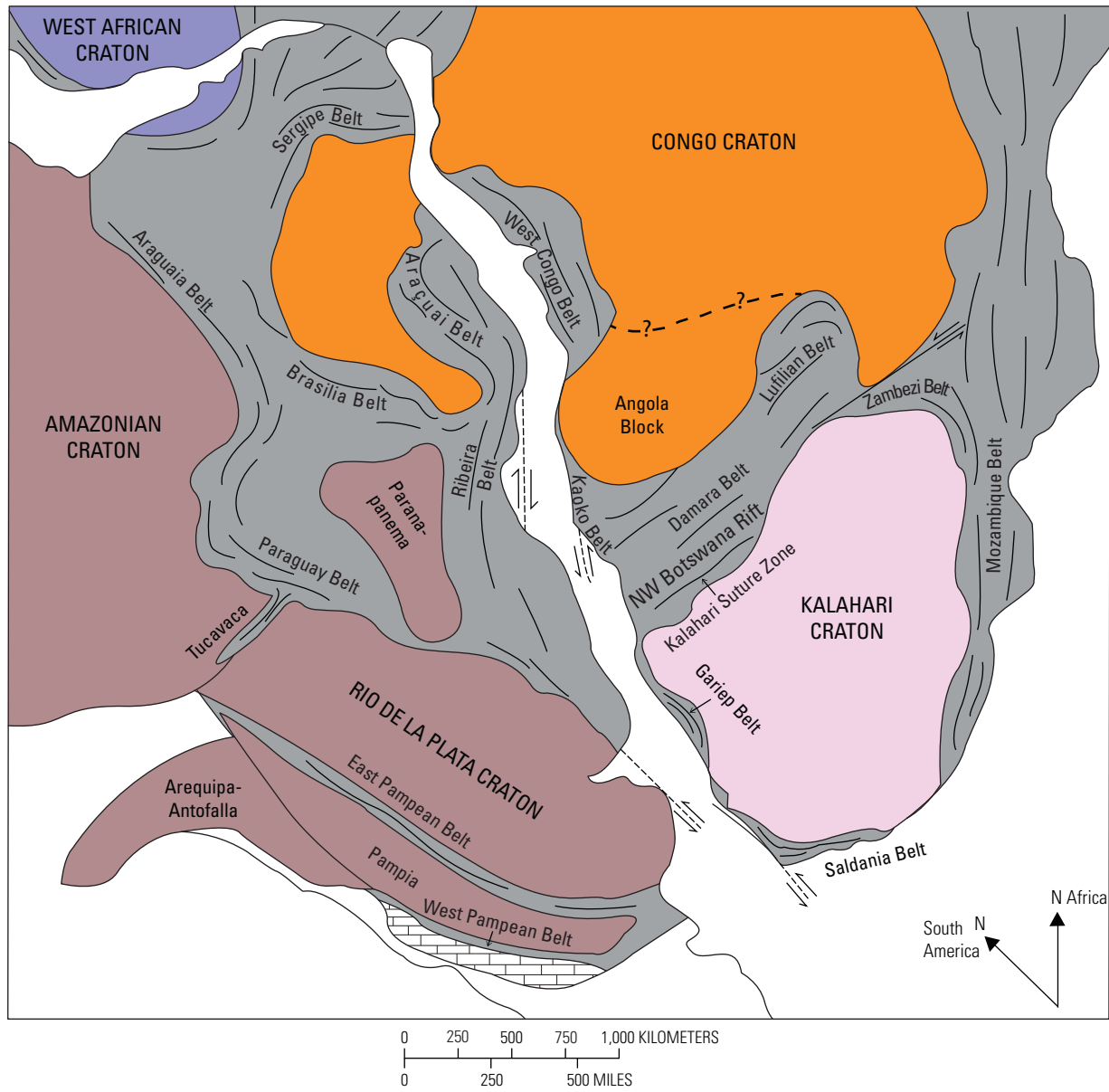
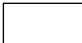


**Figure 2-1.** Map of the Proterozoic rocks associated with the Northwest Botswana Rift, Botswana and Namibia. Modified from Schreiber (1980), Key (1998), Haddon (2001), Singletary and others (2003), Van Der Heever and Arengi (2010), and Discovery Metals Ltd. (2011b).



**EXPLANATION**

- |   |   |   |  |
|---|---|---|--|
|  | <b>Younger crust</b>                                |  | <b>Craton of specific paleogeographic affinity (&gt;1.0 billion years old)</b> |
|  | <b>Precordillera terrane</b>                        |  | <b>Structural grain</b>  |
|  | <b>Neoproterozoic-early Paleozoic orogenic belt</b> |  | <b>Fault</b>   |

**Figure 2-2.** Map showing the reconstruction of southwestern Gondwana supercontinent with the general location of the Northwest Botswana Rift and the Kalahari Suture Zone in relation to the position of cratonic blocks and Neoproterozoic fold belts. Modified from Gaucher and others (2010) and Frimmel and others (2011).



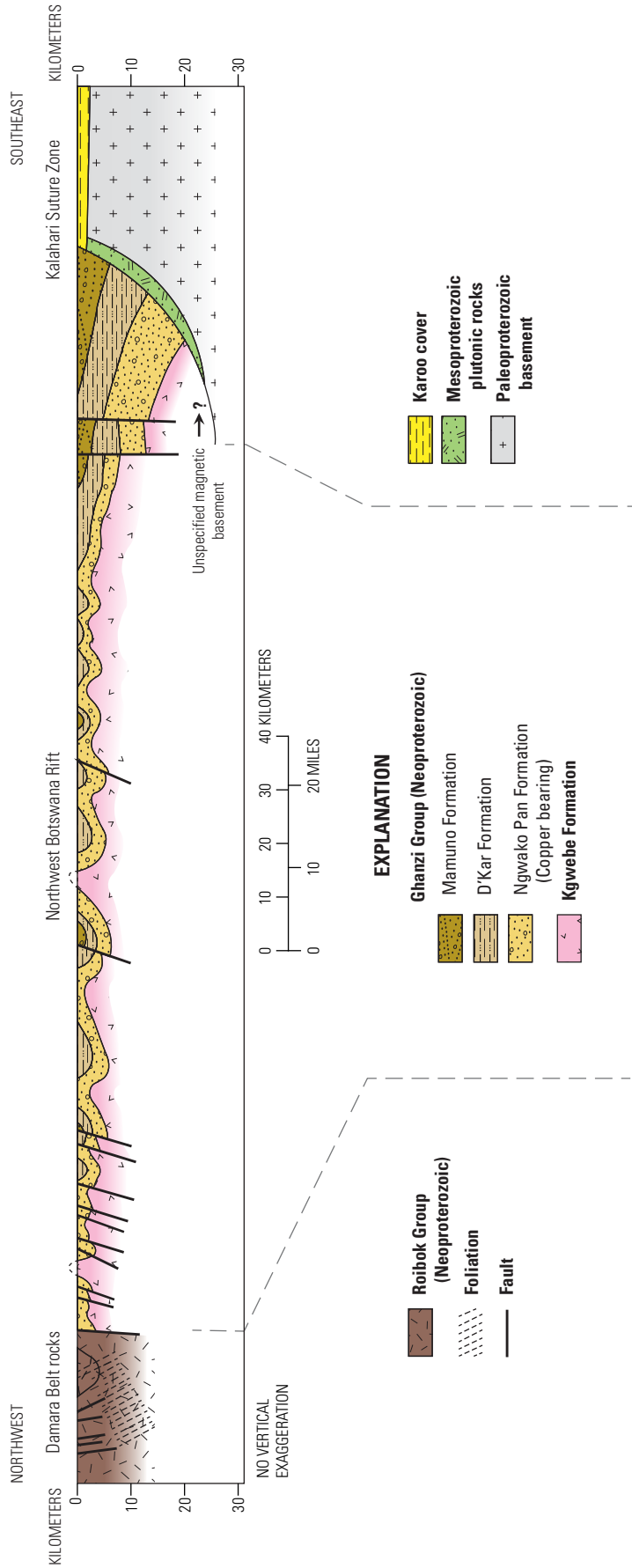


**Figure 2.3.** Cross section through the Northwest Botswana Rift showing folding and faulting of Proterozoic Ghanzi Group rocks that host mineralization associated with the Kalahari Copperbelt. Modified from Key and Maepo (1999).

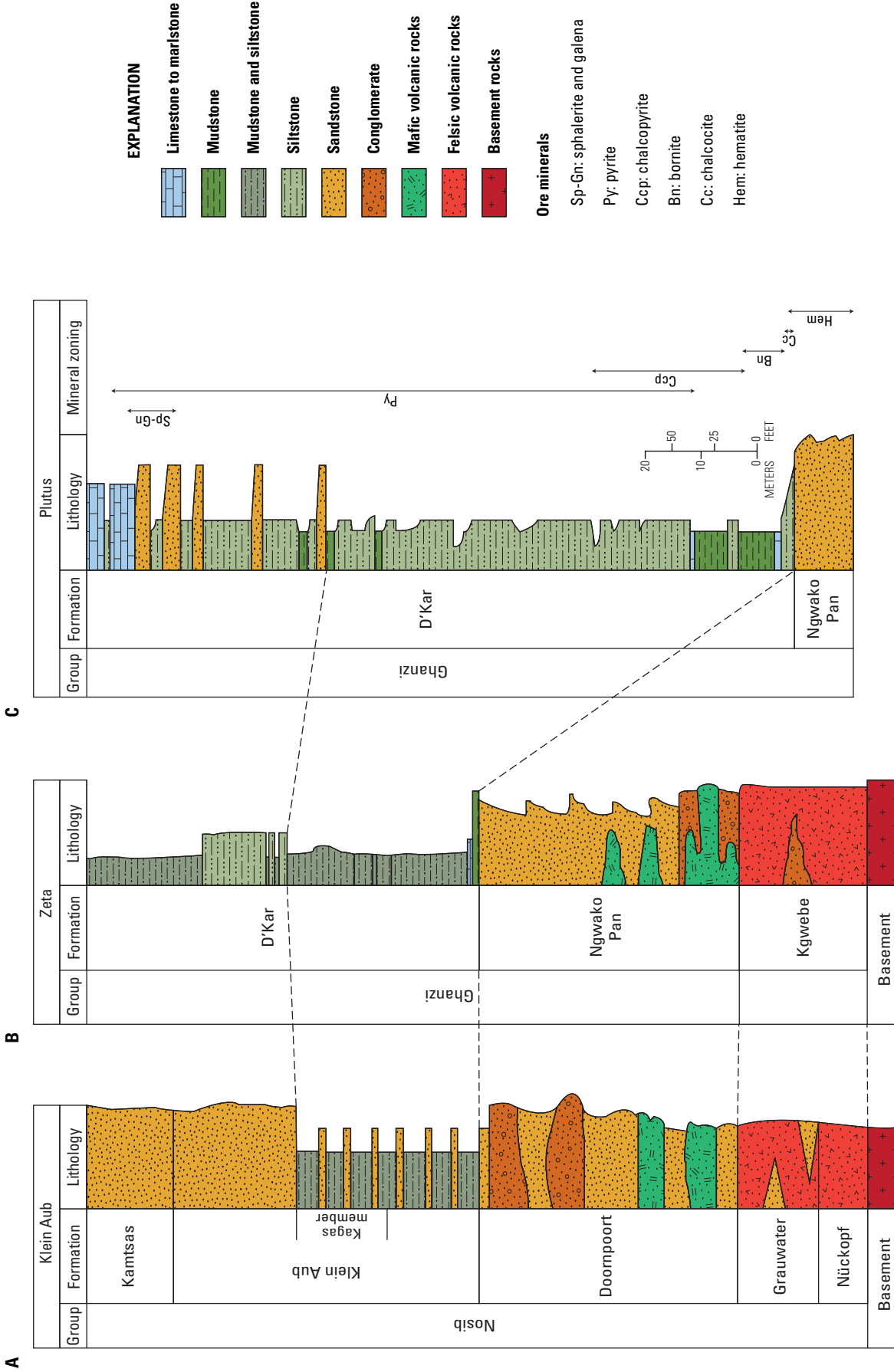


**Figure 2-4.** Stratigraphic columns of the Neoproterozoic rocks that host reduced-facies-type stratabound copper mineralization of the Kalahari Copperbelt, Botswana and Namibia. Columns are for (A) the Klein Aub Mine, in the western part of the area, and (B) the Zeta and (C) Plutus deposit areas, both in the eastern part of the belt. Scale is for Plutus column only. Modified from Borg and Stanistreet (1996), Body and Lomborg (2007), and Hall (2013).

**Table 2-1.** Sediment-hosted stratabound copper deposits within the Northwest Botswana Rift, Botswana and Namibia.

[Abbreviation of mineral names: Bn, bornite; Cc, chalcocite; Ccp, chalcopyrite; Cp, cuprite; Cv, covellite; Dg, digenite. g/t, grams per metric ton; Mt, million metric tons; %, percent; —, no data]

Name	Latitude	Longitude	Ore minerals	Major commodities	Resources (unmined)	Citation
Reduced-facies deposits						
Banana Zone	-21.089	22.738	Cc, Bn, Ccp	Cu, Ag	91.22 Mt at 1.15% Cu; 14.98 g/t Ag	Discovery Metals Ltd. (2011b); Pretorius and Park (2011)
Corner K	-21.146	22.408	—	Cu, Ag	9.5 Mt at 0.91% Cu	MOD Resources Ltd. (2012)
Dordabis (Koperberg)	-22.940	17.749	Cc, native Cu	Cu	1.74 Mt at 0.97% Cu	Kalahari Minerals plc (2008)
Ghanzi project - Zone 5	-20.619	23.222	Cc, Bn, Ccp	Cu, Ag	13.4 Mt at 1.66% Cu; 12.11 g/t Ag	Discovery Metals Ltd. (2011b); Pretorius and Park (2011)
Ghanzi project - Zone 6	-20.414	23.359	Cc, Bn, Ccp	Cu, Ag	6.27 Mt at 1.50% Cu; 6.68 g/t Ag	Discovery Metals Ltd. (2011b); Pretorius and Park (2011)
Klein Aub	-23.800	16.633	Ccp, Bn, Cc, Cp	Cu, Ag	6 Mt at 1.5% Cu	Ruxton (1986); Borg and Maiden (1987); Andritzky (1998); Cox and others (2003)
NE Mango	-20.679	23.150	—	Cu, Ag	33.3 Mt at 1.2% Cu	Discovery Metals Ltd. (2014)
Petra and Plutus	-20.543	22.961	Cc, Bn, Ccp	Cu, Ag	67.4 Mt at 1.4% Cu; 14 g/t Ag	Discovery Metals Ltd. (2010, 2011a, and 2011b)
Selene	-20.472	23.141	—	Cu, Ag	16.0 Mt at 1.0% Cu	Discovery Metals Ltd. (2014)
Zeta	-20.605	23.008	Cc, Bn, Ccp	Cu, Ag	35.4 Mt at 1.4% Cu; 20 g/t Ag	Discovery Metals Ltd. (2011a and 2011b)
Zeta NE	-20.539	23.092	—	Cu, Ag	12.9 Mt at 1.3% Cu	Discovery Metals Ltd (2014)
Sandstone-copper deposits						
Christiadore	-22.417	18.232	—	Cu	1.2 Mt at 2.3% Cu	Andritzky (1998); Kalahari Minerals plc (2006); Extract Resources (2008); Kalahari Minerals plc (2008)
Gemsbockvley	-22.464	18.177	—	Cu	0.4 Mt at 1.8% Cu	Andritzky (1998); Kalahari Minerals plc (2006); Extract Resources (2008); Kalahari Minerals plc (2008)
Malachite Pan	-22.285	18.465	—	Cu	3.0 Mt at 2.1% Cu	Andritzky (1998); Kalahari Minerals plc (2006); Extract Resources (2008); Kalahari Minerals plc (2008)
Oamites	-22.974	17.089	Ccp, Bn, Cc	Cu, Ag	6.1 Mt at 1.33% Cu; 12.3 g/t Ag	Lee and Glenister (1976); Maiden and others (1984); Andritzky (1998); Cox and others (2003)
Ophion	-20.796	22.733	—	Cu	14.0 Mt at 1.0% Cu	Discovery Metals Ltd. (2011b)
Okasewa	-22.390	18.316	—	Cu	6.0 Mt at 1.8% Cu	Andritzky (1998); Kalahari Minerals plc (2006); Extract Resources (2008); Kalahari Minerals plc (2008)
Witvlei (Pos)	-22.339	18.462	Cc, Bn, Ccp, Cv, Dg	Cu, Ag	2.8 Mt at 1.5% Cu	Anhaeusser and Button (1973); Maiden and others (1984); Andritzky (1998); Cox and others (2003); Extract Resources (2008); Kalahari Minerals plc (2008); Cullen Resources Ltd. (2011a)

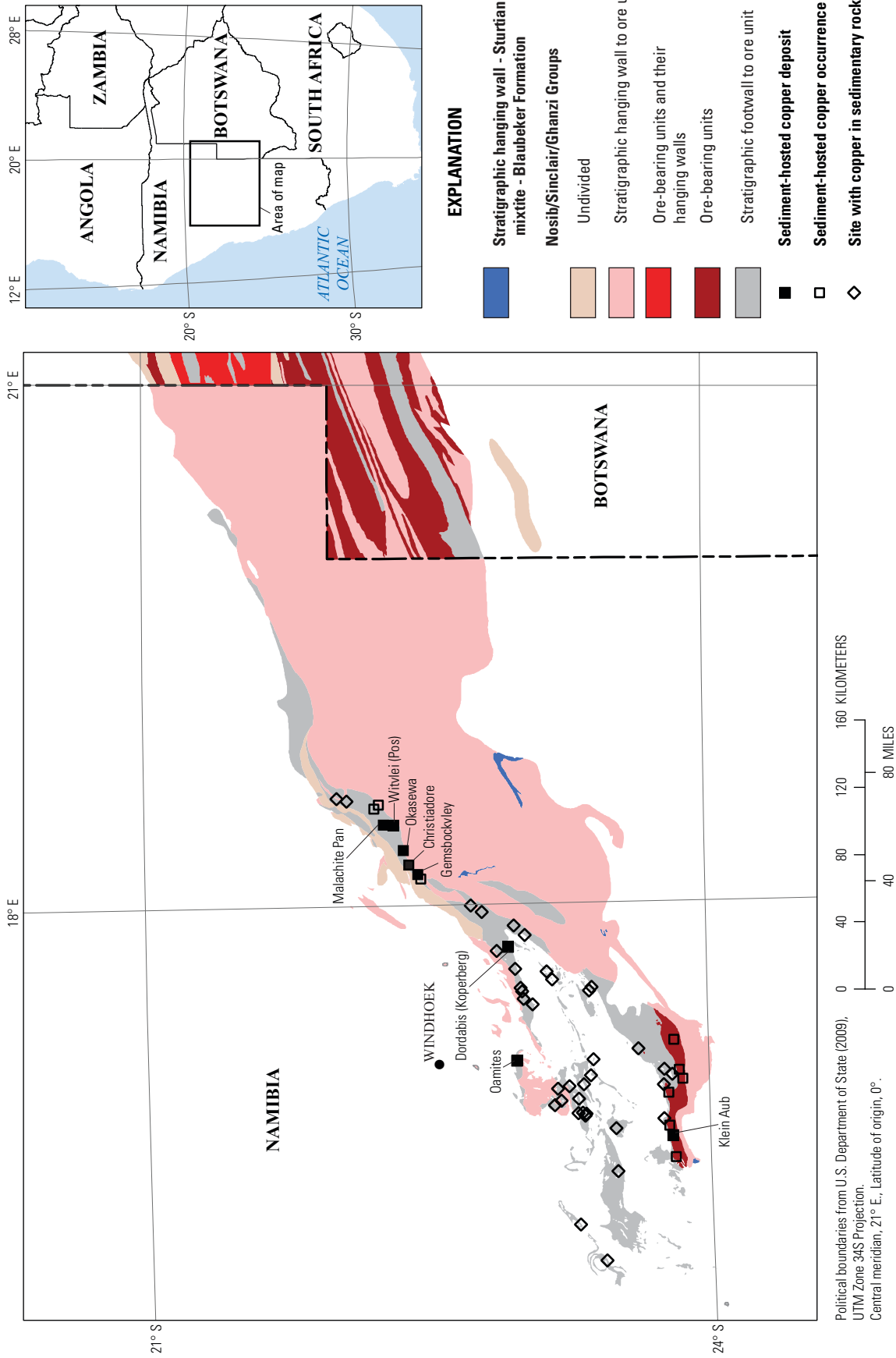


**Figure 2-5.** Geologic map of the western part of the Kalahari Copperbelt, Northwest Botswana Rift, Botswana and Namibia, showing selected geologic units and the location of sediment-hosted copper deposits and occurrences. Geology modified from Schreiber (1980), Key (1998), Haddon (2001), Van Der Heever and Arengi (2010), and Discovery Metals Ltd. (2011b).

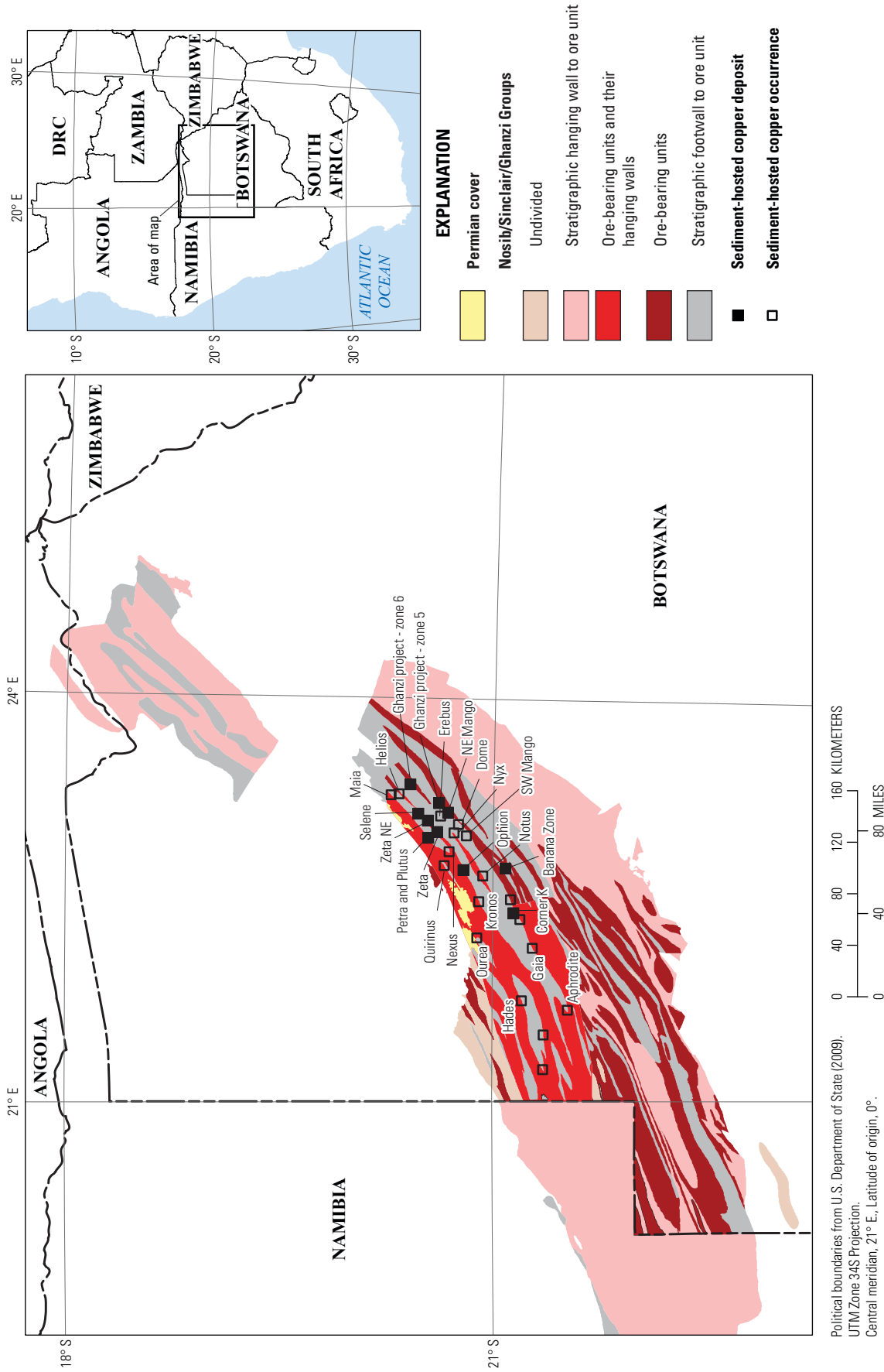


**Figure 2-6.** Geologic map of the eastern part of the Kalahari Copperbelt, Northwest Botswana Rift, Botswana and Namibia, showing selected geologic units and the location of sediment-hosted copper deposits and occurrences. Geology modified from Schreiber (1980), Key (1998), Haddon (2001), Van Der Heever and Arengi (2010), and Discovery Metals Ltd. (2011b).

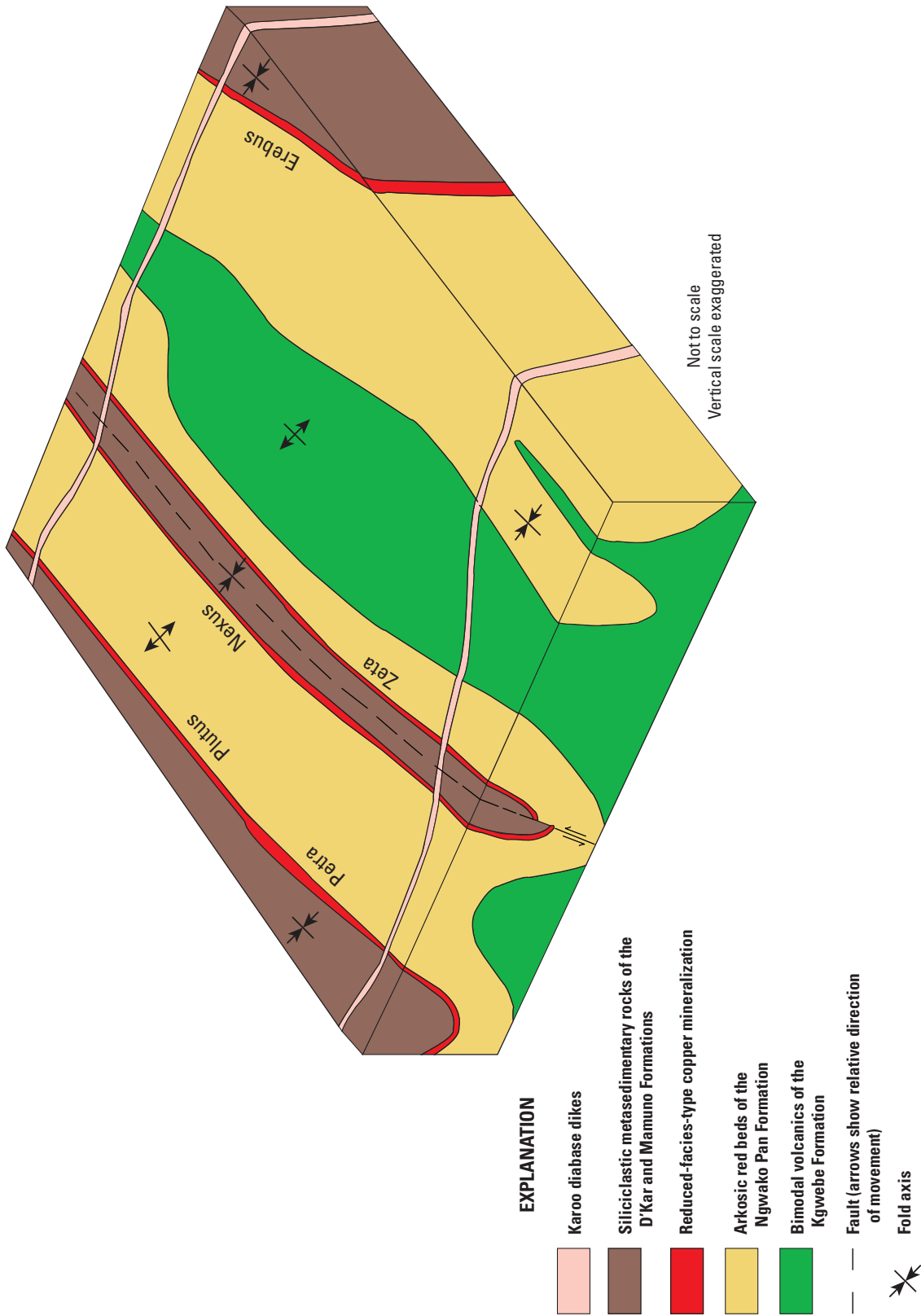


**Figure 2-7.** Schematic block diagram showing the location of several reduced-facies-type sediment-hosted copper deposits and occurrences along the folded contact between the Ngwako Pan and D'Kar Formations. Modified from Discovery Metals Ltd. (2011b).

two companies left the joint venture in 1975, but U.S. Steel continued exploration with additional soil-sample geochemistry, ground geophysics, trenching, and diamond drilling (Van Der Heever and Arengi, 2010). In 1980, U.S. Steel announced a resource at Zeta (Ngwako Pan) of 20 million metric tons of ore at 2 percent copper and 39 grams per ton of silver with an average thickness of 5.8 m to a depth of 650 m. After conducting feasibility studies, U.S. Steel abandoned the project. Anglo American Corporation took over and ran the project from 1989 until 1994. Anglo American ran airborne electromagnetic surveys and drilled electromagnetic conductors. The corporation detected pyrite and pyrrhotite in the hanging wall of a zone of copper mineralization and concluded that the Zeta area was the best prospective area, followed by the Banana Zone. Delta Gold explored the area from 1996 until 2000. Each time, the companies took up approximately the same exploration concessions and then relinquished the property in a prolonged period of low copper prices.

Around 2007, Hana Mining Ltd. entered into an agreement to acquire a 70 percent interest in the Ghanzi Project. After extensive exploration, Hana Mining Ltd. announced indicated and inferred resources totaling 91.2 million metric tons of 1.2 percent copper and 14.98 grams per ton of silver from the Banana Zone and Zones 5 and 6 of the Ghanzi Project (fig. 2-6; Pretorius and Park, 2011). The resources are conducive to open pit mining, and mineralization is believed to continue at similar grades and thicknesses below the open pit. In 2013, Hana Mining Ltd. was acquired by Cupric Canyon Capital.

Discovery Metals Ltd. acquired the rights to seven prospecting licenses that focused on the Zeta deposit in 2005 (fig. 2-6). They collected extensive drill and soil samples around the Zeta deposit, discovered and explored both the Petra and Plutus deposits, and drilled mineralized rock at the Nexus and Quirinus occurrences. Discovery Metals Ltd. acquired the rights to an additional seven prospecting licenses in 2008, and they control licenses that extend 60 km southwest from the town of Maun, Botswana, toward the Namibian border (distance of about 300 km) totaling an area of 10,000 km<sup>2</sup> (fig. 2-6; Discovery Metals Ltd., 2011a). The company used infill drilling in the Zeta-Petra-Plutus area to eventually identify an estimated total geologic resource (measured, indicated, and inferred) of 102.8 million metric tons of 1.4 percent copper and 17.3 grams per ton of silver, and conducted a feasibility study that was completed in August 2010. Discovery Metals Ltd. is developing (as of 2014) the Boseto project, which is predicted to produce 35,000 metric tons of copper and 1 million ounces of silver annually from three closely spaced open pits at Zeta, Petra, and Plutus (fig. 2-6). Boseto resources at depth are sufficient to continue mining underground once the open pit ore is exhausted (Discovery Metals Ltd., 2011a).

As of 2014, MOD Resources holds the license for approximately 7,800 km<sup>2</sup> of area between the Discovery Metals Ltd. Boseto Project and the Cupric Canyon Ghanzi project. On the basis of 138 drill holes, the Discovery Metals Ltd. Corner K deposit has a resource of 9.5 million metric tons with

0.91 percent copper and 18.4 grams per ton of silver (MOD Resources Ltd., 2012).

In the Klein Aub deposit in Namibia, reduced-facies copper mineralization in the Klein Aub Formation (fig. 2-5) comprises 6 to 10 disseminated, zoned, sulfide bodies (Ruxton, 1986). Copper was recognized and prospected as early as 1855 in the vicinity of the Klein Aub Mine (Mietzner, 2011). Between 1967 and 1987, the Klein Aub Mine was developed and produced 7.5 million metric tons of copper ore at a grade of 2 percent (Borg and Maiden, 1987; Cox and others, 2003; Kamona and Gunzel, 2007; McKinney and others, 2009; Discovery Metals Ltd., 2011a; Pretorius and Park, 2011). The decrease in copper prices forced the mine to close in 1987 although reserves were estimated to contain at least as much tonnage at the same grade as was already mined (table 2-1; Dierks, 2005). In 2011, Midnight Sun Mining Corporation, a mineral exploration and development company that trades on the TSX Venture Exchange<sup>4</sup>, entered into an agreement to earn a 60 percent interest in the Klein Aub group of prospecting licenses (Midnight Sun Mining Corporation, 2014).

## Sandstone-Copper Deposits

German colonists discovered copper resources in the Oamites area of Namibia (fig. 2-5) in the late 1800s, but the copper ore was considered uneconomic because the sulfide minerals were too fine grained for existing separation techniques. Exploration drilling in Oamites in the 1960s revealed a substantial ore body that led to mine development by Falconbridge Nickel Mines Ltd. in 1970. The Oamites deposit was mined between 1971 and 1985 and produced more than 6.1 million metric tons of ore at 1.33 percent copper and 12.3 grams per ton of silver (Cox and others, 2003). During active mining years, the Oamites Mine produced 55,000 metric tons of ore per month (Lee and Glenister, 1976). The copper mineralization at the Oamites Mine is hosted in amphibolite-grade metamorphic rocks that may be equivalent to Nosib Group rocks.

Recent reports estimate a total of 13.4 million metric tons of ore at 1.85 percent copper in five separate locations in the Witvlei area of Namibia: Christiadore, Gemsbockvley, Malachite Pan, Okasewa, and Witvlei (Pos) (figs. 2-5 and 2-6; table 2-1; Kalahari Minerals plc, 2008; Cullen Resources Ltd., 2011a). Rimann (1915) was the first to document copper in the Witvlei area, but extensive exploration did not commence until the late 1960s and early 1970s by Anglovaal Southwest Africa Pty Ltd. Borehole samples were analyzed, and the petrography and mineralogy of the Witvlei area were studied in detail during that time. The grade was reported as 1.5 to 2 percent copper and was considered uneconomic for large mining operations; nevertheless, small-scale mining operations were conducted (Anhaeusser and Button, 1973; Borg and Maiden, 1989). In early 2010, Cullen Resources

<sup>4</sup>The TSX Venture Exchange is a stock exchange headquartered in Calgary, Alberta and has offices in Toronto, Vancouver, and Montreal.



Ltd. submitted prospecting applications for approximately 8,000 km<sup>2</sup> (Cullen Resources Ltd., 2011b), and two exclusive prospecting licenses were acquired but later relinquished (Cullen Resources Ltd., 2014). Kalahari Minerals plc (2008) also reported resources of 1.74 million metric tons of copper ore with 0.97 percent copper at the Dordabis deposit (fig. 2-5). This deposit is about 100 km southwest of Witvlei (Pos) and is within the same stratigraphic units as the five deposits and occurrences in the Witvlei area.

## Mineral System Components

Neoproterozoic sedimentary rocks of southwestern Africa host stratabound copper deposits that likely formed during diagenesis of the D'Kar and Klein Aub Formations. Sulfide formation during diagenesis produced disseminated and cementing copper ore minerals in the Lake N'Gami, Witvlei, and Klein Aub outcrop areas, respectively (Ruxton, 1986). A secondary mineralization episode is found in stockwork veinlets at Klein Aub, which likely postdated lithification that produced the Klein Aub Formation (Miller, 1983).

Basalt and red-bed copper sources, evaporite-bearing Lake N'Gami rocks, subsurface brine-rich fluids, and a redox boundary (reduced organic-rich host rocks overlying an oxidized red-bed-type sequence) are all present in this reduced-facies sedimentary basin. The Neoproterozoic Doornpoort Formation basalt flows and their equivalents in Botswana could be the primary copper source rocks (Borg and Maiden, 1987). Regional metamorphism of the basalts resulted in epidote-quartz-chlorite-hematite-muscovite mineral assemblages; during the epidote alteration, copper, zinc, and cobalt were leached from these rocks. Native copper was precipitated in permeable zones such as breccia at the top of lava flows, amygdaloidal zones within flow units, and fractures within and adjacent to the basalts. Copper leached from the basalts is also a possible metal source for the sediment-hosted stratabound deposits. Borg and Maiden (1987) conclude that the volume of metabasalt and the extent of alteration and leaching can account for the amount of copper in the sediment-hosted deposits. Underlying red beds contain copper and were likely a local copper source. Replaced evaporite minerals in the Lake N'Gami area rocks (Borg and Maiden, 1989) indicate saline brine was likely a part of the NWBR mineralizing system.

The Damara Orogeny caused faulting and folding throughout the region (fig. 2-3; Key and Mapeo, 1999). These faults may have served as conduits for brine-rich fluid movement during secondary mineralization. The reductant component for the reduced-facies subtype of sediment-hosted stratabound copper mineralization is a redox boundary that resulted from the chemical contrast between oxidized clastic red beds and the overlying reduced carbonate-bearing rocks. The Klein Aub and D'Kar Formations contain carbonate rocks and pyritic shales that overlie the continental coarse clastic red beds of the Doornpoort and Ngwako Pan Formations. The red beds are interpreted as the infill of protoceanic rifts

that cut Mesoproterozoic basement rocks (Martin and Porada, 1977; Porada, 1989). The Klein Aub Formation in Namibia and the D'Kar Formation in Botswana likely are seal rocks to the mineralizing systems. In the sandstone-copper deposits of the Witvlei area, the reductant was likely a form of petroleum, probably sour gas, and the seal rocks were shale interbeds.

## Principal Sources of Information

A 1:1,000,000-scale geologic map of Namibia (Schreiber, 1980), a 1:2,500,000-scale bedrock geologic map of southwestern Africa (Haddon, 2001), and company reports from Hana Mining Ltd. and Discovery Metals Ltd. (Van Der Heever and Arengi, 2010; Discovery Metals Ltd., 2011b) were sources of geologic information for this assessment. The marked contrast in the detail of the permissive tracts between Botswana and Namibia reflects the use of a national geophysical survey completed in Botswana in the 1990s to map geology under cover. The main sources of mineral deposit and occurrence information included a 1:1,000,000-scale mineral occurrence map of Namibia (Andritzky, 1998), mining company reports from Discovery Metals Ltd., Kalahari Minerals, and Hana Mining Ltd., and references cited in table 2-1.

## Benguela and Cuanza Basins, Angola—Assessment Tract 002rfCu2000

Sedimentary rocks of the Cretaceous Lower and Upper Cuvu Formations in the Benguela and Cuanza Basins of western Angola host red-bed and reduced-facies subtypes of stratabound copper deposits, respectively. The Lower and Upper Cuvu Formations crop out in an arcuate, north-south-trending belt (fig. 2-8) over an area of about 2,300 km<sup>2</sup>. The onshore parts of the Benguela and Cuanza Basins contain 2 deposits, 10 occurrences, and 13 sites (fig. 1-4).

## Tectonic Setting

The Benguela and Cuanza Basins are two of the numerous grabens and half grabens that formed during the breakup of the supercontinent Gondwana and opening of the southern Atlantic Ocean during the Early Cretaceous (Marzoli and others, 1999; Guiraud and others, 2010). Thermally driven subsidence began in the Albian Age and continued through the Miocene Epoch resulting in deposition of alternating marine and terrestrial material as sea level periodically rose and fell (Guiraud and others, 2010). The western offshore part of the Cuanza Basin is an important petroleum-producing basin (Brognon and Verrier, 1966; Brownfield and Charpentier, 2006). Basin fill was locally compressed and inverted because of crustal shortening, which perhaps was due to ridge push

from the Mid-Atlantic Ridge as spreading direction changed during the Santonian Age (Nurnberg and Muller, 1991), or due to an uplift of the African Craton (Hudec and Jackson, 2002). Salt diapirs were emplaced later during the Cretaceous (fig. 2-9; Hudec and Jackson, 2002), and pervasive folding formed many of the anticlines that are structural traps for migrating petroleum (Brownfield and Charpentier, 2006).

## Stratigraphy

The basal rocks in the Benguela and Cuanza Basins are rift-related pre-Aptian tholeiitic basalt and basaltic andesite, which overlie gneissic and quartzitic Precambrian basement rocks (fig. 2-10; Brognon and Verrier, 1966; Marzoli and others, 1999). The volcanic rocks are overlain by red sandstone, dolomitic to calcareous sandstone, siltstone, and argillite of the Lower Cretaceous (pre-Aptian) Lower and Upper Cuvo Formations. The Lower Cuvo Formation consists of basal fanglomerate beds that grade upward to red-bed fluvial sandstone (Van Eden, 1978; Guiraud and others, 2010). The Upper Cuvo Formation is composed of coarse to fine calcareous sandstone with intercalations of siltstone and marl that grade upward into dolomite (Van Eden, 1978). The change in lithology from clastic to calcareous represents a marine transgression (Brognon and Verrier, 1966; Guiraud and others, 2010). The Lower and Upper Cuvo Formations range from 200 to 300 m in thickness. As much as 400 m of anhydrite and halite of the Aptian Loeme Formation disconformably overlies the Upper Cuvo Formations (fig. 2-10; Brognon and Verrier, 1966).

The Loeme Formation in the Benguela and Cuanza Basins is overlain by the Aptian Quianga and Binga Formations; both of these formations have basal anhydrite overlain by carbonate rocks (fig. 2-10). The bitumen-rich Binga Formation is the main petroleum source in the Benguela and Cuanza Basins (Brognon and Verrier, 1966; de Carvalho, 1980–82; de Araújo and Perevalov, 1998; Guiraud and others, 2010). Outcrops of the Binga Formation extend for about 40 km along strike and are as much as 300 m thick (de Araújo and Perevalov, 1998).

## Deposits and Occurrences

Two stratabound copper deposits are hosted in the Lower Cuvo and Upper Cuvo Formations, as well as a number of occurrences. The reduced-facies Cachoeiras de Binga deposit is located in the southern part of the Cuanza Basin (fig. 2-8). The English Mine and associated occurrences in the Benguela Basin are examples of the red-bed-deposit subtype. There are 2 deposits, 10 occurrences, and 13 sites located along the eastern margin of the Benguela and Cuanza Basins (table 2-2; fig. 2-8).

## Reduced-Facies-Subtype Deposits

The Cachoeiras de Binga deposit at the transition between continental clastic and marine carbonate rocks within the Upper Cuvo Formation has a measured resource of 7 million metric tons with 2 percent copper (table 2-2; Caia, 1976; Kirkham and others, 1994). The Cachoeiras de Binga copper deposit was studied by the Angolan Geological Survey in the early 1970s; the study included approximately 6,500 m of drilling (CityView Corporation Ltd., 2006). Studies of the Benguela and Cuanza Basins by the Johannesburg Consolidated Investment Co. Ltd., including the Cachoeiras de Binga copper deposit, were summarized by Van Eden (1978). In the early 1980s, further work in and around the deposit funded by the United Nations Development Program (Smith, 2005) included geochemical traverses immediately to the north of Cachoeiras de Binga, across the Cuvo River. The results of the traverses indicated that the Cachoeiras de Binga deposit may extend to the west and south (Smith, 2005). The Angolan Civil War (1975–2002) halted exploration work on the deposit.

From about 2004 to 2008, the Cachoeiras de Binga license area was held by a number of exploration companies such as Aurum, Simba Jamba Mines, Simba Mines, Zebra Copper, Fortitude Minerals, and CityView Corporation (for example, CityView Corporation Ltd., 2006; Fortitude Minerals Ltd., 2008; Mining Review, 2008; Schustack, 2008). The last of the parent companies, CVI Energy Corporation Ltd. (formerly CityView Corporation Ltd.), was delisted from the Australian stock exchange in 2011. The most significant outcomes of this work are technical reports that summarize previous work on the property (Smith, 2005, 2006). According to Smith (2005), approximately 50 million metric tons of inferred resources with a grade of 2 to 2.14 percent copper may be present to the north and west of the Cachoeiras de Binga deposit.

## Red-Bed-Subtype Deposits

Red-bed copper deposits and occurrences at English Mine, Novo Redondo, and Zenza in the Benguela and Cuanza Basins (fig. 2-8) are hosted in the conglomerate or sandstone of the Lower Cretaceous Cuvo Formation (table 2-2; fig. 2-10; Van Eden, 1978). At the English Mine, copper oxide minerals (such as cuprite) are present with iron oxides in a 100-m long by 10- to 20-m-thick gossan zone. Conglomerate and sandstone below the gossan zone are barren (Van Eden, 1978). The mineralized rocks are overlain by limestone. The conglomerate, sandstone, and limestone are a buttress unconformity against a paleohill of basement granite (Van Eden, 1978; Smith, 2005). Copper ore was extracted from the English Mine in the late 19th century, but no production numbers are published (Van Eden, 1978; Kirkham and

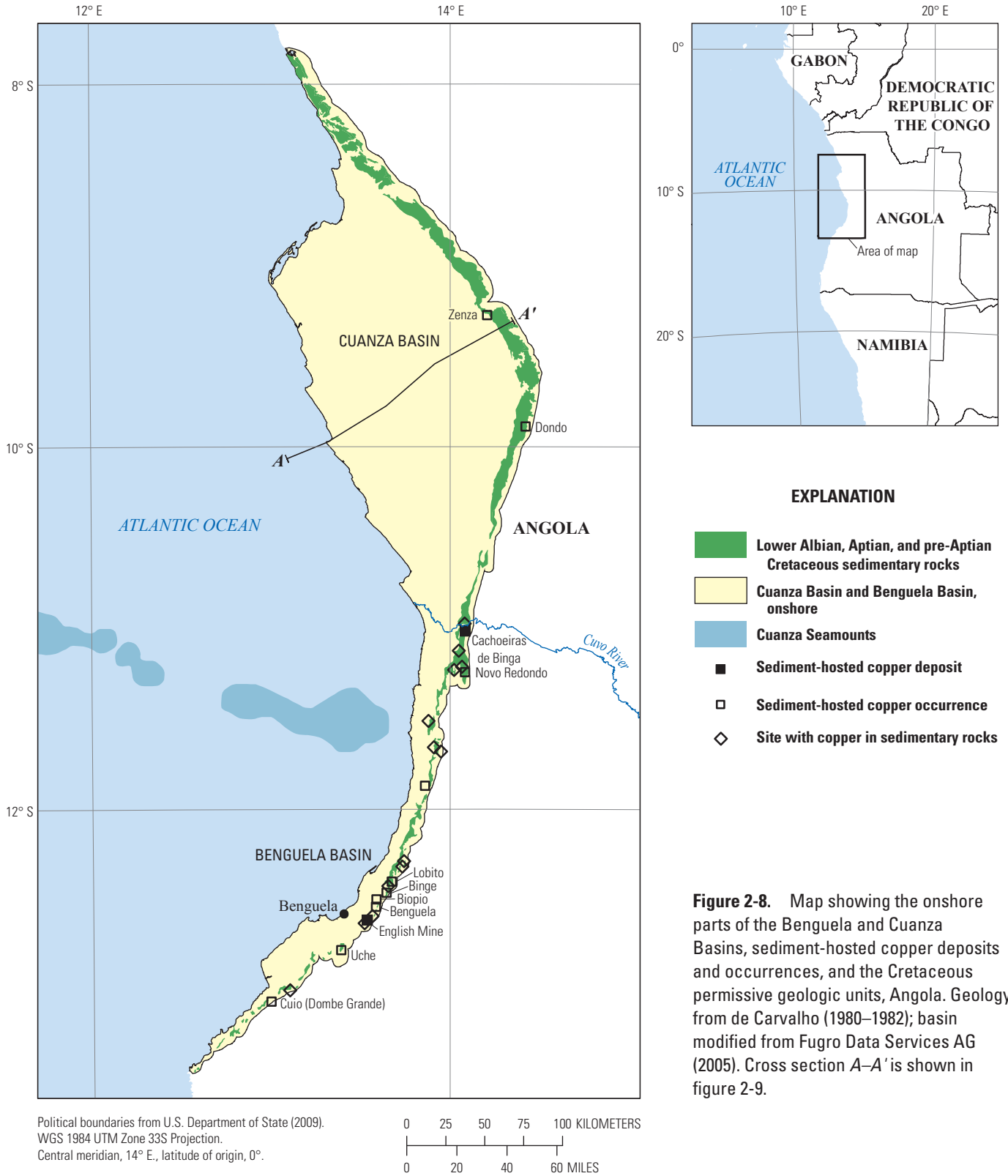


**Figure 2-8.** Map showing the onshore parts of the Benguela and Cuanza Basins, sediment-hosted copper deposits and occurrences, and the Cretaceous permissive geologic units, Angola. Geology from de Carvalho (1980–1982); basin modified from Fugro Data Services AG (2005). Cross section A–A' is shown in figure 2-9.

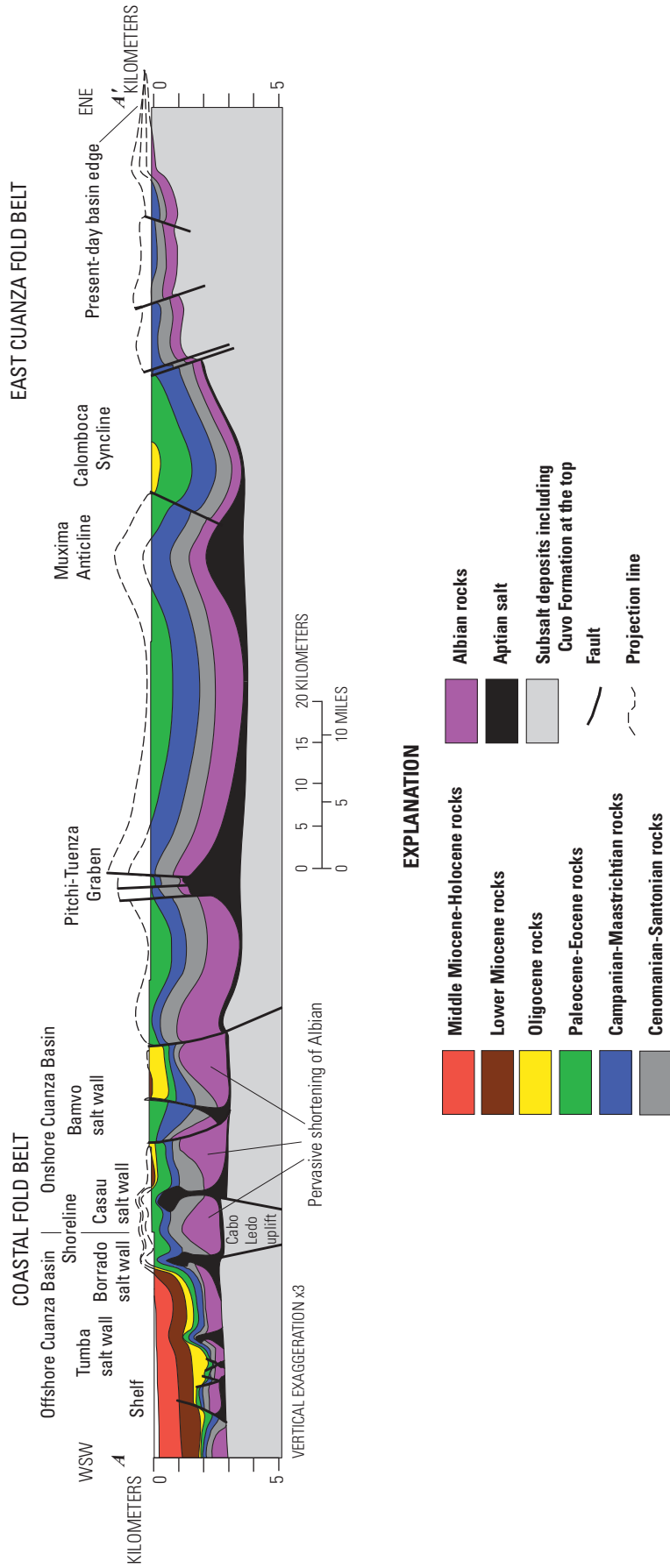


**Figure 2-9.** Geologic cross section of the Cuanza Basin, Angola. Oligocene-Holocene crustal shortening of the Angolan passive margin inverted the west edge of the onshore Cuanza Basin and formed the Coastal fold belt. Modified from Hudec and Jackson (2002). Location of cross section A-A' is shown in figure 2-8.



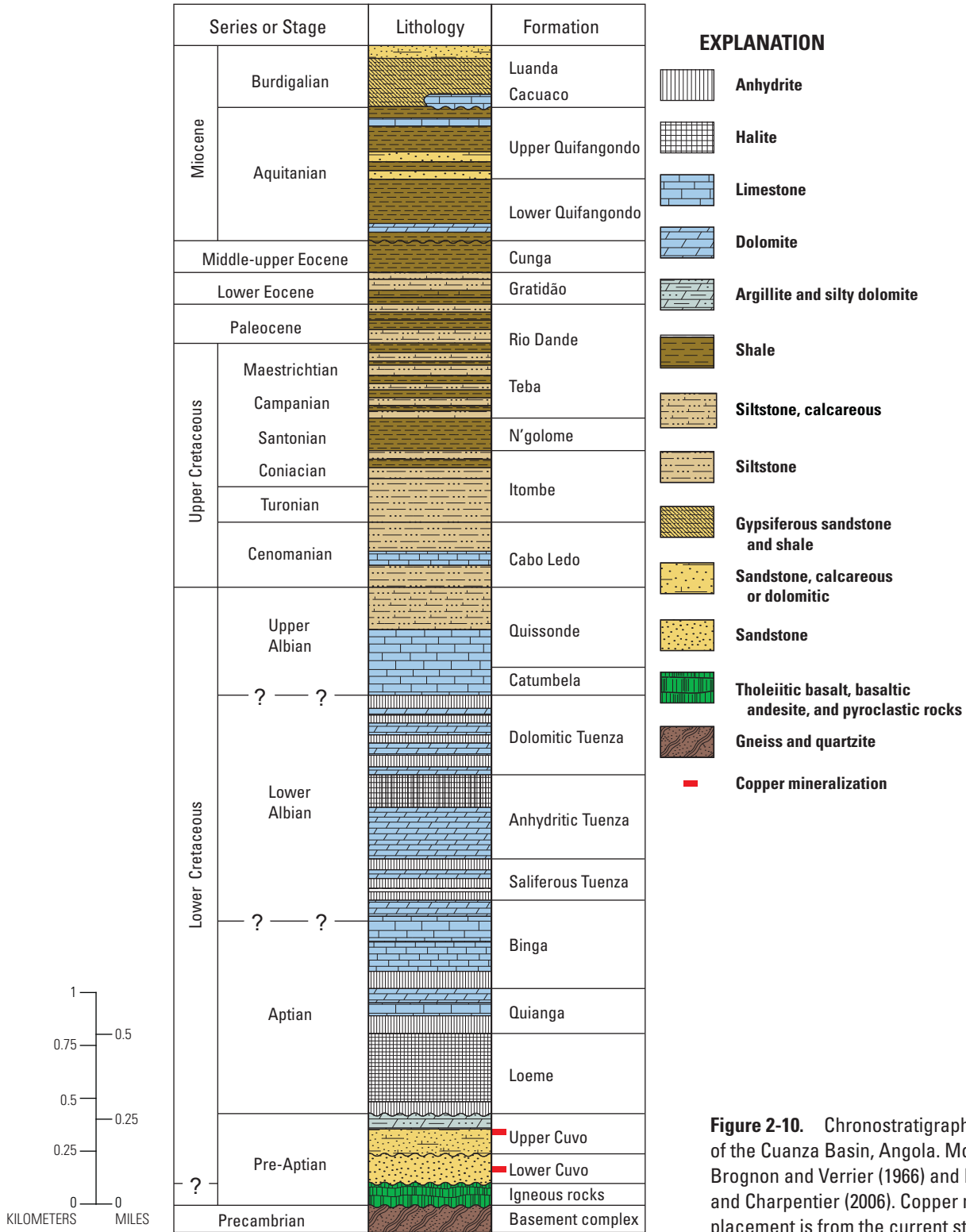


**Figure 2-10.** Chronostratigraphic column of the Cuanza Basin, Angola. Modified from Brognon and Verrier (1966) and Brownfield and Charpentier (2006). Copper mineralization placement is from the current study.

**Table 2-2.** Sediment-hosted stratabound copper deposits within the Cuvo and Binga Formations of the Benguela and Cuanza Basins, Angola.

[Abbreviation of mineral names: Bn, bornite; Cc, chalcocite; Ccp, chalcopyrite. g/t, grams per metric ton; Mt, million metric tons; %, percent; —, no data]

Name (alternate name)	Latitude	Longitude	Major commodities	Subtype of copper mineralization	Ore minerals	Resources (unmined)	Citation
Cachoeiras de Binga	-11.017	14.085	Cu	Reduced facies	Bn, Cc, Ccp	7 Mt at 2% Cu; 2–15 g/t Ag	Caia (1976); Van Eden (1978); Kirkham and others (1994); de Araújo and Perevalov (1998); Cox and others (2003); Kirkham and Rafer (2003); Kirkham and Broughton (2005)
English Mine (Unango)	-12.490	13.628	Cu	Red bed	Bn, Cc, Ccp	—	Van Eden (1978); Kirkham and others (1994); de Araújo and Perevalov (1998); Cox and others (2003)

others, 1994). At Zenza, the mineralization occurs within red conglomeratic sandstone directly below an upward transition to gray coaly rocks. Chrysocolla and pseudomalachite are in the clayey matrix or carbonate cement of the sandstone (Van Eden, 1978). At Novo Redondo, the mineralization crosses stratigraphy and consists of discontinuous layers of chrysocolla as matrix within sandstone. The mineralized sandstone underlies white feldspathic sandstone and overlies limonite-stained conglomeratic sandstone. Some copper mineralization is associated with small coaly pieces (Van Eden, 1978). Mineralization here appears to be supergene and formed at a paleo-water table; copper may have originated from overlying reduced-facies mineralization.

## Mineral System Components

Two copper sources and redox boundaries as well as one evaporitic seal are present in the Benguela and Cuanza Basins. Copper may have originated in the Lower Cuvo underlying formations and carried in brines upward to the Upper Cuvo Formation (fig. 2-10; Van Eden, 1978; Swenson and others, 2004). Potential copper sources include the pre-Aptian tholeiitic basalt and basaltic andesites that underlie the Lower Cuvo Formation. In addition, copper may have dissolved from the clastic lower red beds and precipitated in overlying carbonate-bearing reduced beds (Van Eden, 1978; Swenson and others, 2004). The Upper Cuvo Formation includes thin beds of anhydrite, gypsum, and other salts, as well as finely bedded siltstones with plant and coal remains. Toward the center of the basin, the Upper Cuvo Formation passes laterally into and is overlain by a sequence of saline evaporitic cycles and calcareous units including the Loeme, Quianga, Binga, and Tuenza Formations. No evaporite minerals, which would indicate a brine source, are known to be in the rock units underlying the copper mineralization in the onshore part of the Cuanza Basin. In-place fluids likely were mobilized due to compaction by rapidly deposited sediments. Mobilized fluids could have

migrated to the basin margins through the Lower Cuvo Formation. The stratigraphic transition from the oxidized red beds to the overlying reduced dolomitic-calcareous rocks of the Upper Cuvo Formation represents a marine transgression, which is termed a flooding surface. The redox boundary for the red-bed copper mineralization is in the oxidized clastic Lower Cuvo Formation where coaly plant remains and fragments served as reductants to the mineralizing solutions (Van Eden, 1978). Anhydrite and halite of the Loeme Formation (fig. 2-10; Brognon and Verrier, 1966), which directly overlies the Upper Cuvo Formation, likely served as seal rocks that supported recirculation of copper-rich fluids.

## Principal Sources of Information

Principal sources of information for the assessment included a 1:1,000,000-scale geologic map of Angola (de Carvalho, 1980–82) and a 1:1,000,000-scale mineral resource map of Angola (de Araújo and Perevalov, 1998). World mineral deposit databases from the USGS (Cox and others, 2003) and Geological Survey of Canada (Kirkham and others, 1994; Kirkham and others, 2003) provided information on mineral deposits and occurrences. Additional resources include a publication on stratiform copper mineralization of Angola by Van Eden (1978) and a 1:5,000,000-scale digital metallogenic map of Africa (Veselinovic-Williams and Frost-Killian, 2003).

## Egypt–Israel–Jordan Rift, Egypt, Israel, and Jordan—Assessment Tract 002rfCu2001

Sedimentary rocks of the Cambrian Nasib, Timna, and Burj Formations in Egypt, Israel, and Jordan, respectively, contain reduced-facies stratabound copper mineralization.

Copper deposits and occurrences are localized in an east-west belt that follows a facies change from marine carbonate rocks in the north to near-shore sandstone in the south. This belt extends into the subsurface eastward from Feinan, Jordan, and westward from Timna, Israel. The Egypt–Israel–Jordan Rift permissive tract area delineated during this study is about 26,000 km<sup>2</sup>; the tract contains 4 deposits and 12 occurrences (fig. 1-5).

## Tectonic Setting

Proterozoic collisional tectonics (900 to 620 Ma) sutured numerous fragments of the Arabian-Nubian shield (fig. 2-11) in the closing stages of the East African Orogeny during the final amalgamation of Gondwana (Husseini and Hussein, 1990; Johnson and others, 2011). Isostatic uplift of the sutured basement resulted in a laterally extensive erosional surface along the northern margin of Gondwana that was unconformably overlain by Neoproterozoic to Cretaceous sedimentary and volcanic rocks (Amireh and others, 2008; Johnson and others, 2011). Cambrian platform sedimentary rocks that overlie Neoproterozoic rift basins developed on the Arabian-Nubian shield host copper deposits in Egypt, Israel, and Jordan. In this region, metavolcanic and metasedimentary rocks intruded by calc-alkaline granitoids make up the basement complex (Amireh and others, 2008).

The tectonic setting shifted from compressional to extensional at about 620 Ma (Ediacaran Period of the Neoproterozoic Era) when isolated basins opened along the edge of Gondwana in what is now South Oman, the Arabian Sea, central Iran, and Pakistan (fig. 2-11; Hussein and Hussein, 1990). Two other related rift systems are proposed in areas now largely covered by younger sedimentary deposits: (1) the Jordan Valley Rift which extends north from the Sinai Peninsula across the Jordan Valley to southeast Turkey and (2) the Egypt Rift which extends west from the Sinai Peninsula and North Egypt to northeast Africa. The Jordan Valley Rift was active from about 600 to 510 Ma, and the Egypt Rift was active from 600 to 540 Ma. The left-lateral Najd strike-slip fault system contemporaneously developed with the rift systems (fig. 2-11; Hussein and Hussein, 1990); small rift basins filled with Ediacaran stratified sediment formed along these faults (Johnson and others, 2011, 2013). In southern Jordan, seismic studies show the presence of a series of asymmetrical half grabens bounded by listric faults and filled with Ediacaran and Lower Cambrian strata (fig. 2-12; Amireh and others, 2008).

Following the rifting event, a marine transgression of the proto-Tethys ocean covered an expansive area of northern Africa and Arabia, resulting in deposition of marine clastic sediments (for example, the Cambrian Salib Arkosic Sandstone Formation) and then marine carbonate sediments (the Cambrian Burj Formation) (fig. 2-12; Hussein and Hussein, 1990; Amireh and others, 1994, 2008). Subsequently, as much as 2 km of clastic sediment accumulated atop the carbonate material (Amireh and others, 2008).

Fission-track thermochronology of annealed grains from the Cambrian sandstone (Vermeesch and others, 2009) and K-Ar and Rb-Sr dates from the illite clay fraction of Cambrian Timna Formation dolostone (Segev and others, 1985) indicate a regional tectonothermal event that is interpreted as a partial basin inversion around 380 to 365 Ma (in the Devonian Period). Since the Miocene, landmasses on either side of the Dead Sea Transform Fault were offset by about 110 km in a left-lateral direction (Quennell, 1958; Freund and others, 1970; Garfunkel, 1981; Hatcher and others, 1981; ten Brink and others, 2007).

## Stratigraphy

Ediacaran continental sedimentary and volcanic material was deposited in the extensional basins associated with the Najd strike-slip fault system (fig. 2-11; Johnson and others, 2011, 2013). In the Hammamat and Thalbah Basins in the northeastern desert of Egypt and northwestern Saudi Arabia, respectively, rocks include approximately 4,000 m of cobble and boulder polymict conglomerate, pebbly sandstone, purple sandstone, siltstone, and mudstone (fig. 2-11; Johnson and others, 2013). In Jordan, rocks of the Umm Ghaddah Formation (a fining-upward sequence of terrestrial conglomerates and sandstones) and underlying Sarmuj Conglomerate, Hiyala Volcaniclastic Formation, and the Aheimir Volcanic Suite were deposited in northeast-trending, elongated rift basins (fig. 2-12; Amireh and others, 2008). The Hiyala Volcaniclastic Formation, not shown in figure 2-12, overlies the Sarmuj Conglomerate and underlie the Aheimir Volcanic Suite (Amireh and others, 2008, table 1). The Aheimir volcanic suite is composed of lava flows and pyroclastic rock made up of lithic tuff and ignimbrite material with compositions including basaltic trachyandesite, trachyandesite, trachyte/trachydacite, and rhyolite (Jarrar and others, 2012). The Ghuweir volcanic rocks in the Wadi Araba area of southwest Jordan are predominantly basaltic to andesitic rocks (Jarrar and others, 2008).

The overlying Cambrian continental sedimentary rocks include the laterally equivalent Salib Formation in Jordan, the Amudei Shelomo Formation in Israel, and the Serabit el-Khadim member in Egypt (fig. 2-13; El Sharkawi and others, 1990; Kolodner and others, 2006). Calcareous rocks of the Burj Formation in Jordan and the Timna Formation in Israel record a marine transgression and directly overlie red beds. In Egypt, calcareous rocks of the Carboniferous Umm Bogma Formation overlie the Cambrian Adedia, Nasib, and Abu Hamata Formations, which overlie Cambrian Serabit el-Khadim red beds (El Sharkawi and others, 1990).

The Lower to Middle Cambrian Burj Formation consists of as much as 130 m of dolomite, sandstone, siltstone, and shale (figs. 2-13 and 2-14; Kolodner and others, 2006). The Timna Formation is a Lower to Middle Cambrian mixed siliciclastic and carbonate unit that includes dolomite, sandstone, siltstone, and shale. The Timna Formation is as much as 49 m thick (Kolodner and others, 2006). The Cambro-Ordovician Nasib Formation (about 45 m total thickness) is divided into

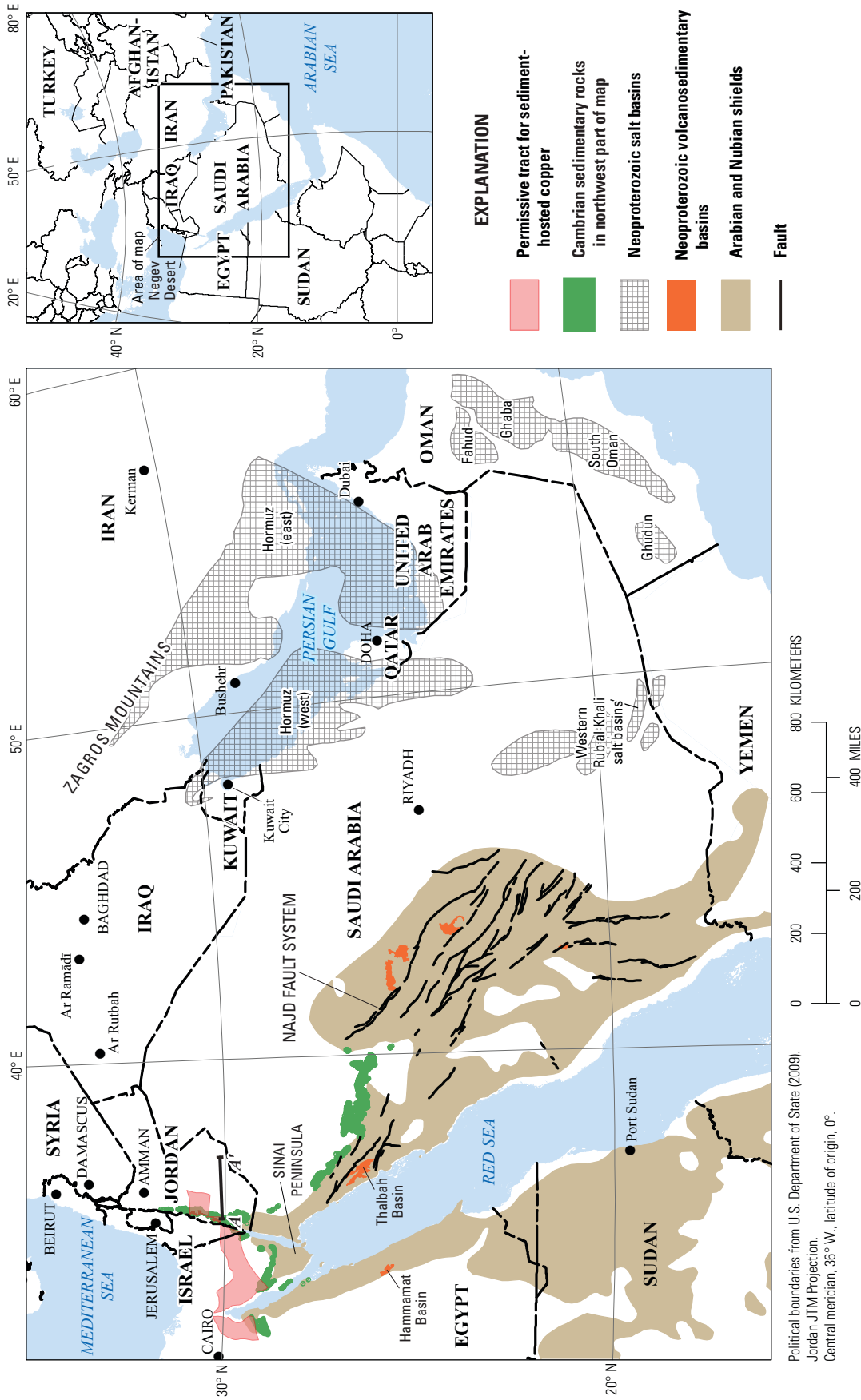


**Figure 2-11.** Map showing the Egypt–Israel–Jordan Rift permissive tract for undiscovered sediment-hosted copper including Cambrian sedimentary rocks, Neoproterozoic salt basins, Neoproterozoic volcanosedimentary basins, and the Arabian and Nubian shields (Hadley, 1972; Moore, 1979; Stern and Johnson, 2010). Cross section A–A' is shown in figure 2-12.

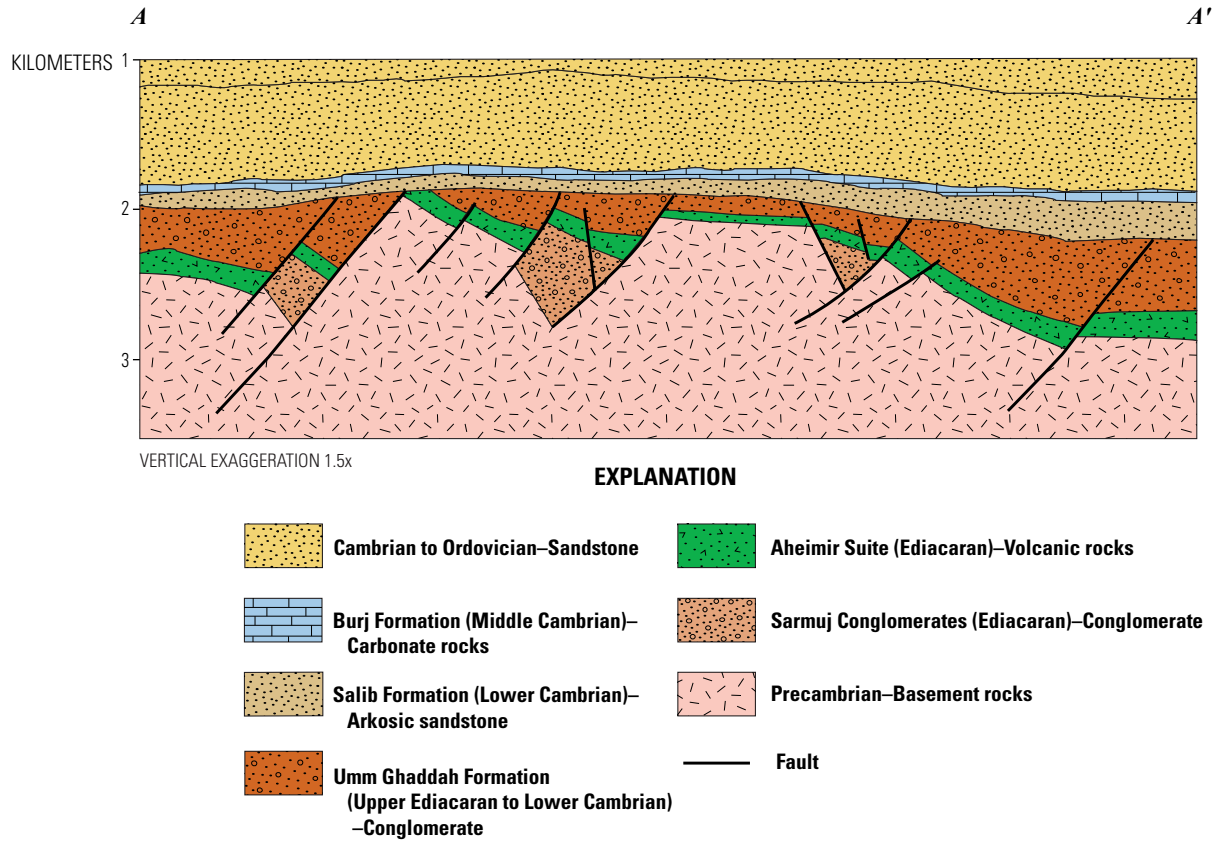


**Figure 2-12.** Geologic cross section based on a seismic profile through southern Jordan that shows the transgressive sequence of the Salib Arkosic Sandstone Formation and the Burj Formation overlying a series of half grabens filled with volcanic rocks (Aheimir Volcanic Suite) and red beds (Umm Ghaddah Formation). Modified from Amireh and others (2008). Location of cross section A–A' is shown in figure 2-11.



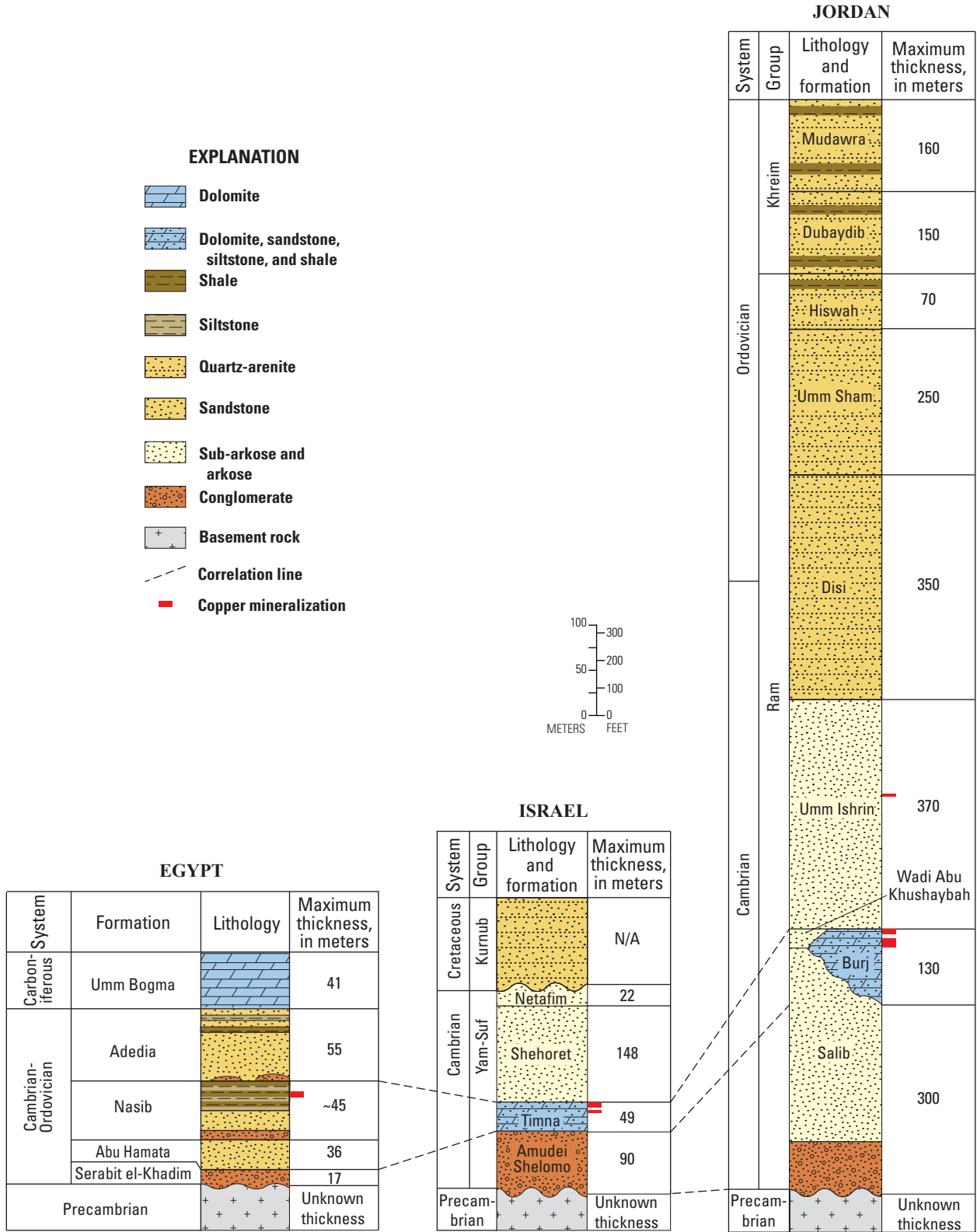


**Figure 2-13.** Stratigraphic columns of lower Paleozoic sedimentary rocks showing the position of copper mineralization in Early to Middle Cambrian strata, Egypt–Israel–Jordan Rift, Egypt, Israel, and Jordan. Column for Timna, Israel, and for Feinan, Jordan, modified from Kolodner and others (2006). Column for Egypt modified from El Sharkawi and others (1990). Stratigraphic position of copper mineralization for Israel and Jordan is from the current study. N/A, not available.

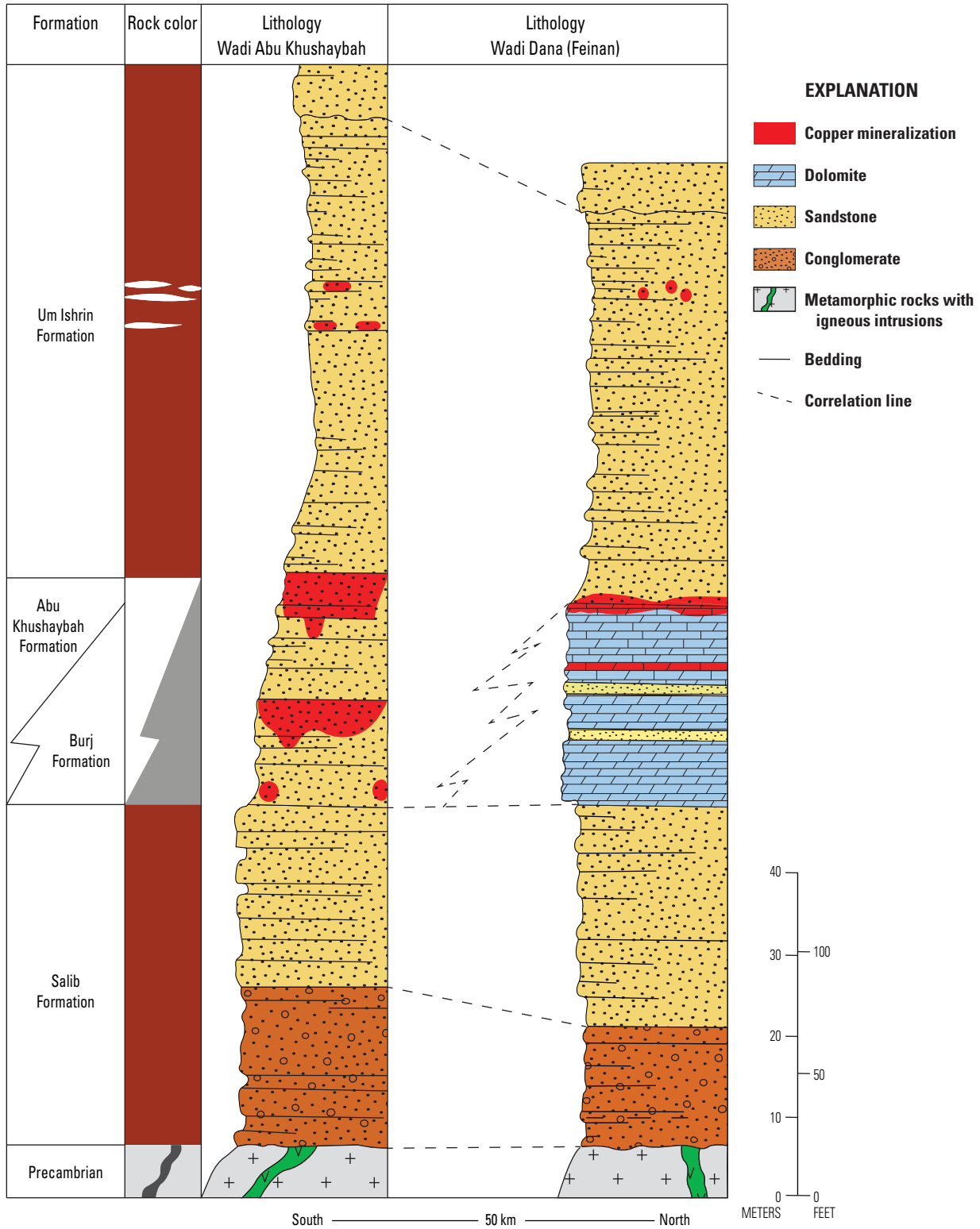


**Figure 2-14.** Stratigraphic columns of Early to Middle Cambrian rocks in Jordan showing the lateral facies change from carbonates of the Burj Formation in the north to sandstones of the Wadi Abu Khushaybah Formation to the south. Copper mineralization occurs in both the Burj and Wadi Abu Khushaybah Formations. Modified from Bender (1965).

a lower member of conglomerate and sandstone and an upper member of siltstone and shale (El Sharkawi and others, 1990).

The host rocks for copper mineralization are from the Burj (Jordan), Timna (Israel), and Nasib (Egypt) Formations. The permissive tract delineated for this area (figs. 2-11 and 2-15) is based on projecting the Timna and Burj Formations to a maximum depth of 2 km. These two formations record a transition from marine to coastal and near-shore facies, resulting from a marine transgression. In selecting the assessment unit, it is presumed that oxidizing metalliferous brines derived from the Cambrian depocenters to the north moved upsection to the south and dissolved copper from coarse arkosic red beds in Infracambrian rift basins and perhaps subjacent basement rocks (Burgath and others, 1984; Beyth, 1987). The mobile metalliferous brines reacted with the organic matter of the Timna Formation and Burj equivalents (deposited from the first postrift marine transgression), reducing sulfate to sulfide and precipitating copper as sulfides at temperatures less than 93 °C, at which djurleite is stable (Roseboom, 1966; Shlomovitch and others, 1999).

The Amudei Shelomo (Israel) or Salib (Jordan) Formations that represent the rift basins, crop out to the north of the Khirbet en Nuhas deposit and extend southeastward in Jordan (fig. 2-15; Amireh and others, 2008). The basins also extended in north-south-elongate troughs into Jordan and Iraq (Jassim, 2006, p. 34). The shelf carbonate rocks that host ore minerals in Israel and Jordan extend northeastward into Syria and northern Iraq and probably into central Iran, Afghanistan, and Pakistan (Husseini and Husseini, 1990). The north-to-south transition from marine carbonate, sandstone, siltstone, and shale rocks to coastal and nearshore sandstone rocks extends westward from Israel into northern Africa and eastward into Jordan (Guiraud, 1999, table 1 and fig. 2; Al-Laboun, 1993, p. 64–65). Only part of the shelf carbonate sequence is thought to be permissive for sediment-hosted stratabound copper mineralization.

In Israel, copper mineralization is localized in an approximately 50-km-wide zone where the host rocks change from coastal and nearshore sandstone in the south to marine carbonate rocks in the north (fig. 2-15). In Israel, the Timna Formation contains ore-grade mineralization in the Timna Valley outcrop exposures, but in the Sinaf-1 drill hole, 39 km to the north (fig. 2-15), the Timna Formation dolostone contains from 8 to 241 parts per million (ppm) copper, of which the higher values are anomalous, but not ore grade (Segev and Sass, 1989, p. 653). At the Har Amram outcrops, 10 km south of the Timna deposit, the rocks are not mineralized. Thus, a north-south belt less than 50-km wide appears to be mineralized. The mineralized belt that parallels (east-west) the important facies change from marine rocks to sandstone is the permissive unit used to delineate the tract.

The Dead Sea Transform Fault offsets the permissive tract (fig. 2-15). The deposits near Timna, in Israel, and Feinan, in Jordan, formed adjacent to each other in the same belt of permissive rocks and are piercing points indicating about 110 km of left-lateral offset along the Dead Sea

Transform Fault since initiation of seafloor spreading in the Red Sea in the early Miocene (figs. 2-11 and 2-15) (Quennell, 1958; Freund and others, 1970; Garfunkel, 1981; Hatcher and others, 1981; ten Brink and others, 2007). Figure 2-16 shows approximate boundaries that limit the permissive tract on cross sections. The steep topographic rise just east of the Dead Sea Transform Fault, near Feinan in Jordan (cross section C-C' in figure 2-16), accounts for the relatively small area of the permissive tract above 2 km depth in Jordan. In contrast, the area of permissive rock within 2 km of the surface is larger on the Israeli side of the transform. The cross sections show that dips are shallow on both sides of the transform. A 50-km-wide belt of rocks, including the Feinan deposit and parallel to the facies change, was extended east into Jordan and truncated where permissive-formation depths exceed 2 km (Rybakov and Segev, 2004). From the Timna area, the tract was extended to the west as far as the subsurface projection of permissive units to a depth of 2 km (Rybakov and Segev, 2004). The depth limit (fig. 2-15) defines the north-northwestern tract boundary.

The tract was extended westward across the Sinai Peninsula to include eight copper occurrences that are in outcrops of the Cambrian Nasib Formation. On the west side of the Red Sea, the tract was extended to include the Wadi Araba occurrence in the eastern desert of Egypt (fig. 2-15). The southern boundary of the tract connects the Har Amram unmineralized outcrops south of Timna (fig. 2-15) with the southern part of the area of copper occurrences in the Nasib Formation of Egypt. A belt of Cambrian outcrops that crosses the Sinai Peninsula to the south and east is excluded. Also excluded are unmineralized outcrops preserved in horst blocks along the coast of the Gulf of Suez. Lastly, an area of unmineralized Cambrian outcrops in the eastern desert south of Wadi Araba is excluded. All three of these outcrop areas are excluded because no copper minerals are observed in outcrop, so it is clear they are not permissive for undiscovered copper. Nonetheless, a sizable part of the tract lies to the north and north-west of the Wadi Araba occurrence.

## Deposits and Occurrences

Cambrian sedimentary rocks in Egypt, Israel, and Jordan host 4 deposits and 12 occurrences (figs. 2-15 and 2-17; table 2-3). Archaeological studies have established that the Feinan area in Jordan and the Timna area in Israel were among the first copper deposits mined on a small industrial scale (fig. 2-17; Rothenberg and Merkel, 1995; Weisgerber, 2006; Hauptmann, 2007). More than 100 chalcolithic mines in the Feinan area date from the fourth millennium B.C. (Weisgerber, 2006). Distinctive pieces of tile ore found at the chalcolithic metallurgical site of Shiqmim in the northern Negev Desert (Golden and others, 2001) resemble ores unique to the massive brown sandstone of the Umm Ishrin Formation (fig. 2-13) at Feinan (Rabb'a and Nawasreh, 2006). An extensive trade network may have brought raw materials from Feinan to Shiqmim

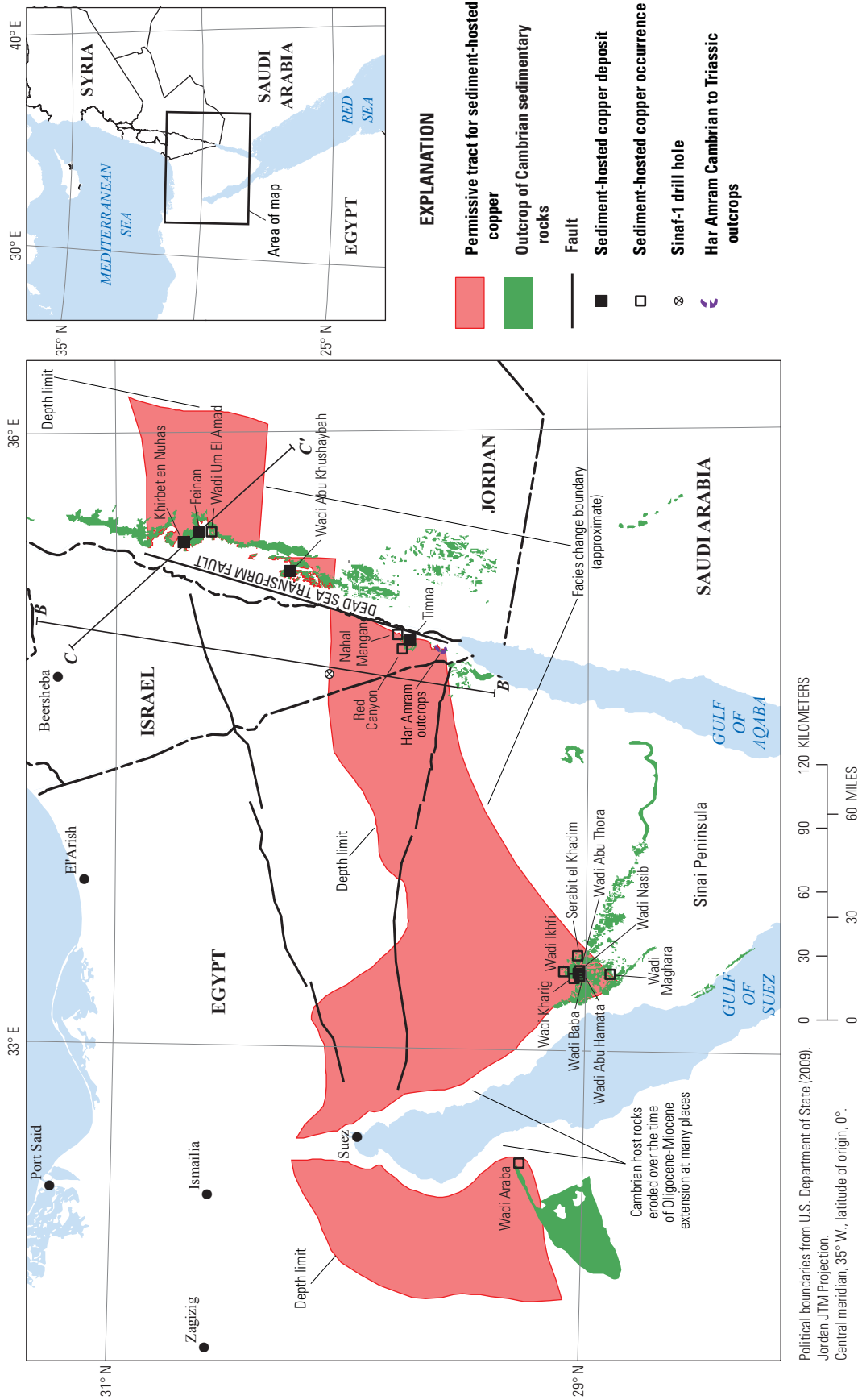


**Figure 2-15.** Map showing sediment-hosted copper permissive tract, deposits, and occurrences in Early to Middle Cambrian rocks in the Egypt–Israel–Jordan Rift, Egypt, Israel, and Jordan. Cross sections B–B' and C–C' are shown in figure 2-16.





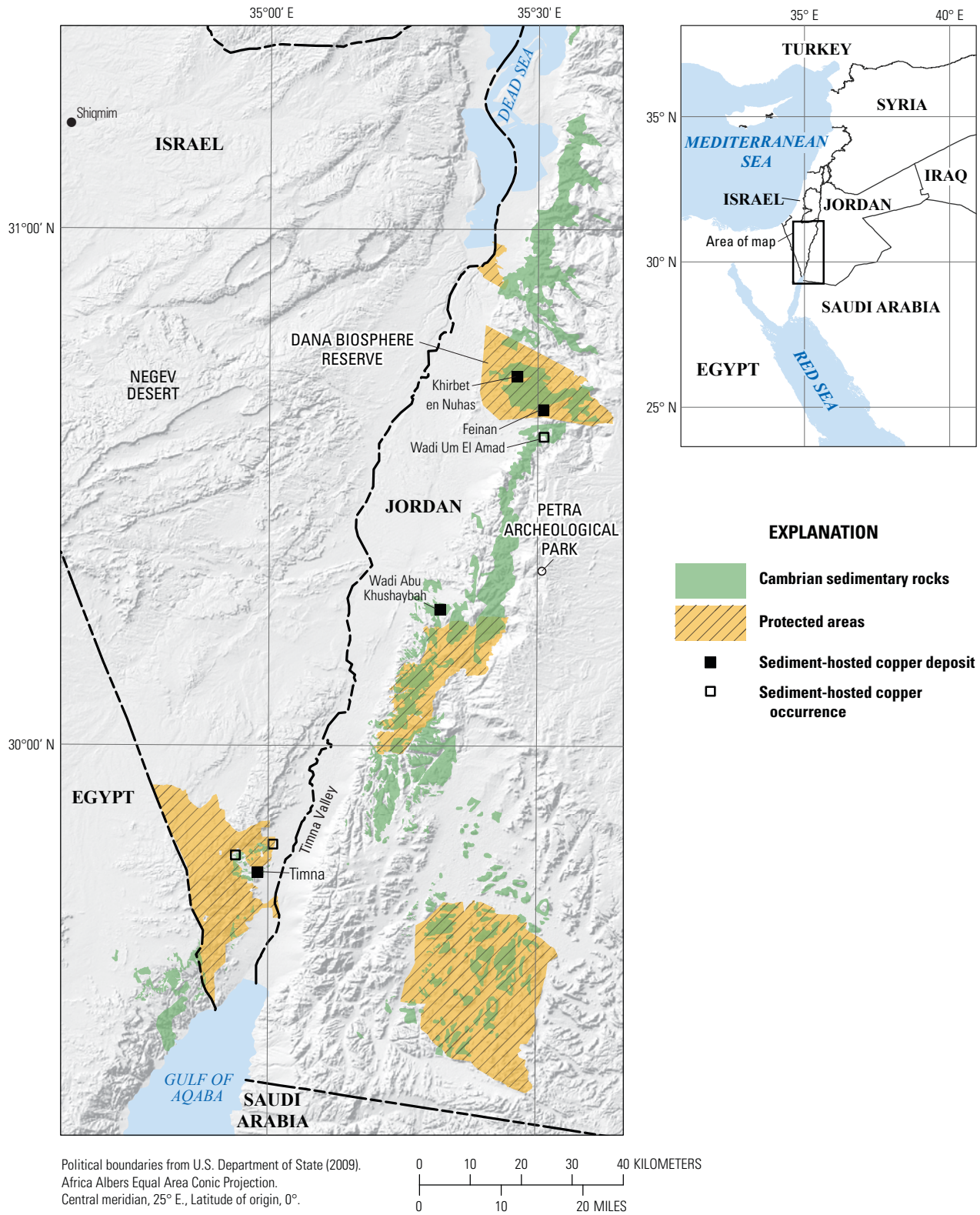


**Figure 2-17.** Map showing the relation between Cambrian sedimentary host rocks and associated sediment-hosted stratabound copper deposits and occurrences to protected areas in Israel and Jordan. Protected areas from <http://www.protectedplanet.net/>.

**Table 2-3.** Sediment-hosted stratabound copper deposits in Early to Middle Cambrian rocks of the Egypt–Israel–Jordan Rift in Egypt, Israel, and Jordan.

[Abbreviation of mineral names: Az, azurite; Ccl, chrysocolla; Dj, djurleite; Holcor, hollandite–coronadite solid solution; Mal, malachite; Patc, paratacamite; Pyl, Pyrolusite. Mt, million metric tons; %, percent]

Name	Latitude	Longitude	Country	Major commodities	Ore minerals	Resources (unmined)	Citation
Reduced-facies deposits							
Feinan	30.643	35.508	Jordan	Cu, Mn	Ccl, Mal, Az, Pyl, Holcor	35.7 Mt at 1.36% Cu	Nimry (1973); Kirkham and others (1994); Rabb'a and Nawasreh (2006)
Khirbet en Nuhas	30.681	35.436	Jordan	Cu	Ccl, Mal, Az	25 Mt at 2.33% Cu	Rabb'a and Nawasreh (2006)
Timna	29.767	34.950	Israel	Cu, U, Zn	Dj, Patc, Ccl, Mal, Pyl, Holcor	28.4 Mt at 1.51% Cu (see text)	Amit Segev, Geological Survey of Israel, oral commun., 1986; Segev and Beyth (1986); Kirkham and others (1994); Rabb'a and Nawasreh (2006)
Sandstone-copper deposit							
Wadi Abu Khushaybah	30.262	35.318	Jordan	Cu	Ccl, Mal, Az	8 Mt at 0.65% Cu	Rabb'a and Nawasreh (2006)

and similar chalcolithic sites near Shiqmim in the southern Levant<sup>5</sup>.

During the third millennium B.C., mining at Feinan shifted from copper ores in the Massive Brown Sandstone to dolomite-limestone-shale, and large-scale smelting was done on site (Weisgerber, 2006). Excavations of the Iron Age copper production site at Khirbat en-Nahas (Feinan) provide the first stratified radiocarbon dates from the Biblical region of Edom (Levy and others, 2004). Use of the deposits at Feinan and Timna continued through the heights of the Egyptian and Assyrian civilizations, reaching historical peak production during the time of Roman occupation (beginning about 64 B.C. and ending about the middle of the 4th century A.D.).

In 2004, Mexican steel producer Altos Hornos de México SA (AHMSA), set up a subsidiary in Israel named Arava Mines and conducted a study to determine if Timna could become productive using solvent extraction-electrowinning. At one point, AHMSA reported resources of more than 500 million metric tons of ore at an unannounced grade (Altos Hornos de México, 2008). The Israeli government initially offered a grant to support the reopening effort but later rescinded the offer. In response, AHMSA suspended their work at Timna in 2009 (Coren, 2009).

In Jordan, the Feinan deposit and adjacent areas were explored following the work of Bender (1965, 1975a). Trenching and drilling by the Mining Division of the Jordanian Natural Resources Authority during 1966, 1967, 1972, and 1973 led to the delineation of 19.8 million metric tons of measured and indicated resources with an average grade of

1.36 percent copper and another 15.9 million metric tons of inferred resources at the same grade at Feinan (Nimry, 1973). Subsequent trenching identified 25 million metric tons of inferred resources at 2.33 percent copper at Khirbet en Nuhas and average grades of about 0.8 percent copper in near-surface mineralization at Wadi Umm El Amad. Research by the Jordanian Natural Resources Authority also identified 8 million metric tons of 0.6 percent copper in sandstones at Wadi Abu Khushaybah (Rabb'a and Nawasreh, 2006). Both the Feinan and Khirbet en Nuhas deposits are unlikely to be mined in the near future because they are within the Dana Biosphere Reserve (also known as Dana Nature Reserve). Wadi Umm El Amad and Wadi Abu Khushaybah are better candidates for future mining because they are outside the Dana Biosphere Reserve and the Petra Archeological Park, a World Heritage Site (fig. 2-17).

The Egyptian copper occurrences in western Sinai include the minerals malachite, chrysocolla, atacamite, azurite, turquoise, langite, spangolite, shattuckite, and crednerite, in descending order of approximated abundance (Hilmy and Mohsen, 1965). Several of the occurrences were turquoise mines for the pharaohs. Serabit el-Khadim (fig. 2-15) is the location of a shrine to the Egyptian goddess Hathor, also known as the “Lady of Turquoise” (Lanckester, 2012). Carved reliefs that date to the third dynasty pharaohs Djoser (2668–2649 B.C.) and Sneferu (2649–2609 B.C.) were discovered at Wadi Maghara (Rothenberg, 1979). Wadi Maghara is a World Heritage Site, and Serabit el-Khadim is an Egyptian national monument.

<sup>5</sup>The eastern part of the Mediterranean, with its islands and adjoining countries.

## Mineral System Components

A copper source, evaporite-bearing rocks, oxidized subsurface fluids, and confining rocks likely were present in the Egypt–Israel–Jordan mineralizing system. Specific copper source beds for this area are not identified. By analogy with other reduced-facies mineralizing systems, the Salib, Amudei Shelomo, and Serabit el-Khadim units contain coarse, arkosic red beds that are candidates for the rocks from which copper was leached (fig. 2-13). Upper Neoproterozoic and Lower Cambrian evaporite minerals (for example, the Hormuz of the Persian Gulf region (fig. 2-11) were deposited in areas to the east and perhaps north of the copper host rocks. The nearest known evaporite minerals are found about 675 km east to northeast of Feinan, between Ar Rutbah and Ar Ramādī, Iraq (Jassim, 2006, p. 93). These evaporite minerals could have partially dissolved in the subsurface to provide highly saline groundwater needed to transport copper in high concentrations (Rose, 1976). Oxidizing metalliferous brines likely dewatered from near the Cambrian depocenters to the north and then moved upsection to the south, dissolving copper from the Amudei Shelomo and Salib coarse arkosic red beds and perhaps subjacent copper-rich basement rocks (Burgath and others, 1984).

Mineralization may have formed in the Early Devonian from a gravity-driven fluid circulation system that developed when the northern basin margin was tectonically elevated. Metal-rich dolomite in the Timna Formation and barite and (or) apatite in the Shehoret sandstone (Weissbrod and Nachmias, 1986) could be alteration products that mark some of the paths taken by the metalliferous brines. A thermal event at 380–365 Ma possibly dates this second mineralization, which was recorded by annealed zircons in the sandstone (Vermeesch and others, 2009) and by illite in dolostone (Segev and others, 1985).

Metalliferous brines likely reacted with the organic matter in the Timna Formation and equivalents in Egypt and Jordan, thereby reducing sulfate to sulfide and precipitating copper as sulfide minerals. Marine carbonaceous strata of the Burj, Timna, and Middle Araba Formations overlie continental clastic Salib, Amudei Shelomo, and basal Middle Araba and Serabit el-Khadim Formations. The stratigraphic bases of the Timna Formation in Israel, Burj Formation in Jordan, and Nasib Formation in Egypt are laterally continuous flooding

surfaces (marine transgressive disconformities) that are considered to be confining beds as well as host rocks.

## Principal Sources of Information

The permissive tract was delineated using geologic maps ranging in scale from 1:20,000 to 1:5,000,000 (table 2-4). Information on deposits and occurrences was obtained from various cited published reports, a mineral deposit database of the world (Kirkham and others, 1994), and a 1:20,000-scale geologic map of the Timna Valley (Segev and Beyth, 1986).

## Redstone Copperbelt, Canada— Assessment Tract 003rfCu3000

The Redstone Copperbelt hosts reduced-facies strat-  
abound copper deposits and occurrences in Neoproterozoic sedimentary rocks of the Mackenzie Mountains Supergroup and the Windermere Supergroup in the Mackenzie Mountains, Northwest Territories, Canada (fig. 2-18). The northwest-trending arcuate belt extends for more than 350 km. There are 3 deposits and 46 occurrences (fig. 1-6) within the Little Dal Group of the Mackenzie Mountains Supergroup and the overlying Coates Lake and Rapitan Groups of the Windermere Supergroup (fig. 2-19).

## Tectonic Setting

As a part of the Foreland Belt in the Canadian Cordillera (Monger and Price, 2002), the Mackenzie Mountains are composed of Neoproterozoic rock units that form an elongated arcuate belt striking north-northwest (Rainbird and others, 1996). This belt reflects the position of the Laurentian platform margin (fig. 2-18; Rainbird and others, 1996) and may be part of a large intracratonic basin that rifted apart in the breakup of the supercontinent Laurentia during the Neoproterozoic (Ross, 1991; Rainbird and others, 1996). Sediment accumulated in the Mackenzie platform area from the Neoproterozoic Era to at least the Devonian Period (Rainbird and others, 1996; Thorkelson and others, 2005).

Five stratigraphic packages are exposed in the Mackenzie Mountains in the Northwest Territories of Canada: (1) the

**Table 2-4.** Geologic maps used by the assessment team for the Egypt–Israel–Jordan Rift.

Map name	Scale	Citation
Geologic map of the Timna Valley	1:20,000	Segev and Beyth (1986)
Geologic map of Israel	1:200,000	Sneh and others (1998)
Geologic map of Egypt	1:500,000	Klitzsch and others (1987)
Geologic map of Jordan	1:500,000	Bender (1975b)
Geologic map of Egypt	1:2,000,000	Egyptian Geological Survey and Mining Authority (1981)
Geology of the Arabian Peninsula	1:5,000,000	Pollastro and others (1997)





Political boundaries from U.S. Department of State (2009).  
 Transverse Mercator Projection.  
 Central meridian, 120° W., latitude of origin, 0°.

#### EXPLANATION

- Neoproterozoic rocks
- Mackenzie Mountains
- Inferred position of the cratonic margin of Laurentia
- Sediment-hosted copper deposits and occurrences

0 75 150 225 300 KILOMETERS  
 0 75 150 MILES

**Figure 2-18.** Map showing the distribution of Neoproterozoic rocks in northwestern Canada, the Mackenzie Mountains, the inferred margin of Laurentia, and sediment-hosted stratabound copper deposits and occurrences of the Redstone Copperbelt. Modified from Rainbird and others (1996) and Garrity and Soller (2009).

Neoproterozoic Mackenzie Mountain Supergroup, formed in an intracratonic basin; (2) the Neoproterozoic Windermere Supergroup, deposited in rift and passive-margin settings; (3) a succession of latest Precambrian to Cambrian rocks, deposited in shelf, ramp, and deep-water settings along a passive margin; (4) Upper Cambrian to lower Silurian rocks, forming the Mackenzie Platform; and (5) Devonian rocks including shallow-water carbonate and evaporite units, which are overlain by shales (Dewing and others, 2006).

Terrane accretion in the Early Jurassic to Paleogene and Laramide Orogeny thrusting in the Late Cretaceous to early Eocene deformed the region (Chartrand and Brown, 1985). During the Laramide Orogeny, the rock units of the Mackenzie Mountains were thrust and folded into broad anticlines and synclines that are part of the Cordilleran fold and thrust belt (Chartrand and Brown, 1985).

## Stratigraphy

Neoproterozoic strata of the Mackenzie Mountains are divided into the Mackenzie Mountains Supergroup and the Windermere Supergroup (fig. 2-19; Narbonne and Aitken, 1995). The Neoproterozoic Mackenzie Mountains Supergroup (4–6 km thick) consists of shallow-water siliciclastic and carbonate strata deposited in fluvial and marine environments. From bottom to top, the Mackenzie Mountains Supergroup consists of the H1 Group (shallow-marine dolostone), the Tsezotene Formation (offshore mudstone and siltstone), the Katherine Group (cyclical, formation-scale marine siltstone and fluvial quartz arenite units), and the Little Dal Group (shallow marine carbonate and evaporite rocks) (Turner and Long, 2008). The unconformably overlying Windermere Supergroup (5–7 km thick) is made up of basal rift deposits and glacial diamictites (Coates Lake Group and Rapitan Group) that are overlain by three kilometer-scale siliclastic to carbonate cycles (Narbonne and Aitken, 1995; Rainbird and others, 1996; Batten and others, 2004).

Syndepositional Neoproterozoic subbasins in parts of the Mackenzie Mountains and Windermere Supergroups are indicated by abrupt changes in stratigraphic thickness and lithofacies patterns over short distances parallel and perpendicular to depositional strike (fig. 2-20; Jefferson, 1983; Jefferson and Parrish, 1989; Turner and Long, 2008). Unit thickness and facies patterns in the Katherine Group and the lower part of the Little Dal Group indicate that the succession developed over a segmented extensional margin marked by listric and transfer faults (Turner and Long, 2008). The Coates Lake and Rapitan Groups of the Windermere Supergroup were deposited in widening rift valleys (Narbonne and Aitken, 1995). The Coates Lake Group shows marked variation in facies and is confined to a number of embayments<sup>6</sup> that are thought to be fault-bounded subbasins (Jefferson, 1983; Jefferson

and Ruelle, 1986; Aitken, 1991). The Neoproterozoic Thundercloud Formation at the base of the Coates Lake Group consists of meter-scale cycles of red-bed siliciclastic rocks grading upward into peritidal carbonates. The overlying Neoproterozoic Redstone River Formation varies laterally from fanglomerates to red mudstones and continental evaporites from embayment margins to centers. The overlying limestone material of the Neoproterozoic Coppercap Formation was deposited in a restricted marine or lacustrine setting. The Neoproterozoic Sayunei and Shezal Formations of the Rapitan Group accumulated in widening rift basins (Narbonne and Aitken, 1995). The base of the group is strongly unconformable where it overlies the Mackenzie Mountains Supergroup (Aitken, 1991; Narbonne and Aitken, 1995). The Sayunei Formation consists of slope and deep-water red mudstone with jasper-hematite iron formations near the top of the unit (Narbonne and Aitken, 1995). Glacial processes are indicated by dropstones and extrabasinal boulders. The Shezal Formation consists of greenish boulder diamictites (Narbonne and Aitken, 1995; Hoffman and Halverson, 2011). These deposits have been correlated with the global Sturtian glacial event (Hoffman and Halverson, 2011). A major marine transgression followed the Rapitan glaciation.

The Little Dal basalt locally overlies the strata of the Mackenzie Mountains Supergroup and underlies the Coates Lake Group (fig. 2-19; Long and Turner, 2014). The lavas of the Little Dal are continental tholeiites and are thought to be part of the same magmatic event that formed the Tsezotene Sills which have a U-Pb baddeleyite age of  $779 \pm 2$  Ma (Dudás and Lustwerk, 1997). Sandeman and others (2014) propose that the Little Dal basalt and the Tsezotene sills are part of the Gunbarrel Igneous Event. Rocks related to this magmatic event extend from the Mackenzie Mountains to Wyoming and could be related to an upwelling mantle plume associated with the protracted Late Proterozoic rifting of the western margin of ancestral North America. These rocks constrained the timing of rift initiation that led to the deposition of the Coates Lake Group.

## Deposits and Occurrences

Three sediment-hosted stratabound copper deposits and 46 occurrences (table 2-5; figs. 2-21 and 2-22) are known within the Redstone Copperbelt. In 1962, the Redstone Copperbelt was discovered, and exploration was conducted by Redstone Mines Ltd. from 1962 to 1970, Cerro Mining Company of Canada from 1970 to 1972, and Shell Canada Resources Ltd. and Rio Tinto Canadian Exploration Ltd. from 1973 to 1976 (Northwest Territories Geoscience Office, 2010).

The most economically favorable sites are reduced-facies deposits and occurrences associated with the contact between continental red beds of the Redstone River and shallow marine

<sup>6</sup>Downwarped areas containing stratified rocks, either sedimentary, volcanic, or both, that extends into a terrain of other rocks (Neuendorf and others, 2005).



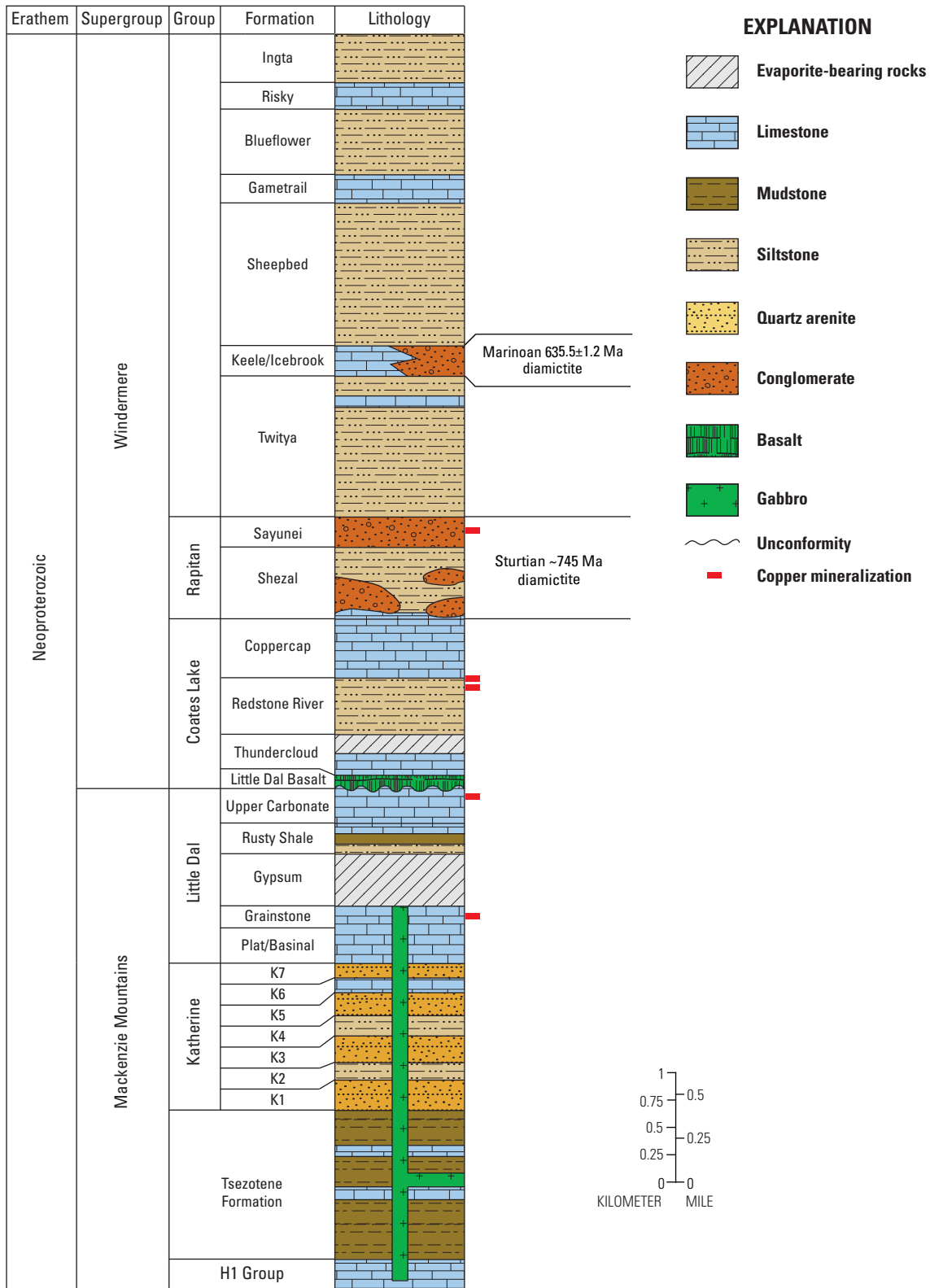


**Figure 2-19.** Stratigraphic column showing the position of reduced-facies-type copper mineralization in Neoproterozoic rocks of the Redstone Copper Belt, Mackenzie Mountains, Northwest Territories, Canada. Most deposits and occurrences are found near the contact between the Redstone River and Coppercap Formations. Modified from Jefferson (1978), Jefferson and Parrish (1989), Rainbird and others (1996), Halverson (2005), and Long and Turner (2014). Copper mineralization placement is from the current study.

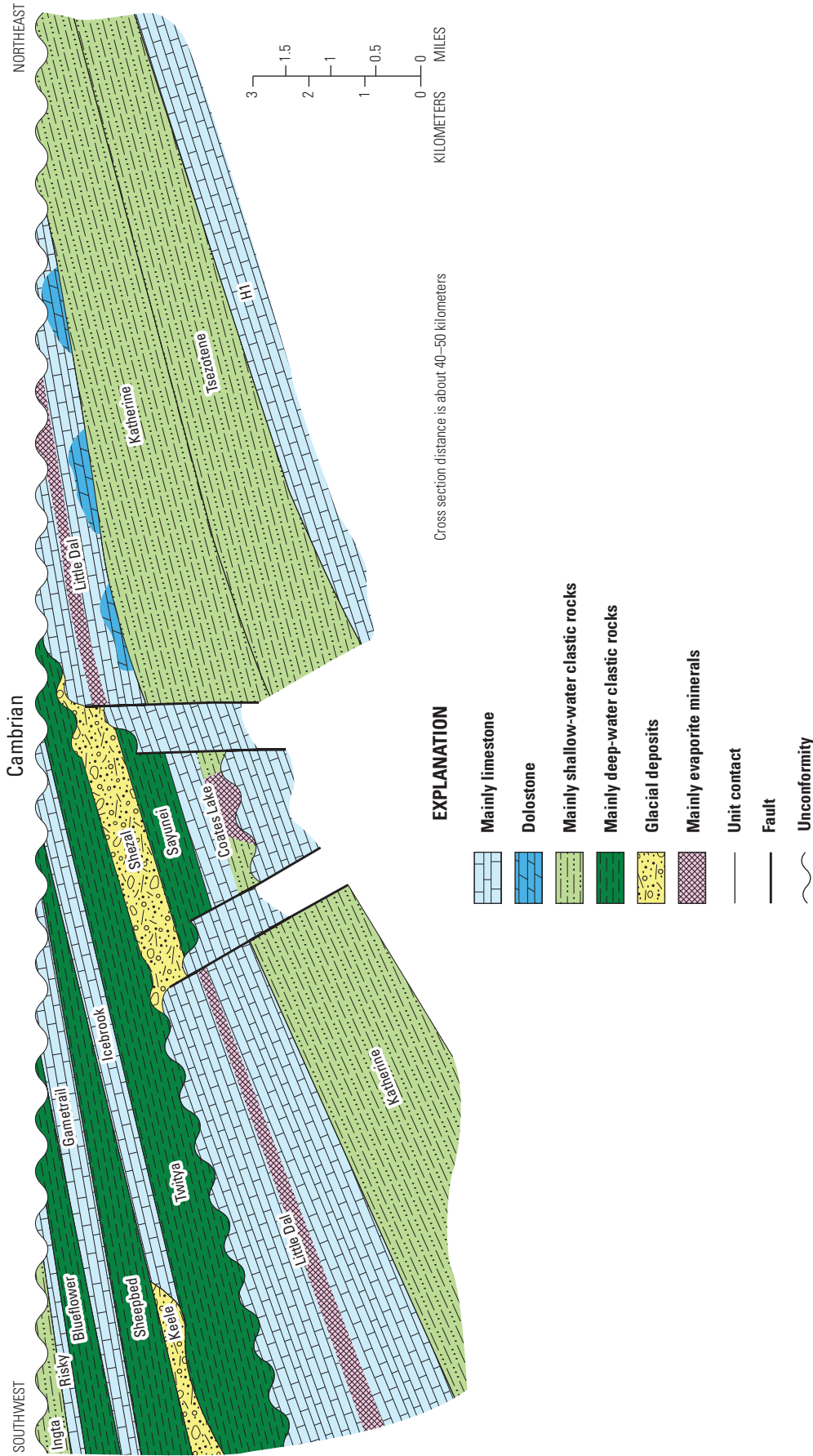


**Figure 2-20.** Schematic cross section illustrating stratigraphic relations of Neoproterozoic units in the central Mackenzie Mountains, Northwest Territories, Canada. The diagram shows that the Coates Lake Group is confined to fault-bounded subbasins (or embayments). Modified from Aitken (1991).

**Table 2-5.** Sediment-hosted stratabound copper deposits in the Redstone Copperbelt, Northwest Territories, Canada.

[Abbreviation of mineral names: Bn, bornite; Cc, chalcocite; Ccp, chalcopyrite; Cv, covellite; Dg, digenite. Mt, million metric tons; t, metric tons; %, percent]

Name	Latitude	Longitude	Ore minerals	Major commodities	Resources (unmined)	Subtype	Citation
Coates Lake	62.700	-126.627	Bn, Cc, Ccp, Cv, Dg	Cu, Ag	61.7 Mt at 2.13% Cu	Reduced-facies	Ruelle (1982); Gourlay (2005)
Jay	63.772	-127.830	Ccp, Bn, Dg, Cc, Cv	Cu	1.2 Mt at 2.7% Cu	Reduced-facies	Ruelle (1982); Kirkham and others (1994)
June Creek	63.831	-127.972	Ccp, Bn, Dg, Cc, Cv	Cu	250,000 t at 3.4% Cu	Reduced-facies	Ruelle (1982); Kirkham and others (1994)

carbonate rocks of the overlying Coppercap Formations (fig. 2-23; Ruelle, 1982; Jefferson, 1983). Deposits and occurrences are localized in areas where the Coppercap Formation overlies three fault-bounded subbasins (embayments) that have thicker accumulations of the Redstone River Formation than areas outside the subbasins (Jefferson and Parrish, 1989). The largest deposit, Coates Lake in the Coates Lake Embayment (fig. 2-22), occurs in a 1-m-thick bed that underlies an area of at least 12 km<sup>2</sup>; grade and thickness are uniform along strike (for 6,000 m) and down dip (to 2,400 m). Rock units are truncated to the west by a high-angle reverse fault (fig. 2-23). Drill-indicated resources are about 37 million metric tons, averaging 3.92 percent copper and 11.3 gram per ton of silver (Ruelle, 1982). Fully diluted, the resource estimate is 61.7 million metric tons, containing 2.13 percent copper (Gourlay, 2005). Detailed drilling on two deposits in the Keele River Embayment, Jay and June Creek, has shown that mineralization is controlled by abrupt facies changes in places and cuts facies boundaries in other places. The mineralized zones may be sinuous over kilometers. Lateral dimensions are about 100 m or less. Drill-indicated thicknesses as great as 52 m, with grading of 2.3 percent copper were found at June Creek; average thickness is 12.5 m and average grade is 2.7 percent copper for the Jay deposit (Ruelle, 1982). Resources for the Jay deposit are 1.2 million metric tons, with grading of 2.7 percent copper; the June Creek deposit has 250,000 metric tons of ore containing 3.4 percent copper (Ruelle, 1982). Mineralization is open for both deposits.

In the Coates Lake area, the transition zone between the Redstone River and Coppercap Formations is as much as 110 m thick and comprises as many as seven cycles of maroon, fine sandstone to mudstone rhythmites overlain by cupriferous, gypsiferous, cryptalgal laminated limestone beds (fig. 2-24; Jefferson, 1978). The transition zone crops out continuously for 11 km within the Coates Lake Embayment (fig. 2-22; Ruelle, 1982). The transition zone is characterized by mineral zoning (with the lowest mineralized bed containing chalcocite and minor bornite) through beds containing chalcopyrite, minor chalcocite, and minor bornite to the upper beds, which contain pyrite (fig. 2-24; Ruelle, 1982; Chartrand and others, 1989). In the Keele River and Hayhook Lake Embayment areas, the transition zone consists of a single cryptalgal-laminated unit that is as much as 8 m thick (figs. 2-21 and 2-22; Ruelle, 1982).

Copper occurrences are also found in the Redstone River Formation and the Rapitan and Little Dal Groups (figs. 2-19, 2-21, and 2-22; Jefferson, 1983; Jefferson and Parrish, 1989; Northwest Territories Geoscience Office, 2010). Examples in the Redstone River Formation include chalcocite and bornite mineralization associated with algal material and green calcareous mudstone interbeds within massive anhydrite units in playa lake facies as well as occurrences of chalcopyrite, pyrite, and minor bornite in the basal part of the fanglomerate facies (Ruelle, 1982). Vein- and breccia-hosted copper mineralization is scattered throughout the Little Dal, Coates Lake, and Rapitan Groups (Jefferson, 1978, 1983).

In 1990, Redstone Mines Ltd. reviewed data, confirmed mapping, identified drill targets, and located potential drill sites. In 2005, Lumina Resources Corporation completed an exploration program and a regional geological evaluation of the Redstone Copperbelt (Gourlay, 2005). In 2006, Western Copper Corporation acquired Lumina Resources. In 2011, Copper North Mining Corporation was formed from Western Copper Corporation and had several discontinuous claims and leases spanning approximately 100 km in a northeast-southwest orientation (Copper North Mining Corp., 2014).

## Mineral System Components

Two primary copper sources and evaporite-bearing rocks were key components to this reduced-facies copper sediment-hosted stratabound mineralizing system. Oxidized red beds of the Neoproterozoic Redstone River (Chartrand and Brown, 1985) and Rusty Shale Formations (Jefferson, 1983) are considered the original copper source for the Redstone copper mineralization (table 1-1). The Little Dal Group also contains basalt that is thought to contribute copper to some sediment-hosted stratabound copper localities (fig. 2-19; Jefferson, 1983). Evaporite minerals of the Neoproterozoic Thundercloud and Gypsum Formations (Jefferson, 1983) may have dissolved and added salinity to ascending hydrothermal fluids. Early diagenetic compaction likely initiated migration of metal-bearing fluids toward the basin margin and upward. Copper-sulfide minerals formed where groundwater containing copper chloride came in contact with pyrite (Chartrand and Brown, 1985).

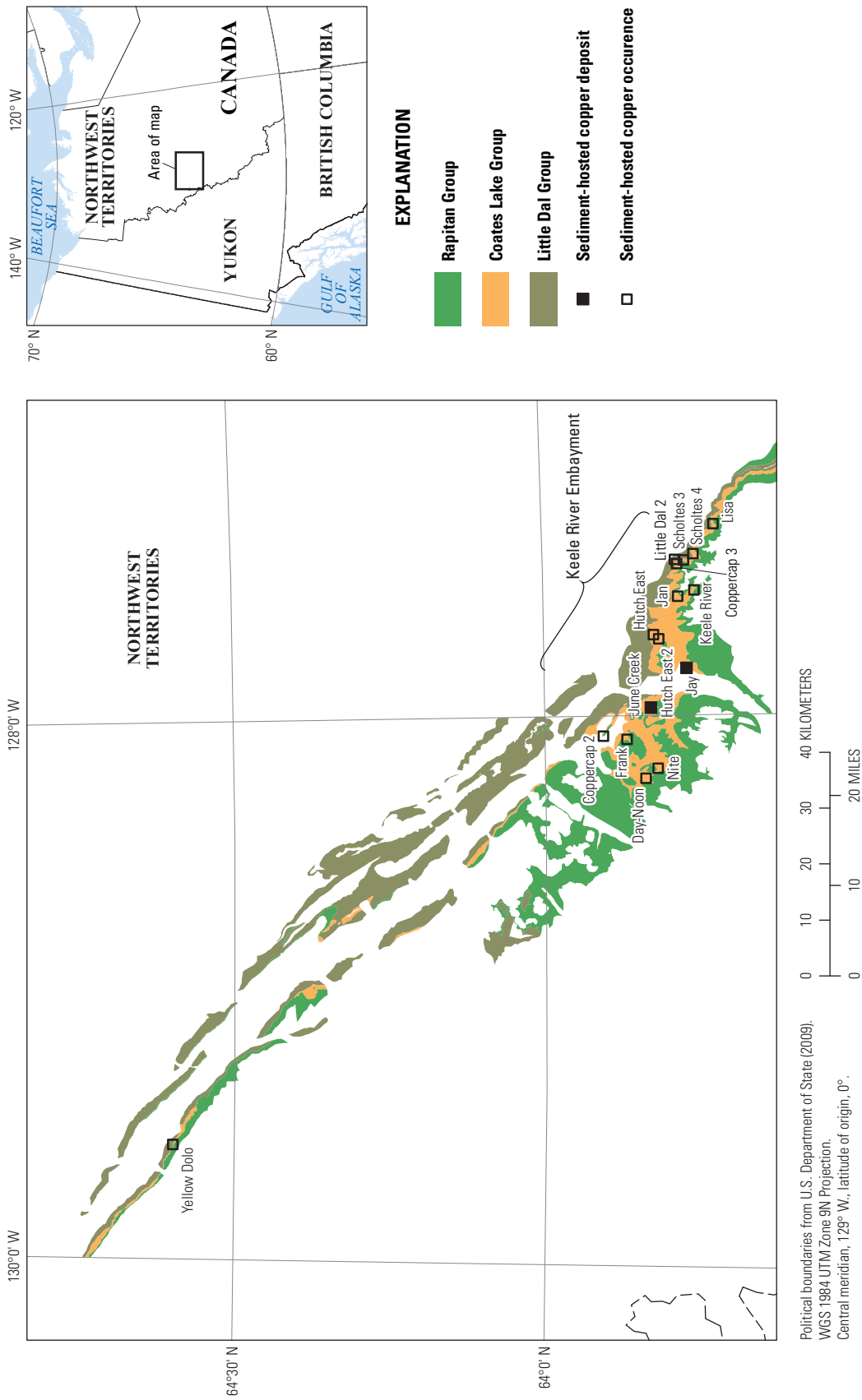


**Figure 2-21.** Map showing sediment-hosted copper permissive geologic units, deposits, and occurrences of the northern part of the Redstone Copperbelt, Mackenzie Mountains, Northwest Territories, Canada. Geology modified from Gabrielse and others (1973a,b); Jefferson and Colpron (1998); MacNaughton and others (2008); Fallas and others (2011); Gordey and others (2011a,b,c); and Roots and others (2011a,b).

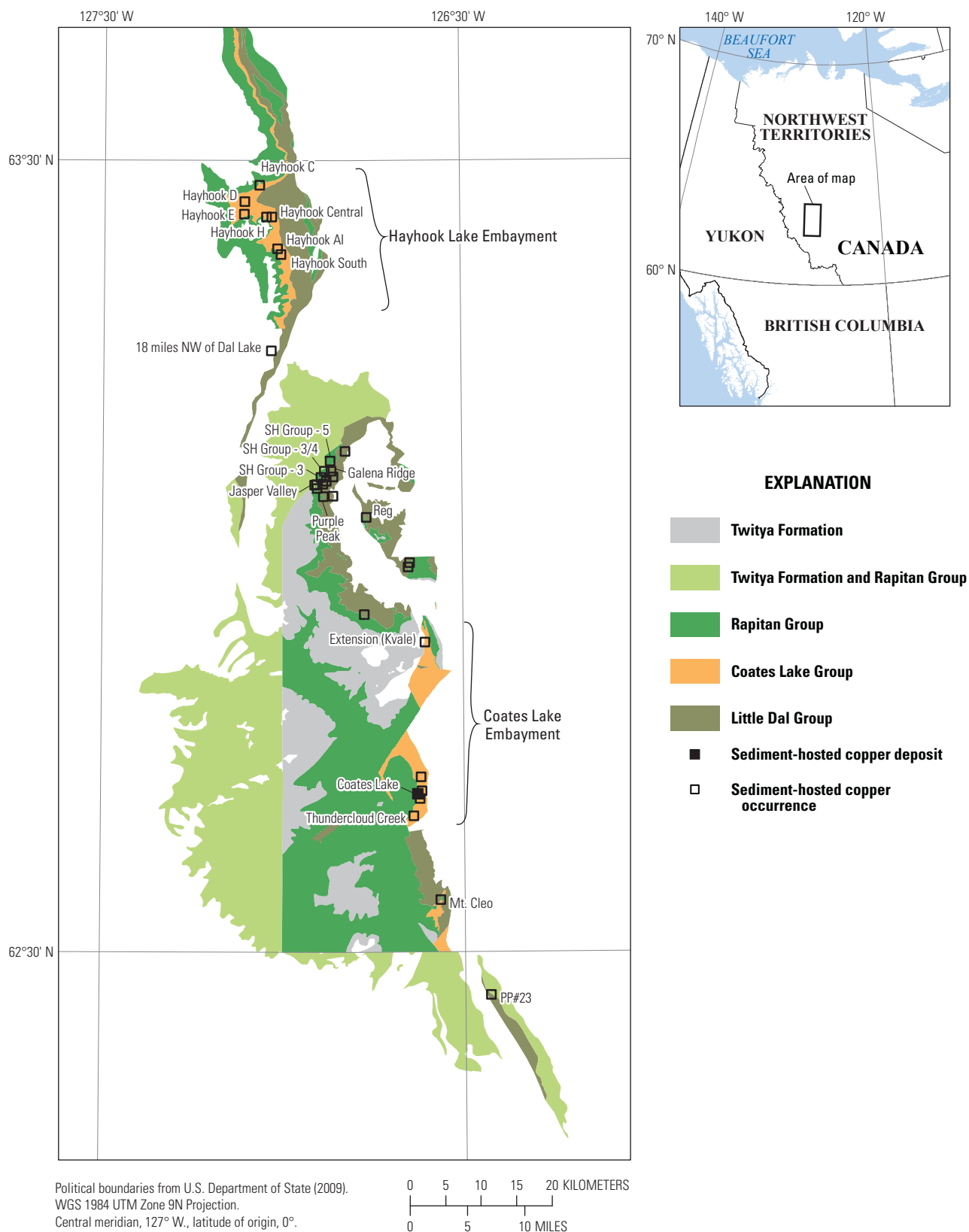


**Figure 2-22.** Map showing sediment-hosted copper permissive geologic units, deposits, and occurrences of the southern part of the Redstone Copperbelt, Mackenzie Mountains, Northwest Territories, Canada. Modified from Gourlay (2005). Geology modified from Gabrielse and others (1973a,b); Jefferson and Colpron (1998); MacNaughton and others (2008); Fallas and others (2011); Gordey and others (2011a,b,c); and Roots and others (2011a,b).



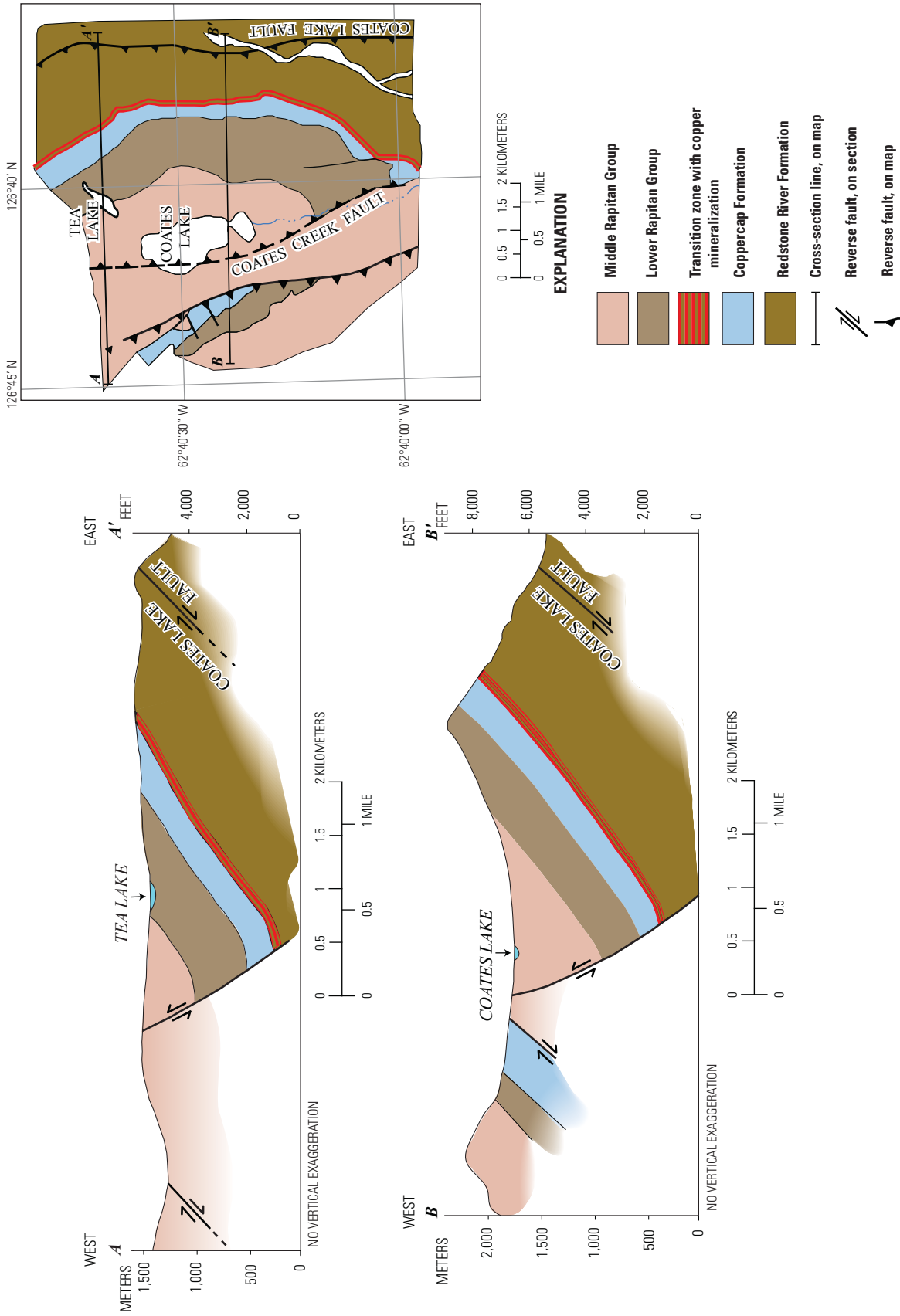


**Figure 2-23.** Map and cross sections through the Coates Lake deposit showing reduced-facies copper mineralization concentrated at the contact between the Redstone River and Coppercap Formations, Mackenzie Mountains, Northwest Territories, Canada. Modified from Gourlay (2005).

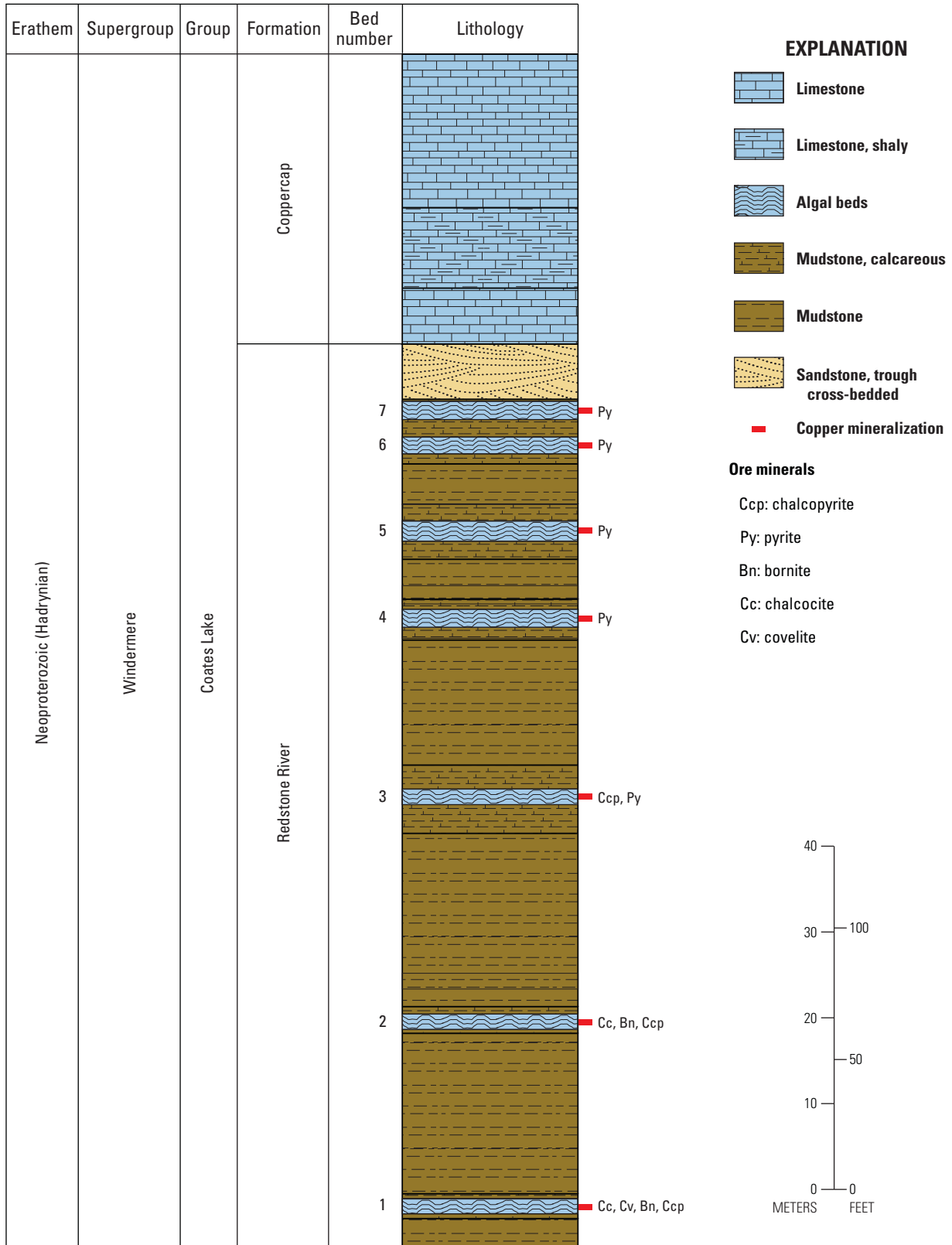


**Figure 2-24.** Stratigraphic column of the mineralized transition zone between the Redstone River and Coppercap Formations of the Coates Lake Group, Mackenzie Mountains, Northwest Territories, Canada. Modified from Jefferson (1978, 1983).

A redox boundary formed by the lithological contrast between oxidized clastic rocks overlain by reduced carbonate rocks is a fundamental component in a reduced-facies sandstone-hosted stratabound-copper mineralizing system. The contrast between gray shallow marine carbonate rocks of the reduced lower Coppercap Formation and underlying continental red-bed strata of the oxidized upper Redstone River Formation formed such a redox boundary, which is where ascending fluids precipitated sulfide minerals. The redox boundary coincides with a flooding surface that represents a marine transgression.

## Principal Sources of Information

Geologic maps, ranging in scale from 1:50,000 to 1:250,000, were used for geologic and mineral deposit information for this assessment (table 2-6). These maps were published by the Northwest Territories Geoscience Office; the Geological Survey of Canada; and the Northwest Territories Geology Division, Department of Indian and Northern Affairs. The information for the three deposits discussed in this assessment was sourced mostly from a Lumina Resources technical report on the Coates Lake copper deposit (Gourlay, 2005), Geologic Association of Canada Special Paper 25 (Ruelle, 1982), and a mineral deposit database of the world (Kirkham and others, 1994). Information for the 46 mineral occurrence sites came from the Northern Minerals Database (NORMIN) (Northwest Territories Geoscience Office, 2011), Northwest Territories geologic maps (table 2-6), and a mineral deposit database of the world (Kirkham and others, 1994). The NORMIN database maintains information on mineral showings and provides references to geology and mineral exploration in the Northwest Territories and Nunavut. Links to publicly available

sources of information, including exploration company assessment reports, are available through the NORMIN database. Numerous scientific publications describing the geology and mineral resources of the Redstone Copperbelt were also used in this assessment.

## Dongchuan Group Rocks, South Central China—Assessment Tract 142rfCu4000

Sedimentary rocks of the Paleo- to Mesoproterozoic Dongchuan Group in the Sichuan and Yunnan Provinces of south central China host reduced-facies stratabound copper mineralization. The permissive rock units extend discontinuously for about 390 km in a north-south direction with outcrop area totaling more than 2,170 km<sup>2</sup> (fig. 1-7). There are 8 deposits and 51 occurrences.

## Tectonic Setting

The Kunyang Aulacogen, an intracratonic rift, developed on the western margin of the Yangtze Craton about 2 to 1.9 Ga (fig. 2-25; Hua, 1991; Lifang, 2002; Zhao and others, 2004; Zhao and others, 2010). The rift is associated with the breakup of the supercontinent Columbia. The early stage of the rift is characterized by voluminous volcanic eruptions, which are represented by alkaline mafic rocks in the Paleoproterozoic Dahongshan Group of Yunnan and the pre-Paleoproterozoic Hekou Formation of southwestern Sichuan (Hua, 1991). Sediments were deposited into elongated grabens associated with the aulacogen (Hua, 1991; Zhao and others, 2010). The sedimentary sequence begins with terrestrial red beds that are

**Table 2-6.** Geologic maps used by the assessment team for the Redstone Copperbelt, Canada.

Map name	Citation
1:50,000-scale	
Geology of the Coppercap Mountain area	Jefferson and Colpron (1998)
Preliminary geology of the Dal Lake area	Colpron and Augereau (1998)
Geology of the Mount Kraft area	Colpron and Jefferson (1998)
1:100,000-scale	
Geology of Wrigley Lake, NTS 95M Northwest	Fallas and others (2011)
Geology of Mount Eduni, NTS 106A Southwest	Gordey and others (2011a)
Geology of Mount Eduni, NTS 106A Southeast	Gordey and others (2011b)
Geology of Mount Eduni, NTS 106A Northwest	Gordey and others (2011c)
Geology of Mount Eduni, NTS 106A Northeast	Roots and others (2011a)
Geology of Sekwi Mountain, NTS 105P Northeast	Roots and others (2011b)
Approx. 1:170,000-scale	
Portion of Plateau Fault in NTS 95M	MacNaughton and others (2008)
1:250,000-scale	
Geology, Glacier Lake, District of Mackenzie	Gabrielse and others (1973a)
Geology, Wrigley Lake area, District of Mackenzie	Gabrielse and others (1973b)

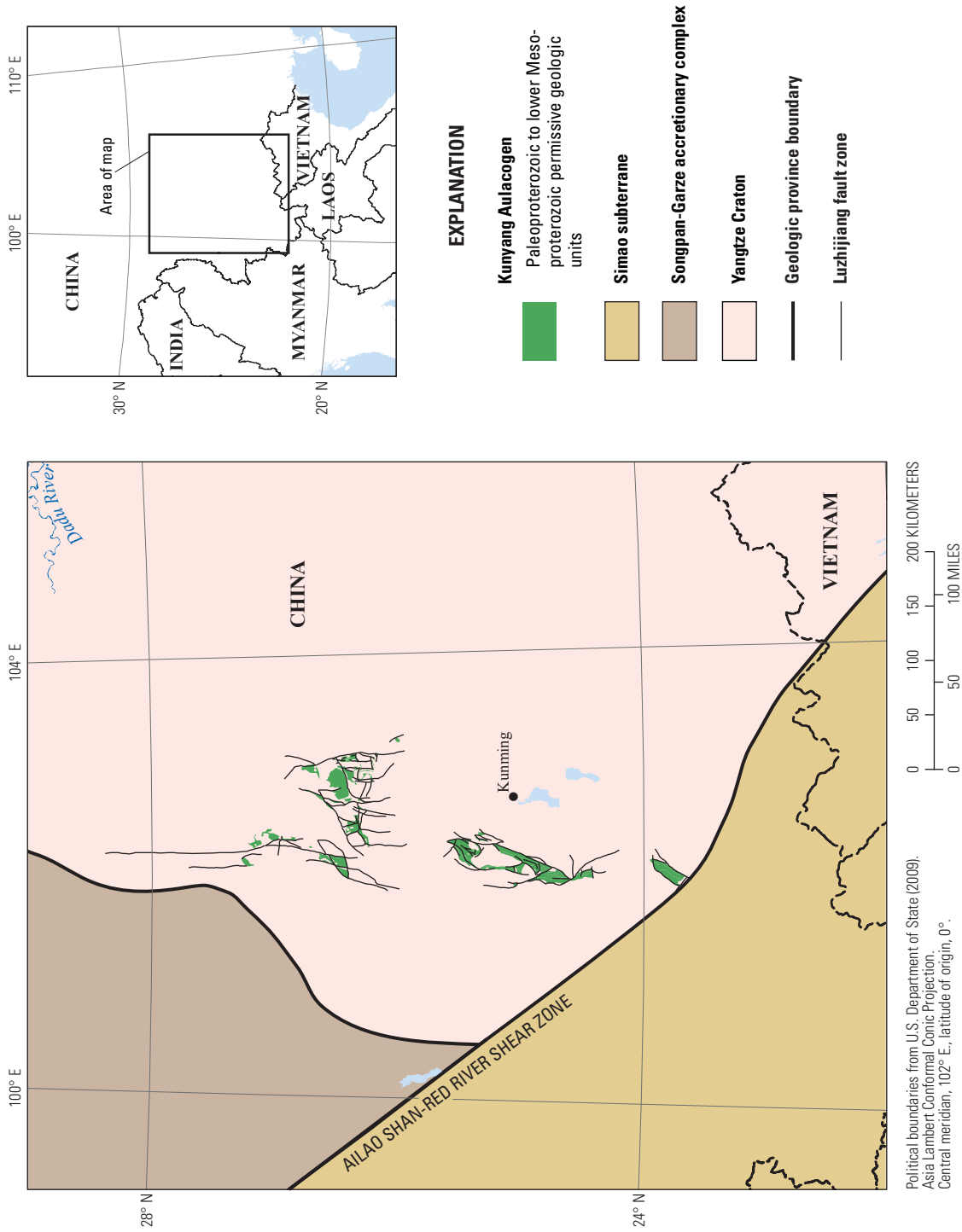


**Figure 2-25.** Simplified tectonic map showing part of the Yangtze Craton and Paleoproterozoic to early Mesoproterozoic rocks associated with the Konyang Aulacogen (Research Institute of Geology, 1982; Bureau of Geology and Mineral Resources of Yunnan Province, 1990; Bureau of Geology and Mineral Resources of Sichuan Province, 1991; Metcalfe, 2011; Pirajno, 2013).

overlain by lagoonal to tidal flat evaporite-bearing dolomitic rocks then marine black shale and carbonate rocks. These rocks were subsequently affected by the Late Proterozoic Jinning Orogeny, the Paleozoic Panxi Rift event, and the Tertiary Himalayan Orogeny (Hua, 1991).

## Stratigraphy

In the western Yangtze Craton, Proterozoic strata are distributed along the Luzhijiang Fault and bounded by subordinate north-northeast-striking faults (fig. 2-25). Fault contacts between rock packages led to confusion about stratigraphic associations; however, recent isotopic dating has clarified the stratigraphic relations of Proterozoic rocks (Chang and others, 1997; Greentree and others, 2006; Zhang and others, 2007; Sun and others, 2009; Wang and others, 2012). The following summary is based on descriptions by Sun and others (2009) (fig. 2-26). The upper Paleoproterozoic to lower Mesoproterozoic Dongchuan Group, consisting of the Yinmin, Luoxue, Etouchang, and Luzhijiang Formations, underwent greenschist facies metamorphism; rocks of the group probably formed between about 1.7 to 1.5 Ga. In central Yunnan, the upper Mesoproterozoic to Neoproterozoic Kunyang Group consists, from the base upward, of the Dayingpan, Heishantou, Dalongkou, and Meidang Formations. In Sichuan, strata equivalent to the Kunyang Group are called the Huili Group. Radiometric dates range from  $1,258 \pm 70$  to  $995 \pm 15$  Ma.

In central Yunnan, rocks of the Dongchuan Group record a change from a terrestrial to a marine or lacustrine paleoenvironment (fig. 2-26; Zhao and others, 2010). The stratigraphically lowest unit, the Yinmin Formation, has rhythmically interbedded sandstone and siltstone with a basal conglomerate layer. Except for the uppermost part of the sequence, these rocks are red beds deposited in a terrestrial fluvial environment (Ruan and others, 1991; Zhao and others, 2010, 2012). The Yinmin Formation is between 480 and 780 m thick (Zhao and others, 2010, 2012). Stratiform and discordant breccias within the Yinmin Formation are interpreted as former salt beds and salt domes (Ruan and others, 1991; Zhao and others, 2012), and the upper part of the Yinmin Formation also contains pseudomorphs of halite and anhydrite (Hua, 1993). Interbedded volcanic rocks, including tuff and basalt, are found in the Yinmin Formation in Yunnan and in the partially correlative Paleoproterozoic Limahe Formation in Sichuan (fig. 2-26).

Marine carbonate rocks of the Paleoproterozoic Luoxue and Fengshan Formations overlie the fine to coarse continental clastic rocks of the Yinmin and Limahe Formations, respectively. The Luoxue Formation is mostly limestone and argillaceous to arenaceous dolostone units that formed in a restricted marine or lacustrine depositional environment (Zhao and others, 2010, 2012). Thickness of the Luoxue Formation

ranges from 130 to 410 m (Ruan and others, 1991; Zhao and others, 2010, 2012).

## Deposits and Occurrences

Rocks hosting reduced-facies-type stratabound copper only occur in the Dongchuan Group and the stratigraphically equivalent Huili Group. Reduced-facies-type sediment-hosted stratabound copper mineralization is localized near the contact between the Yinmin and the Luoxue Formations. The Luzhijiang Formation contains minor copper deposits and a number of small zinc-lead deposits (Zhao and others, 2012). There are 8 deposits and 51 occurrences in the permissive Dongchuan Group rocks (figs. 2-27 and 2-28; table 2-7). More than 90 percent of the reduced-facies copper mineralization is in the upper part of the Yinmin Formation and lower part of the Luoxue Formation (fig. 2-29), and all deposits and occurrences reported here are in these two formations. Copper-bearing vein deposits are also located above some of the stratabound deposits (Ran, 1989a).

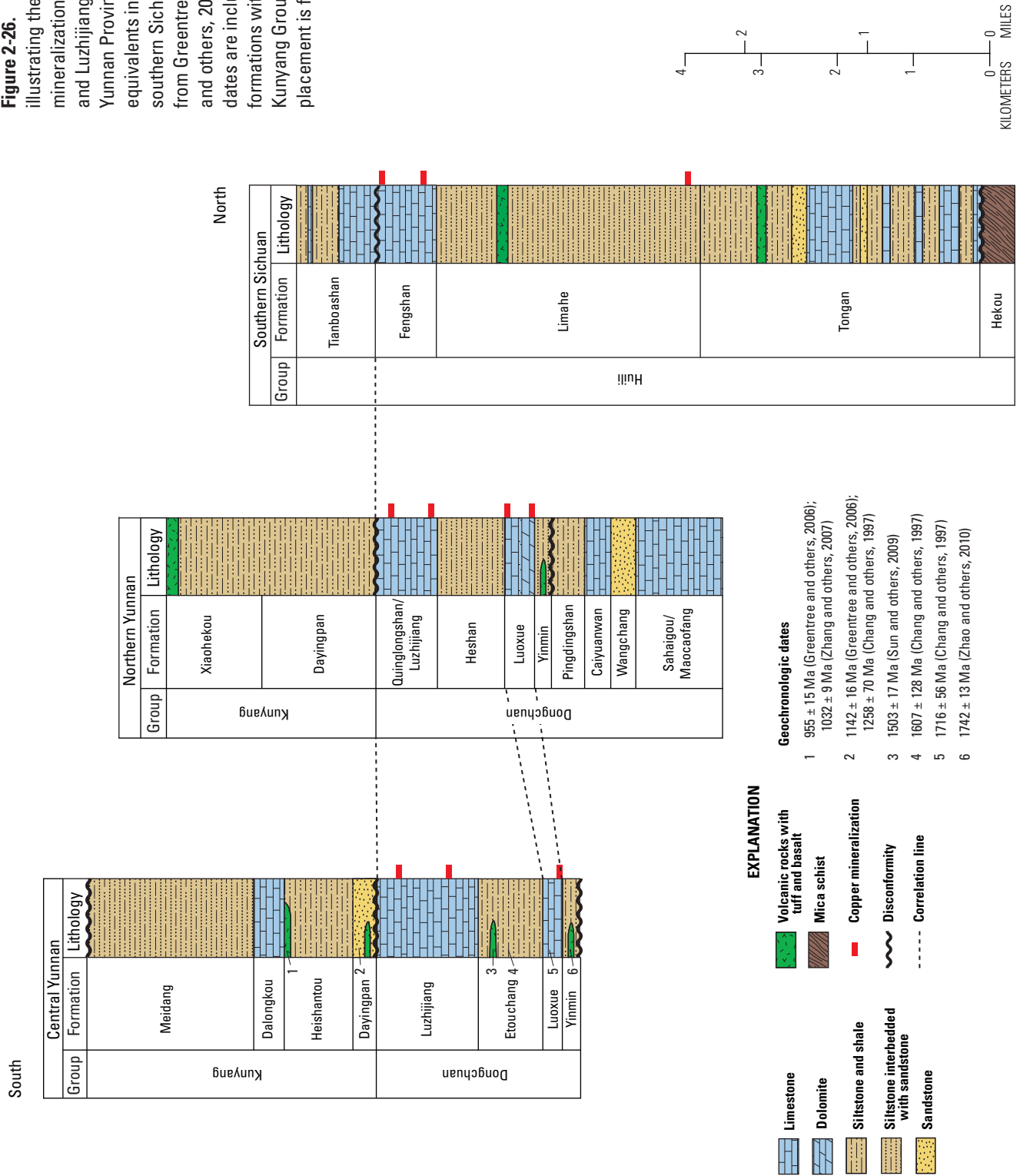
Tangdan, ShiShan, and Luoxue (table 2-7) are the largest copper deposits hosted in Dongchuan Group rocks (figs. 2-27 and 2-28). Within a cluster of deposits and occurrences in northern Yunnan (fig. 2-27), the Tangdan deposit has an estimated resource of 145.6 million metric tons of ore containing 0.87 percent copper (Hua, 1990; Yikang, 2002). To the south, in central Yunnan, the ShiShan deposit (fig. 2-28) contains 52 million metric tons of ore with 1.09 percent copper (Cox and others, 2003). The Luoxue deposit (fig. 2-27), 10 km northwest of the Tangdan deposit in northern Yunnan, has 49 million metric tons of ore containing 1.02 percent copper (Hua, 1990).

Copper-sulfide minerals and a variety of authigenic silicate and carbonate minerals fill former pore spaces along the primary lamination of stromatolites in the Luoxue Formation (Ran, 1989a,b; Ruan and others, 1991; Zhao and others, 2012). The principal ore minerals are bornite, chalcopyrite, chalcocite, digenite, and covellite (table 2-7). The most common authigenic minerals are calcite and iron-rich dolomite; less common minerals include albite, ankerite, apatite, chlorite, hematite, potassium feldspar, quartz, sericite, and tourmaline. Authigenic albite, ankerite quartz, and potassium feldspar replace host rock dolomite (Ran, 1989a; Ruan and others, 1991; Zhao and others, 2012).

Exploration in the Dongchuan mining district has an established history, and production was active as of 2014. Exploration was conducted from 1953 to 1959, and construction of the Dongchuan Mine started in 1958 (SNL Financial, 2014). Production at the Yinmin and Lanniping Mines began in 1960, at the Luoxue Mine in 1970, and at the Tangdan Mazhugong Mine in 1977. In 2001, Dongchuan Mine operators planned to double production capacity, and in 2009 the mine was reported as still operational (SNL Financial, 2014).



**Figure 2-26.** Stratigraphic columns illustrating the position of copper mineralization in the Yinmin, Luoxue, and Luzhijiang Formations in central Yunnan Province and their lateral equivalents in northern Yunnan and southern Sichuan Provinces (modified from Greentree and others, 2006; Zhao and others, 2010). Geochronologic dates are included for various formations within the Dongchuan and Kunyang Groups. Copper mineralization placement is from the current study.



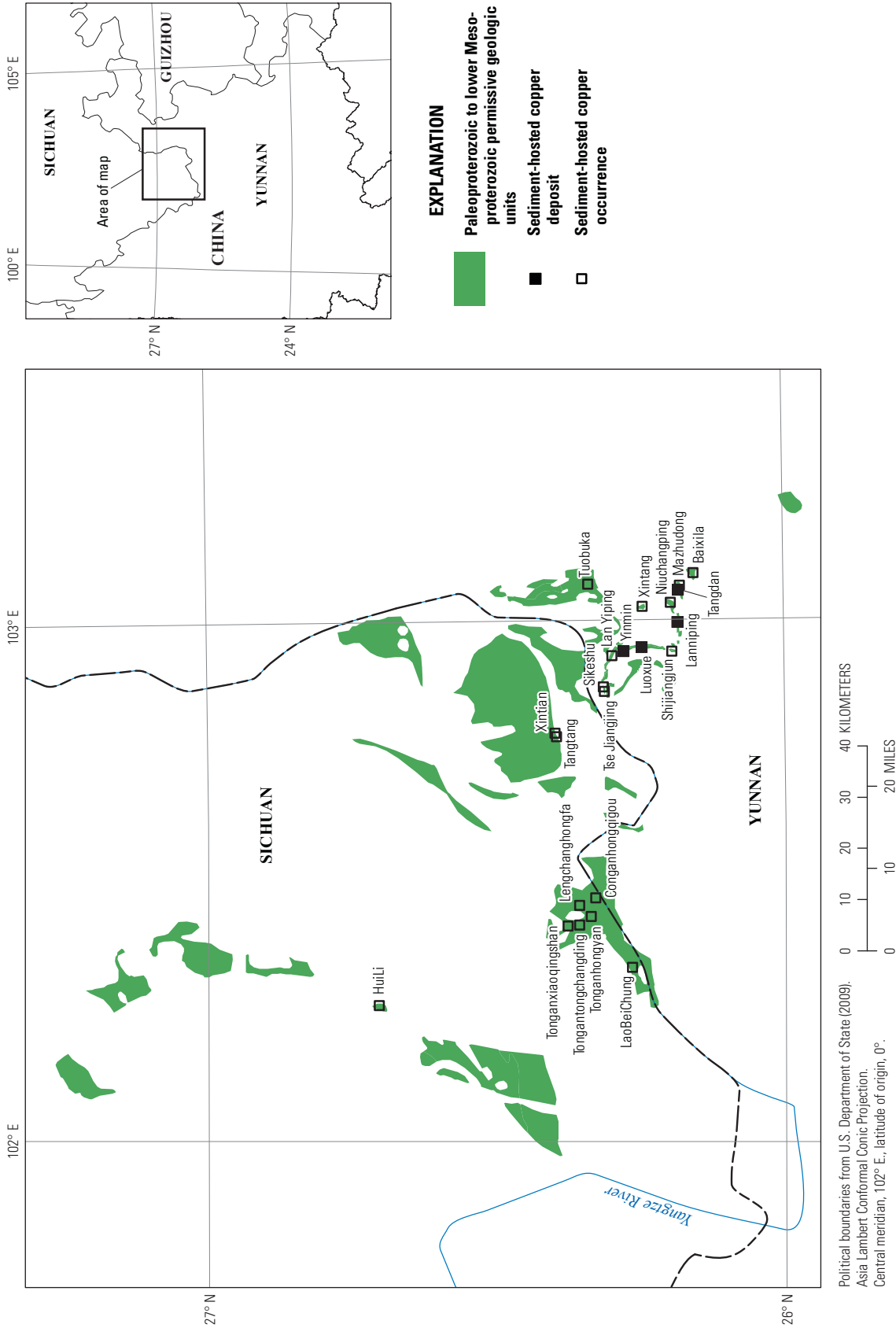


**Figure 2-27.** Map showing the northern part of permissive Paleoproterozoic to early Mesoproterozoic geologic units and associated sediment-hosted copper deposits and occurrences. Geology from Bureau of Geology and Mineral Resources of Yunnan Province (1990) and Bureau of Geology and Mineral Resources of Sichuan Province (1991).

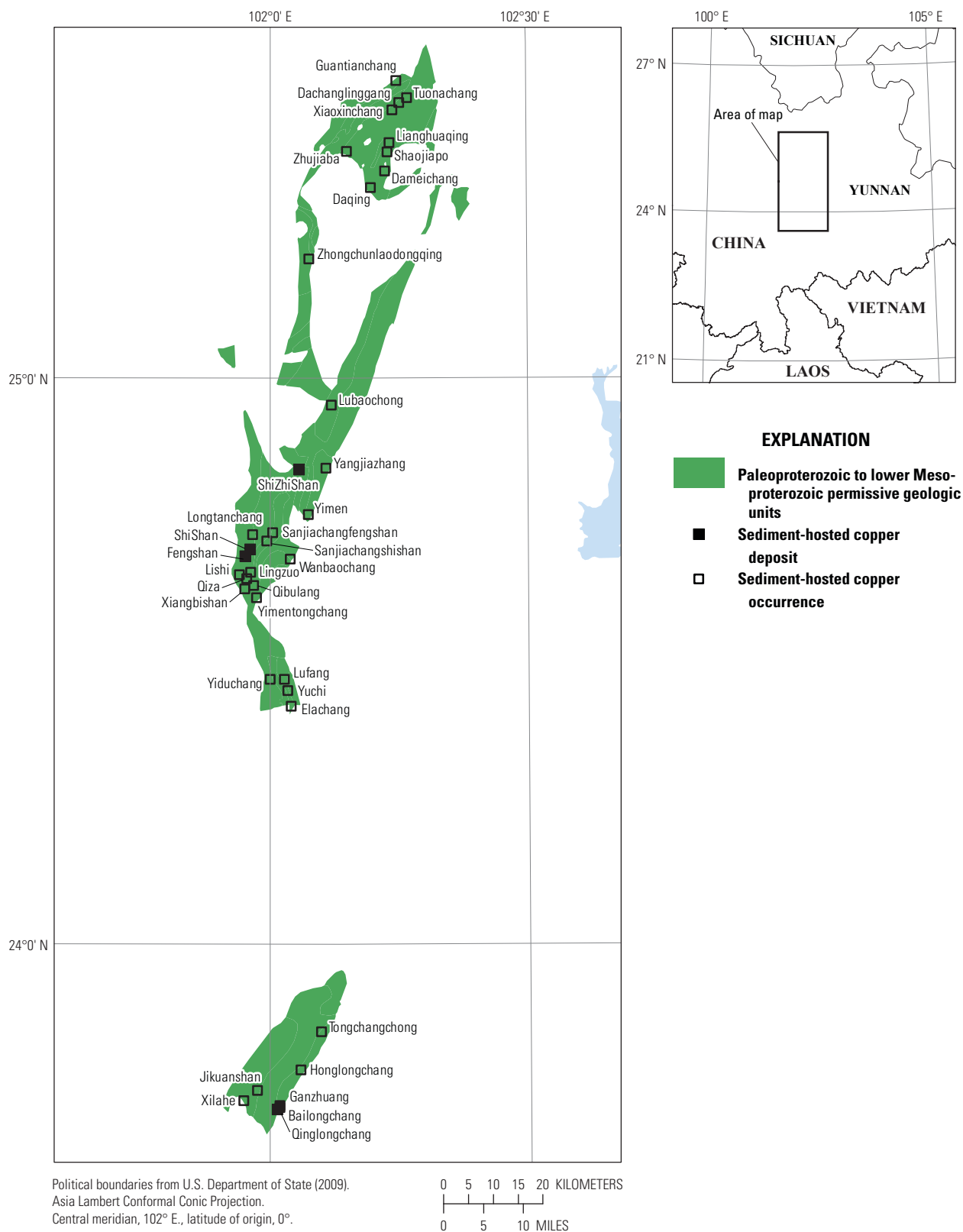
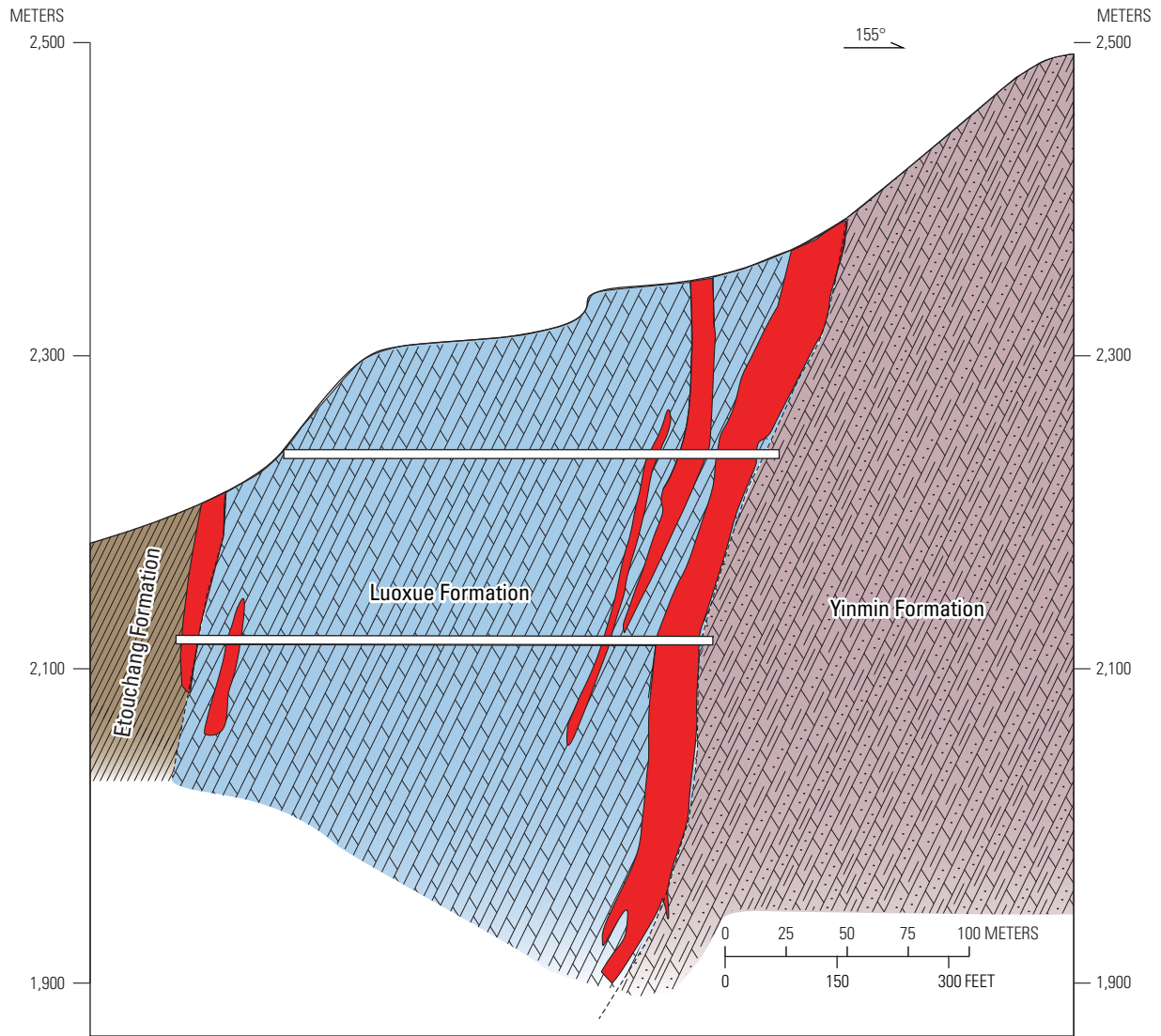


**Figure 2-28.** Map showing the southern part of permissive Paleoproterozoic to early Mesoproterozoic geologic units and associated sediment-hosted copper deposits and occurrences. Geology from Bureau of Geology and Mineral Resources of Yunnan Province (1990) and Bureau of Geology and Mineral Resources of Sichuan Province (1991).

**Table 2-7.** Sediment-hosted stratabound copper deposits within the Proterozoic Dongchuan Group rocks in north-central Yunnan and southern Sichuan, China.

[Abbreviation of mineral names: Bn, bornite; Cc, chalcocite; Ccp, chalcopyrite; Cv, covellite; Dg, digenite; Enr, enargite. Mt, million metric tons; t, metric tons; %, percent; —, no data]

Name	Latitude	Longitude	Major commodities	Ore minerals	Resources (unmined)	Citation
Fengshan	24.685	101.952	Cu	Ccp, Bn	29.0 Mt at 1.2% Cu	Bureau of Geology and Mineral Resources of Sichuan Province (1991); Yang (1996); Cox and others (2003)
Lanniping	26.185	102.995	Cu	Ccp, Bn	170,000 t at 1.26% Cu	Bureau of Geology and Mineral Resources of Sichuan Province (1991); Ruan and others (1991); Zaw and others (1999); Chang and Zhu (2002); Kirkham and others (2003); Yi-Ming and Wu (2006)
LaoXue	26.247	102.947	Cu	Cc, Bn, Ccp, Dg, Cv, Enr	49 Mt at 1.02% Cu	Hua (1990); Ran (1983); Ruan and others (1991); Cox and others (2003); Kirkham and others (2003); Yi-Ming and Wu (2006)
Qinglongchang	23.710	102.014	Cu	—	65,200 t at 0.92% Cu	Bureau of Geology and Mineral Resources of Sichuan Province (1991); Yi-Ming and Wu (2006); Yan and others (2010)
ShiShan	24.697	101.962	Cu	Ccp, Bn	52 Mt at 1.09% Cu	Bureau of Geology and Mineral Resources of Sichuan Province (1991); Yang (1996); Cox and others (2003)
ShiZhiShan	24.838	102.056	Cu	Ccp, Bn	15 Mt at 0.92% Cu	Bureau of Geology and Mineral Resources of Sichuan Province (1991); Cox and others (2003); Yi-Ming and Wu (2006)
Tangdan	26.183	103.056	Cu	Cc, Bn, Ccp, Dg Cv, Enr	145.6 Mt at 0.87% Cu	Ran (1983); Hua (1990); Ruan and others (1991); Yikang (2002); Cox and others (2003); Kirkham and others (2003); Yi-Ming and Wu (2006)
Yinmin	26.278	102.940	Cu	Cc, Bn, Ccp, Dg Cv, Enr	40 Mt at 1% Cu	Ran (1983); Hua (1990); Ruan and others (1991); Cox and others (2003); Kirkham and others (2003) Yi-Ming and Wu (2006)



## EXPLANATION

- Copper ore body**
- Etouchang Formation, carbonaceous slate**
- Luoxue Formation, stromatolitic dolomite**
- Yinmin Formation, interbedded purple slate and arenaceous dolomite**
- Mine workings**
- Approximate contact**

**Figure 2-29.** Cross section of the Tangdan deposit, a reduced-facies deposit in Dongchuan Group strata, China. Ore bodies are located along the upper and lower contacts of the Luoxue Formation and within carbonaceous slate of the lowermost Etouchang Formation. Modified from Zhao and others (2012).



## Mineral System Components

A red-bed copper source and evaporite minerals in the Yinmin Formation as well as a redox boundary were fundamental components of this reduced-facies sediment-hosted stratabound mineralizing system. The primary source for copper in the Dongchuan Group rocks was the Hekou Formation, which is an underlying volcanoclastic and clastic greenschist. Locally, the copper was probably sourced from Yinmin Formation red beds that contain high background copper concentrations (Ran, 1989a; Porter Geoconsultancy, 2011). Evaporite minerals occur in the upper part of the Yinmin Formation in the breccias that likely contributed sulfate and chloride to the metal-transporting fluids (Hua, 1991; Ruan and others, 1991; Zhao and others, 2010). The chemical contrast between the overlying reduced marine Luoxue rocks and the underlying oxidized terrestrial Yinmin rocks formed a redox boundary. Where ascending copper-rich fluids encountered the boundary, copper precipitated (Hua, 1991). In addition to the redox reactions, Zhao and others (2012) attribute copper precipitation to a decrease in pH resulting from dolomite and sulfate mineral dissolution. Minor amounts of organic matter, which can aid copper precipitation (Warren, 2000), are also present in the permissive rock units (Ran, 1990).

Mineralizing fluids likely were warm and saline within the ore-forming system that affected the Dongchuan Group. Quartz fluid inclusions from the stratiform ores have homogenization temperatures ranging from 109 °C to 209 °C with an average of 169 °C (as reported in Zhao and others, 2012, translated from Ran, 1989c). Calculated salinities of the fluid inclusions mostly are in the range of 10 to 23 equivalent weight percent NaCl, but can range as great as 35 percent for some daughter-mineral-bearing inclusions (Zhao and others, 2012). The inclusions in quartz veinlet ore become one phase (vapor or liquid) between 130 and 320 °C, with most between 200 and 320 °C. The inclusions have similar salinities to those in stratiform ore and have daughter minerals, such as NaCl (halite), CaCl<sub>2</sub> (calcium chloride), KCl (sylvite), and BaCl<sub>2</sub> (barium chloride) (Ruan and others, 1991; Zhao and others, 2012). Slate interbeds in the carbonate Luoxue, Luzhijiang, Paleoproterozoic Qinglongshan, and Fengshan Formations, or the carbonaceous slates of the Etouchang Formation, likely served as seals for ascending fluids that contained dissolved copper.

## Principal Sources of Information

A 1:5,000,000-scale mineral resource map (Zhao and Wu, 2006) and 1:1,000,000-scale geologic maps of the Yunnan and Sichuan Provinces (Bureau of Geology and Mineral Resources of Yunnan Province, 1990; Bureau of Geology and Mineral Resources of Sichuan Province, 1991) provided most of the geologic and mineral resource information for this assessment. World mineral deposit databases from the USGS (Cox and others, 2003) and Geological Survey of Canada (Kirkham and

others, 1994; Kirkham and others, 2003) provided information on mineral deposits and occurrences. Key published reports on the geology and mineral deposits of the Dongchuan Group of south central China include papers by Chang and Zhu (2002), Chang and others, (1997) and Zhao and others (2012).

## Belt-Purcell Basin, United States and Canada—Assessment Tract 003ssCu3100

Sedimentary rocks of the Mesoproterozoic Revett/Creston Formation in the Mesoproterozoic Belt-Purcell Basin of northwestern United States and southwestern Canada host sandstone-copper-type stratabound copper deposits. The Belt-Purcell Basin, which is 165,000 km<sup>2</sup> in area and 410 km long, includes 11 deposits and 36 occurrences (fig. 1-8).

## Tectonic Setting

The Mesoproterozoic Belt-Purcell Basin formed about 400 Ma after the consolidation of the Laurentian Craton (Hoffman, 1988) in a tectonic setting that is still debated. Prior to the mid 1990s, proposed settings included aulacogen, miogeoclinal re-entrant, intracratonic basin, impact basin, successor basin, and forearc basin (Link, 1993). More recently, Chandler (2000) suggested the basin formed as a passive-type intracontinental rift. Ross and Villeneuve (2003) suggest that the Belt-Purcell Basin developed within an extensional domain along a convergent plate margin. Sears and others (2004) propose that the basin is part of a large intracratonic rift system involving western Laurentia and the Siberian Craton. The tectonic setting of the basin remains controversial in part because western source areas have been removed or displaced by younger tectonic processes (Ross and Villeneuve, 2003; Sears and others, 2004).

The basin is made up of 15–20 km of marine and non-marine clastic and carbonate strata that crop out over approximately 200,000 km<sup>2</sup> in eastern Washington, northern Idaho, western Montana, southeastern British Columbia, and southwestern Alberta (fig. 2-30; Winston and Link, 1993). Belt-Purcell Supergroup rocks yield depositional dates from 1,469 to 1,401 Ma (Anderson and Davis, 1995; Sears and others, 1998; Evans and others, 2000).

The depositional history of the Belt-Purcell Basin can be divided into two phases based on sedimentation rate and source of detritus (Chandler, 2000; Ross and Villeneuve, 2003). Initially, the basin was characterized by rapid subsidence rates with sediment derived from a source outside of North America. During this rift-phase of the basin, which likely occurred from before 1,470 Ma to about 1,455 Ma, as much as 18 km of sediment was deposited (fig. 2-31; Lydon,

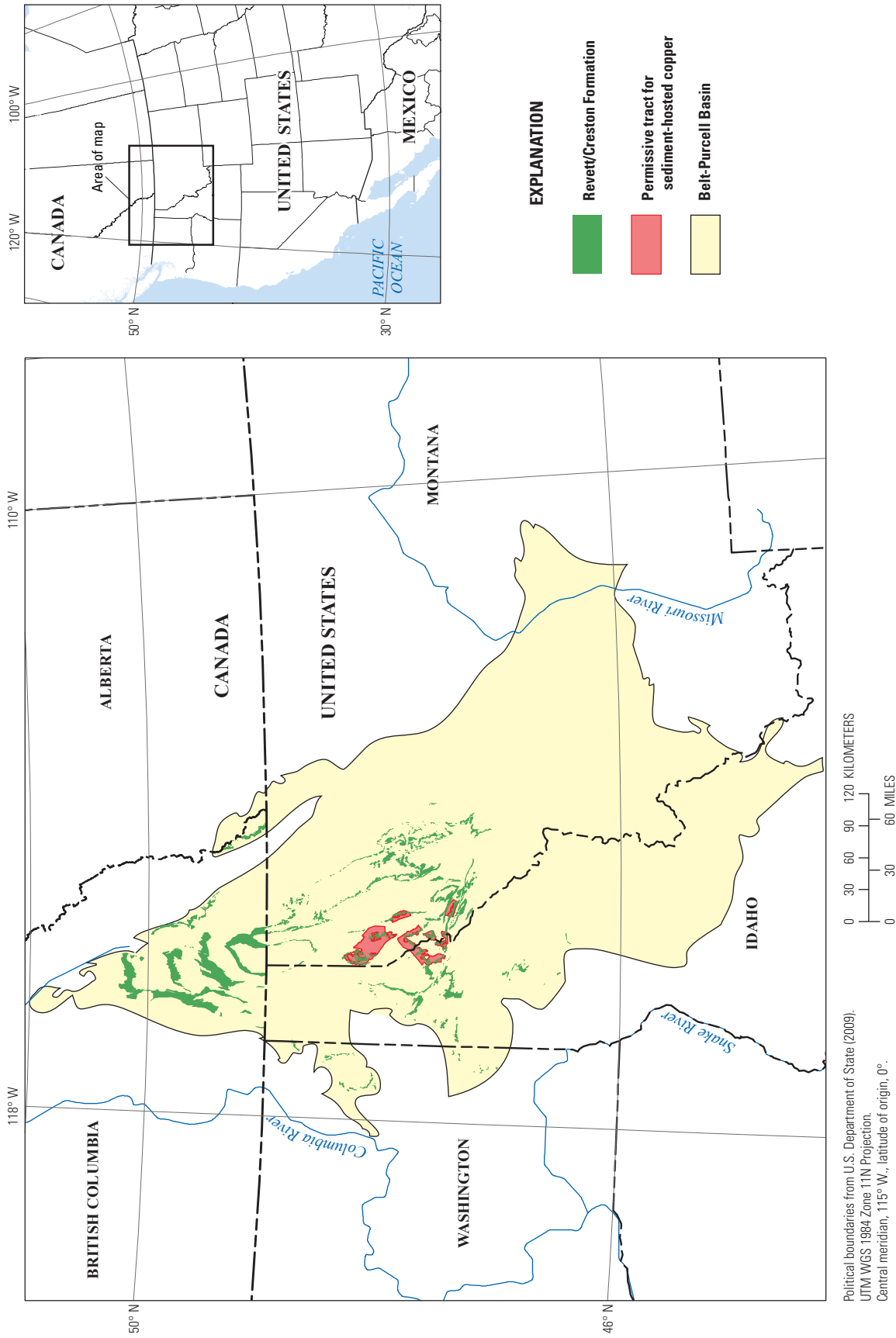


**Figure 2-30.** Map showing the Revett/Creston Formations, Belt-Purcell Basin, and sediment-hosted copper permissive tract for the Belt-Purcell Basin, northwestern United States and southwestern Canada (British Columbia Ministry of Energy, Mines and Petroleum Resources, 2001; Boleneus and others, 2005; Zientek and others, 2005; Garrity and Soller, 2009).

2007). Syndepositional faulting divided the lower Belt-Purcell Basin into subbasins along northeast-striking transform faults (Höy and others, 2000; Turner and others, 2000). This was followed by a period of deposition with lower subsidence rates with sediment derived from both Laurentian (North American) and non-Laurentian sources. During this later sag phase of the basin, only 2.4 km of sediment was deposited (Lydon, 2007).

Belt-Purcell Supergroup rocks generally display greenschist facies burial metamorphism that increases to amphibolite facies, with some partial melting (Doughty and Chamberlain, 1996). Two Mesoproterozoic deformational and metamorphic events affected some rocks of the Belt-Purcell Basin. The older event, about 1,380 Ma based on Lu-Hf ages from metamorphic garnets (Zirakparvar and others, 2010; Nesheim and others, 2012) and U-Pb ages on igneous zircons (Evans and Zartman, 1990; Doughty and Chamberlain, 1996; J. Mortensen, University of British Columbia, unpub. data, reported in Anderson and Parrish, 2000), may be related to the East Kootenay Orogeny described in western Canada where, in places, Lower and Middle Cambrian strata rest unconformably on uplifted, tilted, and mildly deformed Purcell strata (White, 1959). The younger event, from about 1,150 to 1,030 Ma based on both Lu-Hf ages of metamorphic garnets (Zirakparvar and others, 2010; Nesheim and others, 2012) and on U-Pb ages from metamorphic titanite (Anderson and Davis, 1995), overlaps in time with the Grenville Orogeny.

Neoproterozoic and Early Cambrian continental rifting that established the Cordilleran margin of Laurentia truncated the western side of the basin (Stewart, 1972). Most of the rocks of the Belt-Purcell Basin are on the upper plates of an allochthonous thrust sheet that make up the Mesozoic Cordilleran fold and thrust belt (Price and Sears, 2000). Mesozoic deformation transported rocks eastward as much as 250 km and rotated the rocks 20–30° clockwise.

## Stratigraphy

The sedimentary rocks south of the United States–Canada border are divided into four major units (fig. 2-32). At the base of the sequence, the Mesoproterozoic Prichard Formation consists dominantly of turbidites (fig. 2-31) sourced from the southwest (Winston, 1986a) and is thought to be a deep-water clastic wedge (Link and others, 2007). Overlying the Prichard Formation, the Mesoproterozoic Ravalli Group is composed of deltaic foreset and topset lithologies also derived from the southwest (Winston, 1986b) and inferred to have formed in a fluvial system (Link and others, 2007), though Hayes and Einaudi (1986) consider that coastal sandbodies are likely also present. The overlying Mesoproterozoic Piegan Group consists of carbonate-siliciclastic material that represents a complex transgressive to regressive cycle (Link and others, 2007). The overlying Mesoproterozoic Missoula Group is made up of fine-grained shallow water clastic rocks, metasandstone, and minor stromatolitic carbonate rocks; Missoula Group rocks were derived from the south (Harrison, 1972; Winston, 1986a)

and are thought to be a fluvial succession (Link and others, 2007).

Nomenclature for map units varies from place to place because of changes in facies in the basin and differences in naming conventions on either side of the border between Canada and the United States (Harrison, 1972; McMechan, 1981; Winston, 1986a,b; Höy, 1993; Raup and others, 1993).

Sandstone-type sediment-hosted stratabound copper mineralization is hosted in the Mesoproterozoic Revett Formation of the Ravalli Group. The Revett Formation forms a prism of sandy material that was sourced from the southwest. The blocky, crossbedded quartzites found at the western margin of the basin grade into crossbedded or laminated purple-gray, very fine-grained quartzite or medium- to coarse-grained siltite that is interlayered with purple or green argillite at the distal edges of the prism (Boleneus and others, 2005). The well-sorted quartzites of the Revett Formation and the correlative Creston Formation are the coarsest-grained sedimentary rocks in the lower part of the Belt-Purcell Supergroup. The Revett Formation is divided into three informal members: a lower member consisting of alternating quartzite and siltite beds, a middle member consisting dominantly of siltite, and an upper member of alternating quartzite and siltite beds.

## Deposits and Occurrences

Within the Revett/Creston Formation, there are 11 deposits and 36 occurrences of sandstone-copper-type mineralization (table 2-8; fig. 2-33; Cox and others, 2003; Boleneus and others, 2005; Hartlaub, 2009). Ore-grade levels of copper and silver are only in the coarser-grained quartzite facies of the Revett Formation, where argentiferous chalcocite, bornite, and digenite are the predominant sulfide minerals (fig. 2-34). Native silver is also present. The copper-sulfide minerals and native silver are part of a large, zoned system of authigenic and gangue minerals (Hayes and Einaudi, 1986). Ore-grade mineralization occurs where the copper-sulfide minerals and native silver form cements or replace earlier cements or clasts. In some locations, multiple mineralized intervals are found in vertically stacked sequences of quartzites and argillites (fig. 2-34B).

From the 1960s through the early 1980s, three major deposits—Spar Lake (Troy Mine), Rock Creek, and Montanore—and numerous smaller deposits were discovered within the Revett Formation in northwestern Montana (fig. 2-33). Bear Creek Mining Company used exploration geochemistry and outcrop mapping of mineralized rocks to discover the Spar Lake deposit in 1963 (Hayes, 1984) and the Rock Creek deposit in 1966 (Couture and Tanaka, 2005). The Montanore deposit was discovered by U.S. Borax and Chemical Corporation in 1983 (Ristorcelli and Fitch, 2005).

Drilling delineated resources of approximately 2.9 million metric tons of copper and about 26 thousand metric tons of silver, mostly in the Rock Creek (fig. 2-35), Montanore, and Spar Lake (Troy Mine) deposits (fig. 2-33; Boleneus and others, 2005). Montanore contains ore bodies as much as 21

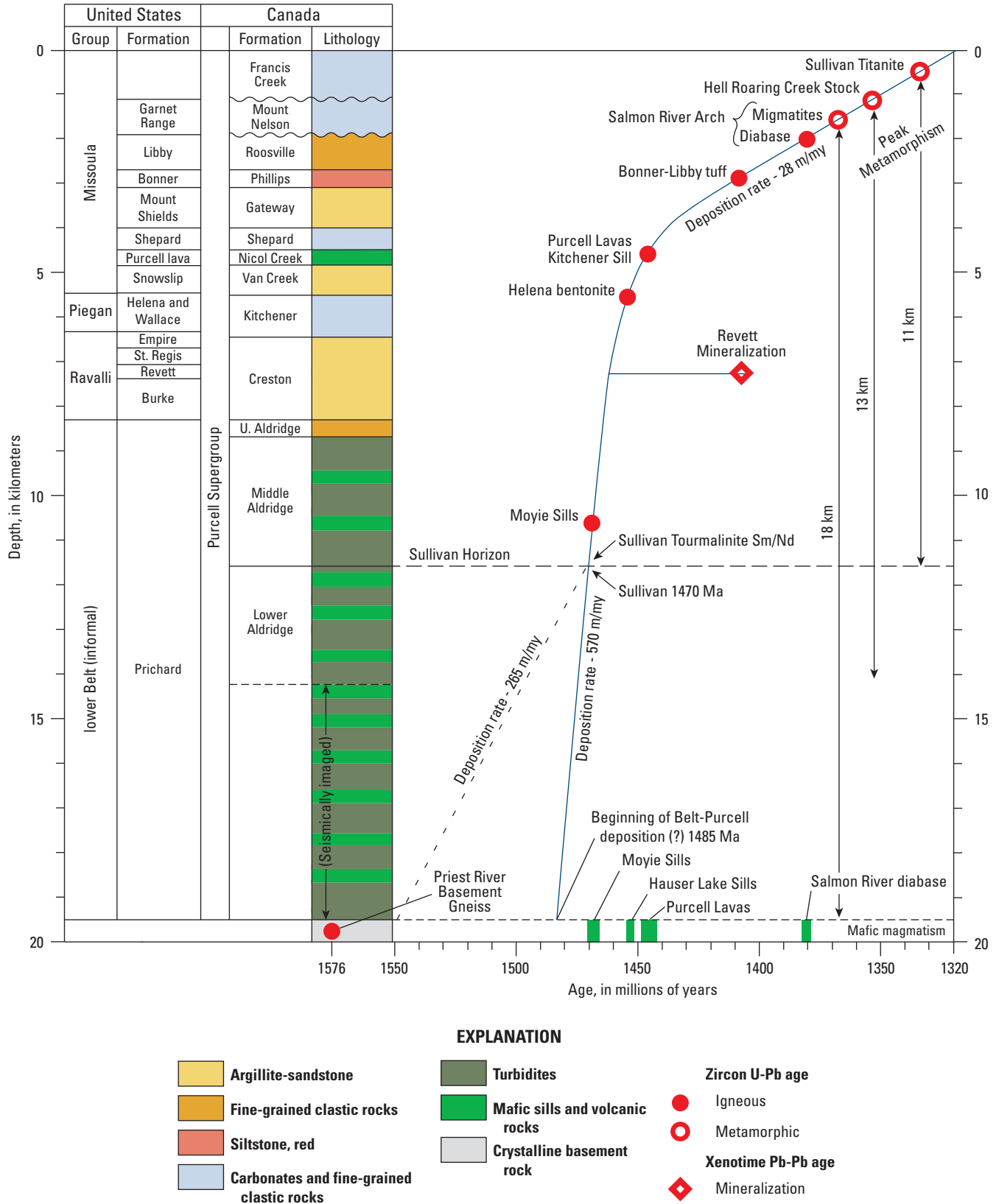
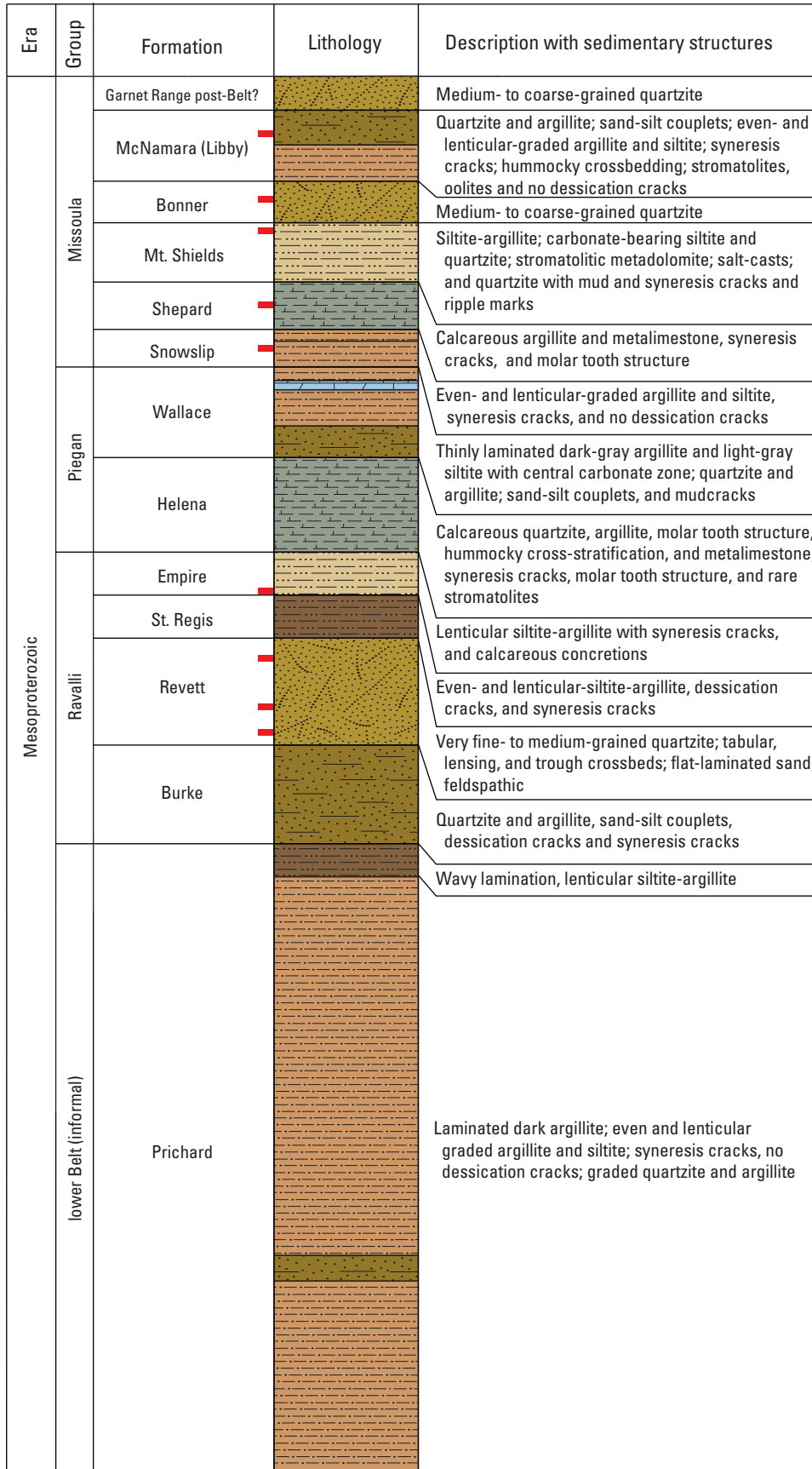


**Figure 2-31.** Diagram showing approximate thicknesses of stratigraphic divisions of the Belt-Purcell Supergroup and stratigraphic or depth-controlled events dated by U-Pb zircons, Pb-Pb titanite, or Pb-Pb xenotime methods. Geochronological data points are joined by a smoothed line that gives average accumulation rates for the Belt-Purcell Basin. Modified from Lydon (2007). km, kilometer; m/my, meters per million years; Ma, millions of years; Sm/Nd, samarium/neodymium; Pb-Pb, lead-lead; U-Pb, uranium-lead.



**EXPLANATION**

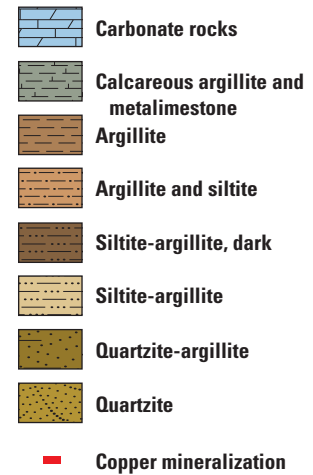


**Figure 2-32.** Stratigraphic column of the Middle Proterozoic Belt-Purcell Supergroup emphasizing sedimentary structures in the area of Revett-hosted deposits and occurrences. Revised stratigraphic nomenclature from Link and others (2007). Copper mineralization placement is from the current study.



**Table 2-8. Sediment-hosted stratabound copper deposits within the Revett Formation of the Belt-Purcell Basin, United States.**

[Abbreviation of mineral names: Bn, bornite; Cc, chalcocite; Ccp, chalcopyrite; Gn, galena; Tet, tetrahedrite. ft, feet; g/t, grams per metric ton; Mt, million metric tons; t, metric tons; %, percent; —, no data]

Name	Latitude	Longitude	Ore minerals	Major commodities	Stratigraphic subunit of the Revett Formation	Alteration minerals	Production (P) and Resources (R)	Additional deposit details	Citations
Copper Gulch	48.080	-115.709	Cc, Bn, Ccp	Cu, Ag	lower member	calcite	R: 13.6 Mt at 0.53% Cu; 52 g/t Ag	Drilled prospect	Thomas Henriksen, written commun. (1998)
Horizon Basin	48.087	-115.669	Cc, Bn, Ccp	Cu, Ag	lower member	calcite	R: 10.1 Mt at 0.6% Cu; 62 g/t Ag	Drilled prospect	Thomas Henriksen, written commun. (1998)
JF	48.199	-115.895	Cc, Ccp, Bn, Gn	Cu, Ag	lower member	calcite	R: 13.6 Mt at 0.4% Cu; 46 g/t Ag	Drilled prospect	Spanski (1992); Long and others (1998); Boleneus and others (2005)
Missoula National	47.501	-115.750	Cc, Bn, Ccp, copper oxides	Cu, Ag	lower member	calcite	R: 4.5 Mt at 0.5% Cu; 35 g/t Ag	Drilled prospect	Garth Crosby, Day Mines, Inc., written commun. (1953); Boleneus and others (2005)
Montanore	48.075	-115.642	Cc, Bn, Ccp, Gn	Cu, Ag	lower member	calcite	R: 136.7 Mt at 0.8% Cu; 76 g/t Ag	—	Long and others (1998); Boleneus and others (2005)
Niagara	47.683	-115.860	Bn, Ccp	Cu, Ag	upper member	feldspar-ankerite	R: 17 Mt at 0.47% Cu; 17 g/t Ag	—	Spanski (1992); Dennis Cox, U.S. Geological Survey, written commun. (1994); Boleneus and others (2005)
Rock Creek	48.080	-115.677	Cc, Ccp, Bn, Gn	Cu, Ag	lower member	calcite	R: 130.5 Mt at 0.8% Cu; 76 g/t Ag	—	Long and others (1998); Couture and Tanaka (2005)
Rock Peak	48.064	-115.665	Cc, Ccp, Bn	Cu, Ag	lower member	calcite	R: 9.9 Mt at 0.65% Cu; 93 g/t	Drilled prospect	Thomas Henriksen, written commun. (1999)
Spar Lake	48.230	-115.904	Cc, Ccp, Bn, Gn	Cu, Ag	upper member; additional mineralization in lower member	calcite	P: 38.65 Mt at 1,379 t of Ag and 176,538 t of Cu; R: 41.95 Mt at 0.68% Cu; 51 g/t Ag	—	Long and others (1998); Boleneus and others (2005); Revett Minerals (2009); Larry Erickson, Revett Minerals, oral commun., (2009)
Snowstorm	47.482	-115.734	Ccp, Tet, Bn, Cc	Cu, Ag, Au	upper member	—	P: 0.8 Mt yielded 128 t of Ag and 25,025 t of Cu; R: 9.1 Mt at 1% Cu; 35 g/t Ag	Historic deposit	Calkins and Jones (1914); Spanski (1992); Earl Bennett, Idaho Geological Survey, oral commun. (1993); Long and others (1998); Brian White, written commun. (1999); Boleneus and others (2005)
Vermilion River/Sims Creek	47.851	-115.370	Bn, Ccp, copper oxides	Cu, Ag	lower member	feldspar-ankerite	R: 13.7 Mt at 0.5% Cu; 31 g/t Ag	Drilled prospect	Spanski (1992); Boleneus and others (2005)

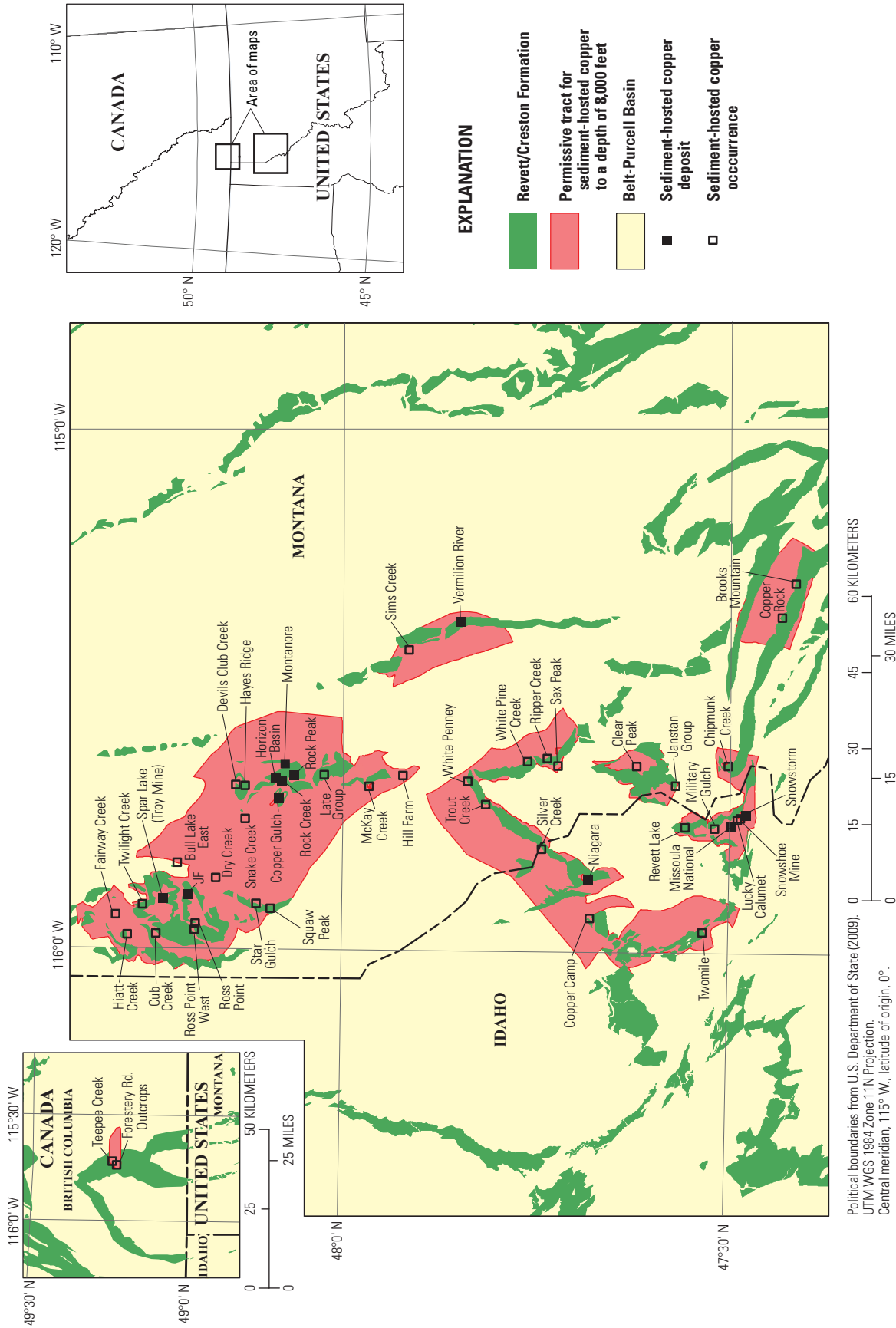
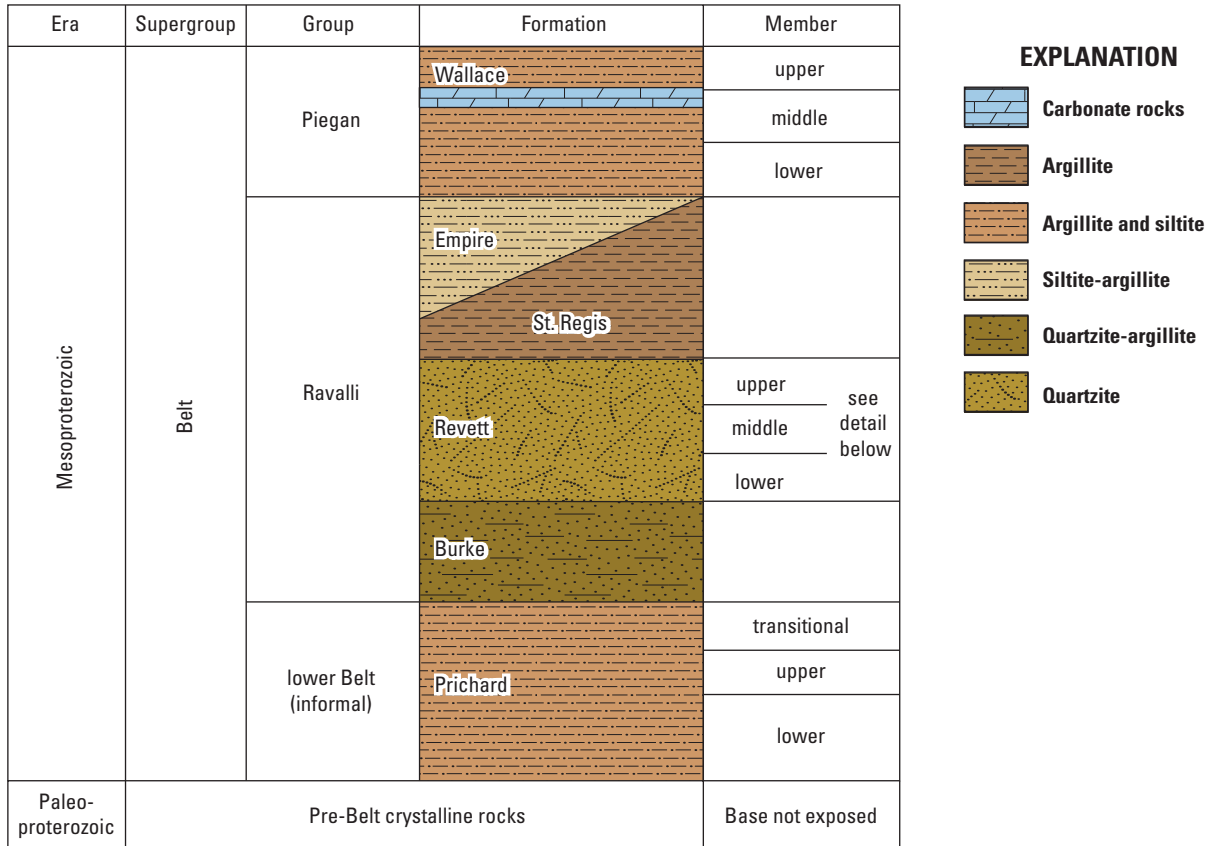


**Figure 2-33.** Map showing the sediment-hosted copper permissive tract, deposits, and occurrences associated with the Revett/Creston Formations, Belt-Purcell Basin, Montana and British Columbia (Boleneus and others, 2005; Zientek and others, 2005; Hartlaub, 2009).

A



B

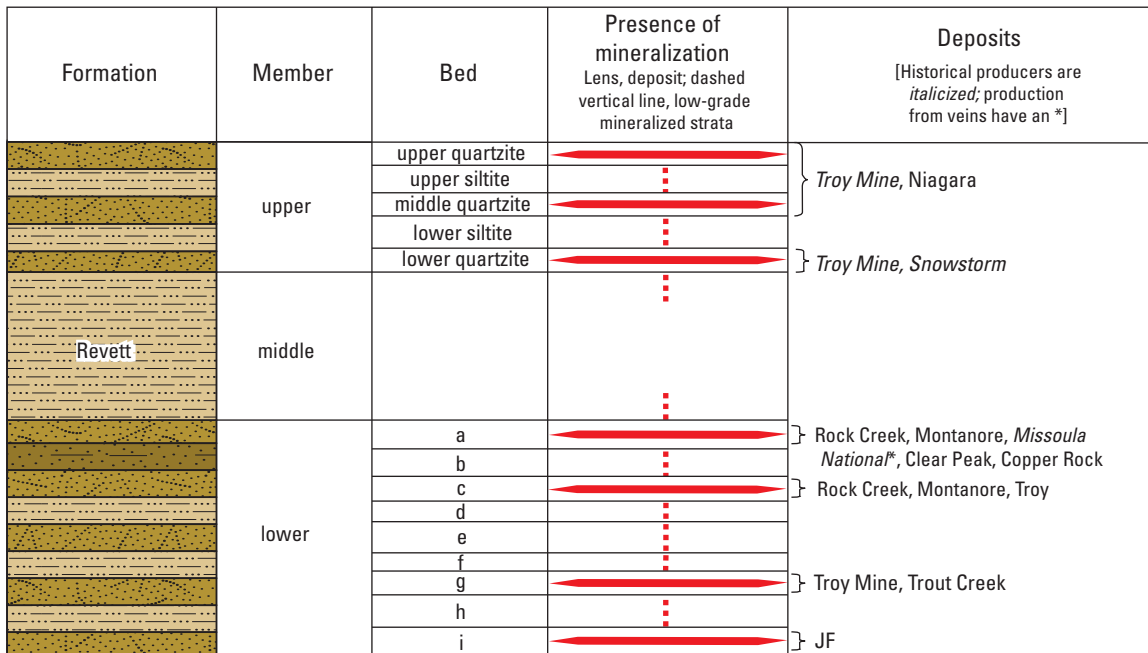


**Figure 2-34.** Stratigraphic columns of the Belt Supergroup of western Montana and northern Idaho. (A) Stratigraphic column of the Belt Supergroup below the Missoula Group. (B) Detailed column of the Revelt Formation showing copper mineralization within the lower and upper members. Modified from Boleneus and others (2005).

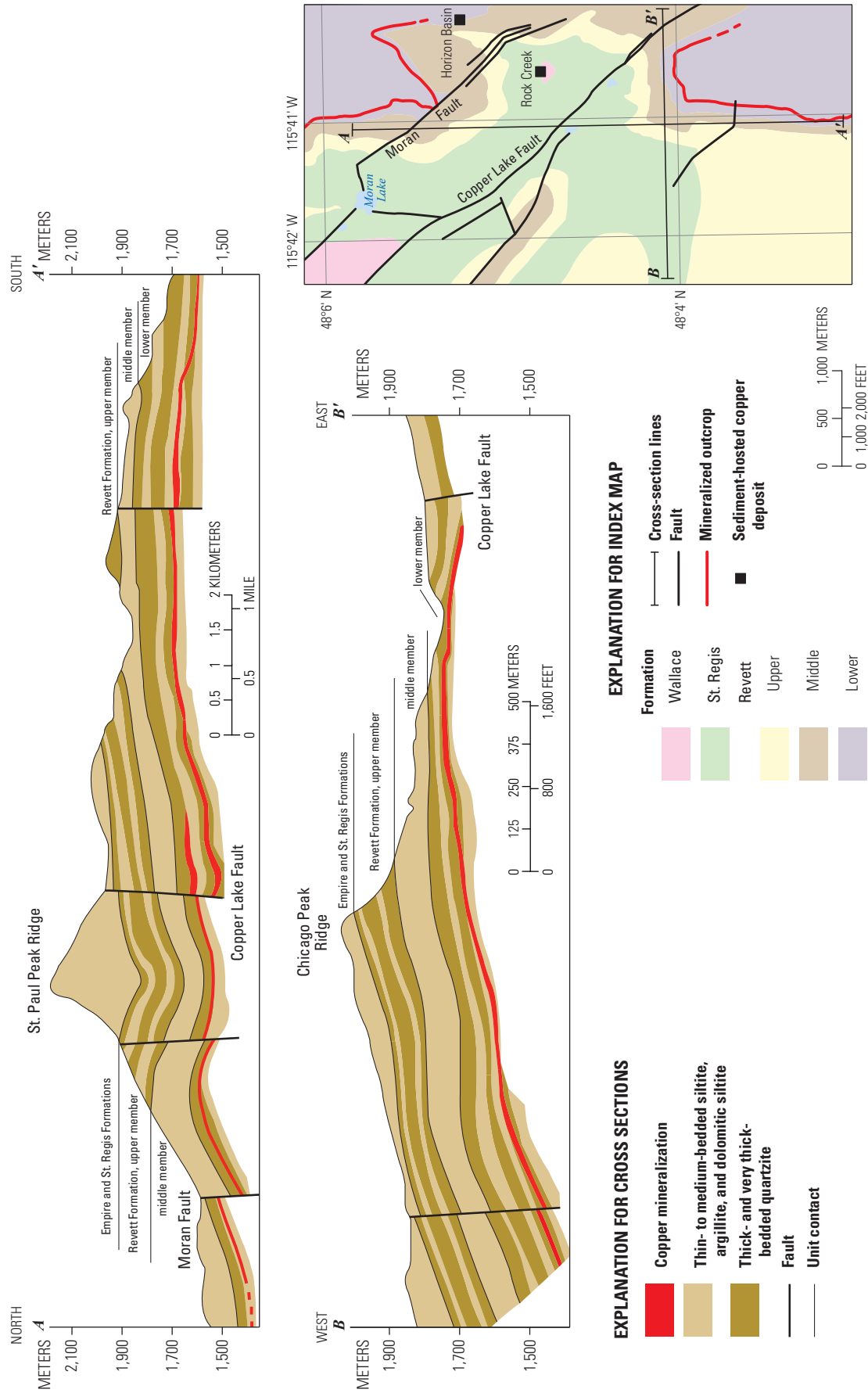


Figure 2-35. Map and cross sections through the Rock Creek deposit within the Belt-Purcell Basin displaying the lateral continuity of sediment-hosted copper mineralization in the Revett Formation, Montana. Modified from Couture and Tanaka (2005).

meters thick (Ristorcelli and Fitch, 2005), and the main ore body at Spar Lake is about 21 meters thick (Hayes, 1984).

The American Smelting and Refining Company operated the Troy Mine from 1981 until April 1993, when low metal prices resulted in closure of the mine. During its first 12 years of operation, the mine produced 222,243 metric tons of copper and 1,569 metric tons of silver (Couture and Tanaka, 2005). Revett Minerals resumed production at the Troy Mine in 2004 and produced an additional 16,144 metric tons of copper and 121 metric tons of silver through 2009. Snowstorm is the only other copper-silver mine in the area with recorded production; between 1906 and 1912, it produced 27,585 metric tons of copper and 141 metric tons of silver (Long and others, 1998). The National and Missoula Mines produced copper and silver from Revett-hosted stratabound ore at the same time as the nearby Snowstorm Mine, but no accurate records of production were kept.

Permissive tracts were delineated as part of a recent USGS assessment for copper-silver deposits in the Revett Formation (figs. 2-30 and 2-33; Boleneus and others, 2005). Delineation was based on the presence of the Revett Formation to a maximum depth of 2.4 km, presence of indicative alteration minerals, and proximity to known stratabound copper-silver deposits or occurrences. Approximately 1,440 km<sup>2</sup> of land was determined to be permissive for stratabound copper and silver deposits. The reader is directed to Boleneus and others (2005) for more detailed description of the tract and its constraints.

Copper occurrences in Canada are within the Creston Formation, which is equivalent to the Revett Formation. Two copper occurrences were discovered in southeastern British Columbia as part of a multiyear field program to investigate copper-silver potential (Hartlaub, 2009). Fine-grained bornite and chalcopyrite along bedding planes of the Creston Formation define the Teepee Creek occurrence (Hartlaub, 2009). Grieve (2010) reports mineralization in southeastern British Columbia on the Silver Fox property, owned by Kootney Gold Inc., that occur in rocks similar to Proterozoic units in Montana with economic copper-silver deposits. The permissive tract (fig. 2-33) for these Canadian occurrences was delineated as part of this assessment; the tract follows the Creston Formation along strike.

## Mineral System Components

Multiple components, such as copper-source rocks, sour-gas reductants, and seal rocks, are known for the Belt-Purcell Basin, but an evaporite source is less certain. Albite- and hematite-bearing rocks (former red beds) of the Revett Formation and the underlying Mesoproterozoic Burke Formation are the likely copper sources in the Belt-Purcell Basin (fig. 2-32; Hayes, 1990). Bedded evaporite accumulations are not found in the Belt-Purcell Basin, but casts and molds of halite, gypsum, and other evaporitic minerals are found in the

Missoula Group, which is upsection from the Revett Formation (Connors and others, 1984; Lyons and others, 1998; Schieber, 1997; Chandler, 2000; Lydon, 2007). Dissolution of evaporite minerals may have contributed to salinity of metal-transporting groundwaters. Copper and silver were then deposited where oxidized metal-bearing basinal brines upwelled (possibly along faults) and subsequently mixed and reacted with trapped sour (hydrogen sulfide-bearing) natural gas (Hayes and others, 2012). The presence of gas in the Mesoproterozoic Prichard Formation (Boberg, 1985) suggests the Prichard Formation was the original source of the reducing and sulfide-sourcing sour gas. Silty argillite beds in the Revett and overlying Mesoproterozoic St. Regis Formations most likely served as seal rocks.

The probable age for mineralization at the Spar Lake deposit is  $1,409 \pm 8$  Ma, based on a weighted average of <sup>207</sup>Pb/<sup>206</sup>Pb spot analyses ( $n = 32$ ) of xenotime overgrowths on detrital zircons determined by using a sensitive high-resolution ion microprobe (fig. 2-31; Aleinikoff and others, 2012). Mineralization was 40 to 60 m.y. after deposition of host rock material. The time of mineralization at Spar Lake is within the error range of a metatuff dated in the Mesoproterozoic Libby Formation ( $1,401 \pm 6$  Ma) about 5 km upsection from the Spar Lake host rocks (Harrison and Cressman, 1993; Evans and others, 2000). Error ranges for the mineralization age ( $1,409 \pm 8$  Ma) and the metatuff ( $1,401 \pm 6$  Ma) overlap, indicating at least 5 km of overburden was present during mineralization. Natural gas reservoirs commonly develop at a depth of about 5 km so the overlapping age dates support natural gas being present in the mineralizing system.

## Principal Sources of Information

Digital 1:250,000-scale geology published by the British Columbia Ministry of Energy and Mines (2013), a USGS Scientific Investigations Report with 1:48,000-scale digital geology (Boleneus and others, 2005), and a USGS Open-File Report with 1:100,000- to 1:250,000-scale digital geology (Zientek and others, 2005) were used for geologic information for this assessment. The USGS Scientific Investigations Report by Boleneus and others (2005) was the main source of deposit and occurrence information. Reports cited in table 2-8 also provided deposit and occurrence information.

## Neuquén Basin, Argentina— Assessment Tract 005ssCu5100

Jurassic and Cretaceous sedimentary rocks of the Neuquén Basin in west-central Argentina host stratabound copper deposits of the sandstone subtype. The Neuquén Basin is about 1,050 km long and covers 170,000 km<sup>2</sup>. The basin hosts 9 deposits, 51 occurrences, and 37 sites (fig. 1-9).



## Tectonic Setting

The polyphase Neuquén Basin (fig. 2-36) is characterized by three stages of evolution: (1) an initial pre-Andean tectonic cycle, when isolated rift basins formed in a strike-slip fault system; (2) the first stage of the Andean tectonic cycle when the isolated rift basins were integrated into an extensional back-arc basin; and (3) the second stage of the Andean tectonic cycle when the basin was inverted and compressed and became a foreland basin (figs. 2-37, 2-38*A* and *B*). The Late Proterozoic to late Paleozoic basement rocks of the Neuquén Basin formed when the western continental margin of South America (then Gondwana) was an active plate margin characterized by terrane accretion and arc magmatism (Charrier and others, 2007).

The earliest phase of the Neuquén Basin is related to a Late Triassic and Early Jurassic strike-slip fault system subparallel to the Gondwana continental margin and superimposed on a Paleozoic Gondwana Orogen (Franzese and Spalletti, 2001; Franzese and others, 2003; Howell and others, 2005). The development of abundant and widely distributed, basically silicic magmatic activity, and a paleogeography dominated by north-northwest-oriented extensional basins are characteristic of this phase of tectonic activity (Charrier and others, 2007). There is no evidence of Late Triassic subduction-related processes in the area west of the Neuquén Basin (Franzese and Spalletti, 2001). Extension related to strike-slip faulting formed long, narrow half-grabens that were initially filled with continental and volcanoclastic rocks followed by lacustrine and shallow marine strata as the separate depositional centers integrated into the Neuquén Basin.

Subduction in the Early Jurassic led to the next phase of basin evolution (Charrier and others, 2007). From the Early Jurassic to the Early Cretaceous, the Neuquén Basin developed in an extensional back-arc setting to a magmatic arc, related to a steeply dipping subducting plate that formed along the western margin of Gondwana (Howell and others, 2005). The first magmas associated with subduction in the Early Jurassic occurred in the Sinemurian–Pliensbachian time (Charrier and others, 2007). From Early Jurassic to Albian time, the Neuquén Basin experienced generalized extension, which is consistent with absolute plate motions where the trench hinge retreats away from the upper plate (trench roll-back) (Heuret and Lallemand 2005; Ramos and Kay, 2006; Ramos, 2010). Early in this extensional back-arc setting, sedimentary rocks characteristic of marine transgressive-regressive cycles were deposited. During the Early Cretaceous, the Neuquén Basin deposition was characterized by transgressive facies, starvation, and anoxia (Franzese and others, 2003).

Although this back-arc phase is largely characterized by extension, the stratigraphic record indicates several episodes of basin inversion that can be linked to the breakup of Gondwana. For example, the Araucanian inversion (fig. 2-37; Milani and Thomaz Filho, 2000) coincides with the opening of the Mozambique Channel and the formation of oceanic crust between Africa and Antarctica (Jokat and others, 2003;

Leinweber and Jokat, 2011). Evidence for the Araucanian cycle of inversions can be found in a regional feature known as the Huincul High (fig. 2-38*A*; Naipauer and others, 2012). The high is a positive topographic element that has acted as a structural and stratigraphic barrier, at least since the Late Jurassic, and divides the basin into two depocenters. The Intraaptian inversion (fig. 2-37) generally corresponds to the initial opening of the South Atlantic Ocean and the breakup of Africa and South America (Heine and others, 2013).

In mid to Late Cretaceous times, the tectonic style of the Andean margin changed from extensional to compressional (Franzese and others, 2003; Charrier and others, 2007; Naipauer and others, 2012). The Neuquén Basin evolved from a back-arc basin controlled by thermal subsidence and extension in Aptian–Albian times to a foreland basin system during the early Cenomanian. These dates are based on the ages of detrital zircons and fission-track data on zircons (Tunik and others, 2010). This transition in tectonic setting caused a hiatus in the stratigraphic record called the Mirano inversion (fig. 2-37; Milani and Thomaz Filho, 2000). This tectonic change can be related to a global-scale plate reorganization event that caused the northeastward displacement of the Farallon Plate and dextral oblique convergence between the oceanic and the South American plates. This change could be related to cessation of subduction in eastern Gondwana (Charrier and others, 2007; Matthews and others, 2012). The magmatic front migrated eastward and major contractional deformation resulted in 45–57 km of crustal shortening in the foreland (Howell and others, 2005; Ramos and Kay, 2006).

## Stratigraphy

As expected, the stratigraphy of the basin is a reflection of its geodynamic history (fig. 2-37). The Lower to Middle Jurassic Cuyo Group, the Middle–Upper Jurassic Lotena Group, the Upper Jurassic to Lower Cretaceous Mendoza Group, and the Lower Cretaceous Rayoso Group (fig. 2-38*B*) were deposited in an extensional back-arc basin formed during the first stage of the Andean tectonic cycle. The Upper Cretaceous Neuquén and Malargüe Groups (fig. 2-38*B*) were deposited in a foreland basin during the second stage of the Andean tectonic cycle. Copper mineralization likely took place during Late Cretaceous compressional tectonics.

During the pre-Andean tectonic cycle, synrift fill composed of volcanic, pyroclastic, and siliciclastic rocks of the Lapa Formation was deposited (Franzese and others, 2006). In the Chachil depocenter in the southern Neuquén Basin, synrift volcanic fill is composed of andesite, rhyolite, and volcanoclastic deposits (Franzese and others, 2006). The overlying sedimentary fill is dominated by coarse-grained, nonmarine rocks.

A marine transgression occurred at the beginning of the first stage of the Andean tectonic cycle and resulted in the deposition of deep-marine shale material of the Lower and Middle Jurassic Los Molles Formation (Vergani and others, 1995; Mosquera and Ramos, 2006). The eastern part of the

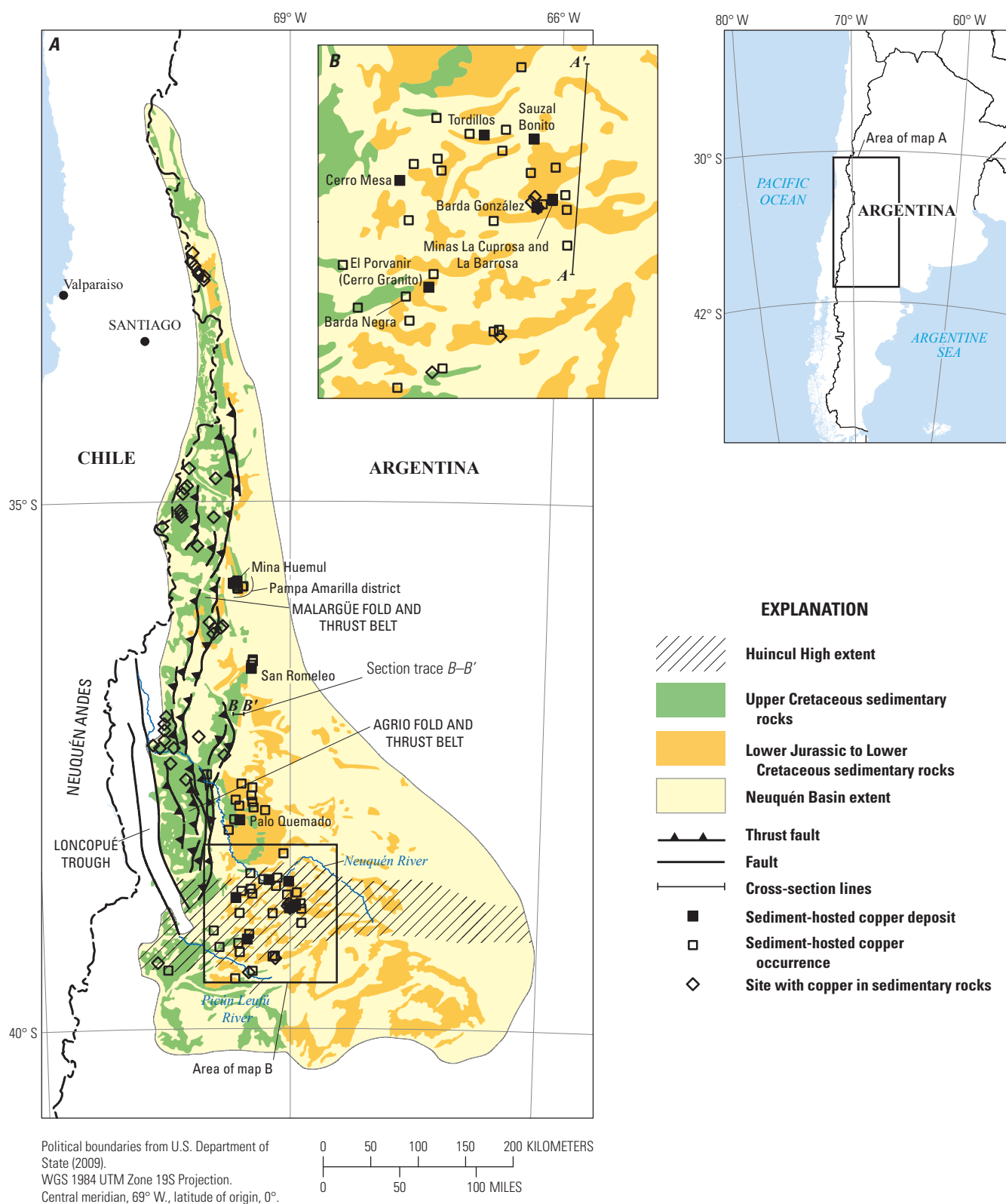


**Figure 2-36.** Map showing the distribution of Lower Jurassic to Upper Cretaceous sedimentary rocks and associated sediment-hosted copper deposits and occurrences in the Neuquén Basin, Argentina. Important structural features include the Huincul High; Andean fold and thrust belts. Modified from Lizuain and others (1997), Mosquera and Ramos (2006); and Ramos and Kay (2006). Cross sections A–A' and B–B' are shown in figure 2-38.

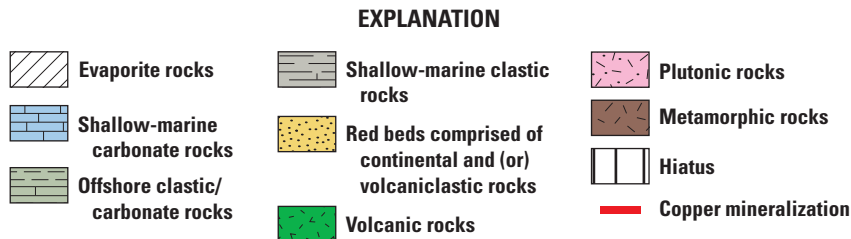
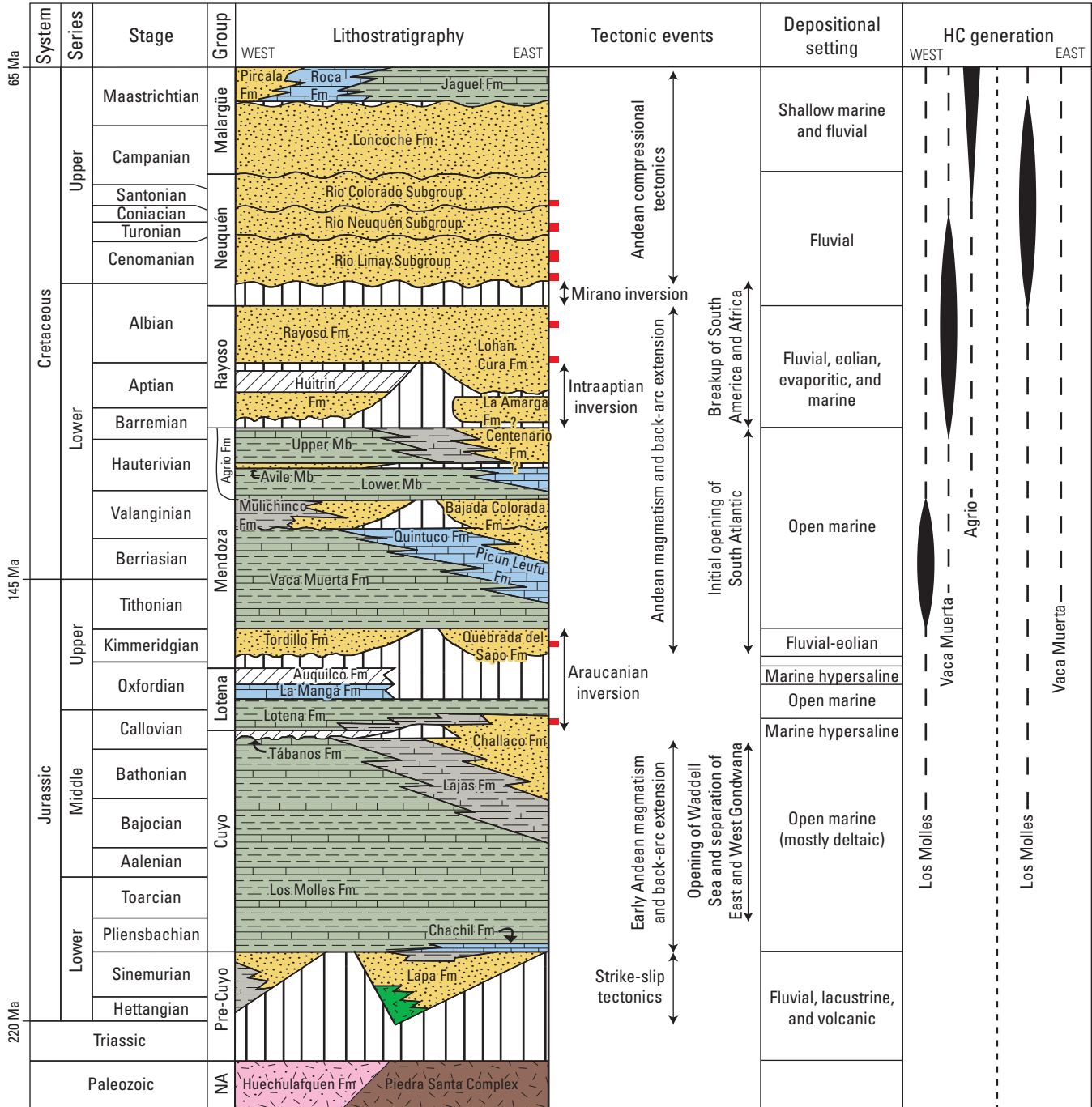
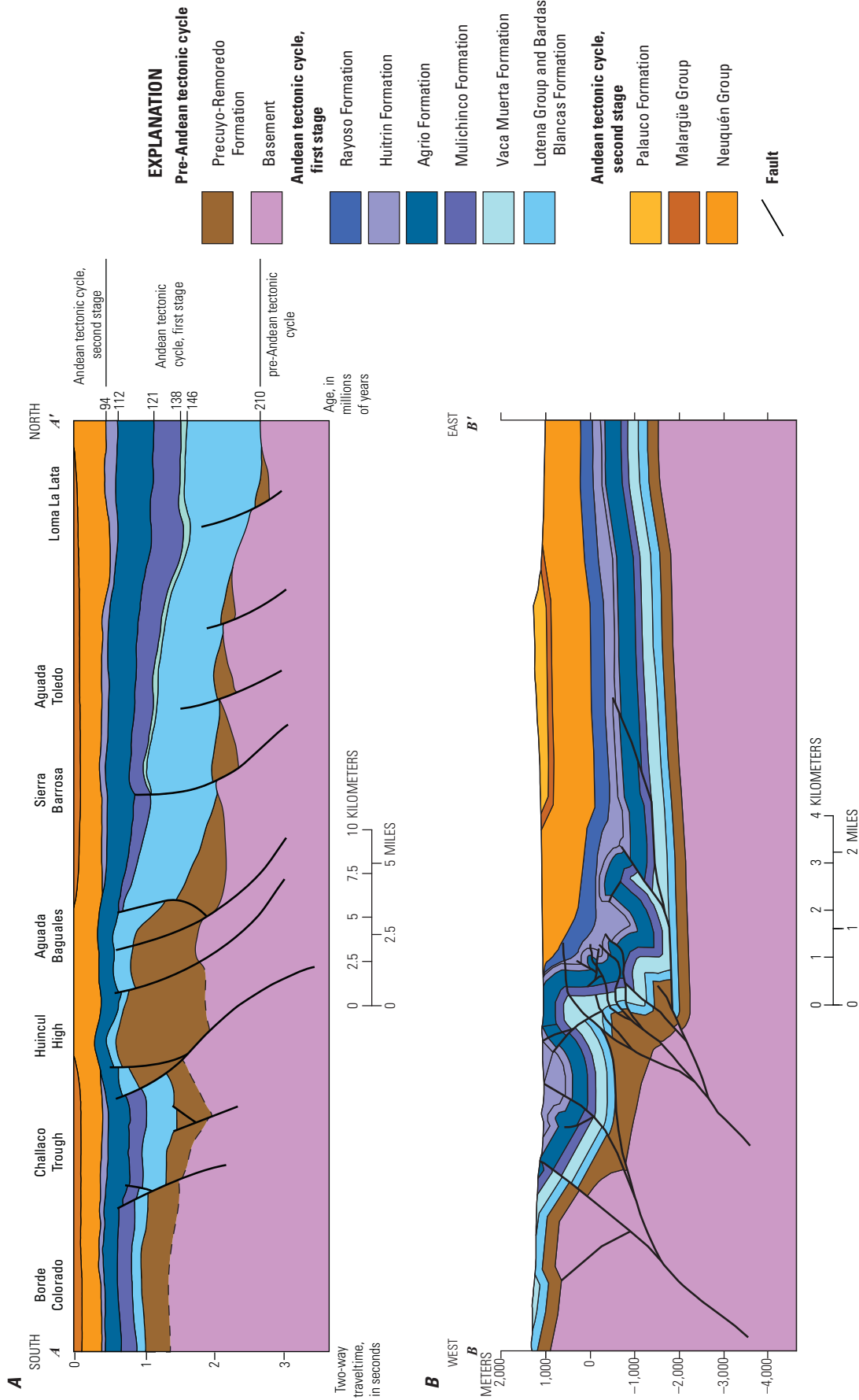


**Figure 2-37.** Stratigraphic column of the Neuquén Basin with regional tectonic history, depositional settings of sedimentary rocks, and hydrocarbon (HC) generation events. Lithostratigraphy modified from Howell and others (2005) and depositional setting and hydrocarbon generation modified from Legarreta and others (2005). See text for sources of information for tectonic events. Copper mineralization placement is from the current study. Fm, formation; Mb, member.



basin is characterized by a coarsening-upward sequence in which shallow marine clastic rocks of the Middle Jurassic Lajas Formation grade upward and laterally into continental fluvial deposits of the Middle Jurassic Challaco Formation. The Los Molles and Lajas Formations are unconformably overlain by marine and marine-hypersaline rocks of the Lotena Group, which include the Middle Jurassic Tabanos Formation (evaporites), the Middle and Upper Jurassic Lotena Formation (deltaic to shallow marine clastic rocks), the La Manga Formation (carbonates), and the Auquilco Formation (evaporites). A hiatus in deposition related to the Araucanian inversion overlies the Auquilco Formation (fig. 2-37).

Rocks of the Mendoza Group, deposited following the Araucanian inversion, indicate at least two major transgressive-regressive cycles (Vergani and others, 1995; Mosquera and Ramos, 2006): (1) deep-marine shaly marl of the Upper Jurassic and Lower Cretaceous Vaca Muerta Formation, grading through shallow marine carbonates of the Upper Jurassic and Lower Cretaceous Picun Leufu and Quintuco Formations, into nonmarine rocks of the Bajada Colorado Formation; and (2) marine shales of the Lower Cretaceous Agrio Formation, grading through shallow marine carbonate and siliclastic rocks, into nonmarine rocks of the Lower Cretaceous Centenario Formation.

Rocks of the Lower Cretaceous Rayoso Group were deposited during and after the Intraaptian inversion. The Lower Cretaceous Huitrin Formation consists of nonmarine siliclastic rocks overlain by evaporite rocks. The overlying Lower Cretaceous Rayoso and Lohan Cura Formations consist of nonmarine siliclastic rocks. Red beds of the Rayoso Group were likely deposited in shallow, perennial lakes (Zavala and others, 2006).

Continental red beds of the Upper Cretaceous Neuquén Group deposited after the Mirano inversion are molassic sedimentary rocks derived from the uplift of the Andes (Tunik and others, 2010; Mescua and others, 2013). An angular unconformity separates the Rayoso and Neuquén Groups. Detrital zircon studies show that rocks above and below the unconformity have different provenances (Tunik and others, 2010). Sediments that make up the Lower Cretaceous Agrio and Rayoso Formations were derived from the east, whereas sediments that formed the Neuquén Formation were derived from the Andean Cordillera to the west.

## Deposits and Occurrences

The Neuquén Basin has 9 deposits and 51 occurrences of sandstone-type sediment-hosted stratabound copper mineralization and 37 sites (table 2-9; fig. 2-36). The 37 sites identified as copper mineralization on metallogenic maps (Ricci, 1970–1971, 1974) are in sedimentary geologic map units associated with the Neuquén Basin; however, no additional information is available about the nature of these sites. Sandstone-hosted copper mineralization is identified in the Jurassic Lotena and Tordillo Formations, the Lower

Cretaceous Rayoso Formation, and the Upper Cretaceous Neuquén Group (Candeleros, Huincul, Portezuelo, and Bajo de la Carpa Formations) (figs. 2-37, 2-38B, and 2-39; Mendez and Zappettini, 1989; Lyons, 1999). Seven of the known deposits are hosted by rocks of the Neuquén Group, and two are in the underlying Rayoso Group. The largest deposits are Barda Gonzáles (35.5 million metric tons with an average grade of 0.368 percent copper) and Tordillos (9.5 million metric tons with an average grade of 0.42 percent copper) (fig. 2-36). The other deposits contain 11,000 to 320,000 metric tons of mineralized rock with grades averaging between 0.37 and 1.86 percent copper (table 2-9). Some of these small deposits have the potential to contain as much as 3 million metric tons of ore if more extensively mined (Lyons, 1999).

Ricardo Wichmann was the first scientist to publish a report on copper mineralization in “Estratos con dinosaurios” (now the Neuquén Group) in Argentina (Wichmann, 1927; Lyons, 1999; Schencman and others, 2013). Fernández Aguilar (1945) described the sandstone-copper mineralization in these rocks and evaluated development potential between the Neuquén and Picún Leufú Rivers, focusing on the El Porvanir (Cerro Granito) deposit. Subsequent exploration activities for sandstone-copper and associated uranium mineralization were summarized for the compilation of “Mineral Resources of the Republic of Argentina” (Zappettini, 1999); in particular, Lyons (1999) provided an overview of the sandstone-copper deposits of the Neuquén Basin. Information about Mina San Romeleo was summarized by Centeno and Fusari (1999). Sandstone-copper-uranium deposits and districts (Barda Negra, Pampa Amarilla, and Rahue-Có) were described by Rojas (1999a,b,c) and Schencman and others (2013). Detailed studies of the two largest sandstone-copper deposits in the Neuquén Basin—Barda Gonzáles and Tordillos—were published by Pons and others (2009 and 2014, respectively).

When viewed collectively, deposits and occurrences in the Neuquén Basin have a number of shared characteristics (Lyons, 1999; Rojas, 1999a,b,c; Consultora Minera R.B., 2008; Giusiano and others, 2008, 2014; Pons and others, 2009, 2014; Rainoldi and others, 2014). Deposits and occurrences are hosted in sandstone and conglomerate rocks in the basin that have fluvial channel facies. Mineralized beds are generally a few meters thick but locally can exceed 30 m. The sandstones and conglomerates are red beds, but those hosting copper minerals are bleached to light colors (gray, cream, or white) and leached (resulting in the development of secondary porosity by dissolution of previous cements, feldspar, and lithic fragments). Copper minerals fill the secondary porosity of permeable and bleached sandstones and are intimately associated with bitumen. The predominant copper minerals are those that form in the supergene environment (malachite and chalcocite). Uranium and vanadium minerals are reported from many of the deposits and occurrences. Table 2-10 summarizes characteristics for some of the deposits and occurrences.



**Table 2-9.** Sediment-hosted stratabound copper deposits within the Neuquén Basin, Argentina.

[Abbreviation of mineral names: Ant, antlerite; Atc, atacamite; Az, azurite; Bh, brochantite; Bn, bornite; Ct, chalcantite; Cc, chalcocite; Ccl, chrysocolla; Cp, cuprite; Cv, covellite; Ida, idaite; Mal, malachite; Trn, tenorite; Turq, turquoise. Mt, million metric tons; %, percent]

Name	Latitude	Longitude	Ore minerals	Major commodities	Resources (unmined)	Citation
Sandstone-copper deposits						
Barda Gonzalez	-38.859	-69.009	Mal, Cc, Cv, Ccp, Az Atc, Bh, Ccl, Trn, Turq	Cu	35.5 Mt at 0.368% Cu	Aguilar (1945); Lyons (1999); Giusiano and others (2008); Pons and others (2009)
Cerro Mesa	-38.759	-69.657	Mal, Az, Cc	Cu	0.035 Mt at 1.75% Cu	Lyons (1999); Giusiano and others (2008); Kirkham and others (2003)
El Porvanir	-39.152	-69.523	Mal, Cc, Az	Cu	0.32 Mt at 1.86% Cu	Aguilar (1945); Lyons (1999); Giusiano and others (2008)
Mina Huemul	-35.775	-69.664	Ccp, Bn, Ida	Cu, U	0.152 Mt at 0.77% Cu	Ricci (1974); Rojas (1999b); Kirkham and others (2003)
Minas La Cuprosa and La Barrosa	-38.829	-68.936	Mal, Az, Ct	Cu	0.225 Mt at 0.37% Cu	Kirkham and others (2003); Consultora Minera R.B. (2008)
Palo Quernado	-38.021	-69.605	Mal	Cu, U	0.011 Mt at 1.9% Cu	Ricci (1970–1971); Lyons (1999); Kirkham and others (2003)
San Romeleo	-36.586	-69.459	Ct, Mal, Az, Bh, Ant, Cc, Cp	Cu	0.257 Mt at 1.29% Cu	Ricci (1974); Zanettini and Carotti (1993); Centeno and Fusari (1999)
Sauzal Bonito	-38.606	-69.022	Mal, Cc, Ccl	Cu	0.12 Mt at 0.55% Cu	Lyons (1999); Kirkham and others (2003); Giusiano and others (2008)
Tordillos	-38.590	-69.258	Cc, Ccp, Bn, Az, Cv, Bh, Mal, Cp, Ccl	Cu	9.5 Mt at 0.42% Cu	Lyons (1999); Giusiano and others (2008); Pons and others (2014)

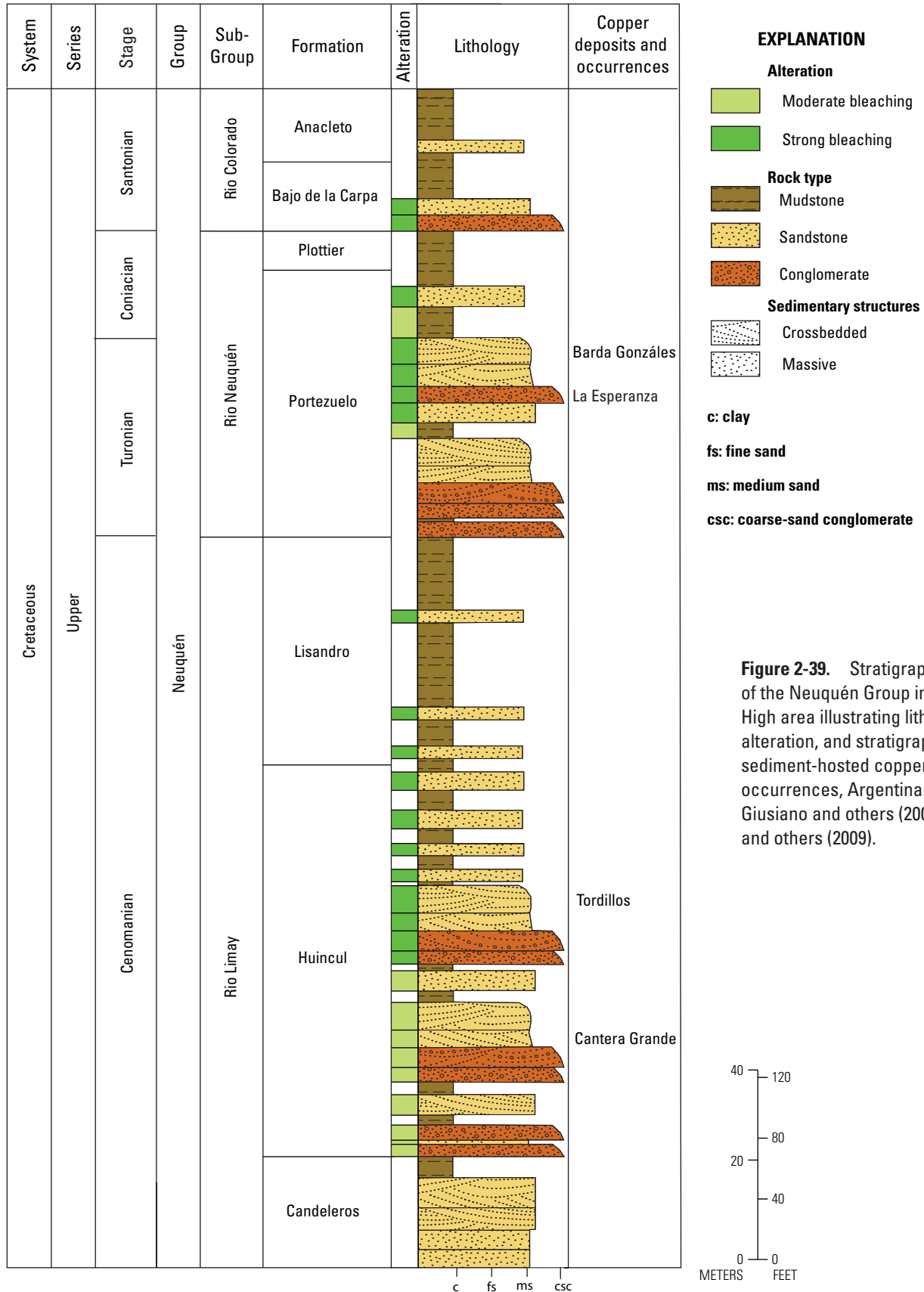


**Table 2-10.** Summary table for selected deposits and occurrences within the Neuquén Basin, Argentina.

[m, meter; km, kilometer, t, metric tons; %, percent; —, no data; RC, reverse circulation]

Site name	Mineralogy	Bitumen	Thickness	Bleaching	Exploration	References
Barda González	Mainly malachite. Small amounts of sulfide minerals: chalcocite and covellite, and traces of chalcopyrite. Besides malachite, other supergene copper minerals include atacamite, azurite, brochantite, chrysocolla, tenorite, and turquoise. Uranium minerals (carnotite, pitchblende) are associated with copper ores. Rare vanadium (volborthite) and iron oxides also present.	Bitumen sheets or granules and small masses are distributed in conjunction with the copper minerals and uranium	Mineralized horizons are 1–30 m thick; generally 1–5 m	Sandstones are irregularly leached and bleached	1969–1979: 325 t selected ore grading 9.7% Cu extracted 1970s: test pits and trenches 1994–1998: 9,434 m drilled in 163 RC holes; resource estimated Additional drilling up through 2002 corroborated previous resource estimate	Lyons (1999); Consultora Minera R.B. (2008); Pons and others (2009)
Tordillos	Chalcocite with relict chalcopyrite and bornite and supergene Cu-V-U minerals (azurite, covellite, brochantite > malachite, copper wad [tenorite], cuprite, chrysocolla, Cu-K-Ba vanadates and urovanadates)	Copper mineralization everywhere in contact with impregnations of bitumen	In central sector, mineralized zone is 20–25 m thick and extends 1.4 km EW and 0.7 km NS	Sandstones are gray to light	1993–1994: 2,506 m drilled in 97 RC holes; resource estimated; 2006: 2,541 m drilled in 50 holes	Lyons (1999); Pons and others (2014)
El Porvanir (Cerro Granito)	Dominantly malachite and chalcocite; some azurite	Bitumen accompanies mineralization	Average thickness 1.73 m	—	1970s: surface exploration 1996–1997: 8,077 m drilled in 16 holes. Only 8 had results with Cu between 0.11 and 0.32%	Lyons (1999)
Cerro Mesa	Predominantly malachite, some azurite and chalcocite as well as the remnants of chrysocolla and traces of uranium ores	Mineralization is accompanied by bitumen	—	—	—	Lyons (1999)
Sauzal Bonito	Malachite, chalcocite, and some chrysocolla	Bitumen, in varying degrees of concentration, is distributed in mineralized horizons in the area	4–15 m	Alteration of the sandstones, with characteristic leaching and discoloration	Evidence of minor and historic workings; 2,467 m drilled in 53 holes	Lyons (1999)
Campeño Norte	Malachite, with rare grains of chalcocite	Bitumen	—	—	1955: 377 m drilled in 17 RC holes	Lyons (1999)
Plaza Huincul	Chalcocite and malachite	Bitumen	—	Bleached and leached	550 m drilled in 16 RC holes	Lyons (1999)
Cerro Bandera Sur	No copper mineralization; only bleached rock	—	—	Bleached and leached	1,063 m drilled in 30 RC holes	Lyons (1999)

Table 2-10. Summary table for selected deposits and occurrences within the Neuquén Basin, Argentina.—Continued

Site name	Mineralogy	Bitumen	Thickness	Bleaching	Exploration	References
Santa Genova and La Olla	Small amounts of chalcocite and some malachite	Small patches of bitumen	—	Sandstone altered to cream to white color	Santa Genova: 1,045 m drilled in 24 RC holes La Olla: 921 m drilled in 24 RC holes	Lyons (1999)
Bordo Colorado	Chalcocite and malachite	—	—	Sandstone, altered to a light or cream color	812 m drilled in 25 RC holes	Lyons (1999)
Barda Negra	Malachite and chalcocite	Copper mineralization accompanied by small amount of bitumen	—	—	Surface sampling, no drilling	Lyons (1999)
Palo Quemado	Malachite and uranophane, possibly some uraninite	—	—	—	Explored in the 1970s by the Argentine National Atomic Energy Commission, judged to contain persistent uranium values which accompany copper mineralization. No drilling	Lyons (1999)
Puesto Lago	Malachite	—	—	—	—	Lyons (1999)
Distrito Uranífero Pampa Amarilla, Mendoza (includes all sites near Huemul deposit)	In the Huemul Mine uranium ore is pitchblende. The other primary minerals are pyrite, marcasite, chalcopyrite, bornite, idaite, sphalerite, and galena. More than 20 secondary uranium minerals.	—	—	—	Uranium minerals noted in copper ores in 1952; exploration from 1954 to 1958; mining of uranium started in 1955 at Huemul	Rojas (1999b)
San Romeleo	Chalcanthite and minor amounts of malachite, azurite, brochantite, antlerite, chalcocite, and cuprite	Disseminated malachite and chalcanthite in a bed of brown sandstone and blackish tar at Agua Amarga area (within 100 m of San Romeleo)	—	—	Work as early as 1967 to determine resources; drilling done by 1971; geochemical surveys in 1998	Centeno and Fusari (1999)

## Mineral System Components

The Neuquén Basin is the leading producer of hydrocarbons in Argentina (Uliana and Legarreta, 1993; Urien and Zambrano, 1994; Legarreta and others, 2005), and several studies have noted the close association of copper mineralization with petroleum systems in the basin (Giusiano and others, 2008; Pons and others, 2009, 2014; Rainoldi and others, 2014). Three marine, organic-rich intervals are petroleum source rocks for the basin (Legarreta and others, 2005). Organic material in the Los Molles Formation was almost entirely converted to hydrocarbons from late Early Cretaceous to Early Tertiary time, whereas the organic material of the Vaca Muerta Formation and the Agrio Formation matured during the Late Cretaceous to Miocene and Eocene to Miocene, respectively. Bitumen associated with the Barda Gonzáles deposit is likely derived from the Vaca Muerta or Los Molles Formations (Pons and others, 2009).

Influx of several pulses of fluids (reduced basinal waters rich in hydrocarbons and oxidized brines carrying copper chloride complexes) and their mixing with interstitial waters containing sulfates may have produced the copper mineralization (Pons and others, 2014). Leaching and bleaching of rocks, which host copper mineralization, is likely caused by the migration of petroleum-bearing fluids (Jon Thorson, oral commun., 2006; Giusiano and others, 2008; Pons and others, 2009, 2014; Rainoldi and others, 2014). A second migration of oxidized brines was responsible for introducing copper that precipitated only in the rocks that were earlier bleached and contained hydrocarbons (Jon Thorson, oral commun., 2006). The source of the copper-bearing oxidized brines is unclear, but red beds of several ages could have sourced copper, as could the volcanic and volcanoclastic rocks of the Lapa Formation or the Paleozoic basement plutonic and metamorphic rocks.

## Principal Sources of Information

Geologic maps used in the assessment include 1:500,000-scale maps of Mendoza and Neuquén Provinces, a 1:750,000-scale geologic map of Río Negro Province, and a 1:2,500,000-scale map of Argentina. Metallogenic maps of Mendoza and Neuquén (1:750,000 scale) show the location of mineral sites, the site name, and the principal mineral commodity present; deposit type is not indicated. Detailed information on mineral deposits and occurrences is from Aguilar (1945), Lyons (1999), Rojas (1999a,b,c), Consultora Minera R.B. (2008), and Pons and others (2009, 2014).

## Maritimes Basin, Canada— Assessment Tract 003shCu1000

Carboniferous sedimentary rocks in Atlantic Canada<sup>7</sup> host sediment-hosted stratabound copper deposits of the red-bed and sandstone-copper subtypes. Red-bed, sandstone-copper, and reduced-facies-type deposits are present. The copper-bearing lithologies (Windsor, Mabou, Cumberland, and Pictou Groups) are present along the coast within the Maritimes Basin in the provinces of New Brunswick, Nova Scotia, Prince Edward Island, Newfoundland, and Labrador. The Maritimes Basin extends over land and sea for about 660 km in an east-west direction (fig. 2-40). There are 2 deposits and 155 occurrences of copper mineralization within the basin (fig. 1-10).

## Tectonic Setting

The Paleozoic Maritimes Basin in the Appalachian Mountains of Atlantic Canada consists of several northeast-trending, partially connected, fault-bounded subbasins. These basins developed in the late Paleozoic following the Devonian Acadian Orogeny (fig. 2-40; Gibling and others, 2008; Allen and others 2013; Waldron and others, 2013). The basin covers approximately 450,000 km<sup>2</sup> and is more than 12 km thick. At least six subbasins developed in various parts of the region (Gibling and others, 2008); the Magdalen, Sydney, and St. Anthony basins are three major depocenters (Dietrich and others, 2009).

The Maritimes Basin formed prior to and during the Carboniferous to Permian Alleghanian Orogeny (Bradley, 1982; Dietrich and others, 2009; Hatcher, 2010). At the time of basin formation, Atlantic Canada was within a zone of dextral megashear that was active during the collision of the continents of Gondwana and Laurussia (Arthaud and Matte, 1977; Bradley, 1982). This intracontinental transform zone lies between the east-west trending Hercynian Belt of Europe and the north-east-trending orogenic belt of the Appalachian Mountains of the United States (Arthaud and Matte, 1977). Tectonism in the Maritimes Basin is diachronous and varies over short distances along strike through regimes of “pure” strike slip, transpressional deformation, and rapid subsidence of extensional basins (Bradley, 1982).

The stratigraphy of the Maritimes subbasins indicates a polycyclic history involving periods of fault-generated subsidence, posttectonic thermal relaxation, and basin inversion (Calder, 1998; Gibling and others, 2008; Allen and others, 2013). Each cycle involves two stages: (1) an initial phase

<sup>7</sup>Atlantic Canada is the region of Canada comprising the four provinces located on the Atlantic coast, excluding Quebec: the three Maritime provinces—New Brunswick, Prince Edward Island, and Nova Scotia—and the easternmost province of Newfoundland and Labrador (<http://www.canadiangeographic.ca/atlas/>).



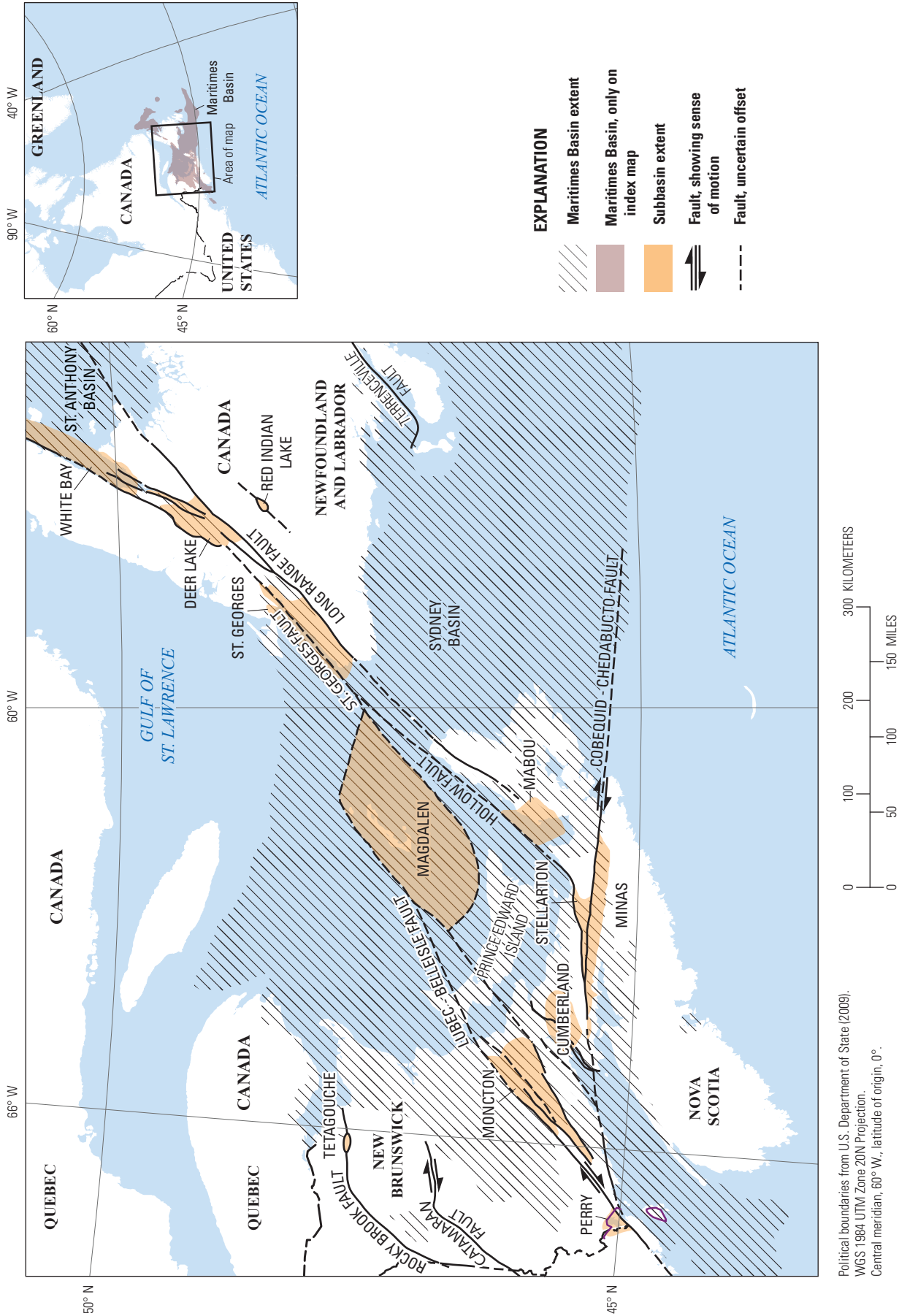


**Figure 2-40.** Map showing late Paleozoic subbasins and faults related to the Maritimes Basin, Canada. Paleozoic subbasins and faults modified from Bradley (1982), Maritimes Basin extent from Gibling and others (2008).

when subsidence was rapid, fault controlled, and often accompanied by volcanism and (2) a subsequent phase where the depositional basins expanded, burying earlier border faults and resulting in younger sedimentary units progressively overlapping basement (Bradley, 1982).

## Stratigraphy

The sedimentary rocks of the Maritimes Basin formed in a predominantly continental setting that was within 5 degrees of the equator from the Early Pennsylvanian through the early Permian (Allen and others, 2013). Individual subbasins within the basin complex had different tectonic and subsidence histories resulting in unique stratigraphies (Allen and others, 2013). Despite the differences between basins, a series of groups can be recognized across much of Atlantic Canada (Gibling and others, 2008). The stratigraphic summary is largely based on the information in Gibling and others (2008) and the lexicon of Canadian geological names (WEBLEX Canada, 2014).

The Middle Devonian to lower Carboniferous Horton Group fills linear, fault-bounded subbasins and consists of sedimentary rocks deposited in lacustrine, fluvial, pro-delta, and flood-plain environments, with instances of restricted marine conditions. Nonmarine, red and gray-to-black, generally coarse-grained clastic rocks are found near the base and top of the group; fine-grained lacustrine and restricted-marine deposits are found in the middle of the unit (fig. 2-41).

The Fountain Lake Group in Nova Scotia, which is time correlative with the Horton Group, has several kilometers of bimodal volcanic rocks, including as much as 1.5 km of continental tholeiitic basalts present in the Diamond Brook Formation (Dessureau and others, 2000). The contact between the Horton Group and the overlying Windsor Group is an angular unconformity. Low-grade regional metamorphism, dated at 335–340 Ma, influences the Horton Group but not the overlying Windsor Group.

The Early Carboniferous Windsor Group, about 800 m thick, is the only open-marine unit in the basin succession (fig. 2-41). As the sediments of this unit accumulated, extension-driven subsidence waned, and a phase of thermal subsidence began. In the type area, the Windsor Group consists of a lower part of thin basal carbonates overlain by massive evaporites; a middle part of interbedded evaporites and minor red clastic rocks, chiefly siltstones and thin carbonates; and an upper part of interbedded clastic and carbonate rocks with minor evaporites (fig. 2-41). The carbonate rocks contain marine faunas, and the clastic rocks are mainly continental and poorly fossiliferous.

The Carboniferous Mabou Group is about 1 km thick and overlies the Windsor Group with conformable to disconformable contacts. The strata are largely nonmarine, but fossils indicate marine influence at some levels. The change from marine conditions during the formation of the Windsor Group to nonmarine conditions for the Mabou Group may reflect the onset of Gondwanan glaciation or tectonic factors. The Mabou

Group consists of interstratified, fine- to medium-grained, red and gray sandstone, and shale. Depositional settings change from gray, shallow lacustrine facies near the base, to red playa and flood-plain deposits near the top. The top contact of the Mabou Group is an unconformity that may represent the onset of a major glacial period or onset of tectonism associated with the Alleghanian Orogeny.

The Mabou Group is overlain by the Late Carboniferous Cumberland Group (figs. 2-41 and 2-42). Cumberland Group rocks were deposited in extensional pull-apart basins related to major strike-slip fault zones; the transpressional and transtensional events in the Maritimes Basin likely correspond to the onset of the Alleghanian Orogeny in the U.S. Appalachian Mountains, which formed a fold-and-thrust belt and the Appalachian Foreland Basin. Rocks of the Cumberland Group formed in fluvial, alluvial plain, lacustrine, estuarine, and shoreline environments with restricted marine influence. Lithologies include red and gray conglomerate; gray, medium- to coarse-grained subarkose to sublitharenite; gray to reddish gray, coarse-grained arkose; red to gray, fine-grained litharenite; gray to reddish-brown mudstone and siltstone; coal seams from 0.01 m to 3.5 m thick; and thin, bituminous, locally fossiliferous limestone and shale.

Basinwide deposition of alluvial red beds of the Late Carboniferous to Permian Pictou Group record a second phase of thermally driven subsidence in the area. The rocks are predominantly fluvial red beds, characterized by abundant sandstone and mudstone, scarce coal, and rare conglomeratic beds.

Most sediment-hosted stratabound copper occurrences lie within three stratigraphic associations in Carboniferous rocks of the Maritimes Basin: reduced-facies-type mineralization that occurs directly above the contact between the Windsor and Horton Groups (Binney and Kirkham 1974; Kirkham 1974); reduced-facies-type mineralization associated with limestones in the upper part of the Windsor Group (Kirkham, 1985); and red-bed-type mineralization found in Upper Mississippian and Pennsylvanian rocks (fig. 2-41; Papenfus, 1931; Brummer, 1958; Binney and Kirkham 1974; Kirkham 1974). Sandstone-type mineralization could also be found in the Upper Mississippian and Pennsylvanian rocks accompanying the red-bed mineralization.

The stratigraphic sequence for the reduced-facies-type occurrences at the contact between the Horton and Windsor Group begins with red conglomerate or fanglomerate of the Horton Group, overlain by green conglomerate, and in turn is overlain by dark, fine-grained, laminated, sandy limestone of the Windsor Group, which grades upward into fossiliferous limestone (Kirkham, 1974). Disseminated pyrite, chalcocopyrite, and, in places bornite and chalcocite, are present in the upper part of the green conglomerate and lower part of the dark, laminated limestone. At most localities, the thickness of the mineralized strata is too thin and copper grades are too low to be of economic interest. Disseminated chalcocopyrite, sphalerite, and galena occur in brown, gray, and black limestone interlayered with red clastic sedimentary rocks in the upper part of

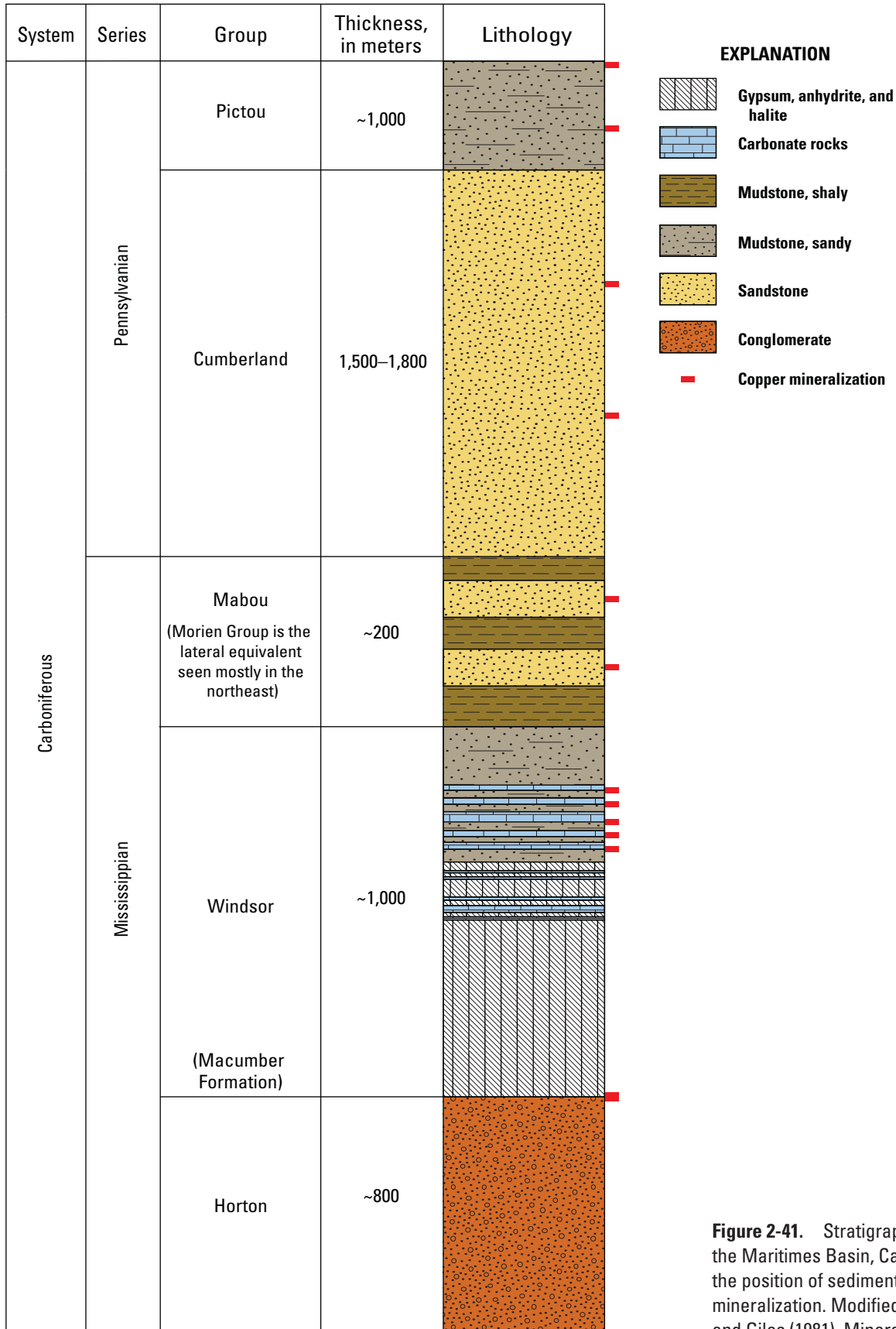
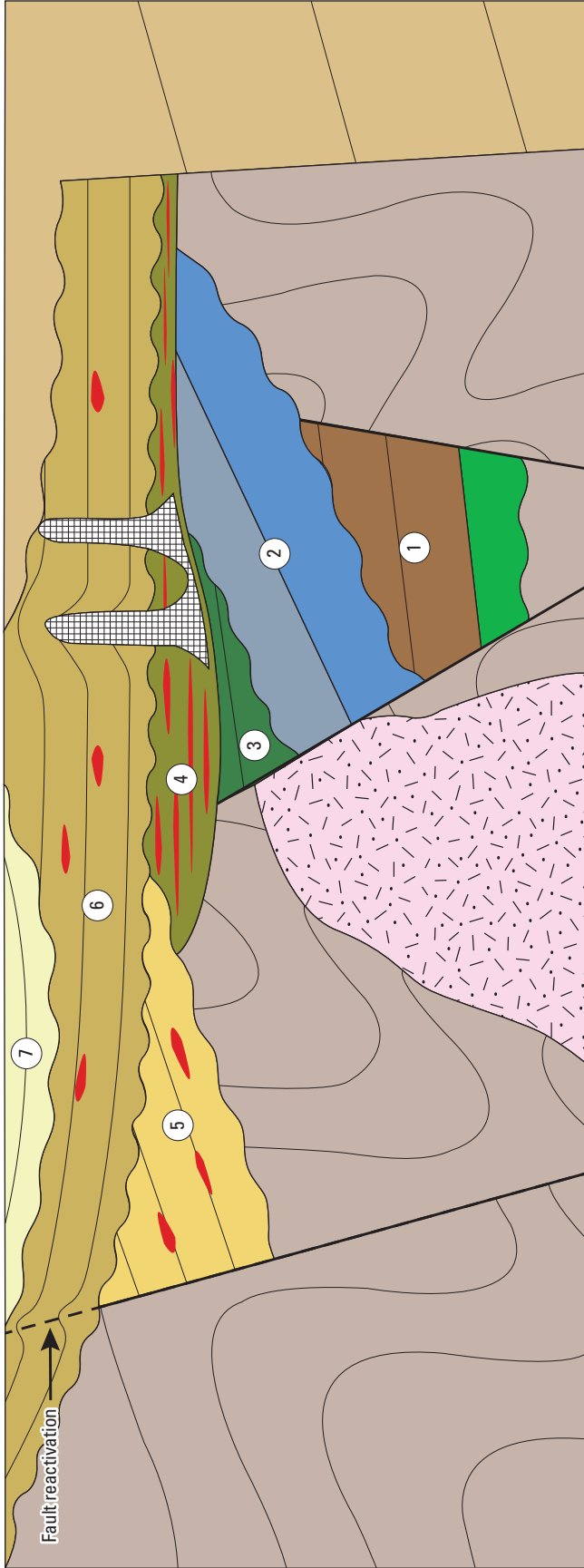


**Figure 2-41.** Stratigraphic column of the Maritimes Basin, Canada, showing the position of sediment-hosted copper mineralization. Modified from Kirkham (1974) and Giles (1981). Mineralization zone location and thickness are based on Kirkham (1985) and Giles (1981).



EXPLANATION

- |  |   |  |   |
|--|---|--|---|
|  | Copper mineralization   |  | Upper Devonian to Mississippian Horton Group—basinal phase 2                    |
|  | Upper Permian to Cenozoic passive margin rocks                              |  | Upper Devonian to Mississippian Fountain Lake Group—basinal phase 2             |
|  | Permian unnamed sandstone—basinal phase 7                                   |  | Middle to Upper Devonian McAdams Lake Formation and equivalents—basinal phase 1 |
|  | Salt diapir   |  | Devonian volcanic rocks   |
|  | Pennsylvanian to Permian Upper Cumberland and Pictou Groups—basinal phase 6 |  | Late Devonian South Mountain Batholith  |
|  | Pennsylvanian Lower Cumberland Group—basinal phase 5                        |  | Metamorphic rocks   |
|  | Mississippian Windsor and Mabou Groups—basinal phase 4                      |  | Unconformity  |
|  | Mississippian Sussex Group—basinal phase 3                                  |  | Fault   |

**Figure 2-42.** Schematic geologic cross section of the Maritimes Basin, Canada, illustrating major basinal phases, intervening periods of inversion (represented by unconformities), and distribution of sediment-hosted copper mineralization. Modified from Gibling and others (2008).

the Windsor Group (Kirkham, 1985). Although the mineralized strata can be as much as 10 m thick and show evidence of lateral continuity, the maximum reported copper concentration is 4,100 parts per million—too low for mining to be economic. Mineral occurrence databases indicate that copper occurrences are found in the Cumberland, Mabou, and Pictou Groups (Kirkham and others, 1994); many, if not most, are red-bed-type deposits. In the red-bed-type occurrences, chalcocite replaces woody material, pyrite, or carbonate cement in green-gray patches or beds in a red-bed sequence (Kirkham, 1974). Few red-bed-type occurrences have sufficient lateral continuity to form economic deposits. Red-bed-type deposits are of minor importance because of the low tonnages and the erratic nature of the mineralization.

## Deposits and Occurrences

The Maritimes Basin was thoroughly explored for reduced-facies deposits because the stratigraphic sequence appeared ideal for that deposit subtype (Kirkham and others, 2003). Although only occurrences of the reduced-facies subtype were found, two deposits of other subtypes were found. Consequently, rocks within the Maritimes Basin host one red-bed-type deposit, one sandstone-copper or red-bed deposit, and 155 sediment-hosted stratabound copper occurrences (tables 2-11, 2-12, and 2-13; figs. 2-43, 2-44, and 2-45). Of the 155 occurrences, 77 are classified as sandstone or red-bed-type copper, 67 are classified as reduced facies, and 11 are not classified. To illustrate the widespread nature of the mineralizing system, numerous red-bed-subtype copper occurrences are shown in figures 2-43, 2-44, and 2-45.

The deposits listed in table 2-11 represent sandstone-copper or red-bed-type mineralization. The Canfield Creek copper deposit (table 2-11; no. 10 in table 2-12; fig. 2-43) occurs within the gray medium- to coarse-grained sandstone of the Cumberland Group that contains abundant plant debris along bedding planes (Ryan and Boehner, 1994). The deposit is along the flank of a salt dome that cuts Upper Carboniferous clastic rocks. Copper mineralization is associated with a zone of carbonaceous detritus in gray, reduced rock units interbedded with red, oxidized units (O'Reilly, 2008). Mineralized sandstone, as much as 5.2 m thick and containing 1.2 percent copper, extends to a depth of at least 110 m. A grid of 27 drill holes delineated 300,000 metric tons of ore containing 1.2 percent copper (Ryan and Boehner, 1994).

The Dorchester deposit occurs in gray, carbonaceous sandstone and conglomerate of fluvial channel sequences at the base of the Pennsylvanian Boss Point Formation (Cumberland Group) immediately overlying Mabou Group red beds (table 2-11; no. 15 in table 2-12; fig. 2-43). The deposit is a 1 km by 2 km, lenticular, northeast-trending zone of low-grade ore (less than 1 percent copper), with high-grade (2–10 percent copper) sections (New Brunswick Mineral Occurrence Database, 2012). Copper minerals replace carbonized plant debris, detrital fragments, and pyrite, and fill interstices

and vugs in the coarser sediments (Boyd, 1977). Exploration identified a 6-meter-thick tabular zone dipping from the surface to a depth of 330 meters along a strike length of 1.1 km; copper grades were less than 1.0 percent (Boyd and Boyd, 1977). Boyd (1977), as reported in Normore and Mitton (2007), calculated a resource of 9.58 million metric tons at 0.73 percent copper that (at the observed dip of 15 degrees) would be an unlikely candidate for profitable mining as of 2014.

Lochaber Lake (no. 115 in fig. 2-44) is downsection from the host rock units defined for the Maritimes Basin (Hooper, 1972; Northcote and others, 1989; Ross, 1998). It is included as an occurrence in this study because the copper mineralization is similar to surrounding occurrences, and identified resources are noteworthy (2.29 million metric tons at 0.33 percent copper; Hooper, 1972).

## Mineral System Components

A copper source and evaporite-bearing rocks were necessary components for copper mineralization to form in the Maritimes Basin. Copper was likely mobilized from bimodal volcanic rocks of the Fountain Lake Group, and later remobilized and precipitated into the Windsor Group (figs. 2-41 and 2-42; Murphy, 2007). Subsequent diagenetic changes could release the copper from the Windsor Group rocks for remineralization (Walker, 1989). The Windsor, Mabou, Cumberland, and Pictou Groups also contain red beds that may have been an additional source of copper in the Maritimes Basin. Dissolution of gypsum and anhydrite in the Windsor Group may have contributed a brine source to the hydrothermal system present during mineralization, which would facilitate transport of copper-sulfide minerals. The evaporite beds in the Windsor Group may also have acted as a seal preventing upward migration of copper-bearing fluids.

Reductants for reduced-facies-type and red-bed-type deposits are scattered throughout sedimentary rocks in the Maritimes Basin. For the reduced-facies-subtype deposits, the contrast between the oxidized continental clastic Horton Group and the overlying reduced marine carbonate Mississippian Macumber Formation (Boehner and Giles, 2008) formed the most laterally consistent redox boundary where copper precipitated. Several cycles of red beds overlain by carbonaceous limestone are higher within the Windsor Group (Boehner and Giles, 2008), so copper mineralization is in more than one host rock sequence. Within the Mabou, Cumberland, and Pictou Groups, carbonized plant fossils in the gray sandstone (Brunner, 1958) served to reduce sulfate to sulfide and precipitate sulfide minerals.

The known deposits and occurrences are reduced-facies-type or red-bed-type, but necessary mineral system components for sandstone-copper-subtype deposits are also present in the Maritimes Basin. Oil shales that contain the necessary petroleum reductant for sandstone-type deposits are present in the lacustrine beds of the middle Horton Group (Hamblin



**Table 2-11.** Sediment-hosted stratabound copper deposits and occurrences within the Maritimes Basin, Canada.

[t, metric tons; Mt, million metric tons; %, percent]

Deposit name	Latitude	Longitude	Major commodities	Resources (unmined)	Citation
Red bed deposit					
Canfield Creek	45.800	-63.667	Cu, Ag	300,000 t at 1.2% Cu	O'Sullivan (1981); Ryan and others (1989); Kirkham and others (1994); Kirkham and others (2003); Keppie (2000); O'Sullivan (2006)
Sandstone-copper or red bed deposit					
Dorchester	45.929	-64.476	Cu, Ag, U, Zn, Pb	9.58 Mt at 0.73% Cu	Boyd (1977) as reported in Normore and Mitton (2007); Kirkham and others (1994); New Brunswick Department of Natural Resources and Energy (2000); New Brunswick Mineral Occurrence Database (2012); Kirkham and others (2003)

**Table 2-12.** Names of deposits and occurrences that correlate to numbers in figure 2-43.

[No., number; Occ, occurrence]

No.	Name	No.	Name	No.	Name	No.	Name
1	Balfroon	22	Feeley Mine	43	Midway Copper Belt - Occ 7	64	Riverside Mine
2	Balfroon - 1	23	Fleming Brook Mine	44	Midway Copper Belt - Pit 1	65	Rockley
3	Balmoral Brook	24	French River Mouth	45	Midway Copper Belt - Pit 2	66	Scotch Hill
4	Biz Brook	25	French River Mouth No 1	46	Midway Copper Belt - Pit 3	67	Scotsburn Brook
5	Black River	26	French River Mouth No 2	47	Midway Copper Belt - Pit 5	68	South Pugwash
6	Blockhouse Claim Group	27	Goshen	48	Midway Copper Belt - Pit 6	69	South Pugwash/ No 1
7	Blockhouse No 2	28	Grant Brook	49	Midway Copper Belt - Shaft No 1	70	South Pugwash/ No 2
8	Blockhouse Point No 1	29	Hopewell	50	Mine Hole Brook	71	South Pugwash/ No 3
9	Brookfield Copper Showing	30	Hopewell Cape (The Rocks)	51	Mine Hole Brook/ No 1	72	Springhill
10	Canfield Creek	31	Kerrs Mills	52	Mine Hole Brook/ No 2	73	Tatamagouche
11	Caribou River	32	King Mine	53	Nappan	74	Telford
12	Central New Annan	33	Knoydart Point and Brook	54	New Horton - Pit 12	75	The Island Roadcut
13	Chisholm Brook	34	Limerock	55	New Horton Mine	76	Treen Point
14	Churchville Road	35	Little Ridge - Pit 13	56	Oliver	77	Union Centre
15	Dorchester	36	Malagash (North Shore)	57	Oliver - No 1	78	Waterside
16	Durham	37	Malagash Centre	58	Oliver - No 2	79	Wentworth
17	East River	38	Malagash Point	59	Oliver North Prospect	80	Woodlock Brook Prospect
18	East Wallace River	39	Matheson Prospect	60	Oliver South	81	Yellow Brook
19	Elgin	40	McLellan Brook (Stewart Brook)	61	Palmer Mine		
20	Eureka (Ferrona Junction)	41	McLellan Brook Holes 1 2 and 3	62	Plainfield Brook		
21	Eureka Hole 1	42	Middle Stewiacke	63	River John (East Branch)		

**Table 2-13.** Names of occurrences that correlate to numbers in figure 2-44.

[No., number]

<b>No.</b>	<b>Name</b>	<b>No.</b>	<b>Name</b>	<b>No.</b>	<b>Name</b>	<b>No.</b>	<b>Name</b>
82	Ballantynes Cove	103	Glen Road	124	Meadow Green (Kennco Hole 6)	145	Whycocomagh
83	Big Marsh	104	Guysborough Area 2-03- ABCD	125	Monastery	146	Willies Brook
84	Black River	105	Guysborough Area 2-03-F	126	Musgrave Showing	147	Yankee Line Road
85	Boisdale	106	Guysborough Area 2-03-K	127	Ohio		
86	Brierly Brook - 2	107	Highway Showing	128	Pitchers Farm - 1		
87	Campbell S Brook	108	Iona	129	Pitchers Farm - 2		
88	Cape Blue	109	James River Station	130	Point Edward		
89	Cape Jack	110	Johnstown	131	Pomquet River		
90	Carr Brook	111	Keaton Point	132	Rights River - Main Showing		
91	Catalone Lake	112	Kirkwood	133	Rights River - Railway Showing		
92	Christmas Island - 1	113	Lakevale	134	Salmon River		
93	Christmas Island - 2	114	Little Judique	135	Soldier Cove North		
94	Christmas Island - 3	115	Lochaber Lake	136	Southwest Mabou River		
95	Coxheath - Contact Zone	116	Lower North Grant	137	Squire Point		
96	Delhanty Brook	117	Mabou	138	St Josephs - 1		
97	East Bay	118	Macbeth Brook	139	St Josephs - 2		
98	Finlay Beach	119	Mackay Showing	140	Steele Crossing		
99	Frenchvale - Leitches Creek	120	Macmullin Brook	141	Steep Creek		
100	Garbarus Lake	121	Mcintyre Lake	142	Sylvan Glen Area		
101	Gillisdale	122	McLeod Point	143	Washabuck		
102	Glen Morrison (GM - 1)	123	McPherson	144	Washabuck - Crow Point		

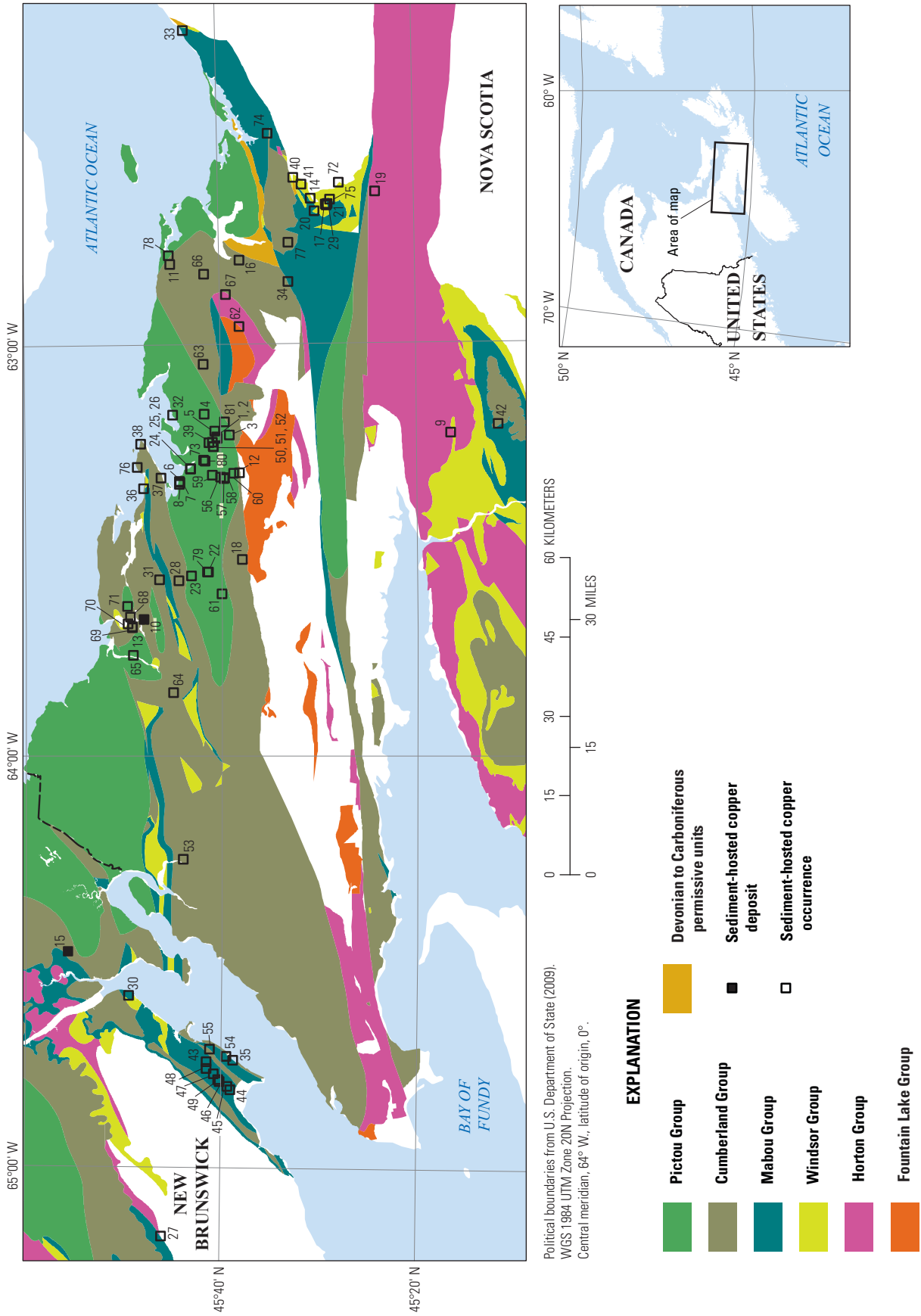


**Figure 2-43.** Geologic map of western Nova Scotia and eastern New Brunswick showing sediment-hosted copper deposits and occurrences associated with the Maritimes Basin, Canada; names that correlate with numbers are listed in table 2-12. Geology from Keppie (2000) and New Brunswick Department of Natural Resources and Energy (2000).

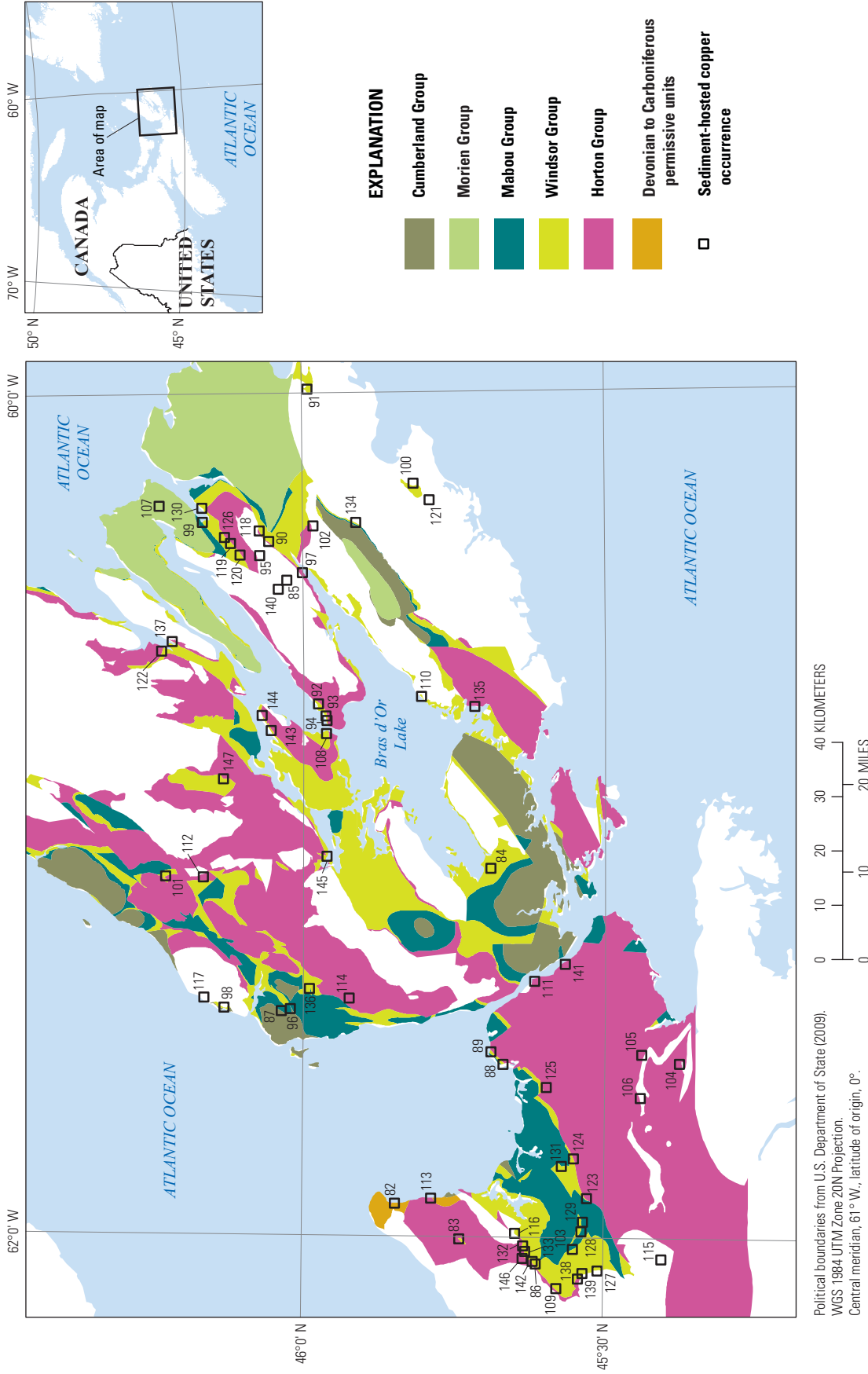


**Figure 2-44.** Geologic map of eastern Nova Scotia showing sediment-hosted copper occurrences associated with the Maritimes Basin, Canada; names that correlate with numbers are listed in table 2-13. Geology from Keppie (2000).

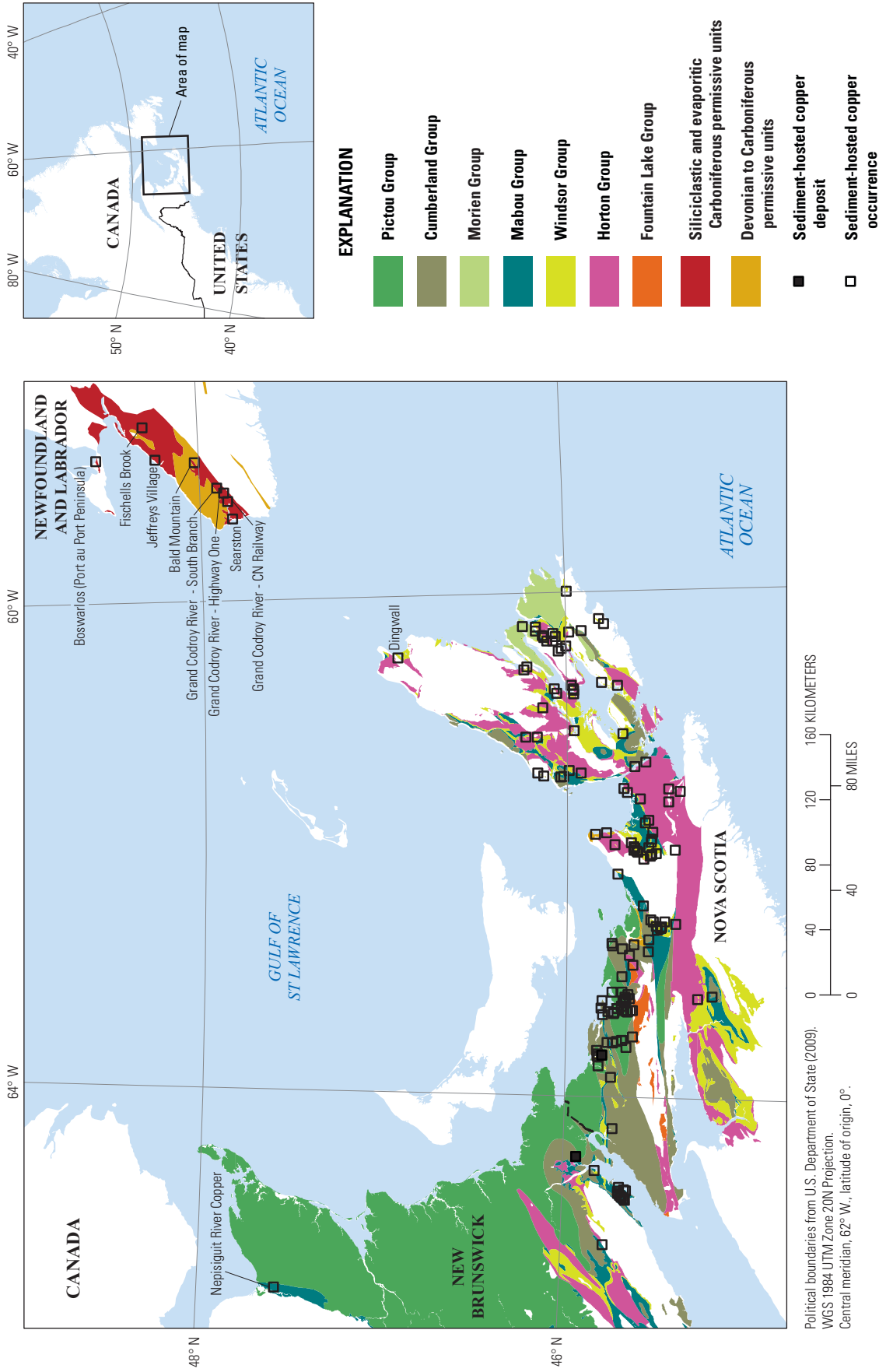


**Figure 2-45.** Geologic map of eastern New Brunswick and western Newfoundland showing sediment-hosted copper deposits and occurrences associated with the Maritimes Basin, Canada. Geology from Davenport and others (1999), Keppie (2000), and New Brunswick Department of Natural Resources and Energy (2000).



and others, 1995). Coal of the Cumberland Group (Boehner and Giles, 2008) is a possible source rock for natural gas, which could act as a reductant and hydrogen sulfide source in the development of sandstone-type deposits. Traps for the copper-bearing liquid or gaseous petroleum are an additional requirement for sandstone-copper-subtype deposits to form. Anticlines might serve as traps for pre-ore natural gas, but a notable potential for traps also exists near the salt domes (fig. 2-42). Fault traps, stratigraphic traps associated with several unconformities in the cross section, and combination traps are present as well (Enachescu, 2006). On the basis of these components, sandstone-copper-subtype deposits within the Maritimes Basin are geologically plausible. Hansley (2007) described low concentrations of pyrobitumens in sandstone pores within samples from the Dorchester deposit; accompanying relicts of carbonized plant fossils suggest that the deposit could be either a red-bed or a sandstone subtype.

## Principal Sources of Information

Digital geologic maps of Nova Scotia, New Brunswick, and Newfoundland provided information on the distribution of permissive rocks for sediment-hosted stratabound deposits in the Maritimes Basin. For New Brunswick and Nova Scotia, source maps are 1:500,000-scale digital maps published by the New Brunswick Department of Natural Resources and Energy and Nova Scotia Department of Natural Resources (Keppie, 2000; New Brunswick Department of Natural Resources and Energy, 2000). The Newfoundland geology was sourced from a 1:1,000,000-scale digital map published by the Newfoundland Department of Mines and Energy, Geological Survey (Davenport and others, 1999). Global sediment-hosted copper deposit databases (Kirkham and others, 2003; Cox and others, 2003), as well as reports of the Geological Survey of Canada, were the main sources of mineral deposit and occurrence information.

## Chuxiong Basin, China—Assessment Tract 142ssCu6000

Sedimentary rocks of the Cretaceous Gaofengsi, Puchanghe, and Matoushan Formations in south-central China host stratabound copper deposits. The Chuxiong Basin, which is 15,400 km<sup>2</sup> in areal extent and 280 km long, hosts at least 12 sandstone-type sediment-hosted copper deposits and 10 occurrences (fig. 1-11).

### Tectonic Setting

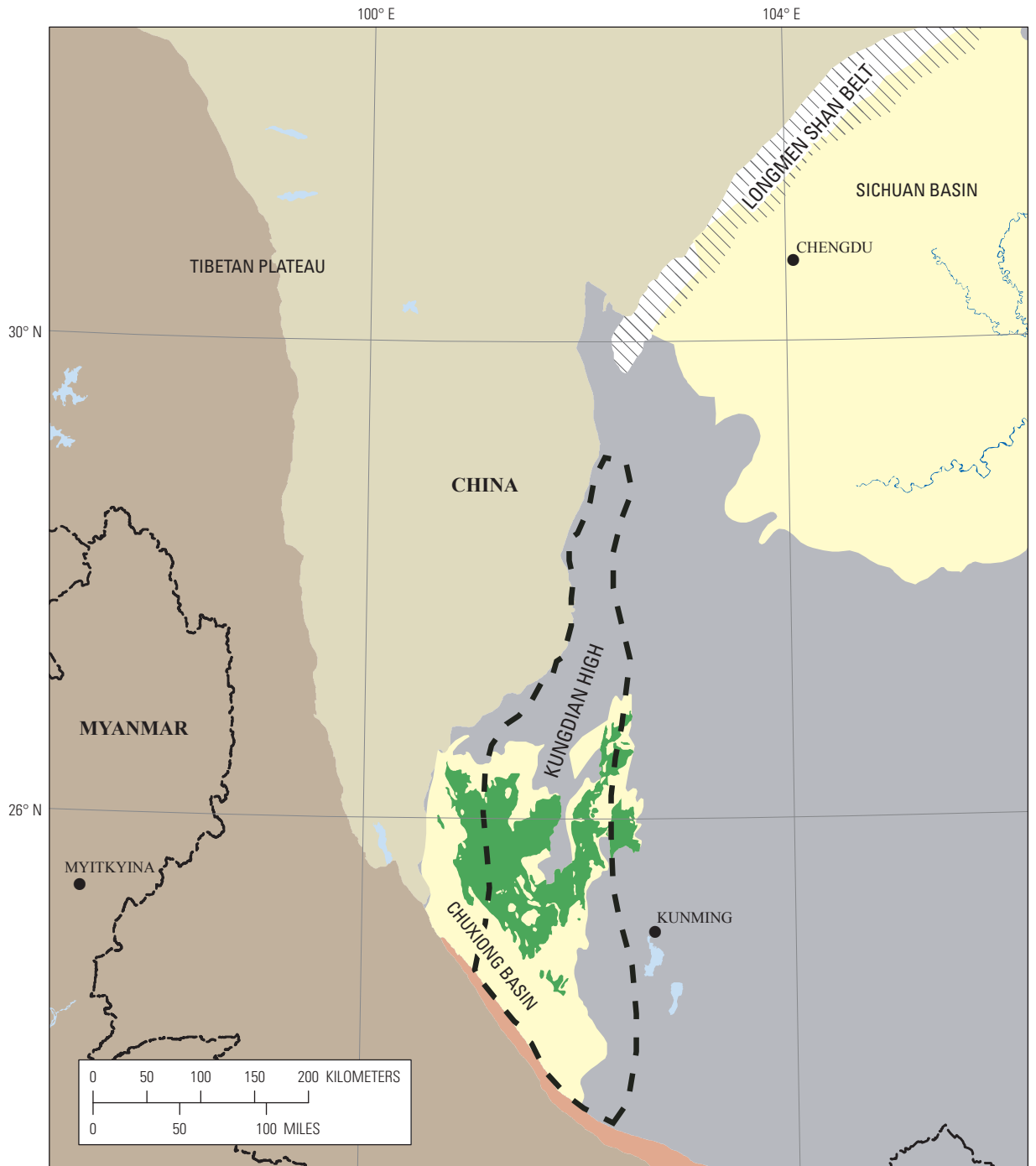
The Chuxiong Basin is the southern part of a north-northeast-trending Triassic foredeep that developed between the advancing northeastern Tibetan Plateau and the Yangtze

Platform (fig. 2-46; Burchfiel and Zhiliang, 2013). The foredeep filled with Upper Triassic to Cretaceous shallow-marine and fluvial material, which became the host sandstone for the copper deposits. The Yangtze tectonic unit, also known as the South China block, consists of a sequence of Paleozoic through Cenozoic shallow-marine and nonmarine sedimentary rocks with numerous unconformities. The Yangtze Platform rocks overlie two continental fragments that were accreted during the Neoproterozoic to early Paleozoic. The southern boundary of the Chuxiong Basin and the Yangtze tectonic unit is the Cenozoic Ailao Shan Metamorphic Belt (fig. 2-46).

The foredeep, which includes the Chuxiong and Sichuan Basins, developed along the eastern margin of the Longmen Shan thrust belt and its southern extension that forms the eastern boundary of the Transitional tectonic unit (fig. 2-46; Burchfiel and Zhiliang, 2013). The northeast-trending Longmen Shan thrust belt formed by southeastward thrusting during the Late Triassic Indosinian Orogeny and was later affected by Cenozoic deformation related to the collision of India and Asia (Burchfiel and others, 1995). A complex allochthon, which underlies the eastern part of the Tibetan Plateau, lies to the west of the thrust belt (Burchfiel and others, 1995). The discontinuity of the Mesozoic outcrops between the Chuxiong and Sichuan Basins is the result of post-Oligocene deformation that uplifted basement rocks along north-south-trending structures (Burchfiel and Zhiliang, 2013).

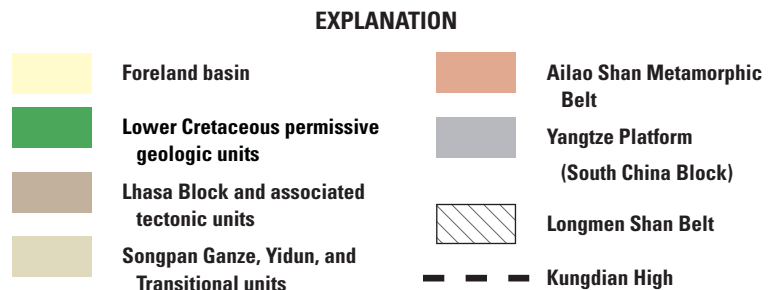
Mesozoic strata of the foredeep were deposited above a north-south trending region shallowly underlain by basement rocks of the Yangtze tectonic unit, the Kungdian High (fig. 2-46). This region was a positive paleogeographic feature during the Paleozoic and early Mesozoic. Paleozoic strata are commonly incomplete, thin, wedge out, or are faulted out on the eastern and western flanks of the high. Flood basalts of the late Permian Emeishan large igneous province covered the western margin of the Yangtze unit and the Tibetan Plateau (Shellnutt, 2014). Along the Kungdian High and in underlying parts of the Chuxiong Basin, however, the Permian Emeishan basalt is missing because of erosion prior to deposition of Upper Triassic strata (Burchfiel and Zhiliang, 2013). The crest of the Kungdian High is overlain by Upper Triassic conglomerate and coarse-grained sandstone.

Late Mesozoic and Cenozoic faults and folds in the Chuxiong Basin form an arcuate pattern that suggests folding in the basin is related to the major thrust fault along the west side (Burchfiel and Zhiliang, 2013). In the northern part of the basin, structures are oriented north-south and extend across the basin margin, dividing the basin margin and the area north of the basin into areas of thick sedimentary rocks separated by uplifts of Precambrian basement rocks. To the south, the structures trend southeastward. The distribution of structures within western and central parts of the basin is consistent with a décollement-style fold and thrust belt that included basement rocks in the north and northeastern parts of the basin. The Paleogene–Neogene structures in the Chuxiong Basin may be related to the same deformational processes that formed the Cenozoic Longmen Shan thrust belt.



Political boundaries from U.S. Department of State (2009).  
 Asia Lambert Conformal Conic Projection.  
 Central meridian, 102° E., latitude of origin, 0°.

**Figure 2-46.** Simplified tectonic map of southern China showing major structural units in the region, the Chuxiong and Sichuan Basins, and Lower Cretaceous sedimentary rocks permissive for the occurrence of sediment-hosted copper deposits. Modified from Bureau of Geology and Mineral Resources of Yunnan Province (1990); Bureau of Geology and Mineral Resources of Sichuan Province (1991); Chen and others (2000); Fugro Data Services AG (2005); Jia and others (2006); and Burchfiel and Zhiliang (2013).



## Stratigraphy

The basin contains a thick section (about 10 km) of Middle Triassic to Paleogene dominantly nonmarine red beds (table 2-14; Burchfiel and Zhiliang, 2013). Stratigraphic unit names of the Chuxiong Basin are different for eastern and western flanks of the basin, which lie on either side of the Kungdian High and within different provinces. Nevertheless, the overall sequence is similar. The section begins with Middle Triassic limestone or Upper Triassic nonmarine basal sandstone and conglomerate. These rocks are overlain by Upper Triassic marine rocks then by Upper Triassic nonmarine strata with coal beds. The rest of the section, from Upper Triassic to Late Cretaceous, consists of nonmarine sandstone, mudstone, shale, and conglomerate, with some lacustrine limestone and minor halite or gypsum in Jiangdihe, which correlate with Xiaoba rocks (table 2-14). The Upper Triassic strata are largely pale brown and tan, but Jurassic and Cretaceous rocks are red and maroon (Yano and others, 1994; Burchfiel and Zhiliang, 2013).

The late Permian Emeishan large igneous province covers the western margin of the Yangtze structural unit and the Tibetan Plateau and underlies the Chuxiong Basin (Zhang and others, 1990; Shellnutt, 2014). The thickness of the continental flood basalts decreases from west to east and north to south in the Chuxiong Basin area. In the west, the basalts are 2 to 3 km thick but are only 0.7 to 1 km thick in the east (Zhang and others, 1990). These mafic rocks are a potential source of copper for the sandstone-copper deposits in the Chuxiong Basin.

## Deposits and Occurrences

Twelve deposits are reported for the Chuxiong Basin (fig. 2-48, table 2-15). The Liuju, Dacun, Moudin, Datongchang, and Haojiahe deposits are the largest in the Chuxiong Basin, each containing more than 10 million metric tons of ore with copper grades between 1.1 and 1.8 percent (table 2-15). Ore minerals include bornite, chalcocite, and chalcopyrite (Kirkham and others, 2003; Kamitani and others, 2007).

Most of the sandstone-copper deposits and occurrences are found in coarse-grained clastic rocks of the Upper Cretaceous Matoushan Formation in the northwestern part of the basin and correlative rocks of the Xiaoba Formation in the northeast (fig. 2-47; Chen, 1988; Editorial Committee of the Mineral Deposits of China, 1990; Qin and others, 1993; Zhuang and others, 1996; Chen and others, 2000; Chen and Xia, 2005; Chen, 2012). Minor occurrences of copper mineralization are noted throughout the underlying Jurassic and Lower Cretaceous sedimentary units in the Chuxiong Basin (Li and others, 1968; Chen, 1988).

The limited information on sediment-hosted stratabound copper deposits in the Chuxiong Basin suggests the deposits are the sandstone-copper subtype. The available literature makes no mention of sulfide minerals replacing wood or carbonized plant matter in these deposits.

Sandstone-copper-subtype deposits occur where migrating oxidized, metal-bearing brines mix and react with accumulations of mobile hydrocarbons, such as oil and gas (for example, Hayes and others, 2012). Evidence for a mobile hydrocarbon reductant at the Haojiahe deposit is supported by the following statement by Qin and others (1993): “there commonly exist postdepositional veinlike, spotted, and cloud dry asphalt, with organic carbon showing positive correlation with Cu and Au content.” Sandstone-type copper deposits may be localized near structural traps, where hydrocarbons can accumulate. The Haojiahe, Datongchang, and Liuju deposits (also known as Luzhou or Liu Zu) are localized near the crest or along the flanks of anticlines (fig. 2-49A; Qin and others, 1993; Chen and Xia, 2005; Chen, 2012). Stacked ore bodies, also characteristic of sandstone-type mineralization, are described at Datongchang (Chen, 1988). At Haojiahe and Liuju, the presence of bleached red beds and zoned ore and gangue minerals is consistent with sandstone-type mineralization (fig. 2-49B; Chen, 1988; Editorial Committee of the Mineral Deposits of China, 1990; Qin and others, 1993; Chen and Xia, 2005).

## Mineral System Components

A basalt and red-bed copper source, evaporite-bearing seal rocks, and sour gas were components of the Chuxiong Basin mineralizing system. Permian continental flood basalt of the Emeishan Formation was likely the original copper source. Downsection from stratabound copper deposits are red beds widely believed to be the immediate sources of copper in the deposits (see Hitzman, 2000, for example). Evaporite-bearing rocks underlying the copper-bearing rock units are not present; however, evaporite-bearing rocks are found in the overlying Upper Cretaceous Zaojiadian and correlative Upper Jiangdihe Formations in Yunnan and the Upper Xiaoba Formation in Sichuan (Chen, 1988). The rock units with evaporite minerals (fig. 2-47) may have served as a seal that prevented fluids from ascending further up the stratigraphy. Compaction by sediment overburden likely caused ascent of mineralizing fluids through pre-existing faults (Chen and others, 2000). The major reductant may have been a form of petroleum, most likely sour gas trapped in the host sandstones. Triassic coal beds in Yunnan (Zhuang and others, 1996), and the lateral equivalents in Sichuan, are good candidates for gas source rocks. A definitive containment structure could not be determined for the Chuxiong Basin. The existence of the Kungdian High may explain why deposits are clustered, because highs can focus mineralization.

As with most sediment-hosted stratabound copper systems, red beds are abundant within the Chuxiong Basin copper mineralizing system. All Jurassic and Cretaceous formations of the Chuxiong Basin contain some red beds (fig. 2-47; Li and others, 1968; Chen, 1988). Red beds, bleached by migrating or trapped petroliferous fluids, can become host rocks for sandstone-copper deposits (Thorson and MacIntyre, 2005).

**Table 2-14.** Stratigraphic units of the Chuxiong Basin, Sichuan and Yunnan, China.

[m, meter; —, no data]

System	Series	Formation	Thickness (m)	Description	Formation	Thickness (m)	Description
Paleogene		Hongyazi	0–966	Western part of basin Boulder conglomerate with sandstone (Zhang and others, 1990).			Eastern part of basin
	Cretaceous	Upper Cretaceous	Zhaojiadian 1,151	Upper part (685 m): Alternating purplish-gray, dark purplish massive feldspathic silicarenites and lateritic thin-bedded mudstone (Chen, 2003).  Lower part (466 m): purplish red thick-bedded to feldspathic silicarenites, interbedded with lateritic mudstones and siltstones (Chen, 2003).	Leidashu	0–1,152	Violet pebble sandstone, siltstone, and mudstone comprising three cycles (Zhang and others, 1990).
		Jiangdihe	239–937	Four members:  Baizitian member (112–883 m): purple-red argillaceous siltstone and gray-green, gray-purple and bright purple laminated calcareous mudstone (Chen, 2003).  Yuanrong member (527–700 m): purple-red and brown-red calcareous siltstone and mudstone with a few gray-green and yellowish green mudstones. Contains rock salt (Chen, 2003).  Liujiushan member (100–172 m): gray-purple and brown-red thick-bedded laminated siltstone (Chen, 2003).  Luojuemei member (200–641 m): brown-red mudstone, sandy claystone, and siltstone, intercalated with numerous layers of dark-gray and gray-green calcareous mudstone and marl that weathers to yellowish green (Chen, 2003).	Xiaoba	0–1,380	Intercalations of marls, mudstone, and siltstone with gypsum in upper and middle parts; siltstone, and sandstone in lower part; and conglomerate at base (Zhang and others, 1990).
		Matoushan	42–640	Purplish red and dark purple thick-bedded sandstone intercalated with a few brown-red siltstone and mudstones, containing copper-bearing sandstone (Chen, 2003).			
	Lower Cretaceous	Puchanghe	363–1,233	Purple-red sandstone intercalated with numerous layers of yellowish green calcareous mudstone or gray-striped marls (Chen, 2003).	Feitian-shan	410–436	Violet medium-to fine-grained sandstone, siltstone with marl, with polymictic conglomerate at base (Zhang and others, 1990).
		Gaofengsi	307–1,041	Alternating grayish white, gray-yellow, gray-green, and purplish gray thick-bedded silicarenites and purplish red sandy mudstones intercalated with thin-bedded yellowish green mudstone (Chen, 2003).			

Table 2-14. Stratigraphic units of the Chuxiong Basin, Sichuan and Yunnan, China.—Continued

System	Series	Western part of basin		Eastern part of basin	
		Formation	Thickness (m)	Formation	Thickness (m)
Jurassic	Upper Jurassic	Tuodian	374	Guangou	799–906
			Alternating purplish red sandstone and mudstone (Wang and others, 1992).		Interbeds of violet calcareous sandstone, mudstone and siltstone, with marl on the top part (Zhang and others, 1990).
Triassic	Middle Jurassic	Shedian	1,086	Niugundang	114–536
			Purplish red coarse sandstone and medium sandstone, intercalated with conglomerate and mudstone (Wang and others, 1992).		Violet mudstone and siltstone with sandstone in upper part, and interbeds of these rocks in lower part (Zhang and others, 1990).
	Zhanghe	80–1,060	Xincuan	503–696	
		Nonmarine red sandstones and mudstones (Chen, 2003).		Violet calcareous siltstone and mudstone with sandstone, with medium- and coarse-grained arkose at base (Zhang and others, 1990).	
	Lower Jurassic	Fengjiahe	166	Yimen	355–856
	Upper Triassic	Baoding	—	Baoding	331–1,102
			Alternating beds of grayish green quartzzone sandstone, siltstone, and mudstone (Zhang, 2009).		Interbeds of gray medium- and fine-grained sandstone, siltstone and mudstone, with mudstone at base (Zhang and others, 1990).
	Upper Triassic	Daqiaodi (Tachiaoti)	—	Daqiaodi	211–2,263
			Calcareous sandstone, muddy limestone, yellow sandstone and conglomerate, with interbeds of yellow shale, and grayish yellow mudstone, with coal-bearing seams (Zhang, 2009).		Gray medium-to-coarse grained sandstone with conglomerate, comprising major coal-series, with conglomerate intercalated with sandstone in upper part (Zhang and others, 1990).
	Upper Triassic	Bingnan	—	Bingnan	0–638
			—		Violet medium-to-coarse conglomerate interbedded with sandstone, with marl, limestone and dolomitic limestone in the top part (Zhang and others, 1990).



**Table 2-15.** Sediment-hosted stratabound copper deposits within the Matoushan Formation, and lateral equivalents, of the Chuxiong Basin.

[Abbreviation of mineral names: Az, azurite; Bn, bornite; Cc, chalcocite; Ccp, chalcopyrite; Mal, malachite; Mo, molybdenite. Mt, million metric tons; t, metric tons; %, percent; —, no data]

Name	Latitude	Longitude	Major commodities	Ore minerals	Resources (unmined)	Citation
Dacun	26.050	101.333	Cu, Ag, Pb, Zn, Mo, Se, U	Cc, Bn	12.8 Mt at 1.8 % Cu	Chen (1988); Bureau of Geology and Mineral Resources of Sichuan Province (1991); Kirkham and others (1994); Zhang (1996); Cox and others (2003); Kirkham and others (2003); Kamitani and others (2007)
Datongchang	26.504	102.226	Cu	Cc, Ccp, Mo, Az	14.8 Mt at 1.2 % Cu	Chen (1988); Bureau of Geology and Mineral Resources of Yunnan Province (1990); Kirkham and others (1994); Zhang (1996); Cox and others (2003); Kirkham and others (2003); Yi-Ming and Wu (2006); Kamitani and others (2007); Yan and others (2010)
Geyiza	25.260	101.631	Cu	—	3.1 Mt at 1.0 % Cu	Bureau of Geology and Mineral Resources of Sichuan Province (1991); Kirkham and others (1994); Cox and others (2003); Kirkham and others (2003); Yi-Ming and Wu (2006); Yan and others (2010)
Haojiahe	25.380	101.610	Cu	—	14.1 Mt at 1.1 % Cu	Chen (1988); Bureau of Geology and Mineral Resources of Sichuan Province (1991); Kirkham and others (1994); Cox and others (2003); Kirkham and others (2003); Yi-Ming and Wu (2006); Yan and others (2010)
Laoqingshan	25.191	101.727	Cu	—	1.4 Mt at 1.2 % Cu	Chen (1988); Bureau of Geology and Mineral Resources of Sichuan Province (1991); Kirkham and others (1994); Cox and others (2003); Kirkham and others (2003); Yi-Ming and Wu (2006); Yan and others (2010)
Liuju	25.913	101.354	Cu	Bn, Cc, Ccp	31.0 Mt at 1.3 % Cu	Chen (1988); Bureau of Geology and Mineral Resources of Sichuan Province (1991); Kirkham and others (1994); Chen and others (2000); Cox and others (2003); Kirkham and others (2003); Chen and Xia (2005); Yi-Ming and Wu (2006); Kamitani and others (2007)
Moboliangzi	26.019	101.272	Cu	—	1.0 Mt at 0.92 % Cu	Yan and others (2010)
Moudin	25.400	101.633	Cu	Cc, Mal	14.4 Mt at 1.3 % Cu	Zhang (1996); Bureau of Geology and Mineral Resources of Sichuan Province (1991); Kamitani and others (2007)
Qingshuihe	25.360	101.591	Cu	—	1.0 Mt at 1.62 % Cu	Bureau of Geology and Mineral Resources of Sichuan Province (1991); Kirkham and others (2003); Yi-Ming and Wu (2006); Yan and others (2010)
Shimenkan	25.830	101.390	Cu	—	1.0 Mt at 1.1 % Cu	Yi-Ming and Wu (2006); Yan and others (2010); Bureau of Geology and Mineral Resources of Sichuan Province (1991); Kirkham and others (2003)
Tongchangjing	25.494	101.572	Cu, Ag, Pb, Zn, Mo, Se, U	—	452,000 t at 1.5 % Cu	Chen (1988); Bureau of Geology and Mineral Resources of Sichuan Province (1991); Kirkham and others (1994); Cox and others (2003); Kirkham and others (2003); Yan and others (2010)
Xiwangmiao	25.253	101.730	Cu	—	886,000 t at 1.0 % Cu	Bureau of Geology and Mineral Resources of Sichuan Province (1991); Kirkham and others (2003); Yi-Ming and Wu (2006); Yan and others (2010)

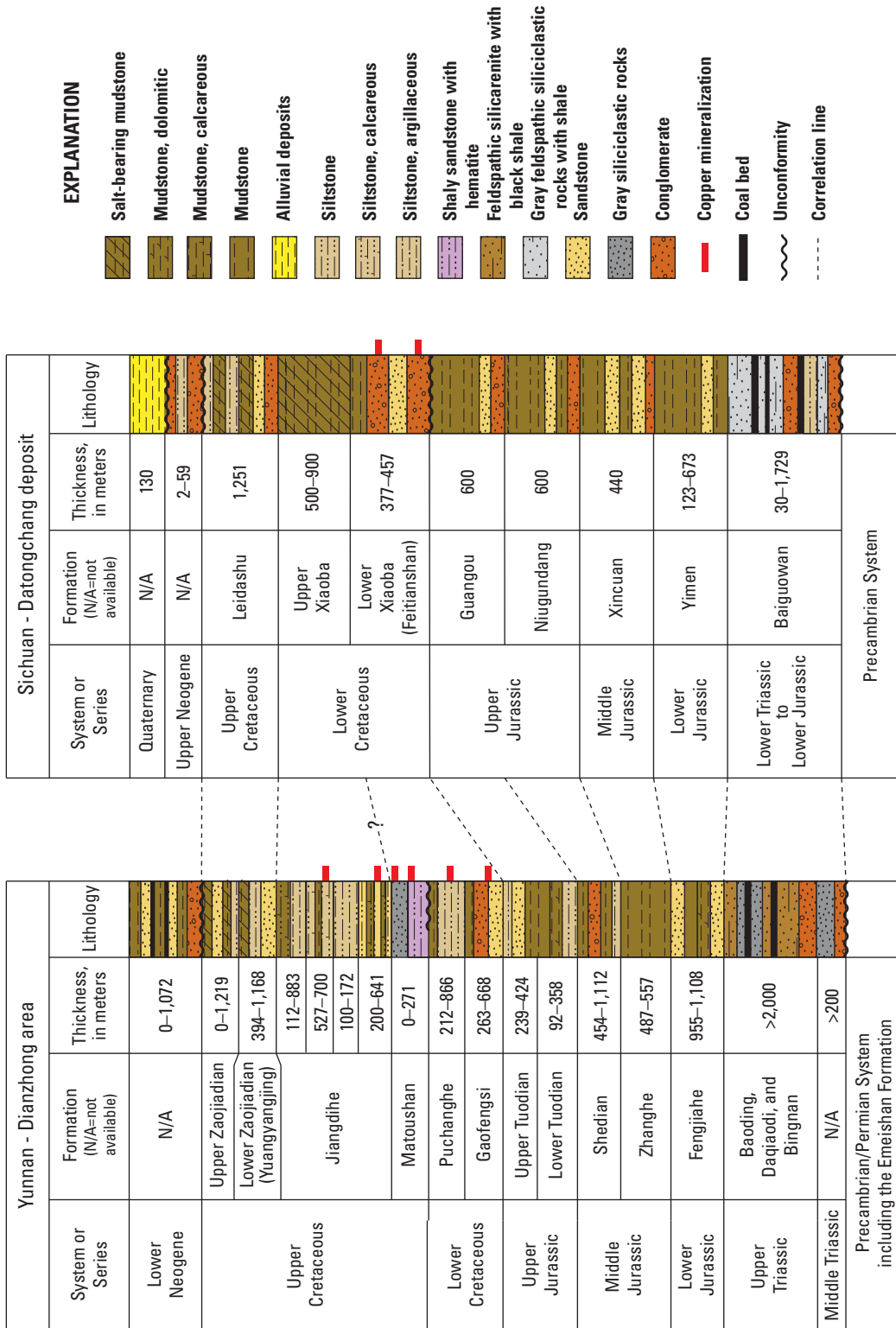


**Figure 2-47.** Correlated stratigraphic columns for the Chuxiong Basin, China, emphasizing the location of sediment-hosted copper mineralization in Cretaceous rock formations. Modified from Chen (1988), Zhang and others (1990), Wang and others (1992), Zhuang and others (1996), Chen (2003), and Zhang (2009).

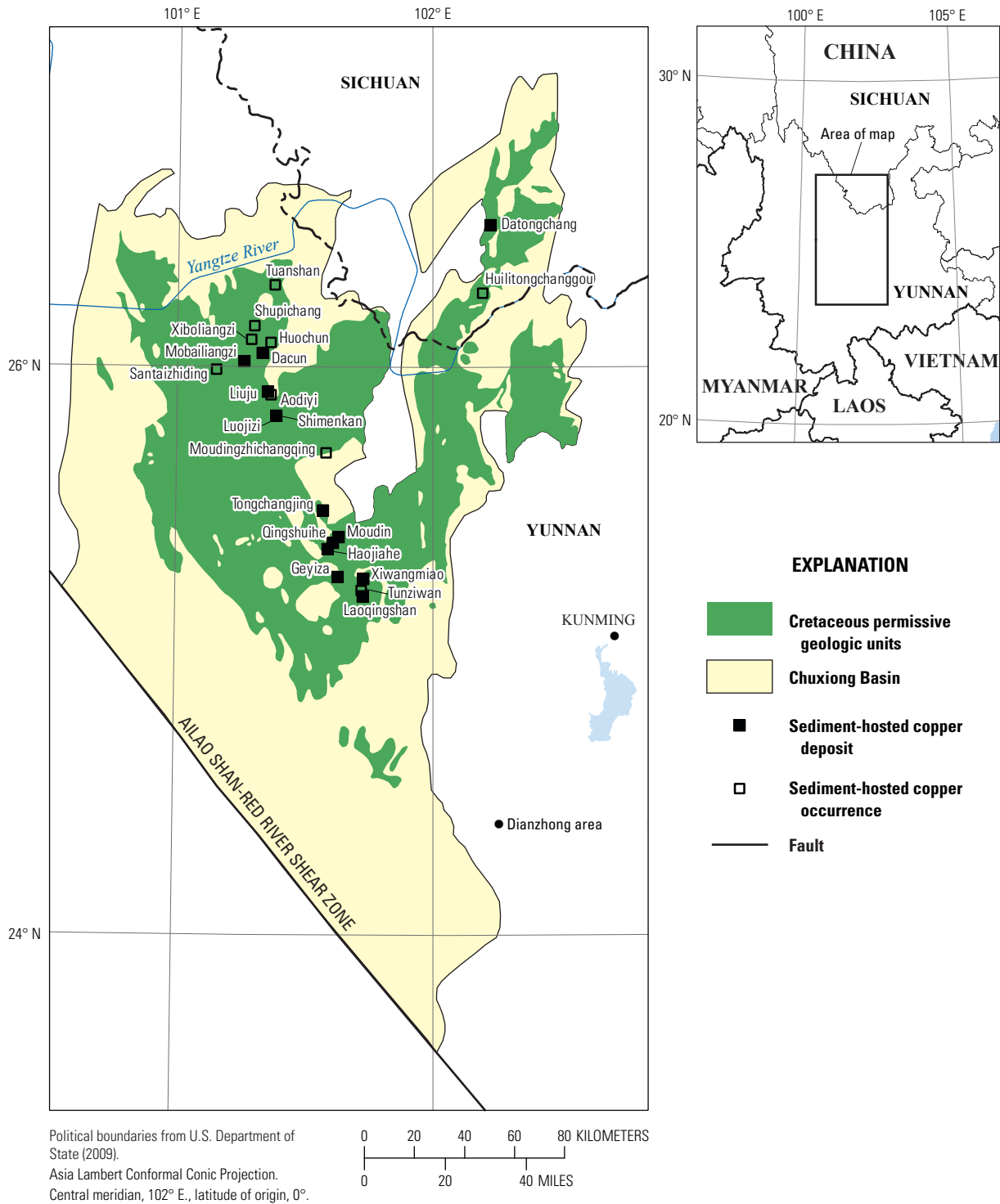


**Figure 2-48.** Map showing the Chuxiong Basin, Cretaceous rocks permissive for sediment-hosted copper mineralization, and sediment-hosted copper deposits and occurrences. The Chuxiong Basin is truncated to the southwest by the Ailao Shan-Red River Shear Zone. Cretaceous rocks from Bureau of Geology and Mineral Resources of Yunnan Province, (1990) and Bureau of Geology and Mineral Resources of Sichuan Province (1991). Basin extent modified from Chen and others (2000) and Fugro Data Services AG (2005).

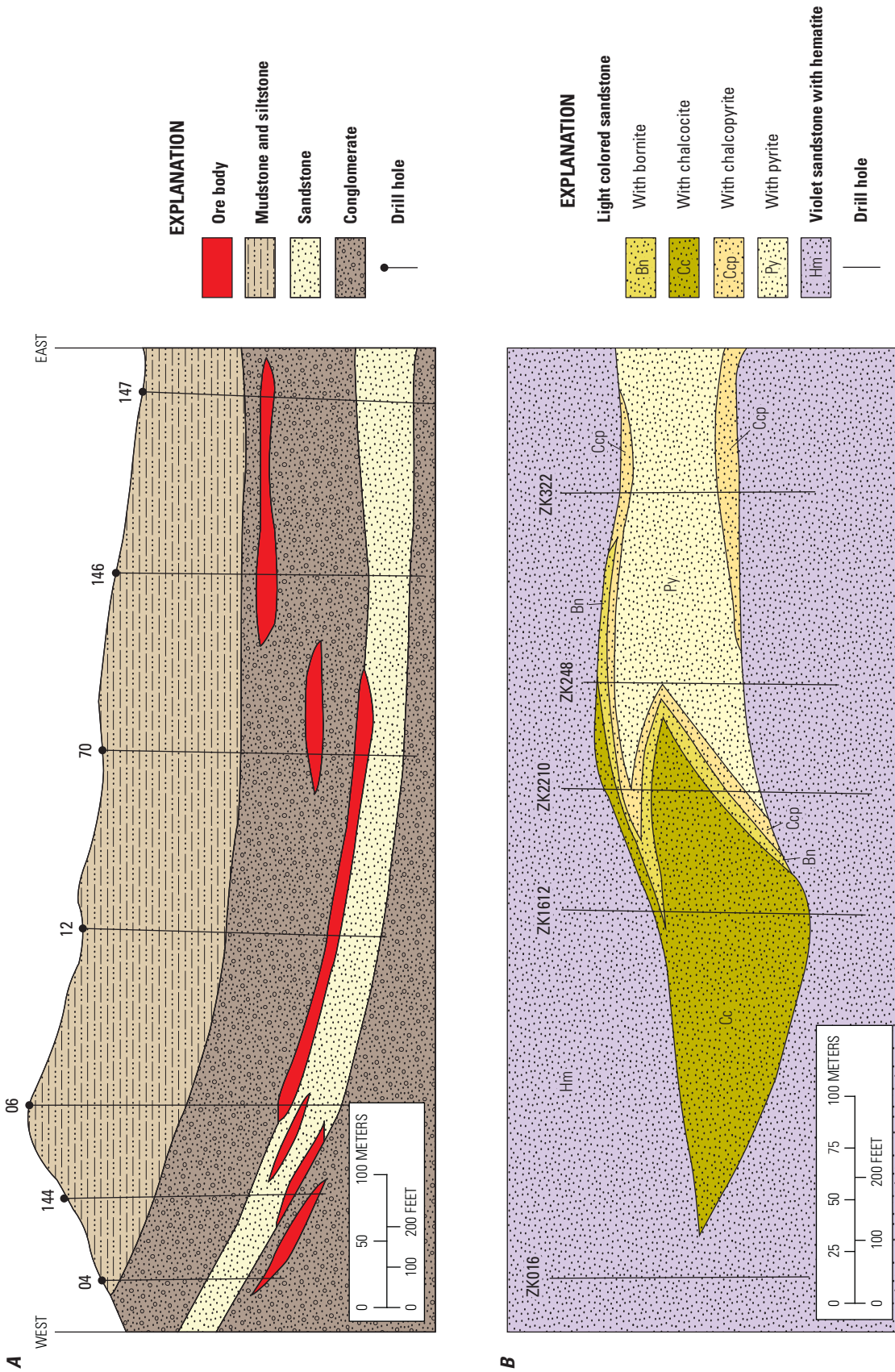


**Figure 2-49.** Cross sections illustrating aspects of sediment-hosted copper mineralization in the Chuxiong Basin, China. (A) Stacked ore bodies in the Datongchang mining area. (B) Mineral zoning in the Liuju deposit. Modified from Chen (1988).

## Principal Sources of Information

A 1:5,000,000-scale mineral resource map (Zhao and Wu, 2006) and two 1:1,000,000-scale geologic maps of the Yunnan and Sichuan Provinces (Bureau of Geology and Mineral Resources of Yunnan Province, 1990; Bureau of Geology and Mineral Resources of Sichuan Province, 1991) provided much of the geologic and mineral resource information for this assessment. World mineral deposit databases from the USGS (Cox and others, 2003) and Geologic Survey of Canada (Kirkham and others, 1994; Kirkham and others, 2003) also provided a substantial amount of information on mineral deposit and occurrence sites as well as reports on the geology and mineral deposits of the Chuxiong Basin cited in table 2-15.

## Salta Rift System, Argentina— Assessment Tract 005ssCu5101

Sedimentary rocks of the Lower Cretaceous to Paleocene Pirgua and Balbuena Subgroups of the Salta Group in the Salta Rift System of northwestern Argentina host stratabound sandstone-copper mineralization. The Salta Rift System extends for 640 km southward from the northern border of Argentina and covers an area of approximately 118,000 km<sup>2</sup> (fig. 2-50). The rift system hosts 2 copper deposits, 4 occurrences, and 14 sites (fig. 1-12).

### Tectonic Setting

The Salta Rift System is one of a series of rifts that developed during the Late Jurassic to Early Cretaceous coincident with the opening of the proto-Atlantic Ocean and the breakup of western Gondwana (fig. 2-50; Ramos and Aleman, 2000; Durieux and Brown, 2007). In the Maastrichtian stage, subsidence spurred the beginning of a sag phase, which continued into the late Eocene (Comínguez and Ramos, 1995). Also during the Maastrichtian stage, sea level rise resulted in a marine transgression that flooded southern South America (Marquillas and Salfity, 1988; Marquillas and others, 2005). The Andean late-Eocene- to early-Oligocene-Inca compressional event subducted the Farallon plate under the South American plate and inverted the Salta Basin. From the early Miocene to the Pleistocene, complex folding and faulting (the Quechua and Diaguita disturbances) deformed the rift zone (Comínguez and Ramos, 1995; Durieux and Brown, 2007; Monaldi and others, 2008).

### Stratigraphy

The stratigraphy of the Cretaceous to Eocene Salta Group varies greatly between the troughs that make up the Salta Rift System (figs. 2-51 and 2-52; Marquillas and Salfity, 1988).

The area is characterized by topographic highs and lows. The lows, or subbasins, generally surround a centrally located high, known as the Salta-Jujuy High (fig. 2-51; Durieux and Brown, 2007). Sedimentation began in the Early Cretaceous as synrift red-bed sedimentary deposits with minor basalts, continued into the Late Cretaceous with postrift carbonates and clastic sediments, and extended into the Paleocene–Eocene with fluvial-lacustrine sediments (Durieux and Brown, 2007). Igneous rocks are mapped in the red-bed sequences in two of the subbasins—the Isonza Basalt in the Alemania Subbasin and the Las Conchas Basalt in the Alemania and Metan Subbasins. These rocks are time correlative with Paraná Volcanic Province magmatism but are derived from different source regions and by different processes (Viramonte and others, 1999).

The Salta Group is subdivided into three subgroups: the Lower and Upper Cretaceous Pirgua Subgroup, the Upper Cretaceous to Paleocene Balbuena Subgroup, and the Paleocene to Eocene Santa Bárbara Subgroup (fig. 2-53). Sediment-hosted copper mineralization is found in the Pirgua and lower Balbuena Subgroups (Durieux and Brown, 2007; Garkus, 2010). The Lower Cretaceous Pirgua Subgroup was deposited during the rifting stage of the Salta Rift System. Thickness of this unit varies widely across the rift system with the thickest areas as much as 4,000 m in some subbasins (fig. 2-52; Marquillas and others, 2005). The Pirgua Subgroup is composed of reddish conglomerate, sandstone, and shale rock units from alluvial fan, fluvial, eolian, and lacustrine depositional environments with intercalated basalts and trachytes (fig. 2-53; Marquillas and others, 2005; Monaldi and others, 2008).

The Balbuena Subgroup was deposited early postrift, beginning in Maastrichtian time, and is generally 400–500 m thick (fig. 2-53; Marquillas and others, 2005). This unit is more laterally consistent across the Salta Rift System than the Pirgua Subgroup (fig. 2-52; Marquillas and Salfity, 1988). The Balbuena Subgroup comprises the lower carbonaceous sandstone Lecho Formation, the middle limestone Yacoraite Formation, and at the top the Olmedo/Tunal Formations that consist mainly of gray to black shale with minor siltstone, limestone, and evaporite minerals (Marquillas and others, 2005). The Yacoraite Formation can be correlated with the limestone of the Totola Formation, found in the Atacama Basin, to the west of the Salta Rift System (figs. 2-51 and 2-52; Mpodozis and others, 2005).

At the top of the Salta Group is the Santa Bárbara Subgroup, which developed in the late postrift stage. This subgroup is typically 700–900 m thick, and is composed of sandstone, siltstone, and mudstone (fig. 2-53; Marquillas and others, 2005).

### Deposits and Occurrences

The Salta Rift System contains 2 deposits, 4 occurrences, and 14 sites (fig. 2-51; table 2-16). The Leon deposit



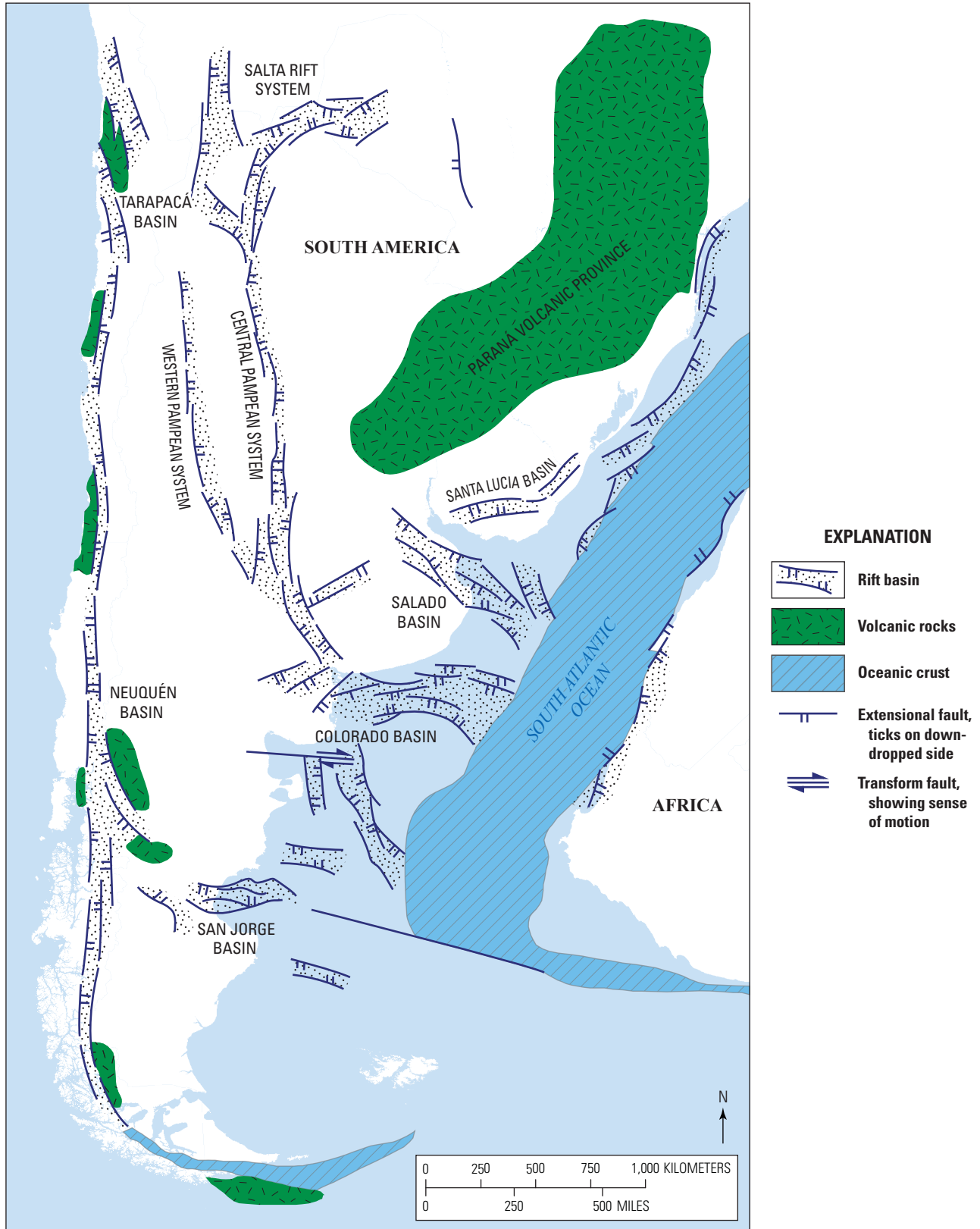


**Figure 2-50.** Map showing areas of Early Cretaceous rifting which formed at the same time as the early opening of the South Atlantic Ocean and breakup of Pangea. Modified from Ramos and Aleman (2000).

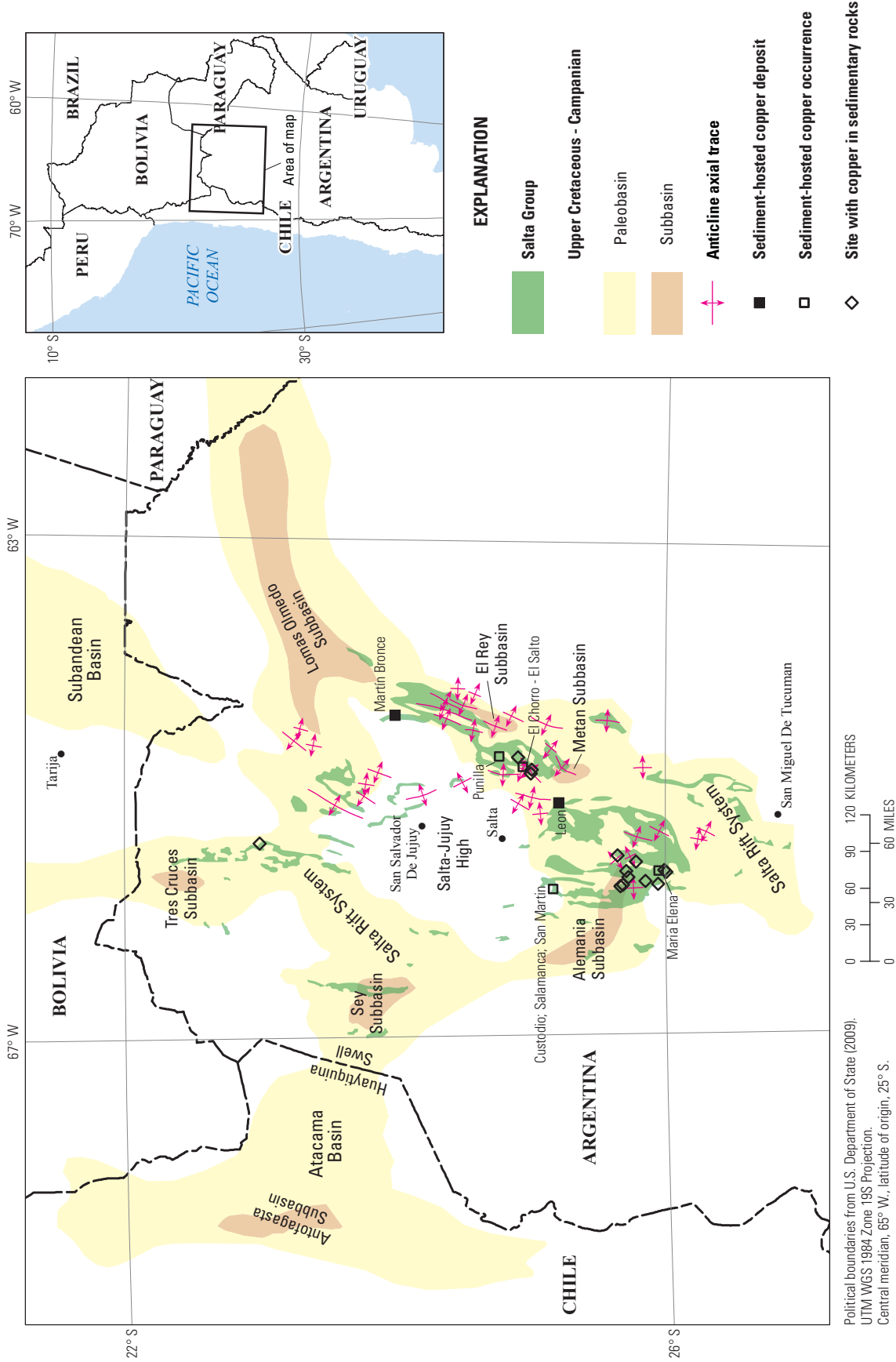


**Figure 2-51.** Map showing the subbasins of the Salta Rift System during the Campanian time; outcrop of the Salta Group; anticlines; and sediment-hosted copper deposits, occurrences, and sites associated with the Salta Rift System, Argentina. Modified from Marquillas and Salfity (1988), Uliana and others (1995), Lizuain and others (1997); Mpodzios and others (2005); Durieux and Brown (2007).

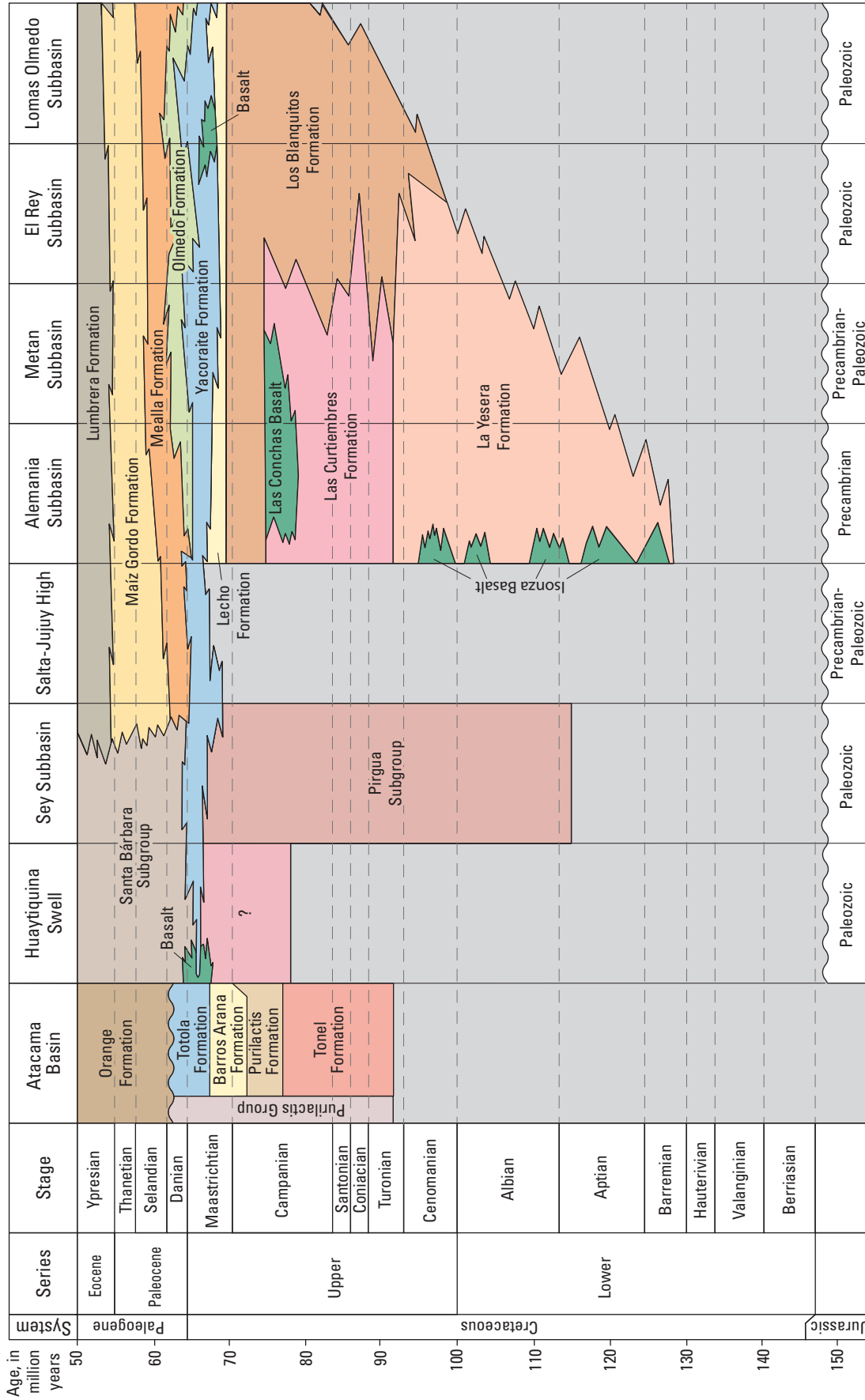


Figure 2-52. Stratigraphic correlation chart showing lateral variation of the Salta Group in northeastern Chile and northern Argentina. Modified from Marquillas and Salffy (1988) and Mpodozis and others (2005). See figure 2-51 for locations of named areas.

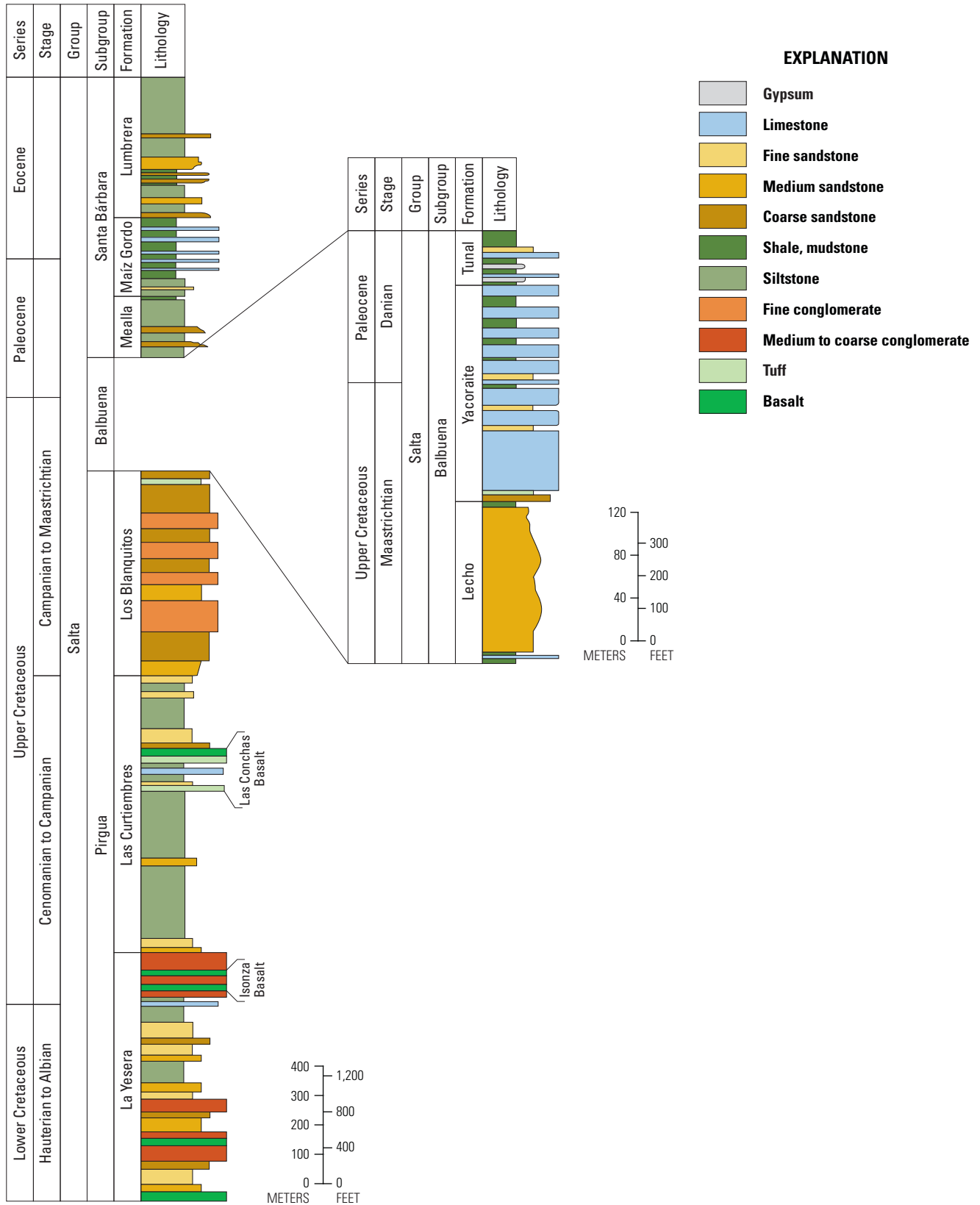


Figure 2-53. Stratigraphic column of the Salta Group, Argentina. Modified from Marquillas and others (2005).

(formerly Juramento) contains a reported 6.66 million metric tons of resources at 0.62 percent copper and 17.98 grams per ton of silver (table 2-16; Alexander Mining plc, 2007). The Leon deposit, which has had several phases of exploration and assessment, is located approximately 55 km southeast of the city of Salta (fig. 2-51; Alexander Mining plc, 2005; Durieux and Brown, 2007). Mineralization is hosted mainly in the carbonate-siltstone Yacoraite Formation of the Balbuena Subgroup with minor amounts also found in the subjacent upper Lecho Formation (figs. 2-54 and 2-55; Durieux and Brown, 2007). The Martín Bronce deposit is located approximately 130 km northeast of the city of Salta (fig. 2-51; Instituto de Geología y Minería, Universidad Nacional de Jujuy, 1996). The Martín Bronce deposit has an estimated 5.6 million metric tons of resources at 3.0 percent copper and is hosted in conglomerate and sandstone rock units (table 2-16; Garkus, 2010). According to Garkus (2010), the deposit is hosted in the Pirgua Subgroup, whereas Avila (1999) places the deposit in the Lecho Formation of the Balbuena Subgroup. The Punilla occurrence is a past producer (about 1942) that produced 3 metric tons of ore with copper grades of approximately 10–15 percent (fig. 2-51; Angelelli, 1984; U.S. Geological Survey, 2010).

## Mineral System Components

Copper source rocks, fluid conduits, and overlying confining beds were crucial components for this sediment-hosted stratabound copper mineralizing system. In the Salta Rift System, red beds of the Pirgua Subgroup are likely the pre-ore copper source rocks (Durieux and Brown, 2007). The Salta Rift System experienced pervasive folding and faulting, which can form pathways for mobile groundwater. The overlying shale and evaporite minerals of the Tertiary Olmedo/Tunal Formation may have contributed to sealing in the ascending fluids, thereby retaining them in mineralizing system. Oxidizing brines, using faults and deformed pathways, could have leached the copper from the source rocks up into the overlying Lecho and Yacoraite Formations. Above the Lecho and Yacoraite Formations lay the shales of the Almedo/Tunal Formation that are also rich in anhydrite and halite, making it a potential seal for the ascending mineral-rich fluids.

The Leon and Martín Bronce deposits are most likely sandstone-copper-subtype deposits. Localization of ore sulfide minerals in former pores within the Lecho sandstone together with the observations that (1) the Yacoraite mineralized carbonate rocks are grainstones, and (2) there is an abundance of pyrobitumens in the Leon deposit (Durieux and Brown, 2007) leads to the interpretation that this mineralization is sandstone subtype at the site of a former petroleum reservoir. Sour gas was, therefore, the likely hydrogen sulfide source and reductant. The Martín Bronce deposit is within the Salta Group (fig. 2-51), like Leon, but the mineral precipitation process is not wholly understood, as Avila (1999) states that neither pelitic materials nor a reducing environment were found at the site. Nonetheless, sandstone-copper subtype is the likely subtype based on available geologic information.

## Principal Sources of Information

A 2,500,000-scale geologic map of Argentina from the Geological and Mining Service of Argentina (SEGEMAR) (Lizuain and others, 1997), a 750,000-scale mineral deposit map from the Argentinian Ministry of Economy (Ricci, 1973), and 500,000-scale provincial maps of Salta and Jujuy (Instituto de Geología y Minería - Universidad Nacional de Jujuy, 1996; Salfity and others, 1998) provided geologic and mineral resource information for this assessment. Mineral deposit localities are derived from multiple sources including Kirkham and others (1994), Kirkham and others (2003), U.S. Geological Survey (2010), and a publication on mineral resources of Argentina by SEGEMAR (Avila, 1999; Peral and Wormald, 1999). Company reports from Alexander Mining plc and AMA Resources (Alexander Mining plc, 2005; Alexander Mining plc, 2007; Garkus, 2010) provided detailed information on the two deposits located in the rift system.

## Conclusions

Geologic information needed to qualitatively assess sediment-hosted stratabound copper potential in several areas of the world is presented in this chapter. These compilations

**Table 2-16.** Sediment-hosted stratabound copper deposits within the Salta Rift System, Argentina.

[Abbreviation of mineral names: Az, Azurite; Bn, bornite; Cc, chalcocite; Ccp, chalcopyrite; Dg, digenite; Mal, malachite. g/t, grams per metric ton; Mt, million metric tons; %, percent]

Name	Latitude	Longitude	Ore minerals	Major commodities	Resources (unmined)	Citation
Leon (formerly Juramento)	-25.217	-65.117	Cc, Dg, Bn, Ccp	Cu, Ag, As	6.66 Mt at 0.62 % Cu and 17.98 g/t Ag	Peral and Wormald (1999); Alexander Mining plc (2005); Alexander Mining plc (2007)
Martín Bronce	-24.003	-64.409	Mal, Az, Cc	Cu, Ag, Au	5.60 Mt at 3.0 % Cu	Kirkham and others (1994); Instituto de Geología y Minería - Universidad Nacional de Jujuy (1996); Avila (1999); Garkus (2010)



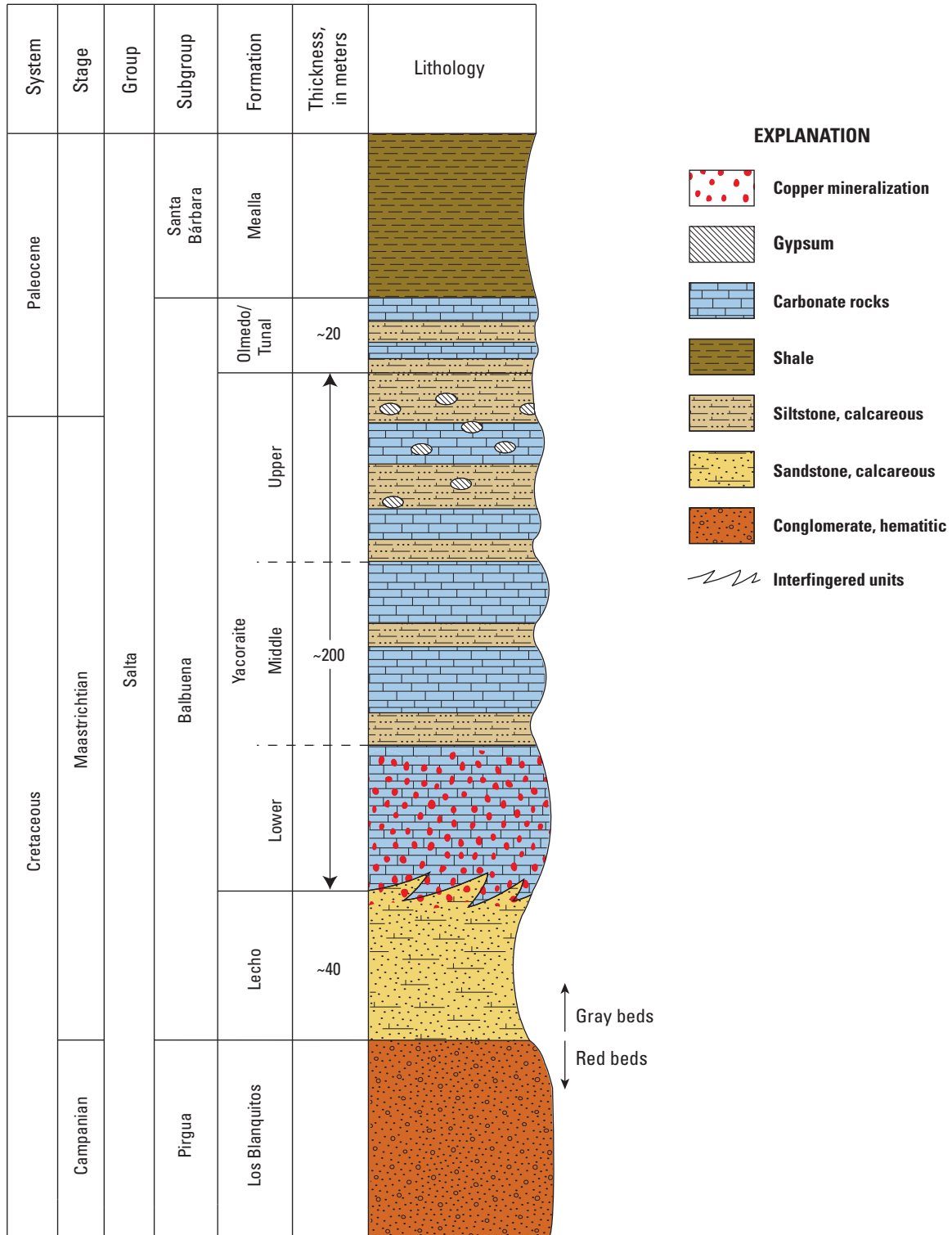


**Figure 2-54.** Stratigraphic column showing sediment-hosted copper mineralization in the Balbuena Subgroup of the Salta Group at the Leon deposit, Argentina. Modified from Durieux and Brown (2007) and Peral and Wormald (1999).

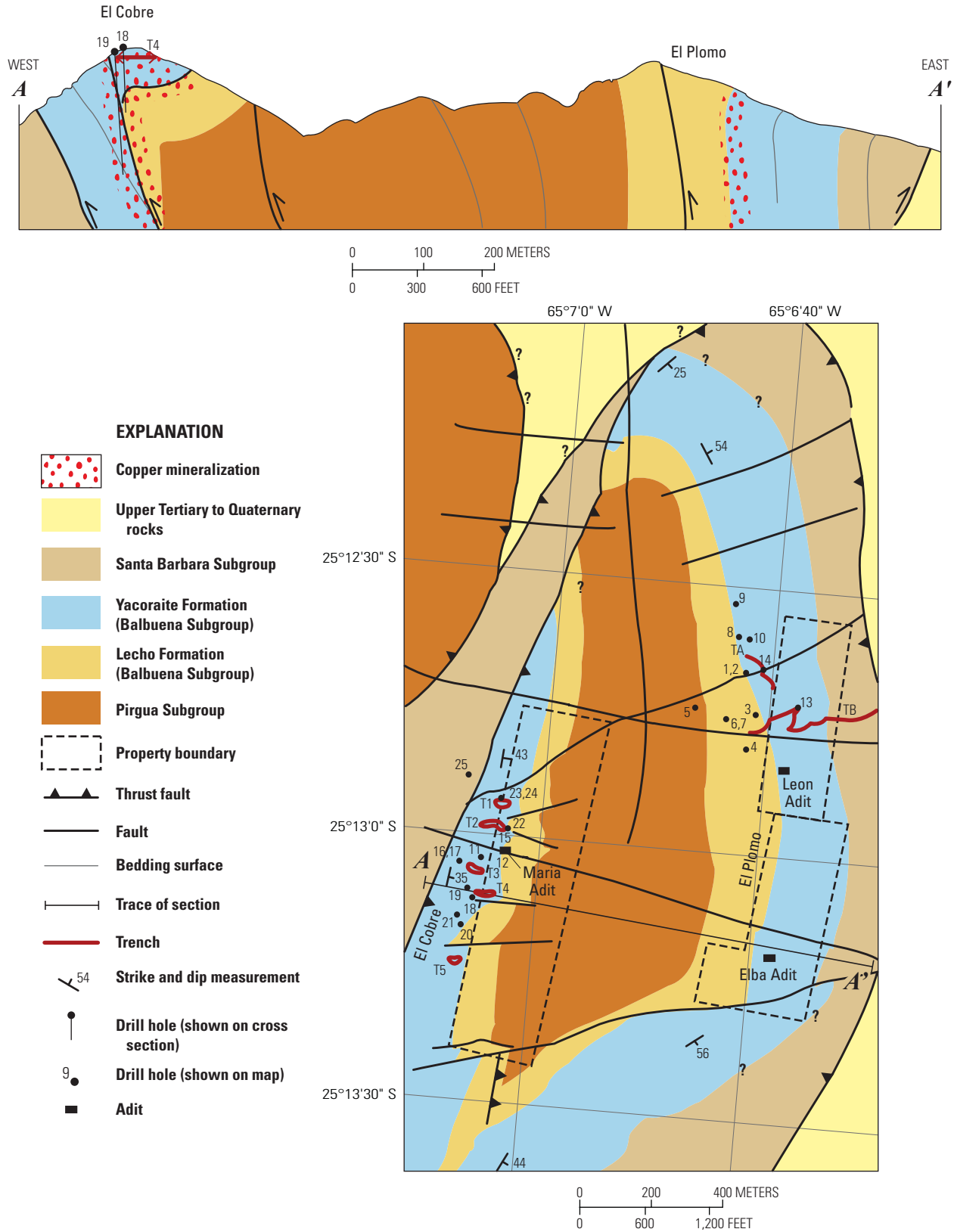


Figure 2-55. Geologic map and cross section through the Leon deposit, Argentina. Modified from Alexander Mining plc (2005).

were initially used to evaluate the quality of the information available and decide how to proceed with the assessment process as part of the USGS Global Mineral Resource Assessment Project. Depending on the quality of the data, we proceeded with either a quantitative assessment using the USGS three-part method or a qualitative assessment. If only limited data were available, the qualitative method was selected. These geologic summaries of the 10 areas permissive for sediment-hosted copper-mineralization in chapter 2 provide the foundation for the qualitative assessment using the analytic hierarchy process (AHP) described in chapter 1.

Mineral-system components for sediment-hosted copper deposits, as outlined by a diagenetic process model, were used to guide the collection of geologic information. This structured outline focused us on the essential ore-forming components of the model and their proxies. Essential mineral system components include a metal source, a chlorine-rich oxidized brine that can carry copper and silver in solution, fluid pathways, and traps that cause mineral precipitation from the brine. Evidence for these components or their proxies was found in stratigraphic columns, cross sections, geologic maps, geologic basin histories, and descriptions of deposits and occurrences. By collecting the same essential geologic information for each permissive area, economic geologists were able to comparatively assess and rank the areas.

A process-based approach that defines what is important to observe provides an advantage that comes with some drawbacks. It can clarify and streamline thinking but at the same time narrows the scope of our observations. Two processes of ore formation, syngeneses and diagenesis, have been debated for sediment-hosted stratabound ore deposits. Literature that is focused on syngeneses does not include observations that support diagenesis and, conversely, literature that is focused on diagenesis does not include observations that support syngeneses. Factual data needed for this compilation was often absent because of differing theoretical viewpoints held by researchers.

Finding a representative proxy for the presence of an oxidized fluid was challenging. We used the presence of sediment-hosted copper deposits and occurrences as evidence for an oxidized fluid but an independent proxy of the feature we are trying to predict would have made for a more robust analysis. The model we used did not distinguish whether subsurface, chlorine-rich brines formed from evaporated seawater or from halite dissolution. Also, the model assumes copper can be leached from hematite in red beds; this hypothesis has not been rigorously evaluated using field data. In hindsight, different system models for reduced-facies and sandstone-type mineralization would have highlighted geologic nuances that significantly affect prospectivity of the deposits. These complications listed do not negate the work presented here, but outline areas for improvement in future research.

When applying our mineral systems model to evaluate mineral potential, we found disparities in what the model would predict and what was actually present. In some areas such as in the Maritimes Basin, all mineral system components

were present but no appreciable ore has been identified. Conversely, some basins with significant sediment-hosted stratabound copper deposits lacked evidence for one or more essential components, as with the Belt-Purcell Basin, where the evaporite source is not certain. This clearly indicates that the mineral systems model needs to be refined.

Availability of relevant information varied widely and posed a difficulty to the assessment process. For example, only publications with basic geologic information were readily available for the Dongchuan Group Rocks. Alternately, data for the Neuquén Basin was ample, including a set of metallogenic maps of Mendoza and Neuquén that show the location of mineral sites, the site names, and the principal mineral commodity information that was key to understanding the mineralizing system. Most of the literature is focused on the geology of deposits and not the larger mineralizing systems in which they occur.

Although available geologic information for each assessment area varied in amount and quality, the focus on compiling data to address the essential mineral-system components provided an effective basis for applying the AHP. For example, more detailed cross sections and more specific information on tectonic setting were available for the Belt-Purcell Basin in Canada and the United States compared with the data for the Dongchuan Group rocks in China. Nonetheless, the Dongchuan Group rocks were ranked above the Belt-Purcell Basin in the AHP (indicating higher potential to contain undiscovered copper deposits) largely because the ore grade and deposit subtype are more favorable.

The approach of identifying and documenting essential mineral-system components used here can be adapted to other deposit types as a basis for either qualitative or quantitative assessments; however, we recommend adjusting the mineral-systems approach as outlined in this section. Our study demonstrates the utility of focusing on mineral system components as well as providing a consistent knowledge base for assessment of sediment-hosted stratabound copper mineralization. Furthermore, identification of missing data about the mineral-system components can guide future research.

## Acknowledgments

Craig Caton, Hannah Campbell, Michael Landkammer, Cassandra Lindsey, Cassandra Hennings, and Andrew Luders, all student interns from Eastern Washington University, made considerable contributions through figure drafting and manuscript proofreading.

The authors thank Mark Mihalasky, USGS, for suggesting the analytic hierarchy process as a tool for this assessment. Stephen E. Box, Jane M. Hammarstrom, Thomas P. Frost, and Steve Ludington (all USGS) greatly improved this manuscript with their detailed constructive reviews. Sincere gratitude is extended to Kathleen M. Johnson, also with USGS, who

provided much-needed guidance throughout the assessment and publication process.

## References Cited

- Aguilar, R.F., 1945, Los yacimientos de areniscas cupríferas del Neuquén: Buenos Aires, Dirección General de Minas, Geología e Hidrogeología, Bulletin 58, 27 p.
- Aitken, J.D., 1991, The Ice Brook Formation and post-Rapitan Late Proterozoic glaciation, Mackenzie Mountains, Northwest Territories: Geological Survey of Canada Bulletin 404, 43 p.
- Aleinikoff, J.N., Hayes, T.S., Evans, K.V., Mazdab, F.K., Pillers, R.M., and Fanning, C.M., 2012, SHRIMP U-Pb ages of xenotime and monazite from the Spar Lake redbed-associated Cu-Ag deposit, western Montana—Implications for ore genesis: *Economic Geology*, v. 107, p. 1143–1175.
- Alexander Mining plc, 2005, Alexander Mining plc placing by Evolution Securing Limited of 66,666,667 ordinary shares at 10p each at 30 pence per ordinary share and admission of the whole to the ordinary share capital to trading on AIM: Alexander Mining plc AIM admission document 24 March 2005, 118 p., accessed September 5, 2011, at [http://www.alexandermining.com/files/AXM\\_Admission\\_Document.pdf](http://www.alexandermining.com/files/AXM_Admission_Document.pdf).
- Alexander Mining plc, 2007, Annual report and accounts 2007: Alexander Mining plc, 52 p., accessed July 9, 2014, at [http://www.alexandermining.com/files/reports/Alexander\\_Mining\\_Annual\\_Report\\_2007.pdf](http://www.alexandermining.com/files/reports/Alexander_Mining_Annual_Report_2007.pdf).
- Al-Laboun, A.A., 1993, Lexicon of the Paleozoic and Lower Mesozoic of Saudi Arabia, Part 1—Lithostratigraphic units—Nomenclature review: Riyadh, Saudi Arabia, Al-Hudhud Publishers, 511 p.
- Allen, J.P., Fielding, C.R., Rygel, M.C., and Gibling, M.R., 2013, Deconvolving signals of tectonic and climatic controls from continental basins—An example from the Late Paleozoic Cumberland Basin, Atlantic Canada: *Journal of Sedimentary Research*, v. 83, p. 847–872.
- Altos Hornos de México, 2008, Israel, a favorable environment for investment: Altos Hornos de México Web page, accessed January 1, 2015, at [http://www.gan.com.mx/Steel/Complements/ahmsa\\_steel\\_israel\\_e/AHMSA\\_steel\\_israel\\_e.htm](http://www.gan.com.mx/Steel/Complements/ahmsa_steel_israel_e/AHMSA_steel_israel_e.htm).
- Amireh, B.S., Amaireh, M.N., and Abdulkader, M.A., 2008, Tectono sedimentary evolution of the Umm Ghaddah Formation (late Ediacaran-early Cambrian) in Jordan: *Journal of Asian Earth Sciences*, v. 33, p. 194–218.
- Amireh, B.S., Schneider, Werner, and Abdulkader, M.A., 1994, Evolving fluvial-transitional-marine deposition through the Cambrian sequence of Jordan: *Sedimentary Geology*, v. 89, p. 65–90.
- Anderson, H.E., and Davis, D.W., 1995, U-Pb geochronology of the Moyie sills, Purcell Supergroup, southeastern British Columbia—Implications for the Mesoproterozoic geologic history of the Purcell (Belt) Basin: *Canadian Journal of Earth Sciences*, v. 32, p. 1180–1193.
- Anderson, H.E., and Parrish, R.R., 2000, U-Pb geochronological evidence for the geological history of the Belt-Purcell Supergroup, southeastern British Columbia, in Lydon, J.W., Höy, T., Slack, J.F., and Knapp, M.E., eds., *The geological environment of the Sullivan deposit, British Columbia: Geological Association of Canada Mineral Deposits Division Special Publication 1*, p. 113–126.
- Andritzky, G., comp., 1998, Mineral map of Namibia: Geological Survey of Namibia, 1 map on 2 sheets, scale 1:1,000,000.
- Angelelli, V., 1984, Yacimientos metalíferos De La Republica Argentina, volume 1: La Plata, Provincia De Buenos Aires, Comisión De Investigaciones Científicas, 291 p.
- Anhaeusser, C.R., and Button, A., 1973, A petrographic and mineragraphic study of the copper-bearing formations in the Witvlei area, South West Africa: *Transactions of the Geological Society of South Africa*, v. 76, p. 279–299.
- Arthaud, François, and Matte, Philippe, 1977, Late Paleozoic strike-slip faulting in southern Europe and northern Africa—Result of a right-lateral shear zone between the Appalachians and the Urals: *Geological Society of America, Bulletin*, v. 88, p. 1305–1320.
- Avila, J.C., 1999, El yacimiento de cobre Martín Bronce, Jujuy, in Zappettini, E.O., ed., *Recursos Minerales de la República Argentina: Buenos Aires, Institute of Geology and Mineral Resources SEGEMAR, anales 35*, p. 947–949.
- Balla, J.C., 2003, Geology of the Rock Creek deposit, Sanders County, Montana, in Balla, J.C., ed., *Mineral deposits of the western Belt Basin: Northwest Mining Association Short Course, 109th Annual Meeting, Spokane, Wash.*, p. 66–78.
- Barnicoat, Andy, 2006, Exploration science—Linking fundamental controls on ore deposition with the exploration process: Predictive Mineral Discovery Cooperative Research Centre, fact sheet, 4 p., accessed June 29, 2012, at [http://www.pmdcrc.com.au/pdfs/brochures\\_exploration\\_science\\_fs.pdf](http://www.pmdcrc.com.au/pdfs/brochures_exploration_science_fs.pdf).
- Batten, K.L., Narbonne, G.M., and James, N.P., 2004, Paleoenvironments and growth of early Neoproterozoic calcimicrobial reefs—Platformal Little Dal Group, northwestern Canada: *Precambrian Research*, v. 133, p. 249–269.

- Bender, Friedrich, 1965, Zur geologie der kupfererzorkommen am ostrand des Wadi Araba, Jordanien: *Geologisches Jahrbuch*, v. 83, p. 181–201.
- Bender, Friedrich, 1975a, Geology of the Arabian Peninsula—Jordan: U.S. Geological Survey Professional Paper 560–I, p. I1–I36.
- Bender, Friedrich, 1975b, Geologic map of Jordan, Plate 1 in Geology of the Arabian Peninsula, Jordan: U.S. Geological Survey Professional Paper 560–I, 36 p., 1 map on 3 plates, scale 1:500,000.
- Beyth, Michael, 1987, The Precambrian magmatic rocks of Timna Valley Southern Israel: *Precambrian Research*, v. 36, p. 21–38.
- Bhatt, B.P., Awasthi, K.D., Heyojoo, B.P., Silwal, Thakur, and Kafle, Gandhiv, 2013, Using geographic information system and analytical hierarchy process in landslide hazard zonation: *Applied Ecology and Environmental Sciences*, v. 1, no. 2, p. 14–22.
- Binney, W.P., and Kirkham, R.V., 1974, A study of copper mineralization in Mississippian rocks of Nova Scotia, in Blackadar, R.G., ed., Report of activities, Part A, April to October 1973: Geological Survey of Canada Paper 74–1 Part A, p. 129–130.
- Blewett, R.S., Henson, P.A., Roy, I.G., Champion, D.C., and Cassidy, K.F., 2010, Scale-integrated architecture of a world-class gold mineral system—The Archaean eastern Yilgarn Craton, Western Australia: *Precambrian Research*, v. 183, p. 230–250.
- Boberg, W.W., 1985, Geological and geophysical review of results of the ARCO 1 Paul Gibbs Well, Flathead County, Montana [abs.]: *American Association of Petroleum Geologists (AAPG) Bulletin*, v. 69, no. 6, p. 1042.
- Body, Kathleen, and Lomberg, Ken, 2007, Ghanzi copper project, Botswana—Independent review of geology and exploration (revised): RSG Global technical report prepared for Hana Mining Ltd., September 11, 2007, 88 p.
- Boehner, R.C., and Giles, P.S., 2008, Geology of the Sydney Basin, Cape Breton and Victoria counties, Cape Breton Island, Nova Scotia: Nova Scotia Mineral Resources Branch Memoir 11, 90 p. (Also available at <http://www.gov.ns.ca/natr/meb/data/pubs/memoir11/memoir11.pdf>)
- Bogdanov, Yu.V., Bur'yanova, E.Z., Kuttyrev, E.I., Feoktistov, V.P., and Trifonov, N.P., 1973, Stratifitsirovannye mestorozhdeniya medi SSSR [Stratabound copper deposits of the USSR]: Leningrad, Nedra Publishing House, 312 p.
- Boleneus, D.E., Appelgate, L.M., Stewart, J.H., and Zientek, M.L., 2005, Stratabound copper-silver deposits of the Mesoproterozoic Revett Formation, Montana and Idaho, with a section on databases and spatial-data files for the geology and mineral deposits of the Revett Formation, by D.E. Boleneus, L.M. Appelgate, M.H. Carlson, D.W. Chase, and M.L. Zientek: U.S. Geological Survey Scientific Investigations Report 2005–5231, 60 p., and data files. (Also available at <http://pubs.usgs.gov/sir/2005/5231/>)
- Borg, Gregor, 1988, The Koras-Sinclair-Ghanzi rift in southern Africa—Volcanism, sedimentation, age relationships and geophysical signature of a late middle Proterozoic rift system: *Precambrian Research*, v. 38, p. 75–90.
- Borg, Gregor, and Maiden, K.J., 1987, Alteration of late Middle Proterozoic volcanics and its relation to stratabound copper-silver-gold mineralization along the margin of the Kalahari Craton in SWA/Namibia and Botswana, in Pharoah, T.C., Beckinsale, R.D., and Rickard, David, eds., *Geochemistry and mineralization of Proterozoic volcanic suites: Geological Society Special Publication No. 33*, p. 347–354.
- Borg, Gregor, and Maiden, K.J., 1989, The Middle Proterozoic Kalahari Copperbelt of Namibia and Botswana, in Boyle, R.W., Brown, A.C., Jefferson, C.W., Jowett, E.C., and Kirkham, R.V., eds., *Sediment-hosted stratiform copper deposits: Geological Association of Canada, Special Paper 36*, p. 525–540.
- Borg, Gregor, and Stanistreet, I.G., 1996, Sedimentation and basin development of the Middle Proterozoic Doornpoort and Klein Aub Formations, central Namibia: *Hallesches Jahrbuch fuer Geowissenschaften—Reihe B, Geologie, Palaeontologie, Mineralogie*, v. 18, p. 1–21.
- Box, S.E., Syusyura, Boris, Hayes, T.S., Taylor, C.D., Zientek, M.L., Hitzman, M.W., Seltmann, Reimer, Chechetkin, Vladimir, Dolgopolova, Alla, Cossette, P.M., and Wallis, J.C., 2012, Sandstone copper assessment of the Chu-Sarysu Basin, Central Kazakhstan: U.S. Geological Survey Scientific Investigations Report 2010–5090–E, v. 1.1, 63 p. and spatial data tables, available at <http://pubs.usgs.gov/sir/2010/5090/e/>.
- Box, S.E., Syusyura, Boris, Seltmann, Reimar, Creaser, R.A., Dolgopolova, Alla, and Zientek, M.L., 2013, Dzhezkazgan and associated sandstone copper deposits of the Chu-Sarysu Basin, central Kazakhstan, in Hedenquist, J.W., Harris, Michael, Camus, Francisco, eds., *Geology and genesis of major copper deposits and districts of the World—A tribute to Richard H. Sillitoe: Society of Economic Geologists Special Publication 16*, p. 303–328.



- Boyd, J.A., 1977, Report on geological investigations, Dorchester copper area, Westmorland County, New Brunswick: New Brunswick Department of Natural Resources Report of Work 470479, 117 p., accessed September 4, 2014, at: <http://dnre-mrne.gnb.ca/parisweb/AssessmentReportSearch.aspx>.
- Boyd, R.T., and Boyd, J.A., 1977, Assessment report on 1977 geological investigations, Dorchester copper area, Westmorland County, New Brunswick: New Brunswick Mineral Report of Work 472201, 31 p., accessed June 24, 2014, at <http://dnre-mrne.gnb.ca/parisweb/AssessmentReportSearch.aspx>.
- Bradley, D.C., 1982, Subsidence in Late Paleozoic basins in the northern Appalachians: *Tectonics*, v. 1, p. 107–123.
- British Columbia Ministry of Energy and Mines, 2013, BC digital geology, version 2.2: British Columbia Ministry of Energy and Mines, Web page, accessed August 11, 2014, at <http://www.empr.gov.bc.ca/Mining/Geoscience/BedrockMapping/Pages/BCGeoMap.aspx>.
- British Columbia Ministry of Energy, Mines and Petroleum Resources, 2001, Geology compilation 1991–96, *geol\_e00.zip*: British Columbia Ministry of Energy, Mines and Petroleum Resources, Geological Survey Geospatial Data Downloads, accessed September 10, 2010, at <http://www.empr.gov.bc.ca/MINING/GEOSCIENCE/MAPPLACE/GEODATA/Pages/default.aspx>.
- Brognon, G.P., and Verrier, G.R., 1966, Oil and geology in Cuanza basin of Angola: *American Association of Petroleum Geologists (AAPG) Bulletin*, v. 50, p. 108–158.
- Brownfield, M.E., and Charpentier, R.R., 2006, Geology and total petroleum systems of the west-central coastal province (7203), West Africa: *U.S. Geological Survey Bulletin* 2207–B, 52 p.
- Brummer, J.J., 1958, Supergene copper-uranium deposits in northern Nova Scotia: *Economic Geology*, v. 53, p. 309–324.
- Burchfiel, B.C., and Chen, Zhiliang, eds., 2013, *Tectonics of the southeastern Tibetan Plateau and its adjacent foreland*: Geological Society of America Memoir 210, 231 p., DVD.
- Burchfiel, B.C., Chen, Zhiliang, Yuping, Liu, and Royden, L.H., 1995, Tectonics of the Longmen Shan and adjacent regions, central China: *International Geology Review*, v. 37, no. 8, p. 661–735.
- Bureau of Geology and Mineral Resources of Sichuan Province, comp., 1991, Geologic map of Sichuan Province, People's Republic of China, Map 1, in Bureau of Geology and Mineral Resources of Sichuan Province, regional geology of Sichuan Province: Beijing, Geological Publishing House, People's Republic of China Ministry of Geology and Mineral Resources Geological Memoirs Series 1, no. 23, 1 map on 4 sheets, scale 1:1,000,000. [In Chinese with English abstract.]
- Bureau of Geology and Mineral Resources of Yunnan Province, comp., 1990, Geologic map of Yunnan Province, People's Republic of China, Map 1, in Bureau of Geology and Mineral Resources of Yunnan Province, regional geology of Yunnan Province: Beijing, Geological Publishing House, People's Republic of China Ministry of Geology and Mineral Resources Geological Memoirs Series 1, no. 21, 1 map on 4 sheets, scale 1:1,000,000. [In Chinese with English abstract.]
- Burgath, K.P., Hagen, C., and Siewers, G., 1984, Geochemistry, geology and primary copper mineralization in Wadi Araba, Jordan: *Geologisches Jahrbuch*, v. 53, p. 3–53.
- Caia, J., 1976, Paleogeographical and sedimentological controls of copper, lead, and zinc mineralization in the lower Cretaceous sandstones of Africa: *Economic Geology*, v. 71, p. 409–422.
- Calder, J.H., 1998, The Carboniferous evolution of Nova Scotia, in Blundell, D.J., and Scott, A.C., eds., *Lyell—The past is the key to the present*: Geological Society, London, Special Publications, v. 143, p. 261–302.
- Calkins, F.C., and Jones, E.L., Jr., 1914, Economic geology of the region around Mullan, Idaho, and Saltese, Montana: *U.S. Geological Survey Bulletin* 540–E, p. 167–211.
- Centeno, Ricardo, and Fusari, Cayetano, 1999, Mina San Romeleo, in Zappettini, E.O., ed., *Recursos Minerales de la República Argentina, Volumen II: Buenos Aires*, Instituto de Geología y Recursos Minerales SEGEMAR, *anales* 35, p. 1147–1148. [In Spanish.]
- Chandler, F.W., 2000, The Belt-Purcell Basin as a low-latitude passive rift—Implications for the geological environment of Sullivan type deposits: Geological Association of Canada Mineral Deposits Division, Special Publication No. 1, p. 82–112.
- Chang, Xiangyang, and Zhu, Bingquan, 2002, Isotope geochemistry of the Dongchuan copper deposit, Yunnan, SE China—Stratigraphic chronology and application of lead isotopes in geochemical exploration: *Chinese Journal of Geochemistry*, v. 21, p. 65–72.

- Chang, Xiangyang, Zhu, Bingquan, Sun, D., Qiu, H., and Zou, R., 1997, Isotope geochemistry study of Dongchuan copper deposits in Middle Yunnan Province, SW China—Stratigraphic chronology and application of geochemical exploration by lead isotopes: *Geochimica*, v. 25, p. 32–38. [In Chinese with English abstract.]
- Charpentier, R.R., and Klett, T.R., 2005, Guiding principles of USGS methodology for assessment of undiscovered conventional oil and gas resources: *Natural Resources Research*, v. 14, no. 3, p. 175–186.
- Charrier, R., Pinto, L., and Rodríguez, M.P., 2007, Tectonostratigraphic evolution of the Andean Orogen in Chile, in Moreno, T., and Gibbons, W., eds., *The geology of Chile*: Bath, United Kingdom, The Geological Society of London, p. 21–114.
- Chartrand, F.M., and Brown, A.C., 1985, The diagenetic origin of stratiform copper mineralization, Coates Lake, Redstone copperbelt, NWT, Canada: *Economic Geology*, v. 80, p. 325–343.
- Chartrand, F.M., Brown, A.C., and Kirkham, R.V., 1989, Diagenesis, sulphides, and metal zoning in the Redstone copper deposit, Northwest Territories, in Boyle, R.W., Brown, A.C., Jefferson, C.W., Jowett, E.C., and Kirkham, R.V., eds., *Sediment-hosted stratiform copper deposits: Geological Association of Canada Special Paper 36*, p. 189–206.
- Chen, Junyu, 2012, The ore genesis and ore-searching prospects of copper deposit in Datongchang, Huili County, Sichuan Province: Chengdu, China, Chengdu University of Technology, Master's thesis, 56 p. [In Chinese, English abstract.]
- Chen, Pei-ji, 2003, Cretaceous biostratigraphy of China, in Zhang, Wentang, Chen, Pei-ji, and Palmer, A.R., eds., *Biostratigraphy of China*: Beijing, Science Press, p. 465–524.
- Chen, Wengen, 1988, Mesozoic and Cenozoic sandstone-hosted copper deposits in South China: *Mineralium Deposita*, v. 23, p. 262–267.
- Chen, Wengen, and Xia, Bin, 2005, Diagenetic origin of the Luzhou copper deposit, Yunnan Province, China, in Mao, Jingwen, and Bierlein, F.P., eds., *Mineral deposit research—Meeting the global challenge*: Berlin, Springer, p. 91–92.
- Chen, Wengen, Xia, Bin, Wu, Yanzhi, Tu, Guangzhi, and Yu, Hengxiang, 2000, The metallogenic mechanism of the sandstone-type copper deposits in the Chuxiong Basin, Yunnan Province: *Science in China, Series D*, v. 43, p. 262–272.
- CityView Corporation Ltd., 2006, Angola—Mineral concessions: ASX Media Release, March 26, 2008, 22 p.
- Colpron, M., and Augereau, C.M., 1998, Preliminary geology of the Dal Lake area, Mackenzie Mountains, Northwest Territories (NTS 95M/2): Canada, NWT Geology Division, Indian and Northern Affairs, EGS 1998–03, scale 1:50,000.
- Colpron, M., and Jefferson, C.W., 1998, Geology of the Mount Kraft area, Mackenzie Mountains, Northwest Territories (NTS 95L/15): Canada, NWT Geology Division, Indian and Northern Affairs, EGS 1998–02, scale 1:50,000.
- Comínguez, A.H., and Ramos, V.A., 1995, Geometry and seismic expression of the Cretaceous Salta Rift System, northwestern Argentina, in Tankard, A.J., Suárez Soruco, R., and Welsink, H.J., *Petroleum basins of South America*: American Association of Petroleum Geologists (AAPG) Memoir 62, p. 325–340.
- Connors, J.J., Reynolds, M.W., and Whipple, J.W., 1984, Stratigraphy of the Ravalli Group, Belt basin, Montana and Idaho, in Hobbs, S.W., ed., 1983, *The Belt—Abstracts with summaries*, Belt Symposium II: Montana Bureau of Mines and Geology, Special Publication 90, p. 13–15.
- Consultora Minera R.B., 2008, Depósitos de cobre sedimentario del Grupo Neuquén—Minas Yaraví Norte, La Cuprosa, La Barrosa y La Nuestra, Barda González-Sierra Barrosa, Departamento Confluentia-Provincia del Neuquén, República Argentina [Sedimentary copper deposits of Neuquén—Yaraví Norte, La Cuprosa, La Barrosa and La Nuestra, Barda González-Sierra Barrosa, Department Confluentia-Neuquén Province, Argentina]: Consultora Minera R.B., Informe Geológico (Relevamiento de Prospección) [Geological survey (Exploration survey)], Mayo de 2008, 58 p. [In Spanish.]
- Copper North Mining Corp., 2014, Projects—Redstone: Copper North Mining Corp. Web page, accessed June 9, 2014, at <http://www.coppernorthmining.com/s/Redstone.asp>.
- Coren, Ora, 2009, Arava mines suspends work at Timna Valley: Haaretz Daily Newspaper/ Israel News, January 9, 2009, accessed on September 7, 2011, at <http://www.haaretz.com/print-edition/business/arava-mines-suspends-work-at-timna-valley-1.268182>.
- Cossette, P.M., Bookstrom, A.A., Hayes, T.S., Robinson, G.R., Jr., Wallis, J.C., and Zientek, M.L., 2014, Sandstone copper assessment of the Teniz Basin, Kazakhstan: U.S. Geological Survey Scientific Investigations Report 2010–5090–R, 42 p., and spatial data, <http://dx.doi.org/10.3133/sir20105090R>.
- Coulter, E.D., Coakley, James, and Sessions, John, 2006, The analytic hierarchy process—A tutorial for use in prioritizing forest road investments to minimize environmental effects: *International Journal of Forest Engineering*, v. 17, no. 2, p. 51–69.

- Couture, J.F., and Tanaka, W.F., 2004 [2005], Independent technical report on the Rock Creek Cu-Ag project, Montana [Prepared for Revett Silver Company]: Toronto, Canada, Steffen Robertson and Kirsten (SRK) Consulting, 71 p. (Also available at <http://www.revettminerals.com/sites/default/files/rockcreekfinaltechreport.pdf>.)
- Cox, D.P., Lindsey, D.A., Singer, D.A., Moring, B.C., and Diggles, M.F., 2003 [2007], Sediment-hosted copper deposits of the world—Deposit models and database: U.S. Geological Survey Open-File Report 03–107, version 1.3, 53 p. (Also available at <http://pubs.usgs.gov/of/2003/of03-107/>.)
- Cullen Resources Ltd., 2011a, Copper, REE Namibia–Africa: Cullen Resources Ltd. Web page accessed May 6, 2011, at [http://www.cullenresources.com.au/pdf/presentations/cullen\\_banner\\_05\\_DAD\\_2010.pdf](http://www.cullenresources.com.au/pdf/presentations/cullen_banner_05_DAD_2010.pdf).
- Cullen Resources Ltd., 2011b, Quarterly report for the period ended 30 June 2010: Cullen Resources Ltd. Web page, accessed May 6, 2011, at [http://www.cullenresources.com.au/pdf/quarterly\\_reports/cullen\\_quarterly\\_100630.pdf](http://www.cullenresources.com.au/pdf/quarterly_reports/cullen_quarterly_100630.pdf).
- Cullen Resources Ltd., 2014, Quarterly report for the period ended 30 January 2014: Cullen Resources Ltd. Web page, accessed May 2, 2014, at [http://www.cullenresources.com.au/pdf/quarterly\\_reports/cullen\\_quarterly\\_140130.pdf](http://www.cullenresources.com.au/pdf/quarterly_reports/cullen_quarterly_140130.pdf).
- Daneshvar, M.R.M., 2014, Landslide susceptibility zonation using analytical hierarchy process and GIS for the Bonjnurd region, northeast of Iran: *Journal of the International Consortium on Landslides*, p. 1–13.
- Davenport, P.H., Nolan, L.W., Butler, A.J., Wagenbauer, H.A., and Honarvar, P., 1999, The geoscience atlas of Newfoundland, version 1.1: Newfoundland Department of Mines and Energy, Geological Survey Open File NFLD/2687, scale 1:1,000,000, CD-ROM.
- Davidson, C.F., 1965, A possible mode of origin of stratabound copper ore: *Economic Geology*, v. 60, p. 942–954.
- de Araújo, A.G., and Perevalov, O.V., 1998, Carta de recursos minerais [Minerals resources map of Angola]: Instituto Geologia de Angola, 1 map on 4 sheets, scale 1:1,000,000. [In Portuguese.]
- de Carvalho, Hector, 1980–82, Geologia de Angola: Laboratória Nacional de Investigação Científica Tropical (Junta de Investigações Científicas do Ultramar), 1 map on 4 sheets, scale 1:1,000,000. [In Portuguese.]
- Dessureau, Gilles, Piper, D.J.W., and Pe-Piper, Georgia, 2000, Geochemical evolution of earliest Carboniferous continental tholeiitic basalts along a crustal-scale shear zone, southwestern Maritimes basin, eastern Canada: *Lithos*, v. 50, p. 27–50.
- Dewing, K.E., Sharp, R.J., Ootes, L., Turner, E.C., and Gleeson, S., 2006, Geological assessment of known Zn-Pb showings—Mackenzie Mountains, Northwest Territories: Geological Survey of Canada Current Research, p. 12.
- Dierks, Klaus, 2005, Chronology of Namibian history—From pre-historical times to independent Namibia: accessed on April 25, 2011, at <http://www.klausdierks.com/Chronology/108.htm>.
- Dietrich, James, Hannigan, Peter, Hu, Kezhen, and Giles, Peter, 2009, Petroleum resource potential of the Carboniferous Maritimes Basin, Eastern Canada: American Association of Petroleum Geologists (AAPG) Search and Discovery Article #90171, CSPG/CSEG/CWLS GeoConvention 2009, Calgary, Alberta, Canada, May 4–8, 2009, 3 p.
- Discovery Metals Ltd., 2010, Boseto Copper Project: Goldman Sachs JBWere Micro Cap Conference, Sydney 2010, 27 p., accessed August 21, 2013, at [http://www.discoverymetals.com/files/media/0\\_85384868.pdf](http://www.discoverymetals.com/files/media/0_85384868.pdf).
- Discovery Metals Ltd., 2011a, Botswana exploration update: accessed July 1, 2011, at <http://www.basemetals.com/content/corporatenews/230611discovery.pdf>.
- Discovery Metals Ltd., 2011b, Mining Indaba, Cape Town: Discovery Metals Ltd., 28 p., accessed July 25, 2011, at [http://www.discoverymetals.com/files/media/mining\\_indaba\\_presentation\\_february\\_2011.pdf](http://www.discoverymetals.com/files/media/mining_indaba_presentation_february_2011.pdf).
- Discovery Metals Ltd., 2014, Botswana resources conference: Discovery Metals Ltd., 21 p., accessed July 28, 2014, at [http://www.discoverymetals.com/files/media/20140611\\_asx\\_announcement\\_presentation\\_at\\_botswana\\_resource\\_sector\\_conference\\_for\\_website\\_2.pdf](http://www.discoverymetals.com/files/media/20140611_asx_announcement_presentation_at_botswana_resource_sector_conference_for_website_2.pdf).
- Doughty, P.T., and Chamberlain, K.R., 1996, Salmon River Arch revisited—New evidence for 1370 Ma rifting near the end of the deposition in the Middle Proterozoic Belt basin: *Canadian Journal of Earth Sciences*, v. 33, p. 1037–1052.
- Dudás, F.O., and Lustwerk, R.L., 1997, Geochemistry of the Little Dal basalts—Continental tholeiites from the Mackenzie Mountains, Northwest Territories, Canada: *Canadian Journal of Earth Science*, v. 34, p. 50–58.
- Durieux, C.G., and Brown, A.C., 2007, Geological context, mineralization, and timing of the Juramento sediment-hosted stratiform copper-silver deposit, Salta district, northwestern Argentina: *Mineralium Deposita*, v. 42, no. 8, p. 879–899.
- Earth Resources Observation and Science (EROS) Center, 2001, HYDRO1k elevation derivative database: U.S. Geological Survey Web page, accessed May 29, 2013, at [http://eros.usgs.gov/#Find\\_Data/Products\\_and\\_Data\\_Available/gtopo30/hydro](http://eros.usgs.gov/#Find_Data/Products_and_Data_Available/gtopo30/hydro).



- Editorial Committee of the Mineral Deposits of China, 1990, *Mineral deposits of China*: Beijing, Geological Publishing House, v. 2, 355 p.
- Egyptian Geological Survey and Mining Authority, 1981, *Geologic map of Egypt*: Egyptian Geological Survey and Mining Authority, 1 sheet, scale 1:2,000,000.
- El Sharkawi, M.A., El Aref, M.M., and Abdel Motelib, A., 1990, Syngenetic and paleokarstic copper mineralization in the Palaeozoic platform sediments of west-central Sinai, Egypt: *Special Publication of the International Association of Sedimentologists*, v. 11, p. 159–172.
- Enachescu, M.E., 2006, Government of Newfoundland and Labrador call for bids 2006 NL06-02, Sydney Basin: Government of Newfoundland and Labrador Department of Natural Resources, 55 p.
- Esri, 2008, Global shaded relief derived from the Shuttle Radar Topography Mission (SRTM): Esri Data & Maps 9.3—Global Imagery and Shaded Relief, DVD.
- Evans, K.V., Aleinikoff, J.N., Obradovich, J.D., and Fanning, C.M., 2000, SHRIMP U-Pb geochronology of volcanic rocks, Belt Supergroup, western Montana—Evidence for rapid deposition of sedimentary strata: *Canadian Journal of Earth Sciences*, v. 37, no. 9, p. 1287–1300.
- Evans, K.V., and Zartman, R.E., 1990, U-Th-Pb and Rb-Sr geochronology of middle Proterozoic granite and augen gneiss, Salmon River Mountains, east-central Idaho: *Geological Society of America Bulletin*, v. 102, p. 63–73.
- Extract Resources, 2008, Company overview: Extract Resources, Kalahari Minerals, May 2008 Company overview, 26 p.
- Fallas, K., Roots, C.F., Martel, E., and MacNaughton, R., comps., 2011, *Geology of Wrigley Lake, NTS 95M Northwest, Mackenzie Mountains, Northwest Territories*: Northwest Territories Geoscience Office, NWT Open File 2010-17 (2d ed.), scale 1:100,000.
- Fortitude Minerals Ltd., 2008, Angolan mineral concessions—Overview: Angola mineral concessions media release, 22 p. (Also available at <http://www.sec.gov/Archives/edgar/data/1023130/000117266508000135/form6kmarch2008.htm>.)
- Franzese, J.R., and Spalletti, L.A., 2001, Late Triassic–early Jurassic continental extension in southwestern Gondwana—tectonic segmentation and pre-break-up rifting: *Journal of South American Earth Sciences*, v. 14, p. 257–270.
- Franzese, J.R., Spalletti, L.A., Pérez, I.G., and Macdonald, D., 2003, Tectonic and paleoenvironmental evolution of Mesozoic sedimentary basins along the Andean foothills of Argentina (32°–54° S): *Journal of South American Earth Sciences*, v. 16, p. 81–90.
- Franzese, J.R., Veiga, G.D., Schwarz, E., and Gómez-Pérez, I., 2006, Tectonostratigraphic evolution of a Mesozoic graben border system—The Chachil depocentre, southern Neuquén Basin, Argentina: *Journal of the Geological Society*, v. 163, p. 707–721.
- Freund, R., Garfunkel, Z., Zak, I., Goldberg, M., Weissbrod, T., and Derin, B., 1970, The shear along the Dead Sea rift: Royal Society, London, *Philosophical Transactions, Series A*, v. 267, p. 107–130.
- Frimmel, H.E., Basei, M.S., and Gaucher, C., 2011, Neoproterozoic geodynamic evolution of SW-Gondwana—A southern African perspective: *International Journal of Earth Sciences*, v. 100, p. 323–354.
- Fugro Data Services, AG, 2005, Fugro Tellus sedimentary basins of the world map: American Association of Petroleum Geologists (AAPG) Web page, accessed May 31, 2011, at <http://www.datapages.com/AssociatedWebsites/GISOpenFiles/FugroTellusSedimentaryBasinsoftheWorldMap.aspx>.
- Gabrielse, H., Roddick, J.A., and Blusson, S.L., 1973a, *Geology, Glacier Lake, District of Mackenzie*: Geological Survey of Canada, “A” Series Map 1314A, scale 1:250,000, doi:10.4095/107938. (Available at [ftp://ftp2.cits.mcan.gc.ca/pub/geott/ess\\_pubs/107/107938/gscmap-a\\_1314a\\_e\\_1973\\_mn01.pdf](ftp://ftp2.cits.mcan.gc.ca/pub/geott/ess_pubs/107/107938/gscmap-a_1314a_e_1973_mn01.pdf).)
- Gabrielse, H., Roddick, J.A., and Blusson, S.L., 1973b, *Geology, Wrigley Lake area, District of Mackenzie*: Geological Survey of Canada, “A” Series Map 1315A, scale 1:250,000, doi:10.4095/107939. (Available at [ftp://ftp2.cits.mcan.gc.ca/pub/geott/ess\\_pubs/107/107939/gscmap-a\\_1315a\\_e\\_1973\\_mn01.pdf](ftp://ftp2.cits.mcan.gc.ca/pub/geott/ess_pubs/107/107939/gscmap-a_1315a_e_1973_mn01.pdf).)
- Gandhi, S.S., and Brown, A.C., 1975, Cupriferous shales of the Adeline Island Formation, Seal Lake Group, Labrador: *Economic Geology*, v. 70, p. 145–163.
- Garfunkel, Z., 1981, Internal structure of the Dead Sea leaky transform (rift) in relation to plate kinematics: *Tectonophysics*, v. 80, p. 81–108.
- Garkus, H.A., 2010, [Technical report on the Martín Bronce deposit]: Servicios Mineros, prepared for AMA Resources, 60 p., accessed June 23, 2014, at <http://amaresourcesinc.com/wp-content/plugins/google-document-embedder/view.php?url=http%3A%2F%2Ftinyurl.com%2Fkmmn8k9&hl=&gpid=2&embedded=true>.
- Garrity, C.P., and Soller, D.R., 2009, Database of the geologic map of North America—Adapted from the map by J.C. Reed, Jr., and others (2005): U.S. Geological Survey Data Series 424, accessed March 22, 2013, at <http://pubs.usgs.gov/ds/424>.

- Gaucher, Claudio, Frimmel, H.E., and Germs, J.B.G., 2010, Tectonic events and palaeogeographic evolution of southwestern Gondwana in the Neoproterozoic and Cambrian, *in* Gaucher, Claudio, Sial, A.N., Halverson, G.P., and Frimmel, H.E., eds., *Neoproterozoic-Cambrian tectonics, global change and evolution—A focus on southwestern Gondwana: Developments in Precambrian Geology*, v. 16, p. 295–316.
- Gibling, M.R., Culshaw, Nicholas, Rygel, M.C., and Pascucci, Vincenzo, 2008, The Maritimes Basin of Atlantic Canada—Basin creation and destruction in the collisional zone of Pangea, *in* Miall, A.D., ed., *Sedimentary basins of the world*, v. 5—The sedimentary basins of the United States and Canada: Amsterdam, Elsevier, p. 211–244.
- Giles, P.S., 1981, Major transgressive-regressive cycles in middle to late Viséan rocks of Nova Scotia: Nova Scotia Department of Mines and Energy Paper 81–2, 27 p.
- Giusiano, Adolfo, Cevallos, Martin, Franchini, Marta, Carbone, Osvaldo, and Rainoldi, Ana, 2014, Evidencias de la circulación de hidrocarburos a través del Grupo Neuquén (Cretácico Superior) en El Doro de Los Chihuidos, Cuenca Neuquina [Evidence of hydrocarbon circulation through the Neuquén Group (Upper Cretaceous) in El Doro de Los Chihuidos, Neuquén Basin]: XIX Congreso Geológico Argentino, Junio 2014, Córdoba—Geología de los Recursos Energeticos, T4–1, 4 p. [In Spanish.]
- Giusiano, Adolfo, Franchini, M.B., Impiccini, Agnes, and Pons, M.J., 2008, Mineralización de Cu en sedimentitas Mesozóicas del Grupo Neuquén y hábitat de los hidrocarburos en la Dorsal de Huincul Neuquén [Cu mineralization in Mesozoic sediments of the Neuquén Group and hydrocarbon habitat in the Dorsal de Huincul, Neuquén]: Salta, 17° Congreso Geológico Argentino, Actas 2, p. 769–770. [In Spanish.]
- Golden, J., Levy, T.E., and Hauptmann, A., 2001, Recent discoveries concerning Chalcolithic metallurgy at Shiqmim, Israel: *Journal of Archaeological Science*, v. 28, p. 951–963.
- Gordey, S.P., Martel, E., Fallas, K., Roots, C.F., MacNaughton, R., and MacDonald, J., comps., 2011a, *Geology of Mount Eduni, NTS 106A Southwest, Mackenzie Mountains, Northwest Territories: Northwest Territories Geoscience Office, NWT Open File 2010–11 (2d ed.)*, scale 1:100,000.
- Gordey, S.P., Martel, E., MacDonald, J., Fallas, K., Roots, C.F., and MacNaughton, R., comps., 2011b, *Geology of Mount Eduni, NTS 106A Southeast, Mackenzie Mountains, Northwest Territories: Northwest Territories Geoscience Office, NWT Open File 2010–12 (2d ed.)*, scale 1:100,000.
- Gordey, S.P., Martel, E., MacDonald, J., MacNaughton, R., Roots, C.F., and Fallas, K., comps., 2011c, *Geology of Mount Eduni, NTS 106A Northwest, Mackenzie Mountains, Northwest Territories: Northwest Territories Geoscience Office, NWT Open File 2010–09 (2d ed.)*, scale 1:100,000.
- Gourlay, A.W., 2005, Technical report on the Coates Lake copper deposit, Nahanni mining district, western Northwest Territories for Lumina Resources Corp.: Lumina Resources Corp. Technical Report, 25 p.
- Greentree, M.R., Li, Zheng-Xiang, Li, Xian-Hua, and Wu, Huaichun, 2006, Late Mesoproterozoic to earliest Neoproterozoic basin record of the Sibao orogenesis in western south China and relationship to the assembly of Rodinia: *Precambrian Research*, v. 151, p. 79–100.
- Grieve, David, 2010, Exploration and mining in Kootenay-boundary region, British Columbia: Exploration Mining in British Columbia, 12 p. (Also available at [http://www.empr.gov.bc.ca/Mining/Geoscience/PublicationsCatalogue/ExplorationinBC/Documents/2010/BCEx-Mining2010\\_06\\_KootenayBoundary.pdf](http://www.empr.gov.bc.ca/Mining/Geoscience/PublicationsCatalogue/ExplorationinBC/Documents/2010/BCEx-Mining2010_06_KootenayBoundary.pdf)).
- Grimaldi, G.O., and Dorobek, S.L., 2011, Fault framework and kinematic evolution of inversion structures—Natural examples from the Neuquén Basin, Argentina: *American Association of Petroleum Geologists (AAPG) Bulletin*, v. 95, p. 27–60.
- Guiraud, M., Buta-Neto, A., and Quesne, D., 2010, Segmentation and differential post-rift uplift at the Angola margin as recorded by the transform-rifted Benguela and oblique-to-orthogonal-rifted Kwanza basins: *Marine and Petroleum Geology*, v. 27, p. 1040–1068.
- Guiraud, Rene, 1999, Paleozoic geodynamic evolution of the northeastern African epicratonic basins—An outline: *Gabhanlungen der Geologischen Bundesanstalt, Band 54*, p. 15–26.
- Haddon, I.G., comp., 1999, Isopach map of the Kalahari Group: Pretoria, South Africa, Council for Geosciences, 1 sheet, scale 1:2,500,000.
- Haddon, I.G., comp., 2001, Sub-Kalahari geological map: Pretoria, South Africa, Council for Geosciences, 1 sheet, scale 1:2,500,000.
- Hadley, D.G., 1972, The taphrogeosynclinal J'balah group in the Mashhad area, northwestern Hijaz, Kingdom of Saudi Arabia: Saudi Arabian Directorate General of Mineral Resources-USGS Saudi Arabian Project Report SA(IR) 151, 37 p.
- Hall, W.S., 2013, Geology and paragenesis of the Boseto copper deposits, Kalahari Copperbelt, Northwest Botswana: Golden, Colorado, Colorado School of Mines, M.S. thesis, 146 p.



- Halverson, G.P., 2005, A Neoproterozoic chronology, *in* Xiao, S., and Kaufman, A.J., eds., *Neoproterozoic geobiology and paleobiology—Topics in geobiology*: New York, Kluwer, v. 27, p. 231–271.
- Halverson, G.P., Hoffman, P.F., Schrag, D.P., Maloof, A.C., and Rice, A.H.N., 2005, Toward a Neoproterozoic composite carbon-isotope record: *Geological Society of America Bulletin*, v. 117, p. 1181–1207.
- Hamblin, A.P., Fowler, M.G., Uttig, J., Hawkins, D., and Riediger, C.L., 1995, Sedimentology, palynology, and source rock potential of Lower Carboniferous (Tournaian) rocks, Conche area, Great Northern Peninsula, Newfoundland: *Journal of Canadian Petroleum Geology*, v. 43, p. 1–19.
- Hansley, Paula, 2007, Petrography of rock samples from the Dorchester and Goshen projects, *in* Normore, Leon, and Mitton, Bruce, First year assessment report of compilation, geological mapping, and rock and stream geochemistry on Claim Group 4949, Dorchester project, NTS 21H/16W, southeast New Brunswick: New Brunswick Department of Natural Resources Report of Work 476473, p. 59–95, accessed September 11, 2014, at <http://dnre-mrne.gnb.ca/parisweb/AssessmentReportSearch.aspx>.
- Harris, D.P., 1984, Mineral resource appraisal—Mineral endowment, resources, and potential supply—Concepts, methods, and cases: New York, Clarendon University Press, 445 p.
- Harrison, J.E., 1972, Precambrian Belt Basin of northwestern United States—Its geometry, sedimentation, and copper occurrences: *Geological Society of America Bulletin*, v. 83, no. 5, p. 1215–1240.
- Harrison, J.E., and Cressman, E.R., 1993, Geology of the Libby Thrust Belt of northwestern Montana and its implications to regional tectonics: U.S. Geological Survey Professional Paper 1524, 42 p.
- Hartlaub, R.P., 2009, Sediment-hosted stratabound copper-silver-cobalt potential of the Creston Formation, Purcell Supergroup, south-eastern British Columbia: *Geoscience BC*, v. 1, p. 123–132.
- Hass, Rainer, and Meixner, Oliver, 2006, An illustrated guide to the Analytical Hierarchy Process: Presentation given to North Pacific Fishery Management Council, Steller Sea Lion Mitigation Committee Meeting July 25–27, 2006, Talaris Conference Center, Seattle, accessed February 9, 2011, at <https://alaskafisheries.noaa.gov/sustainablefisheries/sslmc/july-06/ahptutorial.pdf>.
- Hatcher, R.D., Jr., 2010, The Appalachian Orogen—A brief summary: *Geological Society of America, Memoir* 206, p. 1–19.
- Hatcher, R.D., Jr., Zietz, I., Regan, R.D., and Abu-Ajamieh, M., 1981, Sinistral strike-slip motion on the Dead Sea Rift—Confirmation from new magnetic data: *Geology*, v. 9, p. 458–462.
- Hauptmann, A., 2007, The archaeometallurgy of copper, evidence from Faynan, Jordan: Berlin, Springer-Verlag, 399 p.
- Hayes, T.S., 1984, Geologic studies on the genesis of the Spar Lake stratabound copper-silver deposit, Lincoln County, Montana: Palo Alto, Calif., Stanford University, Ph.D. dissertation, 340 p., 3 pls., 74 figs.
- Hayes, T.S., 1990, A preliminary study of thermometry and metal sources for the Spar Lake stratabound copper-silver deposit, Belt Supergroup, Montana: U.S. Geological Survey Open-File Report 90–0484, 30 p.
- Hayes, T.S., Cox, D.P., Piatak, N.M., and Seal, R.R., II, 2015, Sediment-hosted stratabound copper deposit model: U.S. Geological Survey Scientific Investigations Report 2010–5070–M, 147 p., <http://dx.doi.org/10.3133/sir20105070M>.
- Hayes, T.S., and Einaudi, M.T., 1986, Genesis of the Spar Lake stratabound copper-silver deposit, Montana—Part 1. Controls inherited from sedimentation and pre-ore diagenesis: *Economic Geology*, v. 81, p. 1899–1931.
- Hayes, T.S., Landis, G.P., Whelan, J.F., Rye, R.O., and Moscati, R.J., 2012, The Spar Lake stratabound Cu-Ag formed across a mixing zone between trapped natural gas and metals-bearing brine: *Economic Geology*, v. 107, p. 1223–1249.
- Heine, C., Zoethout, J., and Müller, R.D., 2013, Kinematics of the South Atlantic rift: *Solid Earth*, v. 4, p. 215–253.
- Heuret, Arnaud, and Lallemand, Serge, 2005, Plate motions, slab dynamics and back-arc deformation: *Physics of the Earth and Planetary Interiors*, v. 149, p. 31–51.
- Hilmy, M.E., and Mohsen, L.A., 1965, Secondary copper minerals from west central Sinai: *Journal of Geology of the United Arab Republic*, v. 9, no. 1, p. 1–12.
- Hitzman, M.W., 2000, Source basins for sediment-hosted stratiform Cu deposits—Implications for the structure of the Zambian Copperbelt: *Journal of African Earth Sciences*, v. 30, p. 855–863.
- Hitzman, M.W., Kirkham, Rodney, Broughton, David, Thorson, Jon, and Selley, David, 2005, The sediment-hosted stratiform copper ore system, *in* Hedenquist, J.W., Thompson, J.F.H., Goldfarb, R.J., and Richards, J.P., eds., *Economic Geology—One hundredth anniversary volume 1905–2005*: Littleton, Colo., Society of Economic Geologists, Inc., p. 609–642.

- Hitzman, M.W., Selley, David, and Bull, Stuart, 2010, Formation of sedimentary rock-hosted stratiform copper deposits through Earth history: *Economic Geology*, v. 105, no. 3, p. 627–639.
- Hoffman, P.F., 1988, United plates of America, the birth of a craton—Early Proterozoic assembly and growth of Laurentia: *Annual Review Earth Planetary Sciences*, v. 16, p. 543–603.
- Hoffman, P.F., and Halverson, G.P., 2011, Neoproterozoic glacial record in the Mackenzie Mountains, northern Canadian Cordillera: *Geological Society, London, Memoirs*, v. 36, p. 397–412.
- Hooper, M.J., 1972, Tonnage and grade calculations on Great Horn Mining Syndicate's Lochaber Lake copper property, Antigonish County, Nova Scotia: Nova Scotia Department of Mines and Energy Assessment Report ME 11E/08D 13-B-19(01), 10 p., accessed September 4, 2014, at: <http://gis4.natr.gov.ns.ca/novascan/DocumentQuery.faces>.
- Hosseinali, Farhad, and Alesheikh, A.A., 2008, Weighting spatial information in GIS for copper mining exploration: *American Journal of Applied Sciences*, v. 5, no. 9, p. 1187–1198.
- Howell, J.A., Schwartz, Ernesto, Spalletti, L.A., and Veiga, G.D., 2005, The Neuquén Basin—An overview, *in* Veiga, G.D., Spalletti, L.A., Howell, J.A., and Schwartz Ernesto, eds., *The Neuquén Basin, Argentina—A case study in sequence stratigraphy and basin dynamics*: London, Geological Society of London, Special Publication 252, p. 1–14.
- Høy, Trygve, 1993, Geology of the Purcell Supergroup in the Fernie west-half map area, Southeastern British Columbia: British Columbia Ministry of Energy, Mines, and Petroleum Resources, Geological Survey Branch, Bulletin 84, 157 p.
- Høy, Trygve, Anderson, D., Turner, R.J.W., and Leitch, C.H.B., 2000, Tectonic, magmatic, and metallogenic history of the early synrift phase of the Purcell Basin, southeastern British Columbia, *in* Lydon, J.W., Høy, Trygve., Slack, J.F., and Knapp, M.E. eds., 2000, *The geological environment of the Sullivan deposit, British Columbia*: Geological Association of Canada, Mineral Deposits Division, Special Publication No. 1, p. 32–60.
- Hronsky, J.M.A., 2004, The science of exploration targeting, *in* Muhling, J., Goldfarb, R., Vielreicher, N., Bierlein, F., Stumpfl, E., Groves, D.I., and Kenworthy, S., eds., *SEG 2004 Predictive mineral discovery under cover—Extended abstracts*: Centre for Global Metallogeny, The University of Western Australia Publication 33, p. 129–133.
- Hronsky, J.M.A., and Groves, D.I., 2008, The science of targeting—Definition, strategies, targeting and performance measurement: *Australian Journal of Earth Sciences*, v. 55, p. 3–12.
- Hua, Renmin, 1990, The sedimentation-reworking genesis of Dongchuan-type stratiform copper deposits: *Chinese Journal of Geochemistry*, v. 9, p. 231–243.
- Hua, Renmin, 1991, A study on the Kunyang Aulacogen: *Acta Geologica Sinica*, v. 4, p. 131–144.
- Hua, Renmin, 1993, Some characteristics of sedimentation of the Yinmin Formation: *Acta Sedimentologica Sinica*, v. 11, p. 32–40. [In Chinese with English abstract.]
- Hudec, M.R., and Jackson, M.P.A., 2002, Structural segmentation, inversion, and salt tectonics on a passive margin—Evolution of the inner Kwanza Basin, Angola: *Geological Society of America Bulletin*, v. 114, p. 1222–1244.
- Husseini, M.I., and Husseini, S.I., 1990, Origin of the Infra-cambrian salt basins of the Middle East, *in* Brooks, J., ed., *Classic petroleum provinces*: Geological Society of London Special Publication 50, p. 279–292.
- Ilani, S., Flexer, A., and Kronfeld, J., 1987, Copper mineralization in sedimentary cover associated with tectonic elements and volcanism in Israel: *Mineralium Deposita*, v. 22, p. 269–277.
- Instituto de Geología y Minería, Universidad Nacional de Jujuy, 1996, Mapa geológico de la Provincia de Jujuy República Argentina: Servicio de Geología y Recursos Minerales, scale 1:500,000.
- Jarrar, G.H., Manton, W.I., Stern, R.J., and Zachmann, D., 2008, Late Neoproterozoic A-type granites in the northernmost Arabian-Nubian Shield formed by fractionation of basaltic melts: *Chemie der Erde*, v. 68, p. 295–312.
- Jarrar, G.H., Yaseen, Najel, and Whitehouse, M.J., 2012, The Aheimir Volcanic Suite An Ediacaran post-collisional sequence from the northernmost Arabian Nubian Shield, Wadi Araba, SW Jordan—Age, geochemistry and petrogenesis: Geological Society of America, North-Central Section, 46th Annual Meeting, Abstract, accessed August 11, 2014, at [https://gsa.confex.com/gsa/2012NC/finalprogram/abstract\\_202861.htm](https://gsa.confex.com/gsa/2012NC/finalprogram/abstract_202861.htm).
- Jassim, S.Z., 2006, Palaeozoic megasequences (AP1–AP5), *in* Jassim, S.Z., and Goff, J.C., 2006—*Geology of Iraq*: Prague, Dolin and the Moravian Museum, p. 91–116.

- Jefferson, C.W., 1978, Stratigraphy and sedimentology, Upper Proterozoic Redstone Copper Belt, Mackenzie Mountains, Northwest Territories—A preliminary report, *in* Laporte, P.J., Gibbins, W.A., Hurdle, E.J., Lord, C., Padgham, W.A., and Seaton, J.B., Mineral industry report 1975, Northwest Territories: Indian and Northern Affairs, Northwest Territories, Economic Geology Series, no. 1978–5, p. 157–169.
- Jefferson, C.W., 1983, The upper Proterozoic Redstone Copper Belt, Mackenzie Mountains, N.W.T.: London, Ontario, University of Western Ontario, Ph.D. dissertation, 445 p., 26 pls., 43 figs.
- Jefferson, C.W., and Colpron, M., 1998, Geology of the Copercap Mountain area, Mackenzie Mountains, Northwest Territories (NTS 95L/10): Canada, NWT Geology Division, Indian and Northern Affairs, EGS 1998–04, scale 1:50,000.
- Jefferson, C.W., and Parrish, R.R., 1989, Late Proterozoic, U–Pb zircon ages, and rift tectonics, Mackenzie Mountains, northwestern Canada: *Canadian Journal of Earth Sciences*, v. 26, p. 1784–1801.
- Jefferson, C.W., and Ruelle, J.C.L., 1986, The late Proterozoic Redstone Copper Belt—Mackenzie Mountains, Northwest Territories: *Canadian Institute of Mining and Metallurgy*, v. 37, p. 154–168.
- Jia, Dong, Wei, Guoqi, Chen, Zhuxin, Li, Benlian, Zeng, Qing, and Yang, Guang, 2006, Longmen Shan fold-thrust belt and its relation to the western Sichuan Basin in central China—New insights from hydrocarbon exploration: *American Association of Petroleum Geologists (AAPG) Bulletin*, v. 90, p. 1425–1447.
- Johnson, P.R., Andresen, A., Collins, A.S., Fowler, A.R., Fritz, H., Ghebreab, W., Kusky, T., and Stern, R.J., 2011, Late Cryogenian-Ediacaran history of the Arabian-Nubian Shield—A review of depositional, plutonic, structural, and tectonic events in the closing stages of the northern East African Orogen: *Journal of African Earth Sciences*, v. 61, p. 167–232.
- Johnson, P.R., Halverson, G.P., Kusky, T.M., Stern, R.J., and Pease, Victoria, 2013, Volcanosedimentary basins in the Arabian-Nubian Shield—Markers of repeated exhumation and denudation in a Neoproterozoic accretionary orogeny: *Geosciences*, v. 3, p. 389–445.
- Jokat, Wilfried, Boebel, Tobias, König, Matthias, and Meyer, Uve, 2003, Timing and geometry of early Gondwana breakup [abs.]: *Journal of Geophysical Research*, v. 108, no. B9, p. 2428.
- Kalahari Minerals plc, 2006, Placing of 40,000,000 new ordinary shares at 15p per share—Admission to trading on AIM: Kalahari Minerals plc, March 21, 2006, 97 p. (Also available at <http://www.sedar.com>.)
- Kalahari Minerals plc, 2008, Company overview, May 2008, accessed May 15, 2009, at <http://www.proactiveinvestors.co.uk/genera/files/companies/kah2.pdf>.
- Kamitani, Masaharu, Okumura, Kimio, Teraoka, Yoji, Miyano, Sumiko, and Watanabe, Yasusi, 2007, The mineral deposit data of mineral resources map of east Asia: Geological Survey of Japan, National Institute of Advanced Industrial Science and Technology (AIST), scale 1:3,000,000.
- Kamona, A.F., and Gunzel, A., 2007, Stratigraphy and base metal mineralization in the Otavi Mountain Land, northern Namibia—A review and regional interpretation: *Gondwana Research*, v. 11, p. 396–413.
- Kampunzu, A.B., Akanayang, P., Mapeo, R.B.M., Modie, B.N., and Wendorff, M., 1998, Geochemistry and tectonic significance of Mesoproterozoic Kgwebe metavolcanic rocks in northwest Botswana—Implications for the evolution of the Kibaran Namaqua–Natal Belt: *Geological Magazine*, v. 135, p. 669–683.
- Kampunzu, A.B., Cailteux, J.L.H., Kamona, A.F., Intiomale, M.M., and Melcher, F., 2009, Sediment-hosted Zn–Pb–Cu deposits in the Central African copperbelt: *Ore Geology Reviews*, v. 35, p. 263–297.
- Keppie, J.D., comp., 2000, Geological map of the province of Nova Scotia: Nova Scotia Department of Natural Resources, Minerals and Energy Branch, Map ME 2000–1, scale 1:500,000, digital data.
- Key, R.M., 1998, National geologic map of Botswana: Botswana Geological Survey, scale 1:1,000,000, digital format.
- Key, R.M., and Ayres, Neil, 2000, The 1998 edition of the national geological map of Botswana: *Journal of African Earth Sciences*, v. 30, no. 3, p. 427–451.
- Key, R.M., and Mapeo, R.B.M., 1999, The Mesoproterozoic history of Botswana and the relationship of the NW Botswana rift to Rodinia: *Episodes*, v. 22, p. 118–122. (Also available at <http://www.episodes.co.in/www/backissues/222/118%20CR.pdf>.)
- Kirkham, R.V., 1974, A synopsis of Canadian stratiform copper deposits in sedimentary sequences, *in* Bartholome, P., ed., *Gisements stratiformes et provinces cuprifères*: Liege, Belgium, Société Géologique de Belgique, p. 367–382.
- Kirkham, R.V., 1985, Base metals in Upper Windsor (Codroy) Group oolitic and stromatolitic limestones in the Atlantic Provinces, *in* *Current Research, Part A: Geological Survey of Canada Paper 85–1a*, p. 573–585.



- Kirkham, R.V., 1989, Distribution, settings, and genesis of sediment-hosted stratiform copper deposits, *in* Boyle, R.W., Brown, A.C., Jefferson, C.W., Jowett, E.C., and Kirkham, R.V., eds., *Sediment-hosted stratiform copper deposits: Geological Association of Canada Special Paper 36*, p. 3–38.
- Kirkham, R.V., and Broughton, David, 2005, Supplement to the sediment-hosted stratiform copper ore system, *in* Hedenquist, J.W., Thompson, J.F.H., Goldfarb, R.J., and Richards, J.P., eds., *Economic Geology—One hundredth anniversary volume 1905–2005, Appendix: Littleton, Colo., Society of Economic Geologists, Inc.*, p. 609–642.
- Kirkham, R.V., Carriere, J.J., Laramee, R.M., and Garson, D.F., 1994, Global distribution of sediment-hosted stratiform copper deposits and occurrences: Geological Survey of Canada Open File 2915b, 256 p.
- Kirkham, R.V., Carriere, J.J., and Rafer, A.B. comp., 2003, World distribution of sediment-hosted, stratiform copper deposits and occurrences: Geological Survey of Canada, accessed September 26, 2009, at [http://apps1.gdr.nrcan.gc.ca/gsc\\_minerals/index.phtml?language=en-CA](http://apps1.gdr.nrcan.gc.ca/gsc_minerals/index.phtml?language=en-CA).
- Kirkham, R.V., and Rafer, A.B., 2003, Selected world mineral deposits database: Geological Survey of Canada Open File 1801, 83 p., and digital data.
- Klitzsch, Eberhard, List, F.K., and Pöhlmann, Gerhard, eds., 1987, Geological map of Egypt, NH 36 SE, South Sinai: Cairo Egypt, The Egyptian General Petroleum Corporation, scale 1:500,000.
- Knox-Robinson, C.M., and Wyborn, L.A.I., 1997, Towards a holistic exploration strategy—Using geographic information systems as a tool to enhance exploration: *Australian Journal of Earth Sciences*, v. 44, p. 453–464.
- Kolodner, K., Avigad, D., McWilliams, M., Wooden, J.L., Weissbrod, T., and Feinstein, S., 2006, Provenance of north Gondwana Cambrian—Ordovician sandstone—U-Pb SHRIMP dating of detrital zircons from Israel and Jordan: *Geological Magazine*, v. 143, p. 367–391.
- Komac, Marko, 2006, A landslide susceptibility model using the analytical hierarchy process method and multivariate statistics in perialpine Slovenia: *Geomorphology*, v. 74, p. 17–28.
- Kreuzer, O.P., Etheridge, M.A., Guj, Pietro, McMahan, M.E., and Holden, D.J., 2008, Linking mineral deposit models to quantitative risk analysis and decision-making in exploration: *Economic Geology*, v. 103, p. 829–850.
- Lankester, Francis, 2012, Egyptological online magazine: Serabit el-Khadim, Web page accessed February 9, 2012, at <http://www.egyptological.com/2012/01/serabit-el-khadim-by-francis-lankester-7040>.
- Lee, J.E., and Glenister, D.A., 1976, Stratiform sulfide mineralization at Oamites copper mine, South West Africa: *Economic Geology*, v. 71, p. 369–383.
- Legarreta, Leonardo, Cruz, C.E., Vergani, Gustavo, Laffitte, G.A., and Villar, H.J., 2005, Petroleum mass-balance of the Neuquén Basin, Argentina—A comparative assessment of the productive districts and non-productive trends: *American Association of Petroleum Geologists (AAPG) Search and Discovery Article No. 10080*, 7 p.
- Leinweber, V.R., and Jokat, Wilfried, 2011, The Jurassic history of the Africa-Antarctica corridor—New constraints from magnetic data on the conjugate continental margins: *Tectonophysics*, v. 530–531, p. 87–101.
- Levy, T.E., Adams, R.B., Najjar, M., Hauptmann, A., Anderson, J.D., Brandl, B., Robinson, M.A., and Higham, T., 2004, Reassessing the chronology of Biblical Edom—New excavation and <sup>14</sup>C dates from Khirbat en-Nahas (Jordan): *Antiquity*, v. 78, p. 863–876.
- Li, His-chi, P'an, K'ai-wen, Yang, Ch'eng-fang, and Ts'ai, Chien-ming, 1968, Copper-bearing sandstone (shale) deposits in Yunnan: *International Geology Review*, v. 10, p. 870–882.
- Lifang, Ma [chief compiler], 2002, Geological atlas of China: Beijing, Geological Publishing House, 348 p.
- Lindsey, D.A., and Cox, D.P., 2003 [2007], Descriptive model of Redbed Cu 30b.3, *in* Cox, D.P., Lindsey, D.A., Singer, D.A., Moring, B.C., and Diggles, M.F., *Sediment hosted copper deposits of the world—Deposit models and database: U.S. Geological Survey Open-File Report 03–107, version 1.3*, 5 p. (Also available at <http://pubs.usgs.gov/of/2003/of03-107/>.)
- Link, P.K., ed., 1993, Geologic guidebook to the Belt-Purcell Supergroup, Glacier National Park and vicinity, Montana and adjacent Canada 1993: Belt Association, 3rd Belt Symposium, Guidebook, 125 p.
- Link, P.K., Fanning, C.M., Lund, K.I., and Aleinikoff, J.N., 2007, Detrital zircons, correlation and provenance of Mesoproterozoic Belt Supergroup and correlative strata of east-central Idaho and southwest Montana, *in* Link, P.K., and Lewis, R.S., eds., 2007, *Proterozoic geology of western North America and Siberia: Tulsa, Okla., Society for Sedimentary Geology (SEPM), Special Publication 86*, p. 101–128.
- Lizuain, Antonio, Leanza, H.C., and Panza, J.L., [coordinators], 1997, Mapa geológico de la República Argentina [Geologic map of the Argentine Republic]: Instituto de Geología y Recursos Minerales, Servicio Geológico Minero Argentina (SEGEMAR), 1 map on 2 sheets, scale 1:2,500,000. [In Spanish.]

- Long, D.G.F., and Turner, E.C., 2014, Formal definition of the Neoproterozoic Mackenzie Mountains Supergroup (Northwest Territories), and formal stratigraphic nomenclature for terrigenous clastic units of the Katherine Group: Geological Survey of Canada Open File 7113 (revised), 118 p.
- Long, K.R., DeYoung, J.H., Jr., and Ludington, S.D., 1998, Database of significant deposits of gold, silver, copper, lead, and zinc in the United States: U.S. Geological Survey Open-File Report 98–206, 33 p., digital data.
- Ludington, Steve, and Cox, Dennis, 1996, Data base for a national mineral-resource assessment of undiscovered deposits of gold, silver, copper, lead, and zinc in the conterminous United States: U.S. Geological Survey Open-File Report 96–96, 1 CD-ROM.
- Ludington, Steve, Orris, G.J., Bolm, K.S., Peters, S.G., and U.S. Geological Survey–Afghanistan Ministry of Mines and Industry Joint Mineral Resource Assessment Team, 2007, Preliminary mineral resource assessment of selected mineral deposit types in Afghanistan: U.S. Geological Survey Open-File Report 2007–1005, 44 p., <http://pubs.usgs.gov/of/2007/1005/>.
- Lydon, J.W., 2007, Geology and metallogeny of the Belt-Purcell Basin, in Goodfellow, W.D., ed., 2007, Mineral deposits of Canada—A synthesis of major deposit-types, district metallogeny, the evolution of geological provinces, and exploration methods: Geological Association of Canada Mineral Deposits Division Special Publication No. 5, p. 581–607.
- Lyons, T.W., Frank, T.D., Schreiber, M.E., Winston, D., and Lohmann, K.C., 1998, Geochemical constraints on paleoenvironments within the Belt Supergroup (Middle Proterozoic), Montana, in Berg, R.B., ed., Belt Symposium III, August 14–21, 1993: Whitefish, Mont., Montana Bureau of Mines and Geology, Special Publication 112, p. 190–201.
- Lyons, W.A., 1999, Las areniscas cupríferas del Neuquén, in Zappettini, E.O., ed., Recursos Minerales de la República Argentina, Volumen II: Buenos Aires, Instituto de Geología y Recursos Minerales SEGEMAR, anales 35, p. 1149–1158. [In Spanish.]
- MacNaughton, R.B., Fallas, K.M., and Zantvoort, W., 2008, Qualitative assessment of the Plateau Fault (Mackenzie Mountains, NWT) as a conceptual hydrocarbon play: Geological Survey of Canada Open File 5831, 29 p.
- Magoon, L.B., and Dow, W.G., 1994, The petroleum system, in Magoon, L.B., and Dow, W.G., eds., The petroleum system—From source to trap: American Association of Petroleum Geologists (AAPG) Memoir 60, p. 3–24.
- Magoon, L.B., and Schmoker, J.W., 2000, The total petroleum system—The natural fluid network that constrains the assessment unit, in USGS World Energy Assessment Team, U.S. Geological Survey World petroleum assessment 2000—Description and results: U.S. Geological Survey Digital Data Series 60, chap. PS, 31 p.
- Maiden, K.J., Innes, A.H., King, M.J., Master, S., and Pettitt, I., 1984, Regional controls on the localization of stratabound copper deposits—Proterozoic examples from southern Africa and South Australia: *Precambrian Research*, v. 25, p. 99–118.
- Malczewski, Jacek, 1999, GIS and multicriteria decision analysis: New York, John Wiley & Sons, Inc., p. 217–223.
- Marquillas, R.A., del Papa, Cecilia, and Sabino, I.F., 2005, Sedimentary aspects and paleoenvironmental evolution of a rift basin—Salta Group (Cretaceous–Paleogene), northwestern Argentina: *International Journal of Earth Sciences*, v. 94, p. 94–113.
- Marquillas, R.A., and Salfity, J.A., 1988, Tectonic framework and correlations of the Cretaceous–Eocene Salta Group, in Bahlburg, H., Breikreuz, Ch., and Giese, P., eds., The southern central Andes: Berlin Heidelberg, Springer-Verlag, Lecture Notes in Earth Sciences, v. 17, p. 119–136.
- Martin, H., and Porada, H., 1977, The intracratonic branch of the Damara Orogen in South West Africa—I. Discussion of geodynamics models: *Precambrian Research*, v. 5, p. 311–338.
- Marzoli, A., Melluso, L., Morra, V., Renne, P.R., Sgrosso, I., D’Antonio, M., Morais, D.L., Morais, E.A.A., and Ricci, G., 1999, Geochronology and petrology of Cretaceous basaltic magmatism in the Kwanza basin (western Angola), and relationships with the Parana-Etendeka continental flood basalt province: *Journal of Geodynamics*, v. 28, p. 341–356.
- Master, Sharad, ed., 1996, Excursion guidebook, Paleoproterozoic of Zambia and Zimbabwe: University of Witwatersrand, Economic Geology Research Unit Information Circular 302, 61 p.
- Matthews, K.J., Seton, M., and Müller, R.D., 2012, A global-scale plate reorganization event at 105–100 Ma: *Earth and Planetary Science Letters*, v. 355–356, p. 283–298.
- McCuaig, T.C., Beresford, Steve, and Hronsky, Jon, 2010, Translating the mineral systems approach into an effective exploration targeting system: *Ore Geology Reviews*, v. 38, p. 128–138.



- McKinney, Mark, Brown, Ian, Goldschmidt, Allan, and Lomberg, Ken, 2009, Tschudi copper deposit geological modelling and mineral resource estimate: Coffey Mining Ltd. for Weatherly Mining Namibia Ltd., 83 p., 2 apps., accessed January 22, 2015, at [http://weatherlyplc.com/wp-content/uploads/2013/03/Coffey\\_Tschudi\\_Resource\\_Estimate\\_13112009\\_Final.pdf](http://weatherlyplc.com/wp-content/uploads/2013/03/Coffey_Tschudi_Resource_Estimate_13112009_Final.pdf).
- McMechan, M.E., 1981, The middle Proterozoic Purcell Supergroup in the southeastern Rocky and southeastern Purcell mountains, British Columbia and the initiation of the Cordilleran miogeocline, southern Canada and adjacent United States: *Bulletin of Canadian Petroleum Geology*, v. 29, no. 4, p. 583–621.
- Mendez, V., and Zappettini, E., 1989, Geology and mineral deposits of the Central Andes, Republic of Argentina, chap. 14 of Ericksen, G.E., Canas Pinochet, M.T., and Reine-mund, J.A., eds., *Geology of the Andes and its relation to hydrocarbon and mineral resources*: Houston, Tex., Circum-Pacific Council for Energy and Mineral Resources, Earth Science Series, v. 11, p. 195–206.
- Mescua, J.F., Giambiagi, L.B., and Ramos, V.A., 2013, Late Cretaceous uplift in the Malargue fold-and-thrust belt (36° S), southern Central Andes of Argentina and Chile: *Andean Geology*, v. 40, p. 102–116.
- Metcalf, Ian, 2011, Tectonic framework and Phanerozoic evolution of Sundaland: *Gondwana Research*, v. 19, p. 3–21.
- Meyer, M.A., and Booker, J.M., 2001, Eliciting and analyzing expert judgment—A practical guide: Society for Industrial and Applied Mathematics and American Statistical Association, 459 p.
- Midnight Sun Mining Corp., 2014, Namibian properties: Midnight Sun Mining Corp. Web page, accessed July 29, 2014, at <http://www.midnightsunmining.com/s/Namibian.asp>.
- Mietzner, Peter, 2011, Today in Namibian history, iNamibia, accessed April 25, 2011, at <http://www.inamibia.co.na/news-and-weather/12-entertainment/953-today-in-namibian-history.html>.
- Milani, E.J., and Thomaz Filho, Antonio, 2000, Sedimentary basins of South America, in Cordani, U.G., Milani, E.J., Thomaz Filho, Antonio, and Campos, D.A., eds., *Tectonic evolution of South America: Rio de Janeiro, 31st International Geological Congress, Rio de Janeiro, Brazil, August 6–17, 2000*, p. 389–449.
- Miller, R.McG., 1983, Economic implications of plate tectonic models of the Damara Orogen, in Miller, R.McG., *Evolution of the Damara Orogen of south west Africa/Namibia: Special Publication—Geological Society of South Africa*, v. 11, p. 385–395.
- Mining Review, 2008, Copper project in Angola to undertake drilling campaign: Mining Review Web page, accessed May 19, 2014, at <http://www.miningreview.com/copper-project-in-angola-to-undertake-drilling-campaign/>.
- MOD Resources Ltd., 2012, Botswana copper project—Investor presentation: ASX release, 20 November 2012, 19 p.
- Modie, B.N., 1996, Depositional environments of the Meso- to Neoproterozoic Ghanzi-Chobe Belt, northwest Botswana: *Journal of African Earth Sciences*, v. 22, p. 255–268.
- Modie, B.N., 2000, Geology and mineralization in the Meso- to Neoproterozoic Ghanzi-Chobe Belt of northwest Botswana: *Journal of African Earth Sciences*, v. 30, p. 467–474.
- Monaldi, C.R., Salfity, J.A., and Kley, Jonas, 2008, Preserved extensional structures in an inverted Cretaceous rift basin, northwestern Argentina—Outcrop examples and implications for fault reactivation: *Tectonics*, v. 27, 21 p.
- Monger, Jim, and Price, Ray, 2002, The Canadian Cordillera—Geology and tectonic evolution: CSEG [Canadian Society of Exploration Geophysicists] Recorder, February volume, p. 17–36.
- Moore, J.M., 1979, Primary and secondary faulting in the Najd Fault System, Kingdom of Saudi Arabia: U.S. Geological Survey Open File Report 79–1661, 22 p.
- Moradi, Mehdi, Bazayr, M.H., and Mohammadi, Zargham, 2012, GIS-based landslide susceptibility mapping by AHP method—A case study, Dena City, Iran: *Journal of Basic Applied Science*, v. 2, no. 7, p. 6715–6723.
- Mosquera, Alfonso, and Ramos, V.A., 2006, Intraplate deformation in the Neuquén Embayment, in Kay, S.M., and Ramos, V.A., eds., *Evolution of an Andean margin—A tectonic and magmatic view from the Andes to the Neuquén Basin (35°–39° S lat)*: Geological Society of America Special Paper 407, p. 97–123.
- Mpodozis, Constantino, Arriagada, César, Basso, Matilde, Roperch, Pierrick, Cobbold, Peter, and Reich, Martin, 2005, Late Mesozoic to Paleogene stratigraphy of the Salar de Atacama Basin, Antofagasta, northern Chile—Implications for the tectonic evolution of the Central Andes: *Tectonophysics*, v. 399, no. 1–4, p. 125–154.
- Murphy, J.B., 2007, Geological evolution of middle to late Paleozoic rocks in the Avalon terrane of northern mainland Nova Scotia, Canadian Appalachians—A record of tectono-thermal activity along the northern margin of the Rheic Ocean in the Appalachian-Caledonide Orogen: *Geological Society of America Special Paper 423*, p. 413–434.

- Naipauer, M., Morabito, E.G., Marques, J.C., Tunik, M., Rojas Vera, E.A., Vujovich, G.I., Pimentel, M.P., and Ramos, V.A., 2012, Intraplate late Jurassic deformation and exhumation in western central Argentina—Constraints from surface data and U–Pb detrital zircon ages: *Tectonophysics*, v. 524–525, p. 59–75.
- Narbonne, G.M., and Aitken, J.D., 1995, Neoproterozoic of the Mackenzie Mountains, northwestern Canada: *Precambrian Research*, v. 73, p. 101–121.
- Nesheim, T.O., Vervoort, J.D., McClelland, W.C., Gilotti, J.A., and Lang, H.M., 2012, Mesoproterozoic syntectonic garnet within Belt Supergroup metamorphic tectonites—Evidence of Grenville-age metamorphism and deformation along northwest Laurentia: *Lithos*, v. 134–135, p. 91–97.
- Neuendorf, K.K.E., Mehl, J.P., Jr., and Jackson, J.A., eds., 2005, *Glossary of geology* (5th ed.): Alexandria, Va., American Geological Institute, 779 p.
- New Brunswick Department of Natural Resources and Energy, 2000, *Bedrock geology of New Brunswick* (2000 ed.): Minerals and Energy Division, Map NR–1, scale 1:500,000.
- New Brunswick Mineral Occurrence Database, 2012, Dorchester Mine (Cu), accessed December 18, 2012, at <http://dnre-mrne.gnb.ca/MineralOccurrence/default.aspx?componentID=28>.
- Nimry, Y.F., ed., 1973, *The copper and manganese prospects of the Wadi Araba: Hashemite Kingdom of Jordan*, Natural Resources Authority, Mining Division, 107 p.
- Noori, R., Feizi, F., and Jafari, M.R., 2011, Determination of Cu and Mo potential targets in the Khatunabad based on analytical hierarchy process, west of Mianeh, Iran: *World Academy of Science, Engineering and Technology*, v. 54, p. 598–601.
- Normore, Leon, and Mitton, Bruce, 2007, *First year assessment report of compilation, geological mapping, and rock and stream geochemistry on Claim Group 4949, Dorchester project, NTS 21H/16W, southeast New Brunswick*: New Brunswick Department of Natural Resources report of work 476473, 101 p., accessed September 10, 2014, at <http://dnre-mrne.gnb.ca/parisweb/AssessmentReportSearch.aspx>.
- Northcote, K.E., DeMont, G., and Armitage, A., 1989, Lochaber Lake copper, *in* Open-file report on selected metallic mineral occurrences of the Antigonish area: Nova Scotia Department of Mines and Energy Open-File Report 89–003, p. 13–21.
- Northwest Territories Geoscience Office, 2010, NT GoData, Showings search, accessed August 23, 2010, at <http://ntgodata.nwtgeoscience.ca/showingsQuery.html>.
- Northwest Territories Geoscience Office, 2011, NORMIN—The Northern Minerals Database: Northwest Territories Geoscience Office online database, accessed November 9, 2011, at <http://www.nwtgeoscience.ca/normin/>.
- Nurnberg, Dirk, and Muller, R.D., 1991, The tectonic evolution of the South Atlantic from Late Jurassic to present: *Tectonophysics*, v. 191, p. 27–53.
- O’Reilly, G.A., 2008, From the mineral inventory files—Serendipity and a bit of sleuthing at Canfield Creek: Nova Scotia Minerals Update Autumn 2008, p. 3, accessed June 24, 2014, at <http://novascotia.ca/natr/meb/data/pubs/ftmif/mif25n4.pdf>.
- O’Sullivan, J.R., 1981, Report on geological, geochemical, geophysical, and diamond-drilling surveys on the Pugwash claim group: Nova Scotia Department of Mines and Energy Assessment Report ME 11E/13A 13–E–33(01), 298 p., accessed September 10, 2014, at <http://gis4.natr.gov.ns.ca/novascan/DocumentQuery.faces>.
- O’Sullivan, J.R., 2006, Scott Grant claims, license 06436, Canfield Creek prospect, Cumberland County, Nova Scotia, NTS 11E/13a, report on prospecting and compilation of data: Nova Scotia Department of Natural Resources Mineral Resources Branch, Assessment Report AR2006–083, 16 p., accessed September 5, 2011, at [http://www.gov.ns.ca/natr/meb/data/ar/2006/AR\\_ME\\_2006-083.pdf](http://www.gov.ns.ca/natr/meb/data/ar/2006/AR_ME_2006-083.pdf).
- Papenfus, E.B., 1931, “Red bed” copper deposits in Nova Scotia and New Brunswick: *Economic Geology*, v. 26, no. 3, p. 314–330.
- Pazand, Kaveh, Hezarkhani, Ardeshir, Ataci, Mohammad, and Ghanbari, Yousef, 2011, Combining AHP with GIS for predictive Cu porphyry potential mapping—A case study in Ahar area (NW, Iran): *Natural Resources Research*, v. 20, no. 4, p. 251–262.
- Peral, A.P., and Wormald, P.J., 1999, Mineralización cuprífera del área Juramento, Salta, *in* Zappettini, E.O., Segal, S., Godeas, M., Brodkorb, M.K., and Schalamuk, I.A., eds., *Recursos minerales de la Republica Argentina* [Mineral resources of Argentina]: Instituto de Geología y Recursos Minerales, Servicio Geológico Minero Argentina SEGE-MAR, anales 5, p. 947–949. [In Spanish.]
- Peters, S.G., Ludington, S.D., Orris, G.H., Sutphin, D.M., Bliss, J.D., Rytuba, J.J., and U.S. Geological Survey–Afghanistan Ministry of Mines Joint Mineral Resource Assessment Team, 2007, Preliminary non-fuel mineral resource assessment of Afghanistan: U.S. Geological Survey Open-File Report 2007–1214, 810 p.
- Pirajno, Franco, 2013, Yangtze Craton, Cathaysia and the South China Block, *in* The geology and tectonic setting of China’s mineral deposits: Netherlands, Springerlink, p. 127–247.

- Pollastro, R.M., Karshbaum, A.S., and Viger, R.J., 1997, Maps showing geology, oil and gas fields and geologic provinces of the Arabian Peninsula: U.S. Geological Survey Open File Report 97-470B, CD-ROM.
- Pons, J.M., Franchini, Marta, Giusiano, Adolfo, Impiccini, Agnes, and Godeas, Marta, 2009, Alteración, mineralización de Cu y bitumen en el prospecto Barda González, Neuquén [Alteration, Cu mineralization and bitumen in the Barda González prospect, Neuquén]: *Revista del la Asociación Geológica Argentina*, v. 64, p. 501–513. [In Spanish.]
- Pons, M.J., Franchini, Marta, Giusiano, Adolfo, Maydagán, Laura, and Rainoldi, A.L., 2014, Mineralización de Cu (V-U) en la Formación Huincul, prospecto Tordillos, Cuenca Neuquina [Cu (V-U) mineralization in the Huincul Formation, Tordillos prospect, Neuquén Basin]: *Revista de la Asociación Geológica Argentina*, p. 1–33, accessed July 24, 2014, at [http://www.researchgate.net/publication/263580604\\_MINERALIZACION\\_DE\\_Cu\\_\(V-U\)\\_EN\\_LA\\_FORMACION\\_HUINCUL\\_PROSPECTO\\_TORDILLOS\\_CUENCA\\_NEUQUINA](http://www.researchgate.net/publication/263580604_MINERALIZACION_DE_Cu_(V-U)_EN_LA_FORMACION_HUINCUL_PROSPECTO_TORDILLOS_CUENCA_NEUQUINA). [In Spanish.]
- Porada, H., 1989, Pan-African rifting and orogenesis in southern to equatorial Africa and eastern Brazil: *Precambrian Research*, v. 44, p. 103–136.
- Porter Geoconsultancy, 2011, Dongchuan—Luoxue, Lanniping, Yinmin, Tangdan (Yunnan, China): Porter Geoconsultancy Web page accessed May 18, 2011, at <http://www.portergeo.com.au/database/mineinfo.asp?mineid=mn429>.
- Pretorius, Awie, and Park, Vivian, 2011, Resource estimation update, Hana Mining Ltd., Ghanzi copper-silver project, Ghanzi district, Botswana: Report prepared by Sphynx Consulting CC for Hana Mining Ltd., 116 p. (Also available at <http://www.sedar.com>.)
- Price, R.A., and Sears, J.W., 2000, A preliminary palinspastic map of the Mesoproterozoic Belt-Purcell Supergroup, Canada and USA—Implications for the tectonic setting and structural evolution of the Purcell anticlinorium and Sullivan deposit, in Lydon, J.W., Höy, T., Slack, J.F., and Knapp, M.E., eds., *The Sullivan deposit and its geological environment*: Geological Association of Canada, Mineral Deposits Division, Special Publication 1, p. 61–81.
- Protectedplanet.net, 2014, Israel: Protectedplanet.net Web page, accessed August 8, 2014, at <http://www.protectedplanet.net/countries/106>.
- Qin, Dexian, Meng, Qing, and Yang, Minchu, 1993, The sedimentary-reformation origin of the Haojiahe copper deposit, Mouding County, Yunnan province: *Kuangchuang Dizhi [Mineral Deposits]*, v. 12, p. 97–108. [In Chinese with English abstract.]
- Quennell, A.M., 1958, The structural and geomorphic evolution of the Dead Sea rift: *Quarterly Journal of the Geological Society of London*, v. 114, part 1, p. 1–24.
- Rabb'a, Ibrahim, and Nawasreh, Mohammed, 2006, Mineral status and future opportunity—Copper: Hashemite Kingdom of Jordan, Natural Resources Authority, Geological Survey Administration, 26 p. (Also available at [http://www.nra.gov.jo/images/stories/pdf\\_files/copper.pdf](http://www.nra.gov.jo/images/stories/pdf_files/copper.pdf).)
- Rainbird, R.H., Jefferson, C.W., and Young, G.M., 1996, The early Neoproterozoic sedimentary Succession B of northwestern Laurentia—Correlations and paleogeographic significance: *Geological Society of America Bulletin*, v. 108, p. 454–470.
- Rainoldi, A.L., Franchini, Marta, Beaufort, Daniel, Patrier, Patricia, Giusiano, Adolfo, Impiccini, Agnes, and Pons, Josefina, 2014, Large-scale bleaching of red beds related to upward migration of hydrocarbons—Los Chihuidos High, Neuquén Basin, Argentina: *Journal of Sedimentary Research*, v. 84, p. 373–393.
- Ramos, V.A., 2010, The tectonic regime along the Andes—Present-day and Mesozoic regimes: *Geological Journal*, v. 45, p. 2–25.
- Ramos, V.A., and Aleman, Antenor, 2000, Tectonic evolution of the Andes, in Cordani, U.G., Milani, E.J., Filho, A.T., and Campos, D.A., eds., *Tectonic evolution of South America: Rio De Janeiro, 31st International Geological Congress*, p. 635–685.
- Ramos, V.A., and Kay, S.M., 2006, Overview of the tectonic evolution of the southern Central Andes of Mendoza and Neuquén (35°–39° S latitude), in Kay, S.M., and Ramos, V.A., eds., *Evolution of an Andean margin—A tectonic and magmatic view from the Andes to the Neuquén Basin (35°–39° S latitude)*: Geological Society of America Special Paper 407, p. 1–17.
- Ran, Chongying, 1983, On genetic model of Dongchuan type strata-bound copper deposit: *Scientia Sinica (Series B)*, v. 26, p. 983–995.
- Ran, Chongying, 1989a, Dongchuan-type stratabound copper deposits, China—A genetic model, in Boyle, R.W., Brown, A.C., Jefferson, C.W., Jowett, E.C., and Kirkham, R.V., eds., *Sediment-hosted stratiform copper deposits*: Geological Association of Canada, Special Paper 36, p. 667–677.
- Ran, Chongying, 1989b, Environmental significance of stromatolites and their relation to copper ore in the Luoxue Formation of the Kunyang Group in Dongchuan, Yunnan, China, in Boyle, R.W., Brown, A.C., Jefferson, C.W., Jowett, E.C., and Kirkham, R.V., eds., *Sediment-hosted stratiform copper deposits*: Geological Association of Canada, Special Paper 36, p. 679–685.



- Ran, Chongying, 1989c, Formation mechanism of stratabound copper deposit in Kangdian Axis: Beijing, Geological Publishing House, 50 p. [In Chinese with English abstract.]
- Ran, Chongying, 1990, Geochemical data for the Dongchuan-Yimen stratabound copper deposits, China, *in* Parnell, J., Ye, Linjun, and Chen, Changming, eds., *Sediment-hosted mineral deposits—Proceedings of a symposium held in Beijing, People's Republic of China, July 30–August 4, 1988*: Oxford, United Kingdom, Blackwell Publishing Ltd., 173 p.
- Raup, O.B., Whipple, J.W., and McGimsey, R.G., 1993, Geologic guide for the area of Logan Pass, along the Highline Trail to Granite Park chalet, and the loop on going-to-the-sun road, Glacier National Park, *in* Link, P.K., 1993 [1997], *Geologic guidebook to the Belt-Purcell Supergroup, Glacier National Park and vicinity, Montana and adjacent Canada—Belt Symposium III Field Trip Guidebook, August 14–21, 1993*, Whitefish, Montana: Spokane, Wash., Belt Association, p. 97–112.
- Reed, M.H., 1997, Hydrothermal alteration and its relationship to ore fluid composition, *in* Barnes, H.L., *Geochemistry of hydrothermal ore deposits* (3d ed.): New York, John Wiley & Sons, p. 303–366.
- Research Institute of Geology, comp., 1982, Tectonic map of Asia: Beijing, Chinese Academy of Geological Sciences, 1 map on 6 sheets, scale 1:8,000,000. [In Chinese and English.]
- Revett Minerals, 2009, Troy Mine reserves and resources: Revett Minerals Web page, accessed August 12, 2010, at <http://www.revettminerals.com/revProReserves.php>.
- Ricci, S.M., comp., 1970–71, Provincia del Neuquén mapa minero [Province of Neuquén mining map]: Ministry of Industry and Mining, scale 1:750,000. [In Spanish.]
- Ricci, S.M., comp., 1973, Provincias de Salta y Jujuy, mapa minero: Ministerio De Economía, Republica Argentina: scale 1:750,000. [In Spanish.]
- Ricci, S.M., comp., 1974, Provincia de Mendoza mapa minero [Province of Mendoza mining map]: Ministry of Economy, scale 1:750,000. [In Spanish.]
- Rimann, Ernst, 1915, *Geologische Untersuchungen des Bastardlandes in Deutsch-Südwestafrika*: Berlin, Dietrich Reimer, 100 p.
- Ristorcelli, Steve, and Fitch, David, 2005, Technical report on the copper and silver resources, Montanore project, Lincoln and Sanders counties, Montana [Prepared for Mines Management, Inc.]: Mine Development Associates, NI43–101 Technical report, 151 p. (Also available at <http://www.minesmanagement.com/images/pdfs/Montanore43-101Technical-report.pdf>.)
- Rojas, G.E., 1999a, Distrito uranífero Barda Negra, Neuquén, *in* Zappettini, E.O., ed., *Recursos Minerales de la República Argentina, Volumen II: Buenos Aires*, Instituto de Geología y Recursos Minerales SEGEMAR, anales 35, p. 1073–1074. [In Spanish.]
- Rojas, G.E., 1999b, Distrito uranífero Pampa Amarilla, Mendoza, *in* Zappettini, E.O., ed., *Recursos Minerales de la República Argentina, Volumen II: Buenos Aires*, Instituto de Geología y Recursos Minerales SEGEMAR, anales 35, p. 1135–1140. [In Spanish.]
- Rojas, G.E., 1999c, Distrito uranífero Rahue-Có, Neuquén, *in* Zappettini, E.O., ed., *Recursos Minerales de la República Argentina, Volumen II: Buenos Aires*, Instituto de Geología y Recursos Minerales SEGEMAR, anales 35, p. 1071–1072. [In Spanish.]
- Roots, C.F., Martel, E., Fallas, K., Gordey, S.P., and MacNaughton, R., comps., 2011a, *Geology of Mount Eduni, NTS 106A Northeast, Mackenzie Mountains, Northwest Territories: Northwest Territories Geoscience Office, NWT Open File 2010–10* (2d ed.), scale 1:100,000.
- Roots, C.F., Martel, E., MacNaughton, R., Fallas, K., and Gordey, S.P., comps., 2011b, *Geology of Sekwi Mountain, NTS 105P Northeast, Mackenzie Mountains, Northwest Territories: Northwest Territories Geoscience Office, NWT Open File 2010–14* (2d ed.), scale 1:100,000.
- Rose, A.W., 1976, The effect of cuprous chloride complexes in the origin of red bed copper and related deposits: *Economic Geology*, v. 71, p. 1036–1048.
- Roseboom, E.H., 1966, An investigation of the system Cu-S and some natural copper sulfides between 25° and 700 °C: *Economic Geology*, v. 61, p. 641–672.
- Ross, G.M., 1991, Tectonic setting of the Windermere Supergroup revisited: *Geology*, v. 19, p. 29–35.
- Ross, G.M., and Villeneuve, Mike, 2003, Provenance of the Mesoproterozoic (1.45 Ga) Belt basin (western North America)—Another piece in the pre-Rodinia paleogeographic puzzle: *Geological Society of America, Bulletin*, v. 115, p. 1191–1217.
- Ross, J.D., 1998, Exploration report, Lochaber, Nova Scotia sedimentary copper deposit 11E–8D (Report on trenching, rock sampling, geochemical analyses, a till geochemical survey, and drilling and drill core geochemistry): Nova Scotia Department of Mines and Energy Assessment Report AR98–028, 98 p., accessed September 10, 2014, at <http://gis4.natr.gov.ns.ca/novascan/DocumentQuery.faces>.
- Rothenberg, Benno, 1979, Turquoise, copper and pilgrims—Archaeology of southern Sinai, *in* Rothenberg, Benno, ed., *Sinai—Pharaohs, miners, pilgrims and soldiers*: Bethesda, Md., Binns Publishers, 239 p.

- Rothenberg, Benno, and Merkel, J., 1995, Late Neolithic copper smelting in the Arabah: Institute for Archaeometallurgical Studies Newsletter 19, p. 1–7.
- Rowlands, N.L., 1974, The geology of some Adelaidean stratiform copper occurrence, *in* Bartholomé, Paul, ed., *Gisements stratiformes et provinces cuprifères: Liège, Belgium*, Société Géologique de Belgique, p. 419–427.
- Ruan, Huichu, Hua, Renmin, and Cox, D.P., 1991, Copper deposition by fluid mixing in deformed strata adjacent to a salt diapir, Dongchuan area, Yunnan province, China: *Economic Geology*, v. 86, p. 1539–1545.
- Ruelle, J.C.L., 1982, Depositional environments and genesis of stratiform copper deposits of the Redstone Copper Belt, Mackenzie Mountains, N.W.T., *in* Hutchinson, R.W., Spence, C.D., and Franklin, J.M., eds., *Precambrian sulphide deposits: Geological Association of Canada Special Paper 25*, p. 701–737.
- Ruxton, P.A., 1986, Sedimentology, isotopic signature, and ore genesis of the Klein Aub copper mine, South West Africa/Namibia, *in* Anhaeusser, C.R., and Maske, S., eds., *Mineral deposits of southern Africa: Johannesburg, Geological Society of South Africa*, p. 1725–1738.
- Ryan, R.J., and Boehner, R.C., 1994, Geology of the Cumberland Basin, Cumberland, Colchester and Pictou Counties, Nova Scotia: *Nova Scotia Mines and Energy Branches Memoir 10*, 212 p.
- Ryan, R.J., Boehner, R.C., Stea, R.R., and Rogers, P.J., 1989, Geology, geochemistry, and exploration applications for the Permo-Carboniferous red bed copper deposits of the Cumberland Basin, Nova Scotia, Canada, *in* Boyle, R.W., Brown, A.C., Jefferson, C.W., Jowett, E.C., and Kirkham, R.V., eds., *Sediment-hosted stratiform copper deposits: Geological Association of Canada, Special Paper*, v. 36, p. 245–256.
- Rybakov, Michael, and Segev, Amit, 2004, Top of the crystalline basement in the Levant: *Geochemistry, Geophysics, and Geosystems*, v. 5, p. 1–8, doi: 10.1029/2004GC000690.
- Saaty, T.L., 1980, *The analytic hierarchy process—Planning, priority setting, resource allocation (decision making series)*: New York, McGraw-Hill, 287 p.
- Saaty, T.L., 1990, How to make a decision—The analytic hierarchy process: *European Journal of Operational Research*, v. 48, p. 9–26.
- Saaty, T.L., and Vargas, L.G., 2010, *Decision making with the analytic network process—Economic, political, social and technological applications with benefits, opportunities, costs and risks*: New York, Springer Science+Business Media, LLC, 278 p.
- Saaty, T.L., and Vargas, L.G., 2012, *Models, methods, concepts and applications of the analytic hierarchy process (2d ed.)*: Norwell, Mass., Kluwer Academic Publishers, 333 p.
- Sagripanti, Lucía, Bottesi, Germán, Kietzmann, Diego, Folguera, Andrés, and Ramos, V.S., 2012, Mountain building processes at the orogenic front—A study of the unroofing in Neogene foreland sequence (37° S): *Andean Geology*, v. 39, p. 201–219.
- Salfity, J.A., Monaldi, C.R., Guidi, F., and Salas, R.J., 1998, *Mapa geológico de la Provincia de Salta: Servicio de Geología y Recursos Minerales*, 1 map on 2 sheets, scale 1:500,000.
- Sandeman, H.A., Ootes, Luke, Cousens, Brian, and Kilian, Taylor, 2014, Petrogenesis of Gunbarrel magmatic rocks—Homogeneous continental tholeiites associated with extension and rifting of Neoproterozoic Laurentia: *Precambrian Research*, v. 252, p. 166–179, accessed January 23, 2015, at <http://dx.doi.org/doi:10.1016/j.precamres.2014.07.007>.
- Schenckman, L.J., Leal, P.R., and Perez, D.J., 2013, Caracterización geológica y microtermometría del distrito los mellizos (37° 27' LS, 70° 30' LO), Provincia de Neuquén: *Revista de la Asociación Geológica Argentina*, v. 70, no. 4, p. 549–563. [In Spanish.]
- Schieber, Jurgen, 1997, Sedimentologic, geochemical, and mineralogical features of the Belt Supergroup and their bearing on the lacustrine versus marine debate, *in* Link, P.K., ed., 1997, *Geologic guidebook to the Belt-Purcell Supergroup, Glacier National Park and vicinity, Montana and adjacent Canada (2d ed.)—Belt Symposium III, August 14–21, 1993, Whitefish, Mont: Pocatello, Idaho, Belt Association*, p. 177–189.
- Schreiber, U.M., comp., 1980, *Geological map of Namibia: Geological Survey of Namibia*, scale 1:1,000,000.
- Schustack, Daniel, 2008, CityView Corporation announces results of independent review of company's assets by PricewaterhouseCoopers, accessed May 19, 2014, at [http://www.businesswire.com/news/home/20080618006125/en/CityView-Corporation-Announces-Results-Independent-Review-Companys#.U3p82\\_IdV8E](http://www.businesswire.com/news/home/20080618006125/en/CityView-Corporation-Announces-Results-Independent-Review-Companys#.U3p82_IdV8E).
- Schwartz, M.O., Kwok, Y.Y., Davis, D.W., and Akanyang, P., 1995, The sediment-hosted Ngwako Pan copper deposit, Botswana: *Economic Geology*, v. 90, p. 1118–1147.
- Sears, J.W., Chamberlain, K.R., and Buckley, S.N., 1998, Structural and U-Pb geochronological evidence for 1.47 Ga rifting event in the Belt Basin, western Montana: *Canadian Journal of Earth Sciences*, v. 35, p. 467–475.



- Sears, J.W., Price, R.A., and Khudoley, A.K., 2004, Linking the Mesoproterozoic Belt–Purcell and Udzha basins across the west Laurentia–Siberia connection: *Precambrian Research*, v. 129–308.
- Segev, Amit, and Beyth, M., 1986, Timna Valley geological map: Geological Survey of Israel, scale 1:20,000.
- Segev, Amit, and Sass, Eytan, 1989, Copper-enriched syngenetic dolostones as a source for epigenetic copper mineralization in sandstones and shales (Timna, Israel), *in* Boyle, R.W., Brown, A.C., Jefferson, C.W., Jowett, E.C., and Kirkham, R.B., eds., *Sediment-hosted stratiform copper deposits: Geological Association of Canada Special Paper 36*, p. 647–658.
- Segev, Amit, Steinitz, G., Platzner, I., and Starinsky, A., 1985, An Upper Devonian thermal event in southern Israel based on Rb–Sr and K–Ar ages of illites <2  $\mu\text{m}$  from Cambrian rocks [abs.]: Israel Geological Society Annual Meeting, p. 87–88.
- Shellnutt, G.J., 2014, The Emeishan large igneous province—A synthesis: *Geoscience Frontiers*, v. 5, p. 369–394.
- Shlomovitch, Naama, Bar-Matthews, Miryan, Segev, Amit, and Matthews, Alan, 1999, Sedimentary and epigenetic copper mineral assemblages in the Cambrian Timna Formation, southern Israel: *Israel Journal of Earth Science*, v. 48, p. 195–208.
- Sinclair, A.J., and Blackwell, G.H., 2002, *Applied mineral inventory estimation*: New York, Cambridge University Press, 381 p.
- Singer, D.A., 1995, World-class base and precious metal deposits—A quantitative analysis: *Economic Geology*, v. 90, no. 1, p. 88–104.
- Singer, D.A., and Menzie, W.D., 2010, *Quantitative mineral resource assessments—An integrated approach*: New York, Oxford University Press, 219 p.
- Singletary, S.J., Hanson, R.E., Martin, M.W., Crowley, J.L., Bowring, S.A., Key, R.M., Ramokate, L.V., Direng, B.B., and Krol, M.A., 2003, Geochronology of basement rocks in the Kalahari Desert, Botswana, and implications for regional Proterozoic tectonics: *Precambrian Research*, v. 121, p. 47–71.
- Skinner, B.J., and Barton, P.B., Jr., 1973, Genesis of mineral deposits: *Annual Review Earth Planetary Sciences*, v. 1, p. 183–211.
- Smith, M.H., 2005, Sumbe Base Metal Licence, Simba Jamba Mines Inc. (Sociedade Mineira Simba Jamba Lda), Kwanza Sul, Angola—A review of the mineral potential: Exploration company technical report, 12 p.
- Smith, M.H., 2006, Cachoeiras de Binga Copper Project—Dondo Copper Project—Benguela Copper Project—DRC Copper/Cobalt Project: Exploration company technical report, 7 p., accessed June 16, 2011, at [http://public-exhibition.zoomshare.com/files/Dr\\_Michael\\_Smith\\_Dondo\\_Zenda\\_Cachoeiras\\_report.doc](http://public-exhibition.zoomshare.com/files/Dr_Michael_Smith_Dondo_Zenda_Cachoeiras_report.doc).
- Sneh, A., Bartov, Y., Weissbrod, T., and Rosensaft, M., 1998, Geological map of Israel: Jerusalem, Geological Survey of Israel, 4 sheets, scale 1:200,000, accessed January 14, 2011, at <http://www.gsi.gov.il/eng/>.
- SNL Financial, 2014, Dongchuan property profile: SNL Financial Metals and Mining Properties (Commercial dataset available at <https://www.snl.com/>).
- Spanski, G.T., 1992, Quantitative assessment of future development of copper/silver resources in the Kootenai National Forest, Idaho/Montana, Part I—Estimation of the copper and silver endowments: *Nonrenewable Resources*, v. 1, no. 2, p. 163–183.
- Stensgaard, B.M., Kalvig, Per, and Stendal, Henrik, 2011, Quantitative mineral resource assessment—Sedimentary-hosted copper in Greenland—Reporting the copper assessment workshop, GEUS, Copenhagen, March 2009: *Danmarks og Grønlands Geologiske Undersøgelse Rapport 2011/104*, 104 p. 1 CD–ROM.
- Stern, R.J., and Johnson, Peter, 2010, Continental lithosphere of the Arabian plate—A geologic, petrologic, and geophysical synthesis: *Earth-Science Reviews*, v. 101, p. 29–67.
- Stewart, J.H., 1972, Initial deposits of the Cordilleran geosyncline—Evidence of late Precambrian (<850 m.y.) continental separation: *Geological Society of America, Bulletin*, v. 83, p. 1345–1360.
- Sun, Wei-Hua, Zhou, Mei-Fu, Gao, Jian-Feng, Yang, Yue-Heng, Zhao, Xin-Fu, and Zhao, Jun-Hong, 2009, Detrital zircon U–Pb geochronological and Lu–Hf isotopic constrains on the Precambrian magmatic and crustal evolution of the western Yangtze Block, SW China: *Precambrian Research*, v. 172, p. 99–126.
- Swenson, J.B., Person, M., Raffensperger, J.P., Cannon, W.F., Woodruff, L.G., and Berndt, M.E., 2004, A hydrologic model of stratiform copper mineralization in the midcontinent rift system, northern Michigan, U.S.A.: *Geofluids*, v. 4, p. 1–22.
- Taylor, D., 2000, ‘Soft-rock’ petroleum-type approach to exploration for ‘hard-rock’ minerals in sedimentary basins, *in* Glikson, M., and Mastalerz, M., eds., *Organic matter and mineralization—Thermal alteration, hydrocarbon generation, and role in metallogenesis*: Dordrecht, The Netherlands, Kluwer Academic Publishers, p. 1–12.

- ten Brink, U.S., Rybakov, Michael, Al-Zoubi, A.S., and Rotstein, Yair, 2007, Magnetic character of a large continental transform—An aeromagnetic survey of the Dead Sea Fault: *Geochemistry, Geophysics, Geosystems*, v. 8, no. 7, Q07005, doi: 10.1029/2007GC001582.
- Thomas, R.J., and Jacobs, J., 1998, The contrasting faces of Mesoproterozoic mobile belts in Africa, Laurentia and East Antarctica [abs]: Abstract Volume, International Conference on the role of a national Geological Survey in sustainable development, Gaborone, Botswana, p. 140–143.
- Thorkelson, D.J., Abbott, J.G., Mortensen, J.K., Creaser, R.A., Villeneuve, M.E., McNicoll, V.J., and Layer, P.W., 2005, Early and middle Proterozoic evolution of Yukon, Canada: *Canadian Journal of Earth Sciences*, v. 42, no. 6, p. 1045–1071.
- Thorson, J.P., ed., 2005, Lisbon Valley sediment-hosted copper deposits and Paradox Basin fluids field trip: Society of Economic Geologists Guidebook Series, v. 37, 49 p.
- Thorson, J.P., and MacIntyre, T.J., 2005, Geology of the Cashin Mine sandstone-hosted disseminated copper deposit, Montrose County, Colorado, *in* Thorson, J.P., ed., Lisbon Valley sediment-hosted copper deposits and Paradox Basin fluids field trip: Society of Economic Geologists Guidebook Series, v. 37, p. 43–49.
- Tonkin, G.D., and Creelman, R.A., 1990, Mount Gunson copper deposits, *in* Hughes, F.E., ed., *Geology and mineral deposits of Australia and Papua New Guinea*: Melbourne, Australasian Institute of Mining and Metallurgy, p. 1037–1043.
- Tunik, Maisa, Folguera, Andrés, Naipauer, Maximiliano, Pimentel, Marcio, and Ramos, V.A., 2010, Early uplift and orogenic deformation in the Neuquén Basin—Constraints on the Andean uplift from U–Pb and Hf isotopic data of detrital zircons: *Tectonophysics*, v. 489, p. 258–273.
- Turner, E.C., and Long, D.G.F., 2008, Basin architecture and syndepositional fault activity during the deposition of the Neoproterozoic Mackenzie Mountains Supergroup, Northwest Territories, Canada: *Canadian Journal of Earth Sciences*, v. 45, p. 1159–1184.
- Turner, R.J.W., Leitch, C.H.B., and Delaney, G.D., 2000, Syn-rift structural controls on the paleoenvironmental setting and evolution of the Sullivan ore body, chap. 32 *of* Lydon, J.W., Höy, Trygve, Slack, J.F., and Knapp, M.E., eds., 2000, *The geological environment of the Sullivan deposit*, British Columbia: Geological Association of Canada, Mineral Deposits Division, Special Publication No. 1, p. 582–616.
- Uliana, M.A., and Legarreta, Leonardo, 1993, Hydrocarbons habitat in a Triassic-to-Cretaceous sub-Andean setting—Neuquén Basin, Argentina: *Journal of Petroleum Geology*, v. 16, p. 397–420.
- Uliana, M.A., Arteaga, M.E., Legarreta, Leonardo, Cerdan, J.J., and Peroni, G.O., 1995, Inversion structures and hydrocarbon occurrence in Argentina, *in* Buchanan, J.G., and Buchanan, P.G., eds, *Basin inversion: Geological Society Special Publication No. 88*, p. 211–233.
- Urien, C.M., and Zambrano, J.J., 1994, Petroleum systems in the Neuquén basin, Argentina, *in* Magoon, L.B., and Dow, W.G., *The petroleum system—From source to trap: American Association of Petroleum Geologists (AAPG) Memoir*, v. 60, p. 513–534.
- U.S. Department of State, 2009, Small-scale digital international land boundaries (SSIB)—Lines, edition 10, and polygons, beta edition 1, *in* *Boundaries and sovereignty encyclopedia (B.A.S.E.)*: U.S. Department of State, Office of the Geographer and Global Issues.
- U.S. Geological Survey, 2010, Punilla Mine, Mineral Resource Data System (MRDS): U.S. Geological Survey, accessed September 14, 2010, at [http://mrdata.usgs.gov/mrds/show-mrds.php?dep\\_id=10005468](http://mrdata.usgs.gov/mrds/show-mrds.php?dep_id=10005468).
- Van Der Heever, Deon, and Arengi, Joseph, 2010, Resource estimate update, Hana Mining Ltd., Ghanzi copper-silver project, Ghanzi district, Botswana: GeoLogix, prepared for Hana Mining Ltd., 91 p.
- Van Eden, J.G., 1978, Stratiform copper and zinc mineralization in the Cretaceous of Angola: *Economic Geology*, v. 73, p. 1154–1161.
- Vergani, G.D., Tankard, A.J., Belott, H.J., and Welsink, H.J., 1995, Tectonic evolution and paleogeography of the Neuquén Basin, Argentina, *in* Tankard, A.J., Suarez, Soruco, R., and Welsink, H.J., eds., *Petroleum basins of South America: American Association of Petroleum Geologists (AAPG) Memoirs 62*, p. 383–402.
- Vermeesch, Pieter, Avigar, Dov, and McWilliams, M.O., 2009, 500 m.y. of thermal history elucidated by multi-method detrital thermochronology of North Gondwana Cambrian sandstone (Eilat area, Israel): *Geological Society of America Bulletin*, v. 121, p. 1204–1216.
- Veselinovic-Williams, M., and Frost-Killian, S., 2003 [2007], Digital international metallogenic map of Africa: Council for Geoscience, South Africa and Commission for the Geological Map of the World, scale 1:5,000,000, CD-ROM.
- Viramonte, J.G., Kay, S.M., Becchio, R., Escayola, M., and Novitski, I., 1999, Cretaceous rift related magmatism in central-western South America: *Journal of South American Earth Sciences*, v. 12, p. 109–121.

- Volodin, R.N., Chechetkin, V.S., Bogdanov, Yu.V., Narkelyun, L.F., and Trubachev, A.I., 1994, The Udokan cupriferous sandstone deposit (eastern Siberia): *Geology of Ore Deposits*, v. 36, p. 3–30.
- Waldron, J.W.F., Rygel, M.C., Gibling, M.R., and Calder, J.H., 2013, Evaporite tectonics and the late Paleozoic stratigraphic development of the Cumberland Basin, Appalachians of Atlantic Canada: *Geological Society of America Bulletin*, v. 125, p. 945–960.
- Walker, T.R., 1989, Application of diagenetic alterations in redbeds to the origin of copper in stratiform copper deposits, *in* Boyle, R.W., Brown, A.C., Jefferson, C.W., Jowett, E.C., and Kirkham, R.V., eds., *Sediment-hosted stratiform copper deposits*: Geological Association of Canada, Special Paper 36, p. 85–96.
- Wang, L.J., Yu, J.H., Griffen, W.L., and O'Reilly, S.Y., 2012, Early crustal evolution in the western Yangtze Block—Evidence from U-Pb and Lu-Hf isotopes on detrital zircons from sedimentary rocks: *Precambrian Research*, v. 222–223, p. 368–385.
- Wang, Y.G., Wang, S.E., Liu, P.B., and Yu, J.S., 1992, Eastern China, *in* Westermann, G.E.G., ed., *The Jurassic of the circum-Pacific—World and regional geology 3*: Cambridge, UK, Cambridge University Press, p. 214–224.
- Warren, J.K., 2000, Evaporites, brines and base metals—Low temperature ore emplacement controlled by evaporite diagenesis: *Australian Journal of Earth Sciences*, v. 47, p. 179–208.
- WEBLEX Canada, 2014, *Lexicon of Canadian geological names on-line*: Natural Resources Canada, accessed June 24, 2014, at [http://weblex.nrcan.gc.ca/weblex\\_e.pl](http://weblex.nrcan.gc.ca/weblex_e.pl).
- Weisgerber, G., 2006, The mineral wealth of ancient Arabia and its use, I—Copper mining and smelting at Feinan and Timna—Comparison and evaluation of techniques, production, and strategies: *Arabian Archaeology and Epigraphy*, v. 17, p. 1–30.
- Weissbrod, T., and Nachmias, J., 1986, Stratigraphic significance of heavy minerals in the Late Precambrian—Mesozoic clastic sequence (“Nubian Sandstone”) in the Near East: *Sedimentary Geology*, v. 47, p. 263–291.
- White, W.H., 1959, Cordilleran tectonics in British Columbia: *Bulletin of the American Association of Petroleum Geologists (AAPG)*, v. 43, p. 60–100.
- Wichmann, R., 1927, Los estratos con dinosaurios y su techo en el este del territorio de Neuquén: Buenos Aires, Dirección General de Minas, *Geología e Hidrogeología*, v. 32, p. 1–16.
- Winston, Don, 1986a, Sedimentation and tectonics of the Middle Proterozoic Belt Basin, and their influence on Phanerozoic compression and extension in western Montana and northern Idaho, *in* Peterson, J.A., ed., *Paleotectonics and sedimentation in the Rocky Mountain region, United States*: American Association of Petroleum Geologists (AAPG) Memoir 41, p. 87–118.
- Winston, Don, 1986b, Sedimentology of the Ravalli Group, Middle Belt Carbonate and Missoula Group, Middle Proterozoic Belt Supergroup, Montana, Idaho and Washington, *in* Roberts, S.M., ed., *Belt Supergroup—A guide to Proterozoic rocks of western Montana and adjacent areas*: Montana Bureau of Mines and Geology Special Publication 94, p. 85–124.
- Winston, Don, and Link, P.K., 1993, Middle Proterozoic rocks of Montana, Idaho and eastern Washington; the Belt Supergroup, *in* Reed, J.C., Jr., Bickford, M.E., Houston, R.S., Link, P.K., Rankin, D.W., Sims, P.K., and Van Schmus, W.R., eds., *The geology of North America, Precambrian, Conterminous U.S.*, v. C-2: Boulder, Colo., Geological Society of America, p. 487–517.
- Wyborn, L.A.I., Heinrich, C.A., and Jaques, A.L., 1994, Australian Proterozoic mineral systems—Essential ingredients and mappable criteria: *Proceedings of the Australasian Institute of Mining and Metallurgy Annual Conference*, Darwin, Australia, p. 109–116, accessed May 24, 2012, at [http://www.ga.gov.au/image\\_cache/GA5228.pdf](http://www.ga.gov.au/image_cache/GA5228.pdf).
- Yalcin, Ali, 2008, GIS-based landslide susceptibility mapping using analytical hierarchy process and bivariate statistics in Ardesen (Turkey)—Comparisons of results and confirmations: *Catena*, v. 72, p. 1–12.
- Yan, Guangsheng, Qiu, Ruizhao, Lian, Changyun, Li, Jinyi, Xiao, Keyan, and Mao, Jingwen, 2010, Quantitative assessment on the resource potential of porphyry and sediment-hosted copper deposits in China [English translation]: Beijing, Geological Publishing House, 218 p. [In Chinese].
- Yang, Weihua, 1996, Geochemistry of strata-bound copper deposits, *in* Tu, Guangzhi, ed., *Geochemistry of strata-bound deposits in China*: Beijing, Science Press, p. 470–507.
- Yano, Takao, Genyao, Wu, Mingqing, Tang, and Shaoli, Sha, 1994, Tectono-sedimentary development of backarc continental basin in Yunnan, southern China: *Journal of South-east Asian Earth Sciences*, v. 9, no. 1/2, p. 153–166.
- Yikang, Liu, 2002, Geological overview and mining districts of China: Presentation at Prospectors and Developers Association of Canada (PDAC) meeting, March 12, 2002, Toronto, 59 p., accessed January 3, 2011, at <http://www.gl.ntu.edu.tw/joomla/images/Yikang%201995%20Ore%20deposits%20in%20China.pdf>.

- Zanettini, J.C., 1999, El yacimiento ferrífero Hierro Indio, Mendoza, *in* Zappettini, E.O., ed., Recursos Minerales de la República Argentina: Instituto de Geología y Recursos Minerales, Servicio Geológico Minero Argentino, *anales* 35, v. 2, p. 1547–1552. [In Spanish.]
- Zanettini, J.C.M., and Carotti, M.A., 1993, Yacimientos metalíferos y metalogénesis, capítulo IV-1 [Metal deposits and metallogeny, chap. IV-1], *of* Ramos, V.A., ed., Geología y Recursos Naturales de la provincia de Mendoza: Buenos Aires, Relatorio al XII Congreso Geológico Argentino y 11 Congreso de Exploración de Hidrocarburos [XII Argentina Geological Congress and 11th Congressional Geological Oil Exploration] Report IV, p. 485–504.
- Zappettini, E.O., ed., 1999, Recursos Minerales de la República Argentina: Instituto de Geología y Recursos Minerales, Servicio Geológico Minero Argentino, *anales* 35, 2 v., 1976 p.
- Zavala, Carlos, Ponce, J.J., Arcuri, Mariano, Drittanti, Daniel, Freije, Hugo, and Asenio, Marcos, 2006, Ancient lacustrine hyperpycnites—A depositional model from a case study in the Rayoso Formation (Cretaceous) of west-central Argentina: *Journal of Sedimentary Research*, v. 76, p. 41–59.
- Zaw, Khin, Burrett, C.F., Berry, R.F., and Bruce, E., 1999, Geological, tectonic and metallogenic relationships of mineral deposits in mainland Southeast Asia (P390A): University of Tasmania Centre for Ore Deposits Research AMIRA Project P390A, CD-ROM.
- Zhang, C.H., Gao, L.Z., Wu, Z.J., Shi, X.Y., Yan, Q.R., and Li, D.J., 2007, SHRIMP U-Pb zircon age and Hf-O isotope evidence for Paleoproterozoic metamorphic event in South China: *Precambrian Research*, v. 151, p. 265–288.
- Zhang, Shouxin, ed., 2009, Geological formation names of China (1866–2000): Beijing, Higher Education Press, 2 volumes, 1537 p.
- Zhang, Yunxiang, Yaonan, Luo, and Chongxi, Yang, eds., 1990, Panxi Rift and its geodynamics: Beijing, Geological Publishing House, 415 p.
- Zhang, Z., ed., 1996, The discovery history of mineral deposits of Xinjiang Uygur Autonomous Region, China: Beijing, Geological Publishing House, 181 p.
- Zhao, Guochun, Sun, Min, Wilde, S.A., and Li, Sanzhong, 2004, A Paleo-Mesoproterozoic supercontinent—Assembly, growth and breakup: *Earth-Science Reviews*, v. 67, p. 91–123.
- Zhao, Xin-Fu, Zhou, Mei-Fu, Hitzman, M.W., Li, Jian-Wei, Bennett, Mitchell, Meighan, Corey, and Anderson, Eric, 2012, Late Paleoproterozoic to Early Mesoproterozoic Tangdan sedimentary rock-hosted stratabound copper deposit, Yunnan Province, Southwest China: *Economic Geology*, v. 107, p. 357–375.
- Zhao, Xin-Fu, Zhou, Mei-Fu, Li, Jian-Wei, Sun, Min, Gao, Jian-Feng, Sun, Wei-Hua, and Yang, Jin-Hui, 2010, Late Paleoproterozoic to early Mesoproterozoic Dongchuan group in Yunnan, SW China—Implications for tectonic evolution of the Yangtze Block: *Precambrian Research*, v. 182, p. 57–69.
- Zhao, Yi-Ming, and Wu, Liangshi, 2006, China's copper mineral resource map [English translation]: China Geological Publishing House, scale 1:5,000,000, also available at <http://infomine-china.com/Report/China-Copper-Resource-Map.htm>. [In Chinese.]
- Zhuang, Hanping, Ran, Chongying, He, Mingqin, and Lu, Jialan, 1996, Interactions of copper, evaporite, and organic matter and genesis of sandstone-hosted copper deposits in the Chuxiong Basin, Yunnan Province: *Acta Geologica Sinica*, v. 9, p. 407–419.
- Zientek, M.L., Bliss, J.D., Broughton, D.W., Christie, Michael, Denning, P.D., Hayes, T.S., Hitzman, M.W., Horton, J.D., Frost-Killian, Susan, Jack, D.J., Master, Sharad, Parks, H.L., Taylor, C.D., Wilson, A.B., Wintzer, N.E., and Woodhead, Jon, 2014, Sediment-hosted stratabound copper assessment of the Neoproterozoic Roan Group, Central African Copperbelt, Katanga Basin, Democratic Republic of the Congo and Zambia: U.S. Geological Survey Scientific Investigations Report 2010–5090–T, 162 p., and spatial data, <http://dx.doi.org/10.3133/sir20105090T>.
- Zientek, M.L., Chechetkin, V.S., Parks, H.L., Box, S.E., Briggs, D.A., Cossette, P.M., Dolgoplova, A., Hayes, T.S., Seltmann, R., Syusyura, B., Taylor, C.D., and Wintzer, N.E., 2014, Assessment of undiscovered sandstone copper deposits of the Kodar-Udokan area, Russia: U.S. Geological Survey Scientific Investigations Report 2010–5090–M, 129 p., and spatial data, <http://dx.doi.org/10.3133/sir20105090M>.
- Zientek, M.L., Derkey, P.D., Miller, R.J., Causey, J.D., Bookstrom, A.A., Carlson, M.H., Green, G.N., Frost, T.P., Bole-neus, D.E., Evans, K.V., Van Gosen, B.S., Wilson, A.B., Larsen, J.C., Kayser, H.Z., Kelley, W.N., and Assmus, K.C., 2005, Spatial databases for the geology of the northern Rocky Mountains—Idaho, Montana, and Washington: U.S. Geological Survey Open-File Report 2005–1235, 206 p., and data files, <http://pubs.usgs.gov/of/2005/1235/>.



- Zientek, M.L., Hayes, T.S., and Hammarstrom, J.M., 2013, Overview of a new descriptive model for sediment-hosted stratabound copper deposits, chap. 1 *of* Taylor, C.D., Causey, J.D., Denning, P.D., Hayes, T.S., Hammarstrom, J.M., Horton, J.D., Kirschbaum, M.J., Parks, H.L., Wilson, A.B., and Zientek, M.L., Descriptive models, grade-tonnage relationships, and databases for the assessment of sediment-hosted copper deposits—With emphasis on deposits in the Central Africa Copperbelt, Democratic Republic of the Congo and Zambia: U.S. Geological Survey Scientific Investigations Report 2010–5090–J, p. 2–16, <http://pubs.usgs.gov/sir/2010/5090/j/>.
- Zientek, M.L., Hayes, T.S., and Taylor, C.D., 2013, Grade and tonnage relations for sediment-hosted stratabound copper deposits, chap. 2 *of* Taylor, C.D., Causey, J.D., Denning, P.D., Hayes, T.S., Hammarstrom, J.M., Horton, J.D., Kirschbaum, M.J., Parks, H.L., Wilson, A.B., and Zientek, M.L., Descriptive models, grade-tonnage relationships, and databases for the assessment of sediment-hosted copper deposits—With emphasis on deposits in the Central African Copperbelt, Democratic Republic of the Congo and Zambia: U.S. Geological Survey Scientific Investigations Report 2010–5090–J, p. 17–59, <http://pubs.usgs.gov/sir/2010/5090/j/>.
- Zientek, M.L., Oszczepalski, Sławomir, Parks, H.L., Bliss, J.D., Borg, Gregor, Box, S.E., Denning, P.D., Hayes, T.S., Spieth, Volker, and Taylor, C.D., 2015, Assessment of undiscovered copper resources associated with the Permian Kupferschiefer, Southern Permian Basin, Europe: U.S. Geological Survey Scientific Investigations Report 2010–5090–U, 94 p. and spatial data, <http://dx.doi.org/10.3133/sir20105090U>.
- Zirakparvar, N.A., Vervoort, J.D., McClelland, W., and Lewis, R.S., 2010, Insights into the metamorphic evolution of the Belt–Purcell Basin—Evidence from Lu–Hf garnet geochronology: Canadian Journal of Earth Sciences, v. 47, p. 161–179.



## Appendix A. Description of GIS Files

By Heather L. Parks and Michael L. Zientek

Two Esri shapefiles (.shp), two extensible markup language files (.xml), and an Excel spreadsheet (.xlsx) are included with this report. These files may be downloaded from the USGS Web site as zipped file **sir20105090y\_gis.zip**.

**GMRA\_SSCqual\_pts.shp** is a point shapefile that represents the locations for known deposits, occurrences, and sites. For this report, deposits are defined as sediment-hosted stratabound copper localities with identified resources that have a defined tonnage and copper grade, occurrences are sediment-hosted stratabound copper localities with no known tonnage or grade, and sites are copper localities with an unknown deposit type and development status. The deposits and occurrences

are shown in figures 1-3–1-12 in this report, and the deposits are listed in tables in chapter 2. Attribute table fields include the permissive tract in which the site is located, site name and alternate names, site status, location information, commodities, source rock information, mineralogy, grade and tonnage information, comments, short references, and other miscellaneous descriptive information. The “Tract\_name” field correlates to the assessed areas discussed in this report. Attributes are defined in the accompanying metadata (GMRA\_SSCqual\_pts\_metadata.xml) and in table A1.

**GMRA\_SSCqual\_tracts.shp** is a polygon shapefile that represents areas permissive for sediment-hosted stratabound

**Table A1.** Definitions of GMRA\_SSCqual\_pts.shp attribute table fields.

Field name	Description
Tract_name	Name of permissive tract in which site is located. Same as “Tract_name” field in the GMRA_SSCqual_tracts.shp shapefile
Tract_ID	Identification number for permissive tract in which site is located
Name	Name of site
Name_other	Other names used for the site
SiteStatus	Status of site: “deposits” are sediment-hosted copper localities with reported mineral inventory or past production, “occurrences” are sediment-hosted copper localities with no reported inventory, and “sites” occur in sedimentary rock, but have an unknown deposit type
SiteStat2	Additional comments on the status of the site
Country	Country in which the site is located
State_Prov	State or province in which the site is located
Latitude	Latitude in decimal degrees. –90.000 to 90.000. Negative south of the equator
Longitude	Longitude in decimal degrees. –180.000 to 180.000. Negative west of the Greenwich meridian
Comm_major	Major commodities, in decreasing order of economic importance
Comm_minor	Minor commodities, in decreasing order of economic importance
Age_host	Age of host rock, in standard divisions of geologic time
HostRocks	Simplified lithologic description of host rocks
GeolProv	Geologic province in which site is located
Unit	Geologic unit in which site is located
Footwall	Lithology of footwall rocks
Hangwall	Lithology of hanging wall rocks
Mineralogy	Ore and gangue minerals in approximate order of abundance
Type	Mineral deposit type
Subtype	Sediment-hosted copper subtype
Tonnage_Mt	Ore tonnage, in millions of metric tons, -9999 indicates no data
Cu_pct	Average copper grade, in weight percent, -9999 indicates no data
Con_Cu_Mt	Contained copper, in million metric tons, -9999 indicates no data
Comments	Miscellaneous comments about the site
Size	Descriptive term for the size of the site as described in source document
Ref_short	Short reference; abbreviated citation for reference; full reference is provided in accompanying “GIS references.xlsx” file

copper deposits. These areas, or “permissive tracts,” represent either the areal extent or surface projection of rocks down to a specified depth where undiscovered mineral resources could be present. Information on permissive tract delineation is discussed in the “Permissive Tract Delineation” section of the main text. The permissive tracts are shown in figures 1-3–1-12 of this report. Attributes include the permissive tract name, location information, deposit type, general geology of the permissive rocks, age, and other miscellaneous descriptive information. These areas have been qualitatively assessed; therefore, the assessment result fields in the attribute table show 0 or “Not assessed” values. Each permissive tract correlates to

an assessed area discussed in this report. Attributes are defined in the accompanying metadata (GMRA\_SSCqual\_tracts\_metadata.xml) and in table A2.

**GMRA\_SSCqual\_pts\_metadata.xml** and **GMRA\_SSCqual\_tracts\_metadata.xml** contain the metadata for the **GMRA\_SSCqual\_pts.shp** and **GMRA\_SSCqual\_tracts.shp** shapefiles, respectively.

**GIS references.xlsx** is an excel spreadsheet that contains the full references for the **GMRA\_SSCqual\_pts.shp** file. The short references listed in the “Short\_ref” field in the **GMRA\_SSCqual\_pts.shp** file correlate to the “Short reference” column in the GIS references.xlsx spreadsheet.

**Table A2.** Definitions of GMRA\_SSCqual\_tracts.shp attribute table fields.

Field name	Description
Tract_ID	Identification number for permissive tract
Tract_name	Name of permissive tract. Same as “Tract_name” field in the GMRA_SSCqual_pts.shp shapefile
Unregcode	Three digit UN code for the region that underlies most of the permissive tract
Country	Country(ies) in which the permissive tract is located
Commodity	Primary commodity being assessed
Dep_type	Name of the deposit type assessed
GT_model	Grade-tonnage model used for the undiscovered deposit estimate
Geology	Geologic feature assessed
Age	Age of the assessed geologic feature
Asmt_date	Year assessment was conducted
Asmt_depth	Maximum depth beneath the Earth's surface used for the assessment, in kilometers
Est_levels	The set of percentile (probability) levels at which undiscovered deposit estimates were made
N90	Estimated number of deposits associated with the 90th percentile (90 percent chance of at least the indicated number of deposits)
N50	Estimated number of deposits associated with the 50th percentile (50 percent chance of at least the indicated number of deposits)
N10	Estimated number of deposits associated with the 10th percentile (10 percent chance of at least the indicated number of deposits)
N05	Estimated number of deposits associated with the 5th percentile (5 percent chance of at least the indicated number of deposits)
N01	Estimated number of deposits associated with the 1st percentile (1 percent chance of at least the indicated number of deposits)
N_Expected	Expected (mean) number of deposits. $N\_Expected = (0.233*N90) + (0.4*N50) + (0.225*N10) + (0.045*N05) + (0.03*N01)$
s	Standard deviation. $s = 0.121 - (0.237*N90) - (0.093*N50) + (0.183*N10) + (0.073*N05) + (0.123*N01)$
Cv_percent	Coefficient of variance, in percent. $Cv = (s/N\_Expected) * 100$
N_known	Number of known deposits in the tract
N_total	Total number of deposits. $N\_total = N\_Expected + N\_Known$
Area_km <sup>2</sup>	Area of permissive tract, in square kilometers
DepDensity	Deposit density (total number of deposits per square kilometer). $DepDensity = N\_total/Area\_km2$
DepDen10E5	Deposit density per 100,000 square kilometers. $DepDen10E5 = DepDensity*100,000$
Estimators	Names of people on the estimation team

## Appendix B. Analytic Hierarchy Process Input

By Niki E. Wintzer and Michael L. Zientek

Input used for the analytic hierarchy process (AHP; Saaty, 1980, 1990) analysis of the 10 worldwide sediment-hosted stratabound copper mineralized areas is included with this report as an Excel workbook. **AHP Input.xlsx** has multiple tabs reflecting hierarchy order with numerous tables in each worksheet. Both pairwise and direct rating methods were used to analyze the potential for undiscovered copper, thus two main types of inputs are within the tables—ratios and integers. Pairwise comparison involved each assessment area set opposite the other localities for one criterion (deposit subtype present for example). A rating (from one to nine) was chosen toward one assessment area or the other and then expressed as a ratio. In direct rating, predetermined numerical values were entered into the online software for each basin under each of the criteria.

For this analysis, we used MakeItRational<sup>1</sup>, an online AHP analysis tool ([www.makeitrational.com](http://www.makeitrational.com)). For those who anticipate using the MakeItRational software, note that a mathematical option was used to eliminate rank reversal. Other AHP analysis software services are available online.

### References Cited

- Saaty, T.L., 1980, *The analytic hierarchy process—Planning, priority setting, resource allocation (decision making series)*: New York, McGraw-Hill, 287 p.
- Saaty, T.L., 1990, How to make a decision—The analytic hierarchy process: *European Journal of Operational Research*, v. 48, p. 9–26.

---

<sup>1</sup>Use of trade, product, or firm names is for descriptive purposes only and does not imply endorsement by the U.S. Government.

## Appendix C. Assessment Team

**Deborah A. Briggs** is a geographic information system (GIS) specialist with the USGS in Spokane, Washington. She earned a B.S. degree in Geotechnical Engineering from the University of Idaho and a GIS certificate from Eastern Washington University.

**J. Douglas Causey** is a (retired) economic geologist with the USGS in Spokane, Washington. He designed and provided project-specific mineral resource databases for this mineral resource assessment.

**Shyla A. Hatch** is a student at Eastern Washington University working to obtain a B.S. in Geology and a B.S. in Environmental Science as of 2014. She provided thorough figure and text revisions using ArcMap GIS, Adobe Illustrator, and Microsoft Word.

**Timothy S. Hayes** has worked as a research hydrologist and geologist for the USGS for more than 30 years following several years in minerals exploration for private companies. His greatest expertise is sediment-hosted metal deposits, including sandstone-hosted uranium deposits, sediment-hosted stratabound copper deposits, Mississippi Valley-type lead-zinc deposits, and salt-related carbonate-hosted zinc-lead deposits.

**M. Christopher Jenkins** is a student at Eastern Washington University completing undergraduate geology coursework as preparation for graduate school in geology. Chris

earned a B.A. in Political Science and Social Studies from Western Washington University (2011). He provided figure preparation using ArcMap GIS and Adobe Illustrator as well as text revisions.

**Heather L. Parks** is a geologist with the USGS in Spokane, Washington. She earned a B.S. in Geology from Eastern Washington University (2009). She specializes in GIS and contributed to numerous assessments within the USGS Global Mineral Resource Assessment Project.

**Niki E. Wintzer** is a geologist with the USGS in Spokane, Washington. She earned a B.S. in Earth Sciences from California Polytechnic State University (2004) and an M.S. in Geology from San Jose State University (2009). She specializes in structural geology and economic geology.

**David J. Williams** earned a B.S. in Geology from Eastern Washington University (2010). He served as a GIS specialist for the USGS Global Mineral Resource Assessment Project.

**Michael L. Zientek** is a research geologist with the USGS in Spokane, Washington. He earned a B.S. in Geology from University of Texas (1976) and a Ph.D. in Geology from Stanford University (1984). He is an economic geologist with expertise in magmatic ore deposits and mineral resource assessment. He is co-chief of the USGS Global Mineral Resource Assessment Project.



Zientek and others—**Qualitative Assessment of Selected Areas of the World for Undiscovered Sediment-Hosted Stratabound Copper Deposits—Scientific Investigations Report 2010–5090–Y**